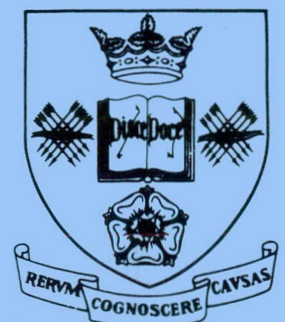
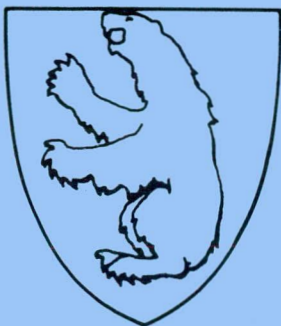


1166

**SHEFFIELD UNIVERSITY NORTH EAST
GREENLAND EXPEDITION
1982**

**FINAL REPORT
MAY 1983**



SHEFFIELD UNIVERSITY NORTH EAST GREENLAND EXPEDITION

1982

FINAL REPORT

FOREWORD

This is the final report of the 1982 Sheffield University N.E. Greenland Expedition. It is in three parts. Part 1 is an Introduction detailing the aims and members, and briefly describing the field work. Part 2, under the general heading "Science", reports each project in detail. Each project report stands complete and is followed immediately by its own figures. Part 3 describes the logistics and administration. This has been kept short, as the details are similar to previous expeditions to the area. A complete list of supporters is appended, although we have also acknowledged support where appropriate in the report. To all these supporters we offer our thanks; if any have been accidentally omitted, we apologise.

The author of each section is shown on the contents pages. The contributions have been subjected to a minimum of editing. I hope that the contrasting styles will provide some variety. I would like to thank Mrs. Norma Parkes for typing this, Eann Patterson and John Allen for assistance with proof reading, and the University Print Unit for printing.

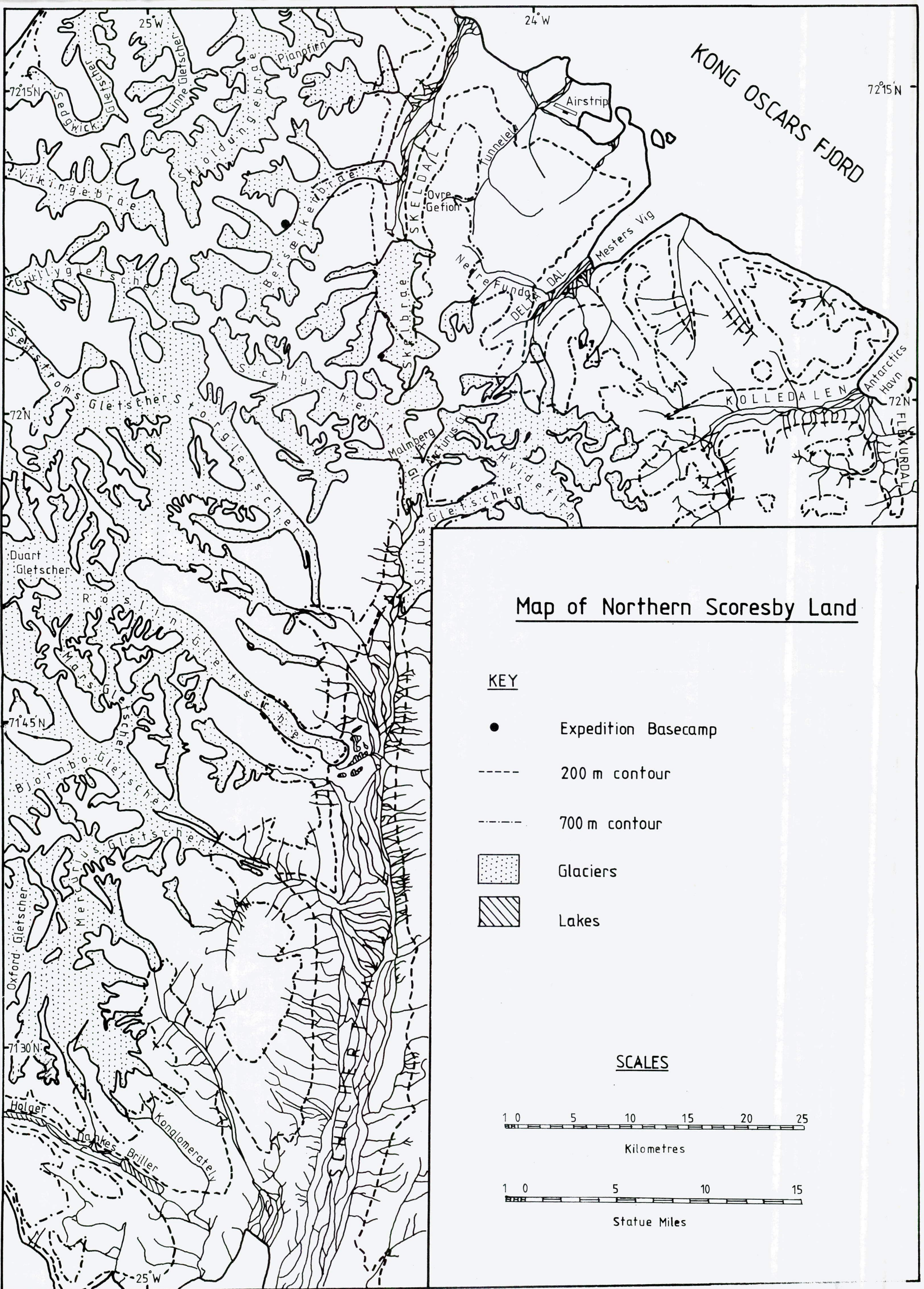
R. M. Andrews
Sheffield.
May 1983

ABSTRACT

Final report of the 1982 Sheffield University N.E. Greenland Expedition to the Bersaerkerbrae Glacier, 72° 10' N, 24° 30' W. Projects were: testing of a low powered CMOS data logging system; measurement of the fracture toughness of glacier ice; monitoring the formation of perched blocks; a study of the geomorphology of a glacial melt stream; a study of Jurassic sediments (at Antarctic Havn); a report of observations of Muskox and a study of blood plasma cortisol levels. Brief logistic and administrative details are included.

CONTENTS

1.	Introduction	R. M. Andrews	1
2.	Science		
2.1	Solar Powered Data-Logger Report	J. P. Allen	4
2.2	Measurement of the Fracture Toughness of Glacier Ice	R. M. Andrews	27
2.3	Perched Block Report	E. A. Patterson	60
2.4	Melt Stream Geomorphology	K. J. Senior	84
2.5	Lower Jurassic Sediments at AntarcticHavn, North East Greenland	A. P. Hillier	102
2.6	A Report of Muskox Observations for 1982	E. A. Patterson	112
2.7	Determination of Plasma Cortisol Levels	J. P. Thompson	120
2.8	Meteorological Conditions Observed in the Northern Stauning Alps during July and August, 1982	J. P. Allen	130
3.	Logistics		
3.1	Permission to Enter Greenland and Travel to the Area	R. M. Andrews	131
3.2	Travel Within the Stauning Alps	R. M. Andrews	133
3.3	Financial Report	E. A. Patterson	134
3.4	Food Report	A. P. Hillier	136
3.5	Equipment	E.A. Patterson, R.M. Andrews	138
3.6	Maps, Aerial Photographs and Landsat Image	R.M. Andrews, J.P. Allen	143
3.7	Medical Report	J. P. Thompson	145
3.8	Radio Report	J. P. Thompson	146
3.9	Mountaineering Report	K. L. Martin	147
4.	Acknowledgements		150

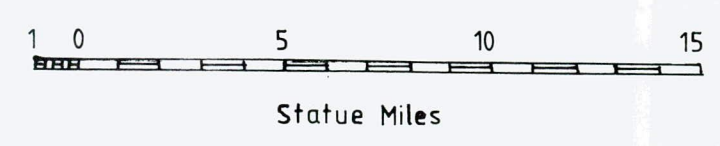
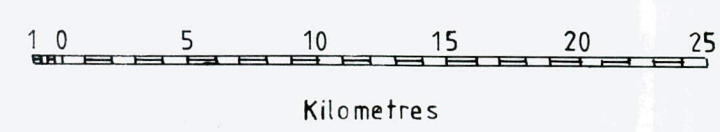


Map of Northern Scoresby Land

KEY

- Expedition Basecamp
- 200 m contour
- - - 700 m contour
- ▤ Glaciers
- ▨ Lakes

SCALES



BERSAERKERBRAE MAP

The map of the Bersaerkerbrae Glacier, shown on the following page, was compiled from several sources of information.

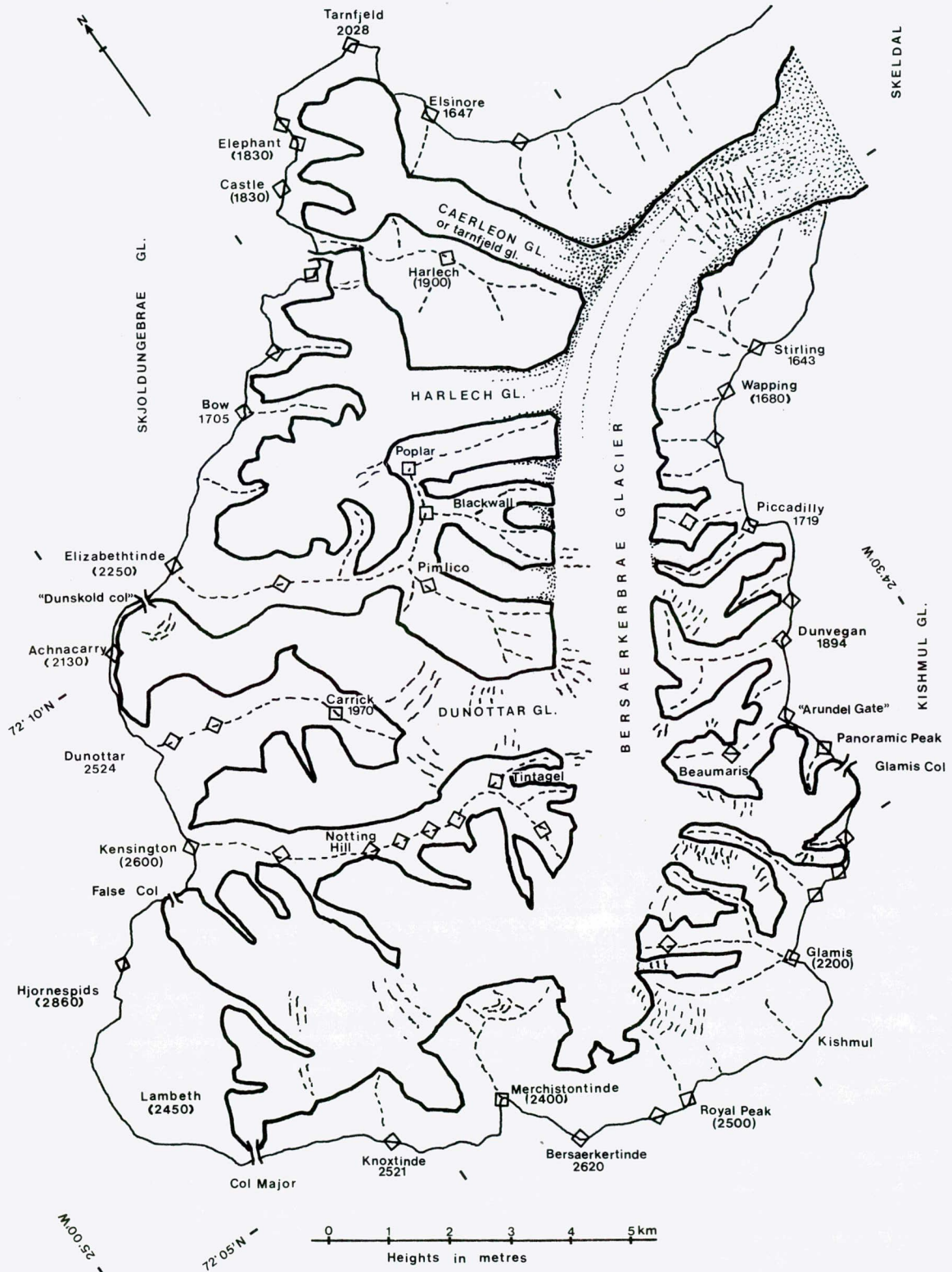
The outline of the glacier and the catchment area were derived from the Landsat scene for Path 248 Row 9, 3 July 1979. Using a film positive copy of the scene the outlines were digitized with a Carl Zeiss Steko 1818 stereocomparator in the Photogrammetry section of the Department of Civil Engineering at the University. The digital information was then transferred onto one of the main-frame computers at the University and plotted using a Calcomp plotter.

There was still extensive snow cover over the Bersaerkerbrae area when the scene was recorded. Combined with an unfavourable sun azimuth this meant that the terrain in the south-west corner of the glacier was particularly difficult to interpret from the image, as a result of this there may be some minor inaccuracies on this part of the map.

The heights and names of the peaks were compiled by Ken Martin from several sources, these include the Danish Geodetic Institute's 1:250,000 scale sheets of the area and the climbing guide to the Stauning Alps by Bennet. Those heights given in brackets are of questionable accuracy. Other details, such as crevasses and moraines, were plotted using information gathered whilst in the field and from air photographs of the area.

THE BERSAERKERBRAE GLACIER

STAUNINGS ALPS, NORTH-EAST GREENLAND



1 INTRODUCTION

This part of the report gives the aims of the expedition, and lists the members. A brief narrative of the field work then follows. The expedition was a multidisciplinary scientific project of seven members, which operated for eight weeks in the Stauning Alps, N.E. Greenland. Most of the studies were carried out on the Bersaerkerbrae Glacier, 72° 10' N, 24° 30' W, a sub polar valley glacier.

AIMS

The expedition left the U.K. with the following aims:

1. To assess the feasibility of using a low-powered CMOS data logger for geomorphological experiments in remote areas.
2. To measure the fracture toughness of glacier ice.
3. To study the geology of a cliff section at Antarctic Havn.
5. To study the effect of exposure to cold on blood plasma cortisol levels.
6. To record details of any Muskox herds encountered.
7. To carry out limited survey work on the Roslin Glacier.
8. To inventory and re-pack supply dumps from previous Cambridge and Sheffield expeditions.
9. To collect Saxifrage specimens on behalf of Mr. John Peach.

Overall, these aims were achieved. The collection of Saxifrages was not successful, owing largely to the botanical ignorance of the members. The results of the survey work were found to be of little value, and have not been included in this report. An additional project was included whilst in the field - a study of the geomorphology of the lateral melt stream of the glacier.

MEMBERS

These details are as at the date of the expedition, with changes noted if necessary. Except for Kev Senior, all members are (or were) students of the University of Sheffield.

BOB ANDREWS (25), leader. A research student in the Mechanical Engineering department. Responsible for the fracture toughness of ice project. He was a member of the 1978 Sheffield expedition to the area.

JOHN ALLEN (24) A research student in the Civil Engineering department. Designed and built data logger and carried out the field tests. A member of the 1978 expedition and also the survey party of the 1980 International Karakoram Project. He now works as a research assistant in the Mechanical Engineering department.

ANDY HILLIER (23) Graduated in geology in 1981, and now works as a geologist in the North Sea. Organized the food, as he did for the 1978 expedition. He carried out the geological study at Antarctic Havn.

KEN MARTIN (21) Final year student in Civil Engineering, now working for West Yorkshire County Council. Organized the equipment for the expedition.

EANN PATTERSON (22). Final year undergraduate in Mechanical Engineering, and a Sub Lieutenant in the Royal Navy. Expedition treasurer and carried out the Perched Block project. Wrote up the collected observations of Muskox herds. Has since resigned from the Navy and now works as a research assistant in the Mechanical Engineering department.

KEV SENIOR (24) Graduated in Geology from Southampton University in 1971, and now works for IBM. On this expedition he carried out the melt stream geomorphology study; previously he was a member of three caving expeditions to the Picos mountains.

JOHN THOMPSON (21) A fourth year medical student, currently reading an intercalated degree in Medical Physics. He was responsible for the plasma cortisol project and acted as the expedition medical officer and radio operator.

The members can be contacted through the leader, whose address is at the end of this part of the report.

CHRONOLOGY

October 1981 - June 1982 This was the planning and preparation phase. By January 1982 applications for financial support and permission to enter the National Park had been made. During the following months interviews were attended, many letters written and equipment designed and constructed. In May and June the pace was increasing, as the departure date approached. Early in May permission to enter the area was received, whereupon the expedition bank balance fell dramatically as reservations were confirmed.

30 June - 2 July Eann and John Allen drove the stores to Glasgow Airport. These were to be airfreighted to Iceland ready for the main party on 2 July. Due to loading problems at Glasgow, the stores actually accompanied the main party. We are grateful for the assistance of Mr. Ronnie Macaulay of Iceland Airtours, the British Embassy in Reykjavik and the staff of Icelandair Flugfrakt in Reykjavik in resolving the problem. The party and stores were re-united in Iceland by the evening of 2 July

3 July The Twin Otter chartered from Flugfelag Nordurlands collected the party and equipment from Keflavik for the flight to Mesters Vig. On arrival, the stores were transferred to the helicopter, and we were treated to coffee and cakes in the canteen. Our thanks are extended to the station staff for their hospitality. The helicopter then flew us out to the Bersaerkerbrae Glacier, landing in a light snowfall. After protecting the stores, we pitched the tents on the first level snow patch encountered in the moraines.

4 - 5 July A site for a permanent base camp was located and levelled on the moraine. After pitching the tents, a porters' route was made through the recent snow, and the stores carried in. A firm base had been established.

6 - 19 July The effort during this period was concentrated on the scientific programme. The data loggers were debugged where necessary and tested, including 24 hour monitoring as a check. Much effort was expended on the fracture toughness project, initially on testing and modifying the equipment and then on coring and testing specimens. Perched blocks of varying sizes were located and surveyed. A regular morning event was the extraction of a blood sample, followed by the cranking of the hand centrifuge. The melt stream below the moraine was intensively monitored.

20 July - 2 August During this period John Allen, Kev, Ken and Andy made a journey to the Roslin Glacier, travelling via the Skel Pass and Schuchert Dal. Whilst there, they resurveyed a series of larger boulders previously surveyed in 1976 and 1978. They found the dump at the site of the main base camp of previous Cambridge expeditions had burst open due to subsidence of the ice cored moraine. The spoiled items were burnt, the area cleaned up and the remainder inventoried and re-packed. Due to bad weather it was not possible to open and check any other dumps. A theodolite tripod was recovered for eventual return to Sheffield. Meanwhile on the Bersaerkerbrae, Eann, John Thompson and Bob continued the scientific work, concentrating on perched blocks and fracture toughness testing, including ice crystal photography.

2 August - 12 August On the 2nd, the Roslin party returned to base and we were also joined by a four man party led by Keith Miller. During this period we completed the scientific work, including two survey profiles of the Bersaerkerbrae snout. Various short local trips were made, including an ascent of Beaumaris, an exploration of the upper Dunottar Glacier and a crossing into the Skjoldungebrae Glacier. Some food was also ferried up from the snout for future use.

13 August - 20 August A geological party of John Allen, Andy and Kev left for Antarctic Havn, walking via the Gefion Pass, Delta Dal and Oksedal. They re-joined the main party at the old lead mine at Blyklippen on August 23rd. Keith Miller and Hal Lister returned to Mesters Vig due to injury, while the remainder of us made a journey down to the Roslin Glacier. This journey, made in two groups, was notable for strong winds and rain.

21 August - 26 August This was the final phase. Base camp on the Bersaerkerbrae was cleaned up; spare food and other useable items were carried up the glacier and packed into a dump at Sun Valley camp. Items for recovery to the U.K. were taken down to the snout, and thence over the Gefion Pass to Blyklippen. En route the data logger monitoring perched block rotation had been collected and the rotation meters removed from the boulders. The equipment was driven into Mesters Vig from Blyklippen by a visiting member of Sirius, saving us some effort. We followed on foot the next day, in mist and a light snowfall. The flight back to Iceland on 26 August, and the return to the U.K. on 27 August were uneventful.

A NOTE ON PLACE NAMES

Place names on the East coast of Greenland are an echo of the exploration by different nationalities. We have tried to follow the spellings used on the Geodaetisk Institut's maps. Due to the limitations of English typewriters, the Danish letter "æ" has been rendered as "ae". The English forms glacier, Greenland and Copenhagen have also been used. We apologise to our Danish readers.

It should be noted that names, especially of peaks, not shown on the official maps, may not have been approved by the Danish authorities.

CORRESPONDENCE

Any correspondence to the expedition should be sent to:

R. M. ANDREWS,
C/O MECHANICAL ENGINEERING DEPARTMENT,
UNIVERSITY OF SHEFFIELD,
MAPPIN STREET,
SHEFFIELD.
S1 3JD

2.1 SOLAR POWERED DATA-LOGGER PROJECT

We would be grateful if anyone constructing one of these units would acknowledge the source in any publications. A copy of the results would also be appreciated, together with any comments or suggestions.

1. Design Philosophy

The current upsurge of interest in micro-electronics has led to two diametrically opposite design philosophies. The first exploits the capabilities of current technology and then tries to find an application suitable for the machine (home computers), the second finds an application and then exploits the capabilities of current technology to build a machine that is suitable. We would like to think that the design of this data-logger was guided by the latter.

One of the first design decisions which had to be made was whether the unit should be controlled by discrete logic (AND, OR, NOR gates etc) or whether the control should be provided by a processor. Discrete logic would produce a cheap solution and would consume little power, however the tremendous increase in flexibility offered by the use of a processor far outweighed the increased cost and by incorporating some recently introduced ICs (Integrated Circuits) the power consumption could still be kept very low. Using a processor to control the functions of the unit meant that its precise specifications could be decided upon much later in the design procedure than would have been the case had discrete logic been used. Hence it was possible to include additions and modifications right until the time when the program was burned into EPROM (Erasable Programmable Read Only Memory). The final design was based on the various needs of the different projects and around the results of a survey carried out by the BGRG (British Geomorphological Research Group) into the needs of geomorphologists as regards data-logging facilities.

The range of sensors which could be used with the unit would depend on the types of electrical inputs provided. Sixteen of the inputs would be for analogue signals i.e. signals where the information is conveyed as a voltage level. Two inputs would be counters; to make this as flexible as possible the inputs to the counters would be triggered by a voltage level and the count interval would be under software control. A further eight inputs would be available to test the settings of mechanical or electrical switches.

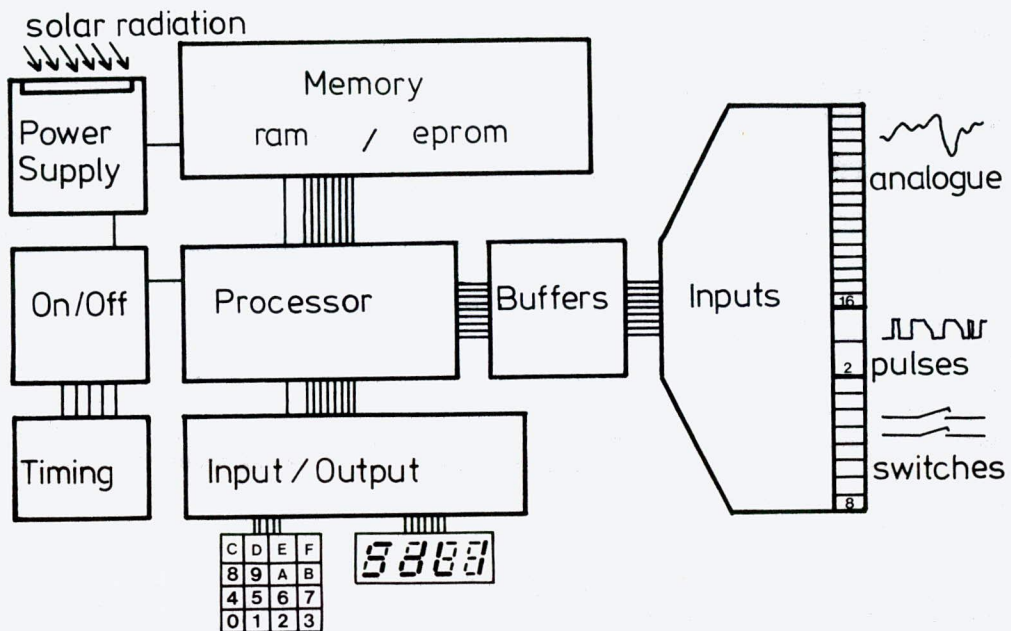
The amount of data storage which could have been provided was unlimited, in theory, but the need for reliability meant that devices such as cassette recorders were discounted very early in the design. The final decision was that there should be just 750 memory locations, a decision forced by the method used for producing a permanent copy of the data (see later) but one which did not seriously hamper the scientific programme. For example, it still allows hourly temperature readings for more than 30 days. The scanning interval had to range from 200 samples/second for the ice fracture toughness project to intervals of one hour or longer between samples for the perched block project. The final design had software controlled (the desired value is entered on the keyboard) intervals up to 15 seconds duration, switchable intervals up to 20 minutes duration and then combined software and hardware for intervals greater than 20 minutes.

Work started on the design in February, just five months before the expedition was due to start. By April construction of the prototype was well under way. Initially only an occasional hour on weekday evenings could be devoted to the project. As the departure date approached the increased sense of urgency meant that daytime at weekends was included, then evenings of weekends and finally any 'spare' moments during weekdays. The prototype and one of the copies became operational a few days before departure,

unfortunately completion of the third unit occurred on the wrong side of our departure date. Being deprived of the usual pieces of test equipment (e.g. Oscilloscope) meant that fault-tracing on this unit became the unwelcome chore of the first two weeks in the field. A summary of the experiments performed using the three data-loggers is given later in this report.

2. Method of Operation

The functional layout of the unit is shown in the diagram below. This is followed by a brief description of each of the functional components. A more detailed description of individual electronic components and their operation can be found in the appendices at the end of this report.



The Processor

The heart of the unit is a RCA CDP1802C COSMAC microprocessor. For this type of application it is ideal; simple to use, well established and relatively cheap. It is fabricated using CMOS (Complementary Metal Oxide Semi-conductor) construction which means that it has a typical current drain of just $0.1\mu\text{A}$ when the clock input is static, yet data internal to the processor will not be lost in this state. The other advantage of this processor is that only a small additional circuit is required to transfer programs stored in another micro-computer across into the memory of the system. This significantly reduces the development time as the programs can then be rapidly and easily modified using the second computer (see SDL TN 4).

EPROM (Erasable Programmable Read Only Memory)

EPROMs retain the information programmed into them even when the power is removed. They are therefore used to store the main set of instructions which will be used by the processor. To keep the operating current of the unit to a minimum the design incorporates a CMOS EPROM. These are relatively new and hence more expensive than conventional EPROMs. However, the current consumed when in standby mode is one thousand times smaller than that required by conventional EPROMs.

RAM (Random Access Memory)

1024 bytes of RAM are provided in the system, 256 of these can be programmed by the user with his set of operating instructions (see later). The remaining 768 bytes are for data storage (see SDL TN 12).

Power Supply

The unit is powered by two 12V 50mA solar panels, with 8 AA sized Ni-Cad batteries to store the excess power for use when the solar panels are not operating. In power-down mode the unit consumes less than 100 μ A, when running just 1 mA. Over 99% of the time that the unit is operational is spent in power-down mode. When fully charged the batteries could therefore provide sufficient power for over two months of continuous operation; with the solar panels attached this period is greatly extended. A CMOS voltage regulator is used to provide the 5V stabilized supply required by the processor and memory (see SDL TN 14).

Keypad and Display

The unit is controlled with a 'Program Select' switch and a 16 key keypad. The keys are used to enter all the instructions required by the unit and their function depends on the program currently running. Key de-bounce is provided in software by the processor, hence cheap switches can be used.

The display is a large four digit liquid crystal display, this is easy to read and requires very little power.

Power-Up/Power-Down Circuit

Typically the unit will spend at least 99% of its time waiting between readings. To save power the unit switches itself off leaving only a timer running which, after a user selected interval, switches the unit on again. Power-down is initiated when the processor executes a power-down instruction; this is entered by the user in his data collection program (see SDL TN 3).

Analogue/Digital Inputs

Conversion of the analogue input voltages to a numerical value is performed by an ADC0816 A/D (Analogue-to-Digital) converter. This 8 bit CMOS converter will resolve the input signal into a numeric value between 000 and 255 i.e. it will resolve to 0.4% full scale. This IC has 16 inputs and has an expansion control so that further analogue inputs can be added. The clock for this device is only enabled when the unit is in 'Execute' mode; if during 'Execute' the power-down instruction is encountered, then the clock will be disabled during the power-down period. Sixty four clock cycles are required by this IC to perform a conversion; this limits the maximum number of samples per second to approximately 1500 for a 100 kHz clock. However, the time required by the processor to transfer the data and to initiate another conversion means that the maximum sampling rate is limited to 200 samples per second.

The full scale (255) input voltage level is set and held constant using four 1.22V bandgap reference diodes. These are stable over a wide range of supply currents and ambient temperatures, typically they require just 50 μ A to operate.

Eight of the analogue voltage inputs go directly to the A/D converter, this allows input voltages ranging from 0.0V to 4.88V. The remaining eight inputs are taken to voltage comparators and the outputs from these are amplified ten-fold before they too are taken to the A/D converter. These inputs have only a 0.488V range, but it can be anywhere between 0V and 8V. Each of the amplified inputs has an 'enable' signal, a 6.1V pulse which starts 0.1 sec. before a conversion is due and which ends after the conversion has been completed. It can be used to power external devices.

Other Inputs

Two counters are provided. These also have voltage comparator inputs, hence the signal can be a fluctuating voltage (it does not need to be in the form of digital pulses).

The count interval is set by the user and can be from 1 to 15 seconds, hence where the pulse frequency is not known a priori several different count intervals can be specified to ensure a usable result. An unregulated 'device-enable' is switched on during the count period and can be used to power external devices.

The parallel input tests the setting of up to eight switches and records these settings as a binary code the value of which lies between 0 and 255.

For further information see SDL TNs 2 and 6.

3. Control and Programming of the Unit

Four modes of operation were programmed into the unit

LOAD
RECALL
WAIT
EXECUTE

The mode required is selected using a simple rotary switch (shown as individual switches on the cct. diagram, labelled 'Program select'). Unused switch settings cause the processor to look for its next instruction at the address location immediately after those of the EPROM fitted, this allows for easy program expansion.

The program is run by selecting the mode required then depressing the 'reset' switch. Pressing 'reset' again will restart the program. There is no other way of transferring from one mode to another.

LOAD

This program allows the user to load the unit with a set of instructions which it will then execute when set to the appropriate mode. The keyboard is scanned and the value of each key pressed is displayed then stored, the memory is not altered until a key is pressed. Up to 240 values can be stored, permitting a total of 120 instructions (two keystrokes are required per instruction, see later).

RECALL

The user memory has been sub-divided into eight 128 byte pages; pages 0 and 1 are for the user instructions and pages 2 to 7 are for the data. This program displays a page of data, first prompting for the page number then for the mode of display. Two display modes are available; STEP requires that a key be pressed before the next data value is displayed and CONTINUOUS displays the data values with approximately 1½ seconds delay between each value. When the program has displayed a complete page it then prompts and waits for a new page number.

WAIT

This program powers down the unit, power consumption is then at a minimum, yet all data are retained. This mode is particularly useful when transporting the unit between the data collection site and a comfortable working environment.

EXECUTE

Immediately after the unit enters this mode it will execute the first instruction entered by the user and then continue sequentially through the user program until it executes a 'repeat' instruction. Each instruction is composed of two key strokes, the first is the function (scan, delay etc) the second is the parameter (channel no., multiplier etc). 'Execute' is the only way in which data memory can be altered (apart from completely switching off the whole unit). The unit will automatically leave execute mode when the last location in data memory is filled, it then loops indefinitely in 'power-down' until a new mode is selected.

During 'Execute' it is possible to blank the display. The program routine which displays the recorded number takes a variable time to execute depending on the number

of iterations required for the binary to decimal conversion. Therefore when scanning channels at a rate faster than once per second the variable time interval between scans can become unacceptable. Blanking the display will make the interval of constant length and will also reduce the power consumption.

Instruction Set

The following instructions are available (note: each requires two key strokes):-

Scan/Channel no.	Initiates the A/D converter; on channels 0-7 there is a 0.1 sec delay with individual 'enables' for each channel.
Delay (short)/multiplier	Multiples of 10ms delays, from 1 to 15, by default set to one 10ms delay period.
Delay (long)/multiplier	Multiples of 100ms delays, from 1 to 15, by default set to one 100ms delay period.
Counter 1/delay (secs)	Counter 1 enabled for 1 to 15 seconds.
Counter 2/delay (secs)	Counter 2 enabled for 1 to 15 seconds.
Parallel/dummy	Scans the keyboard input lines, can be used to test up to eight switches. Dummy is any key and does not affect operation of the program but must be present.
Powerdown/continue or repeat	When the unit executes this instruction it switches several parts of the circuitry off, thus saving a considerable amount of power. After a preset time (set by the switch 'power-up time select') the unit executes the second part of the instruction. If the key is 0-7 then the unit continues to the next instruction, if it is 8-15 then the unit returns to the start of the user program.
Repeat/dummy	When the unit executes this instruction it then loops back to the start of the user program, the dummy key can be omitted.

Program Examples

The key codes are:

key no.	function
0	power-down
1	scan channel
2	counter 1
4	delay (short)
6	counter 2
8	parallel input
12	delay (long)
14	repeat

Example 1 Scan channels 0 and 1 every 22 minutes indefinitely (22.3 minutes is the longest powerdown available - see SDL TN 3)

This would require the following key strokes

1	0	scan/0
1	1	scan/1
0	14	pdn/repeat

Example 2 Scan the parallel input every 45 minutes

8	8	par/dummy
0	0	pdn/cont
0	14	pdn/repeat

Example 3 Scan channel 15 every 250 milli-seconds (note: channels 8 to 15 do not have the 0.1 sec delay).

1	15	scan/1
12	2	del long/x2
4	5	del short/x5
14		repeat/not reqd

Example 4 Enable counter 2 for 1 second and then counter 1 for 10 seconds, scan channel 8 then wait 22 minutes and scan channel 8 again, after a further 22 minutes repeat the whole sequence

6	1	ct 2/1 sec
2	10	ct 1/10 sec
1	8	scan/8
0	0	pdn/cont
1	8	scan/8
0	14	pdn/repeat

Note: the power-down interval can also be set to 11.1 min, 5.6 min, 2.3 min, etc (see SDL TN 3)

4. Construction

The unit was built on two pieces of Vero strip-board, the smaller (150 x 120 mm) held the A/D converter, the input amplifiers and those ICs requiring V Batt, and the larger (235 x 120 mm) held the processor and its associated circuitry. Due to the large dimensions of the crystal required for the oscillator (100 kHz) this was mounted on a separate piece of board 30 x 20 mm in size. Layout of the components is not critical, but on the A/D board IC 34 should be situated as close to IC 2 as possible and the analogue signal lines should be routed as far away from the digital lines as possible. The relatively slow speed at which the processor was being driven and the fact that all the circuitry was CMOS meant that it was unlikely that there would be any problems with interference between closely packed wires on the processor board. Hence strip-board was satisfactory and all wiring was done with fine gauge wire (e.g. wire-wrap wire). Both boards and batteries were housed in the same 230 x 150 x 65 mm metal box.

Temperature sensors etc were attached via 5 pin DIN sockets mounted on the side of the box, these being the cheapest type of connector available. No problems were encountered with this connector although for reliable long term use in the field, particularly in wet conditions, a more robust gold-plated connector is recommended.

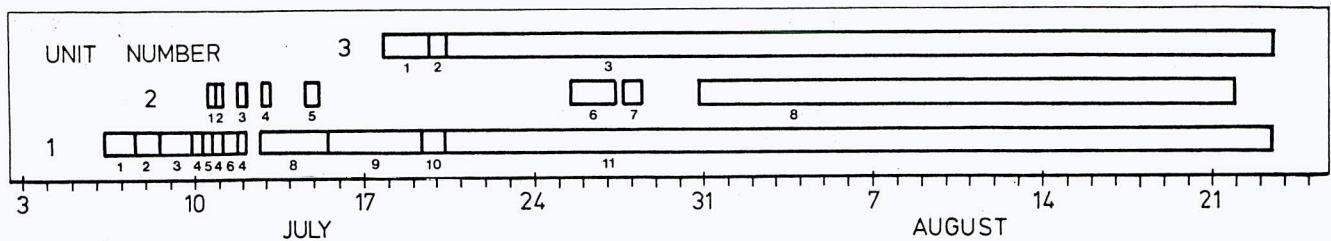
Switches were mounted according to the individual constructors preferences, to prevent accidental erasure of all data the main on/off switch was usually put well out of easy reach.

No special treatment was given to the solar panels, these appeared to function satisfactorily even when full with water! But this will cause long-term problems and a water-tight cover is desirable when rain is common.

Construction of the complete unit took one person about two weeks. Two copies were made of the prototype, both by people with no previous experience in micro-electronics. The only construction problems encountered with these copies were an occasional solder bridge between adjacent tracks on the strip-board and a few wires crossed on the data-bus. The main precaution taken during construction was to avoid the build-up of static electricity whilst handling the ICs, as the high voltages generated can destroy the CMOS circuitry. Avoiding wool/nylon clothing combinations should keep the generation of static to a minimum.

5. Field Operation Summary

During the expedition the three data loggers collected more than 10,300 readings over a period exceeding 2600 hours, fig. illustrates for each unit the period over which it was used and the experiment numbering system used with each unit. The table below summarises the operation of the three units:



Unit No.	Total hours collecting data	Total No. of readings	Comments
1	1125	5184	Prototype
2	657	3860	Copy, start delayed by faulty IC
3	864	1298	Copy, completed in the field

The prototype had been fully tested prior to departure and ran almost uninterrupted for the whole duration of the expedition, no problems were experienced with this unit. Unit 2 had been completed but not fully tested prior to departure, a faulty IC meant that the unit could not be used with the automatic switch-off facility, when the fault had been traced the faulty IC was replaced with one from unit 3. Unit 3 was completed in the field and despite some initial problems provided extensive data-logging facilities for a major part of the expedition. The list below is just a brief summary of the experiments which can be performed using the data-loggers and confirms that the design aim of a flexible system was achieved.

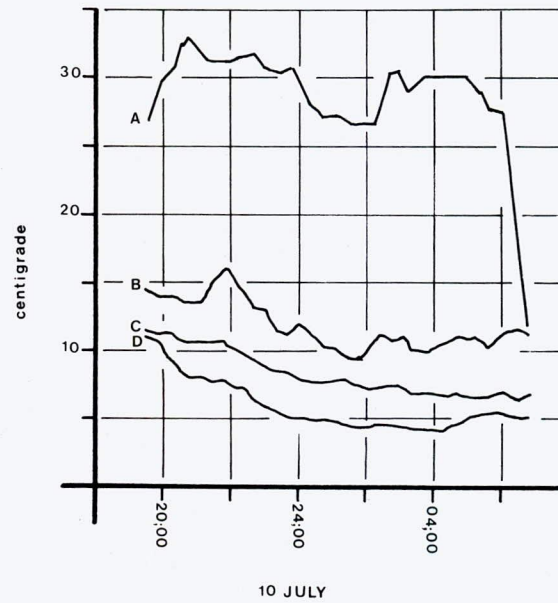
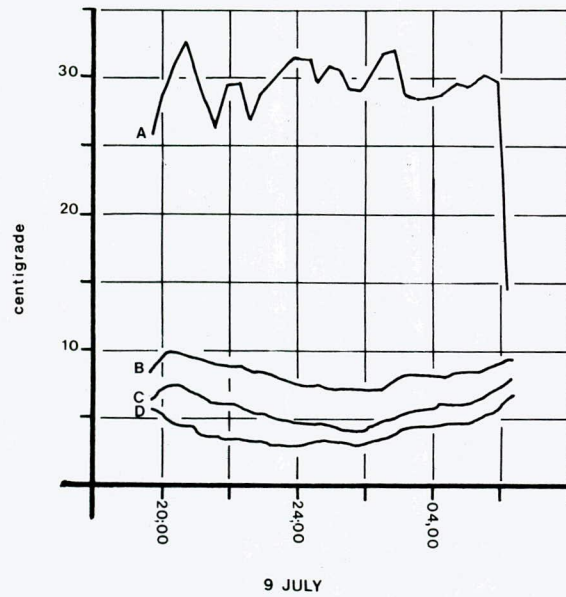
Unit No. 1 - summary of field operations and experiments

- Expt 1: Monitoring the data-logger temperature and input voltages to see how solar radiation affects the stability of the voltage reference.
- Expt 2: Monitoring the temperature inside the cool box used for storing the blood samples.
- Expt 3: Similar to expt 2, but including measurement of incoming solar radiation.
- Expt 4: Monitoring air temperatures, temperatures inside tent and sleeping bags overnight.
- Expt 5: Solar radiation and wind direction at base camp.
- Expt 6: Solar radiation only, to provide additional data for the hydrology expts.
- Expt 7: Automatic stage recorder, abandoned when channel erosion left the recorder above water level.
- Expt 8: Moraine surface temperatures, air temperature and solar radiation.
- Expt 9: Similar to 8 but with increased number of temperature sensors, looking at the effect of water from the ice-core on the surface temperatures.
- Expt 10: Testing data-logger prior to expt 11.
- Expt 11: Recording ground level temperatures in the Skel Valley at hourly intervals for a continuous period of 34 days, unit left unattended.

Experiment 1

So that the units could be easily and safely transported from one location to another, they were housed in robust metal boxes coated with black plastic. The black surface would clearly absorb heat from the sun, so the first experiment was devised to test whether the heating of the circuitry would detriment the accuracy of the data-logger, if necessary the data-loggers could then be coated with reflective aluminium foil.

Four temperature sensors were monitored; the first was situated inside the unit next to the voltage reference circuitry. The second and third temperature sensors were placed on the ground near the unit but so that they were shaded from the sun, these were used to measure the air temperature near ground level. The fourth sensor monitored the air temperature a short distance above ground level. To provide a fixed input voltage one of the rotation sensors was attached to the fifth input channel. The rotation sensor was also placed on the ground in the shade, provided that it was not moved it would give a constant output, if the reference circuit was not stable then the values



Experiment 4 Tent and sleeping bag temperatures on three consecutive nights.

9th/10th July: A Temperature inside sleeping bag at waist level.

B Temperature inside tent.

C Temperature between tent inner and flysheet.

D Temperature of air outside tent.

11th July : A and B Sleeping bag temperatures for two people, sensors at waist level.

C Tent temperature, sensor inside 200mm below ridge pole.

recorded for this channel would change.

The unit was placed on the ground in a position where it would be exposed to the full effect of solar heating and to the cooling effect of the down glacier wind at night. The experiment was allowed to run for one complete day. The table below gives the readings recorded by the unit at approximately two-hourly intervals (see SDL TN 3 for an explanation of how the delay intervals are derived).

Temperatures recorded during Experiment 1 (centigrade)

Time	Internal	Air Temperatures		Rotation Sensor
10:04	14.2	5.0	5.0	154
12:07	20.2	6.2	6.2	154
14:10	26.2	8.4	7.4	154
16:02	26.6	11.2	8.4	154
17:53	27.6	15.4	9.8	154
19:01	16.0	10.2	8.0	154
21:04	4.0	4.8	4.0	154
23:07	2.8	2.8	2.6	154
01:10	1.4	1.2	1.2	154
03:02	0.6	0.8	0.6	154
05:05	2.2	1.2	1.0	154
07:08	6.0	2.8	2.4	155
09:11	11.2	5.0	4.8	155
11:03	16.2	6.6	6.2	155

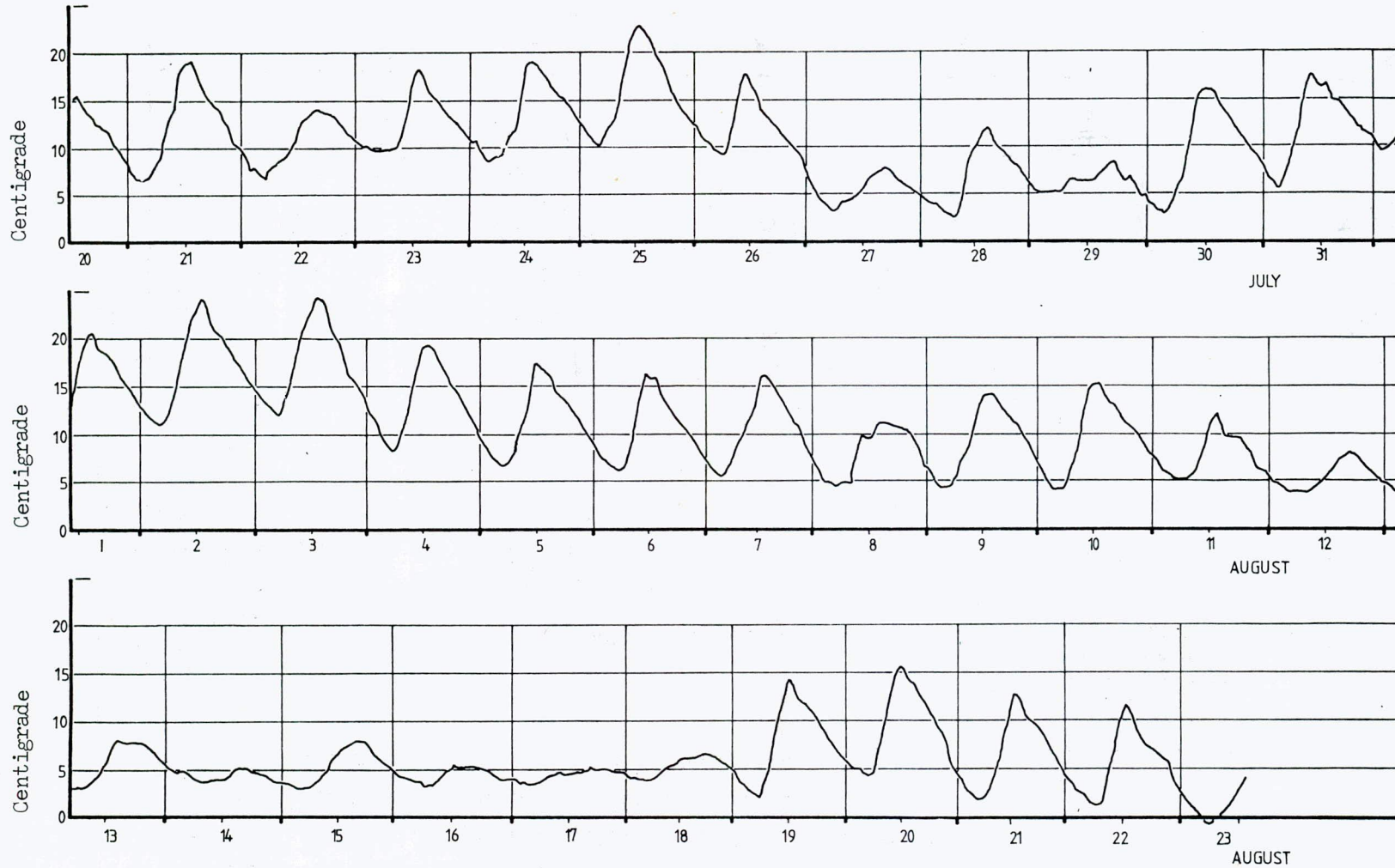
Whilst the air temperature at ground level only varied over a 15°C range, the circuitry inside the data-logger experienced a temperature fluctuation of over 27°C due to the heating by the sun. The two external temperature sensors did not give exactly the same reading during the day time as no precautions were taken to ensure that both were exposed to exactly the same amount of reflected radiation and wind. During the night, when reflected radiation was not significant, the two sensors tracked each other to within 0.1 C (the resolution of the unit was set so that 1 digit was equal to 0.2°C). The temperature of the unit dropped suddenly after 19:00 as the sun went behind the mountain beside which base camp was situated. The rotation sensor reading remained constant, as expected, until 07:08 when the reading rose by one digit. This small increase may have been caused by the rotation sensor being disturbed as it does not appear to be related to any of the temperature changes.

Based on the results obtained in this Experiment, it was decided that the data-loggers did not need to have reflective coating applied to their cases and that changes in ambient temperature would not significantly affect the accuracy of the data-logger.

Experiment 11

Remote areas are inherently difficult to travel around in (unless large amounts of financial support are available) hence performing experiments at more than a few sites becomes impossible unless the experiment can be left unattended for several days or weeks. Experiment 11 was devised to test whether the unit could be left unattended for 30 days or longer whilst programmed to collect air temperatures at hourly intervals. If car batteries had been available then there would have been no worries about the power supply, however finding volunteers to carry the batteries would have been difficult. The alternative was to rely upon the small solar panels to maintain the charge level in the eight 'pen-cell' batteries. Two solar panels were connected to the unit in series, one was positioned so that it would receive the maximum amount of solar radiation at about 11 am and the second panel was positioned to receive maximum radiation at 3 pm. Earlier tests had shown that the panels had a wide angle of acceptance and that configured in this manner they would provide power from 6 am to 8 pm. Mirror reflectors were not attached to the panels as these might have caused problems with stability in high winds.

The unit was placed at ground level in the Skel Valley, about 300m above the valley bottom. The temperature sensor was also placed at ground level and was protected from direct solar radiation. After 34 days (818 hours) the site was revisited and the unit

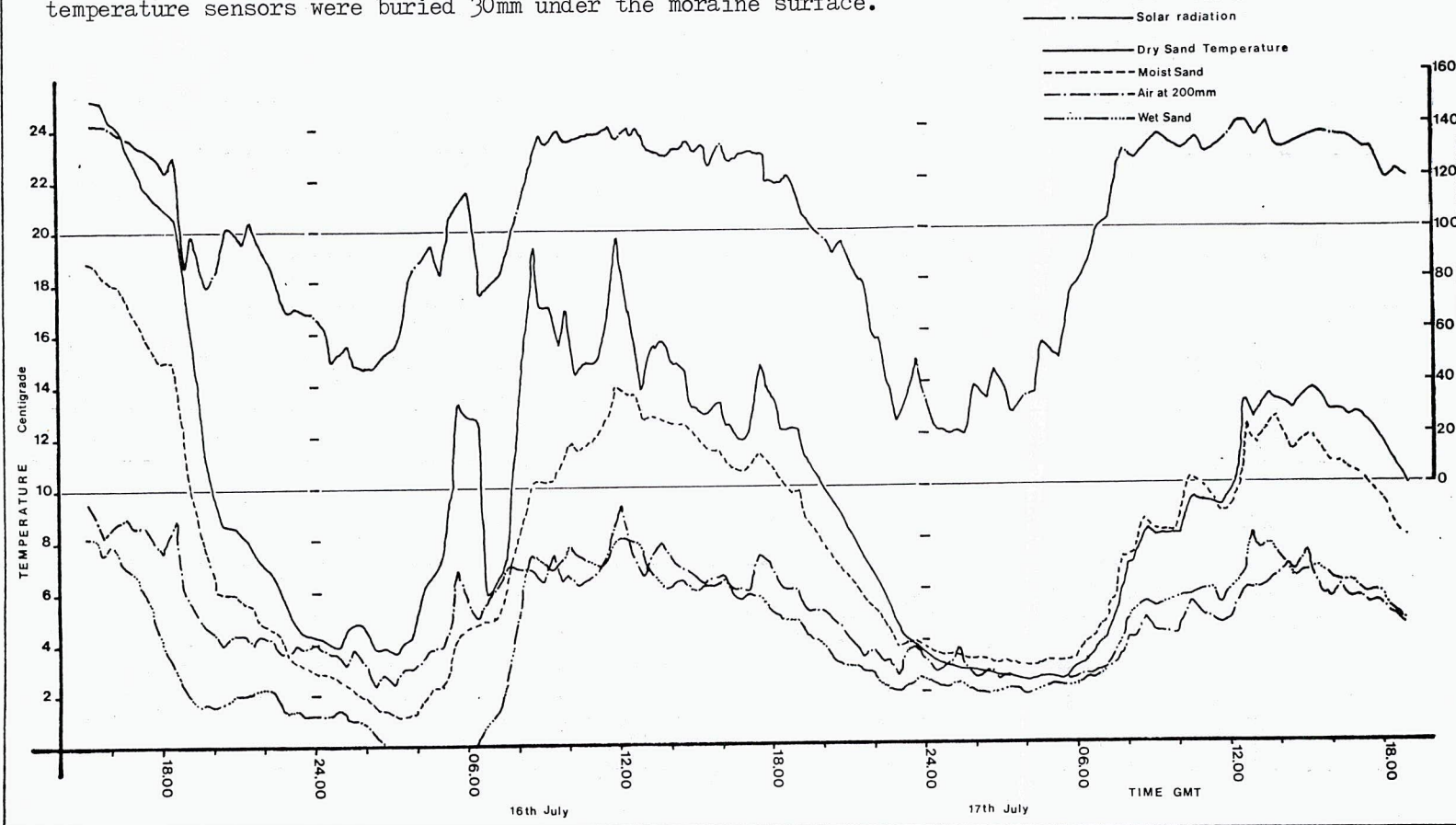


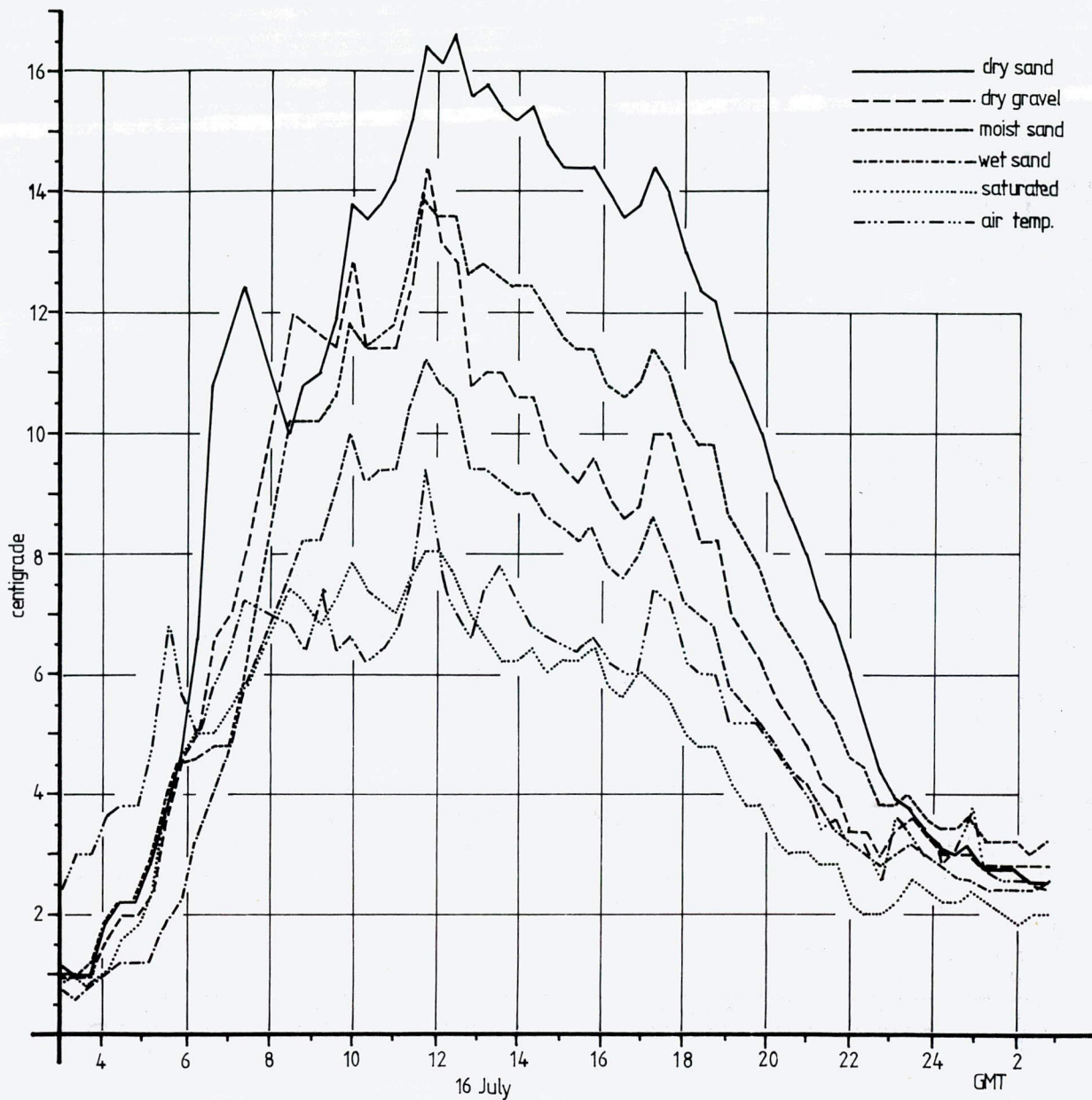
Experiment 11 Prolonged data collection

The figure shows grass temperatures in the Skel valley from 20 July to 23 Aug. The temperatures were recorded by one data-logger at hourly intervals, during data collection the unit was completely unattended.

Experiment 9 Multisensor experiment

Solar radiation, air and ground temperatures were recorded at twentytwo minute intervals over a period of two days during which the weather conditions deteriorated to total overcast. The ground temperature sensors were buried 30mm under the moraine surface.



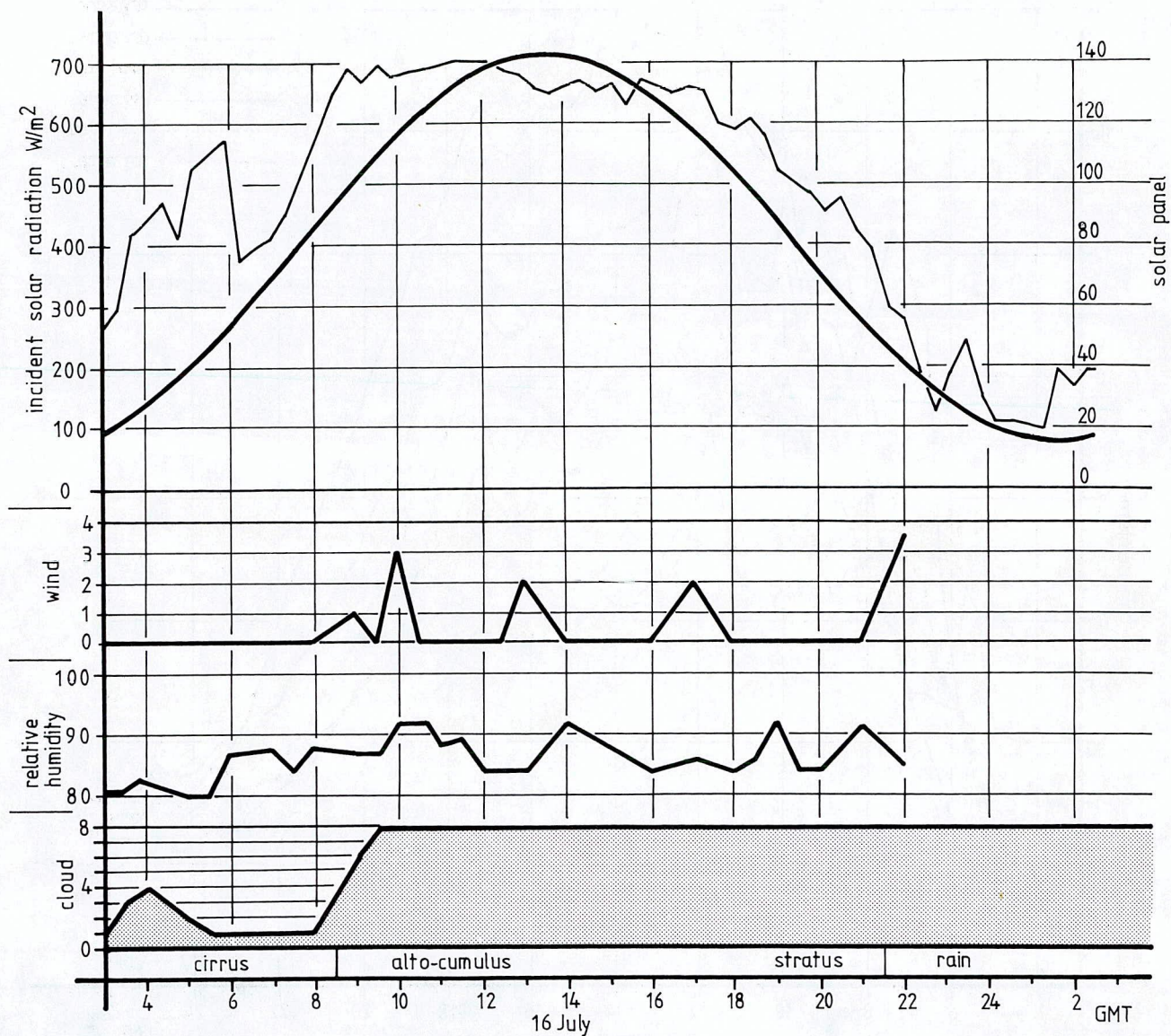


Multisensor Experiment

This figure, with that shown on the following page, shows the full set of data recorded during one of the days when experiment 9 was in progress. The data was recorded by observers and one data-logger and the horizontal axes of the two figures are identical to allow easy correlation between the various values.

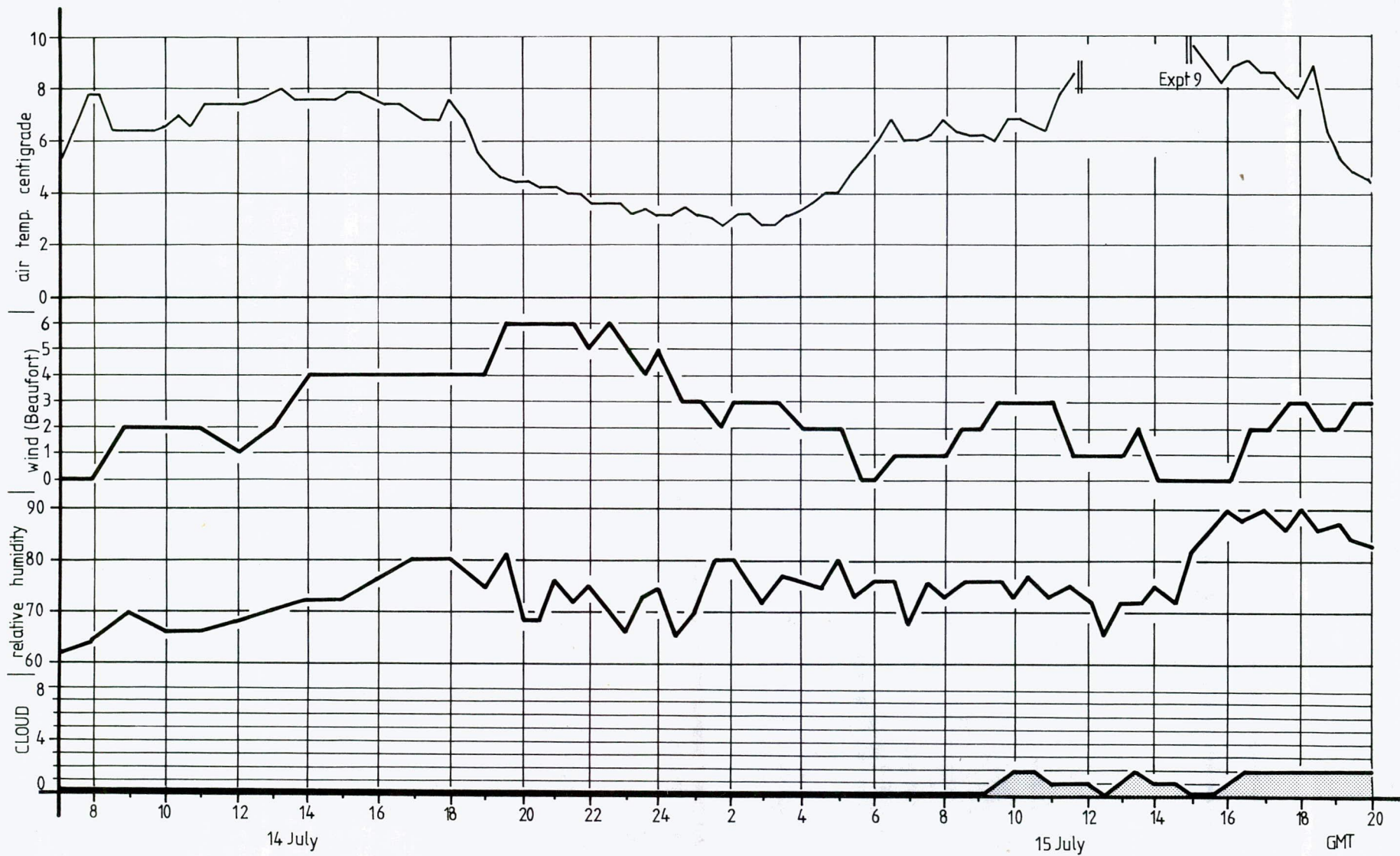
The ground temperatures were recorded with the temperature sensors buried 20mm beneath the surface of the ice-cored moraine.

The heavy line on the solar radiation plot shows the theoretical radiation curve calculated with the appropriate latitude and date parameters for a cloud free day, the light line shows the radiation actually recorded by the solar panel.



Multisensor Experiment

see previous page for details.



Meteorological conditions observed and recorded
for two days prior to experiment no. 9.

was removed so that the data could be unloaded. During the 34 days the unit had recorded 733 temperature readings and was still functioning normally when stopped. The memory available for data storage in the prototype was 768 bytes, had we not returned before the memory was full then the unit would have automatically terminated the data collection and would not have over-written any previously recorded data.

The solar panels had not been protected with any form of weather-proof covering, therefore we were not surprised to find one of them full with rain water, testing the panel with a multimeter showed that it was still providing power although this panel then failed after a further two weeks of operation. For long term use the panels need to be made water-tight.

The temperatures recorded by the unit are shown in fig. . The highest air temperature recorded near ground level was 24.4°C , the lowest was -0.6°C .

The results confirmed that long term unattended operation of the unit was possible and that the unit would work reliably over the temperature range $0-25^{\circ}\text{C}$.

6. Solar Power Data Logger - Technical Specifications

Size: 230 x 150 x 65 mm
Weight: 950 gm

Components

RCA1802 CMOS Processor, 100 kHz crystal
Intersil 6654 CMOS EPROM (512 bytes)
Hitachi 4334 CMOS RAM 1K bytes, used as follows:
16 bytes: processor workspace
240 bytes: user program
768 bytes: data storage

Power supply

2 x 12V 50mA Solar Panels (size: 150 x 110 x 12 mm)
8xAA sized Ni-Cad cells for backup (rating: 500mAh)

Power consumption (approximate figures)

Load/recall 900 μA
Wait 150 μA
Execute 900+ μA when scanning channels; 80 μA when powered-down

Inputs

16 Analogue, 0.0-4.88V range, 8 bit A/D converter
2 Counters, voltage comparator input, 1-15 second programmable count interval
8 Switch test lines, used to test whether up to 8 electrical switches are open or closed
16 Key keypad for programme entry, key de-bounce provided by software
Program select switch, display ON/OFF switch

Outputs

0.5" 4 digit Liquid Crystal Display
6.1V regulated enable for channels 0-7, ON for 0.1 sec before channel is scanned
10V unregulated, switched on whilst the counters are enabled

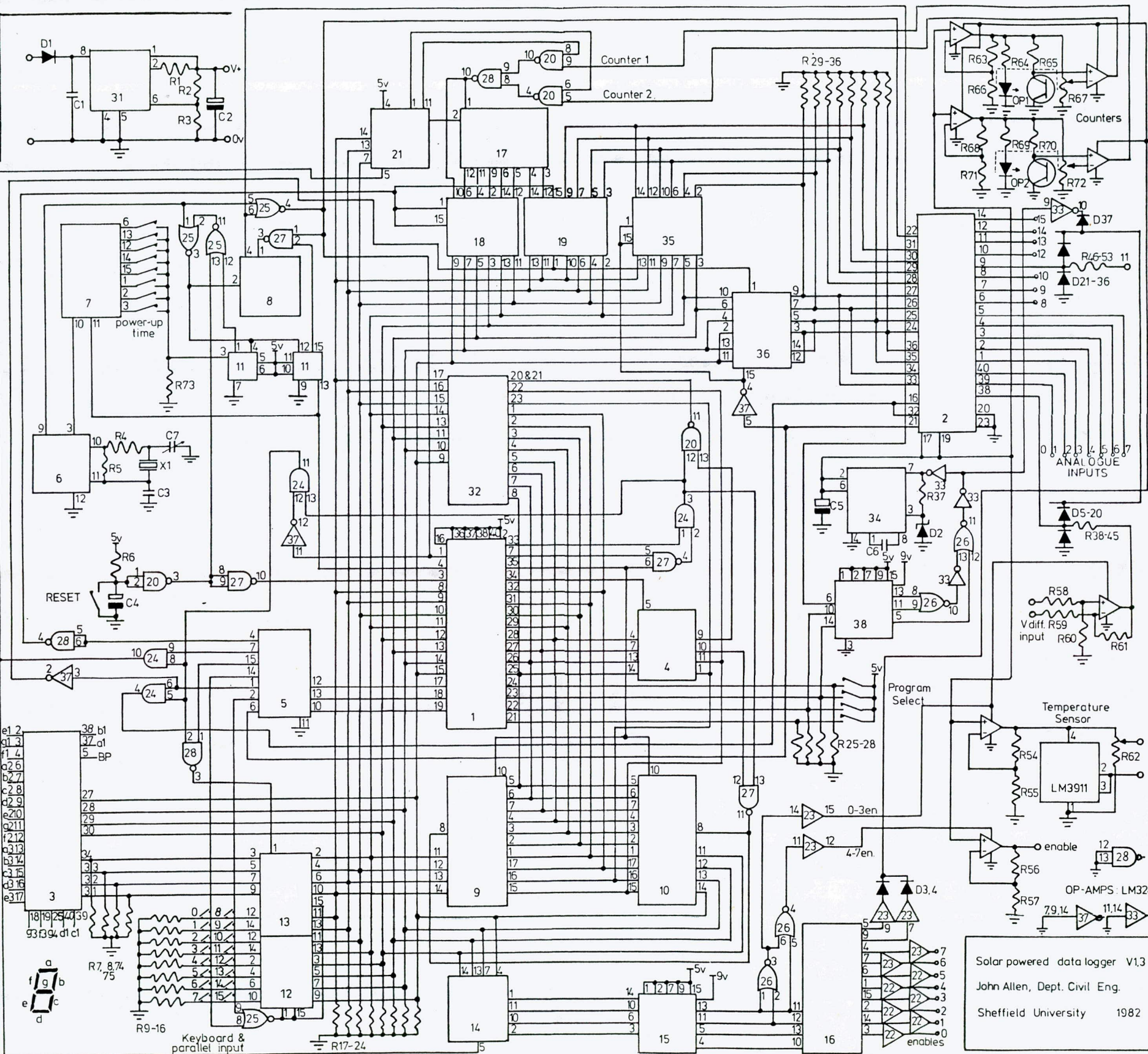
Cost

£150 approximately, June 1982 prices

SDL TN 2 Voltage Reference and Enable Circuits

The A/D converter (analogue-to-digit) used in this unit is a ratiometric converter, the output value is the ratio of the input voltage V_{in} to the voltage difference (V_{ref+}) - (V_{ref-}). In this unit V_{ref-} is 0V and V_{ref+} is 4.88V, hence the range of input voltages which can be converted is 0-4.88V. If the level of V_{ref+} changes, then the output value

SDL-TN1 Data-logger circuit diagram



ICs	Resistors	Diodes
1 CDP1802C	1 18n	1 0A91
2 ADC0816CCN	2 2M85	2 9491BJ ^a
3 ICL7211AIPL ^a	3 1M	3,4 1N4148
4 4042	4 100K	5-37 1N4148
5 4028	5 1M	-----
6 4060	6 47K	C1 0.047µ cer.
7 4020	7,8-16 100K	C2 10µ 10v tant.
8 4024	17-24 47K	C3 22p cer.
9,10 4334 ^e	25-36 100K	C4 4µ7 10v tant.
11 4027	37 33K	C5 10µ 10v tant.
12,13 4503	38-53 2K2	C6 1000p cer.
14 4042	54 25K	C7 6-45pF
15 40109 ^b	55 100K	X1 100kHz
16 4028 ^b	56 25K	OP1,2 RS306-061
17 4024	57 100K	Display RS587-305
18,19 4503	58,59 100K	-----
20 4093	60,61 1M	Switches
21 4042	62 100K pot.	s.p. push to make
22,23 4050 ^d	63	s.p. 12 way (pwr up)
24 4081	64	see 3p. 4w. (prog sel)
25,26 4001 ^e	65	SDL-TN10 ^f
27,28 4011	66	s.p. toggle (EF1) ^h
29,30 LM324	67 100K pot.	s.p. toggle (on/off)
31 ICL7663CPA	68	-----
32 IM6654IJG	69	Sockets
33 4049 ^d	70	see 40 pin x 3
34 LM301	71	24 pin x 1
35,36 4503	72 100K pot.	18 pin x 2
37 4049	73 100K	16 pin x 20
38 40109 ^b	74,75 100K	14 pin x 10
		8 pin x 2

NOTES

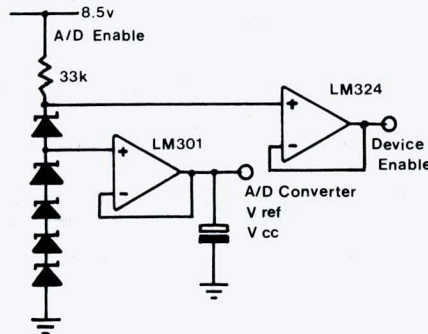
- a) RS Stock No. 304-807
- b) These devices have V_{dd} connected to +9V instead of +5V as for the other devices.
- c) 1k x 4 CMOS RAM, could use HM6514 instead.
- d) Note V_{dd} for these is connected to pin 1.
- e) IC25 V_{cc}=5V, IC26 connect V_{cc} to V_{dd}.
- f) Solar data logger Technical Note 10 'interfacing anemometer'
- g) Bandgap reference, RS283-283, see SDL-TN2
- h) Taking EF1 (pin24 IC1) to +5V enables the display during data collection. Pins 21,22 & 23 on IC1 (EF4,3 & 2) are used for program selection.

Solar powered data logger V1.3
 John Allen, Dept. Civil Eng.
 Sheffield University 1982

will also change, hence it is important that the drift of V_{ref+} due to supply voltage and temperature changes is less than the desired accuracy of the A/D converter over the full range of temperatures in which the unit is expected to work.

The voltage references for the unit are provided by five 9491BJ bandgap voltage reference diodes (RS283-283). The temperature coefficient for these diodes is typically 30 ppm/ $^{\circ}$ C, thus over a 30 $^{\circ}$ C range the output voltage will change by less than 1000ppm, i.e. less than 0.1%. For an 8-bit A/D converter 1000ppm represents $\frac{1}{4}$ l.s.d. (least significant digit) and is therefore just within the limits of acceptability. The voltage across each diode is 1.22V, to produce the 4.88V required by the converter four are used in series. The reference voltage is buffered by op-amp IC34 and a 10 μ F tantalum smoothing capacitor. Setting the V_{ref+} level to 4.88V makes the input voltage change/l.s.d. = 19.06mV for this 8-bit converter.

A fifth reference diode is used to provide the 6.1V reference for the external device enable signal, voltage follower buffers allow this signal to be used to power external devices.



On the main circuit diagram (SDL-TN 1) the enables are shown as being derived from V_{ref+} (4.88V) with op-amps to level shift the voltage, by varying the values of the feedback resistors it is then possible to alter the level of the enable signal, however this then makes it difficult to match the Venables from one channel to the next. Where a 6.1V enable is adequate the circuit in this note is to be preferred due to its greater temperature stability.

During field trials the unit was subjected to ambient temperatures ranging from 0.6 $^{\circ}$ C to +27 $^{\circ}$ C, there was no observed drift in the output readings when a fixed input voltage was applied to one of the converter inputs over the full temperature range.

The long-term stability of the voltage reference was also checked by accurately measuring the output voltages with a 5 digit Solartron DVM. The voltages were measured prior to departure and then re-measured using the same instrument three months later, the values recorded are given below and show that the drift in output voltage was negligible.

Date	V_{ref+}	Venable
June 27	4.9147	6.1633
Sept. 23	4.9152	6.1624

SDL-TN 3 Power-up/power-down circuits

The components and connections referred to in this note are shown on the main circuit diagram, SDL-TN 1.

To save power when the unit is not collecting data, the circuit has been designed so that the clock to the processor and the power to several devices can be stopped when only the timer is required. When this happens the unit is 'powered-down', a pulse from the timer then re-enables the circuit causing the unit to 'power-up'.

Power-down is initialized by the Q output on the processor (pin 4) being set high

then low, this occurs when the processor encounters the power-down command in the user instruction list (see main report). The pulse from Q resets counter IC7 and sets output pin 15 on IC11 high, thus enabling pulses from the clock into counter IC8. After 32 clock cycles, output pin 4 on the counter also goes high disabling the NOR gate and preventing further clock cycles from reaching the processor, counter and A/D converter.

The processor performs two instruction cycles in 32 clock cycles, the second instruction after that which sets Q low was selected to be one which puts the data-bus into a high impedance state, thus reducing the current through the pull-down resistors R17-24 when the unit is powered-down. The output from the counter IC8 is also taken to IC38 which shifts the level of the signal from the +5V used on the processor board to the Vbatt used on the A/D converter board. When the output goes high the supply to the voltage reference D2/IC34 and hence the A/D converter is switched off and the upper protection rail on the A/D inputs is pulled low, IC33/D37.

The time interval which elapses until the unit powers-up is selected by closing just one of the switches connected to the outputs from IC7. This IC is a binary counter, each output changes state at half the rate of the previous output, the oscillator IC6 is also a binary counter, output pin 3 goes high after 2^{21} oscillations. The crystal used with the prototype unit was cut for oscillation at 100 kHz, thus the time intervals will be $2^n/100,000$ secs where n is selected by the switches connected to IC7. The resulting time intervals are 11.1848, 22.3696 min. etc., however as the data will be processed by computer these intervals should cause no hardships.

On power-up input pin 3 on IC11 goes high, this enables one clock pulse through IC25 which is used to reset IC11 and the counter IC8, when reset the counter then enables clock pulses to the processor and A/D converter, the processor then executes the next instruction in memory after that which set the data-bus into a high impedance state.

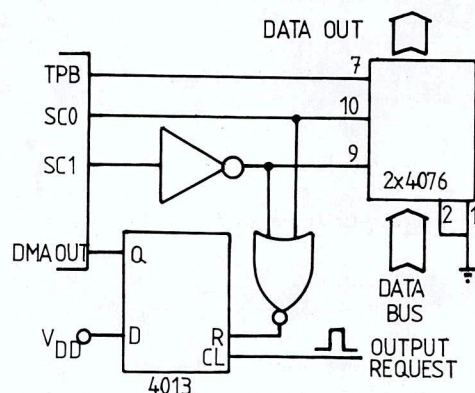
SDL-TN 4: Direct Memory Access (DMA) Facility

Manually unloading the data from the logger, whilst reliable, can become tedious when all 768 bytes have to be recorded, the time required for this task can be reduced to less than one second if a second microcomputer is available. Setting EF2 lo and EF3.4 hi (pins 23, 22 and 21 on IC1 respectively) will cause the processor to start execution of a short program loop (situated 01F2-01FF) when Reset is pressed. The program first loads the start address of the user memory (user program and data) into Register 0 of the processor then repeatedly executes an IDLE instruction. During IDLE the processor waits for DMA OUT (pin 37) to go low, then transfers one byte from memory onto the data bus and increments register 0. Using the circuit shown below DMA OUT can be triggered by a pulse from a second microcomputer and the byte held until the second micro is ready to read the byte. One millisecond delay should be allowed between each byte transfer to allow the processor to execute the program loop thus all 1024 bytes of user memory can be transferred in just over one second. For further information the reader is advised to consult the RCA COS/MOS Integrated Circuits Manual CMS-272. RCA 1979. chpt. XI.

```

01F2 DMA: LDI 01 ; initialise R(3)
          FHI R3
          LDI F9
          FLO R3
          SEF R3 ; prog. counter R(3)
          GHI RB ; put RAM address in
          FHI R0 ; R(0)
          GLO RB
          FLO R0
LOOP:    IDL ; wait for DMA
          BR LOOP

```



SDL-TN 5 Monitor Program V1.1 (100 kHz clock)

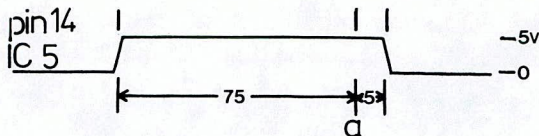
The program completely fills the 512 byte CMOS EPROM used in this data-logger.
The EPROMs were programmed by:

Farnell Electronic Components Ltd.,
Canal Road,
LEEDS
LS12 2TH
(0532 636311)

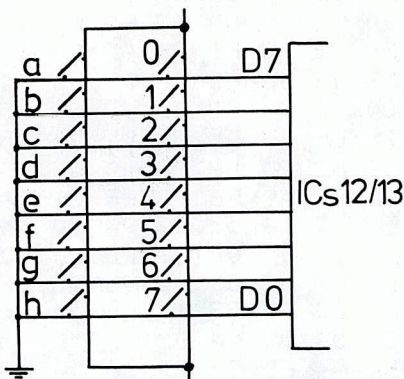
	0	1	2	3	4	5	6	7	8	9	A	B	C	D	E	F
000	71	00	63	FF	66	0F	F8	00	BD	F8	D0	AD	F8	00	BC	F8
010	A5	AC	F8	04	BE	F8	F0	AE	F8	04	BE	F8	00	AB	35	23
020	C0	00	F8	36	28	C0	00	37	3F	2D	C0	01	26	63	FA	78
030	7A	13	C4	C4	C4	30	2F	37	3C	C0	01	F2	E0	63	FF	63
040	2E	63	8A	EE	F8	00	AF	69	FA	FF	32	47	FE	33	52	1F
050	30	4C	8F	F9	80	5E	63	2E	DD	F8	04	BB	F8	00	AB	8F
060	F6	AF	3B	67	F8	80	AB	8F	F6	AF	3B	70	9B	FC	01	BB
070	8F	F6	3B	78	9B	FC	02	BB	E9	FA	FF	32	82	F8	00	AF
080	30	3A	6A	FA	FF	32	78	F8	FF	AF	F8	81	A9	29	89	32
090	3C	F8	00	A8	EE	4B	DC	DD	8F	32	9D	30	8D	69	FA	FF
0A0	32	9D	30	8D	D0	FF	64	3B	AC	18	30	A5	FC	64	B3	88
0B0	F9	20	5E	E3	2E	F8	00	A8	98	FF	0A	3B	C0	18	30	B9
0C0	FC	0A	F9	80	5E	63	2E	88	F9	40	5E	63	2E	30	A4	D0
0D0	EE	F8	02	A7	F8	20	A8	F8	FF	FF	01	3A	D9	28	88	3A
0E0	D7	27	87	32	EC	F8	1A	5E	63	2E	30	D4	F8	1F	5E	63
0F0	2E	30	CF	36	F8	C0	02	00	37	FD	C0	02	00	63	CA	EE
100	F8	00	AF	69	FA	FF	32	0E	FE	33	1C	1F	30	08	F8	08
110	AF	6A	FA	FF	32	00	FE	33	1C	1F	30	16	F8	00	A8	8F
120	5B	DC	DD	1B	30	00	34	2A	63	8B	F8	05	B6	F8	00	A6
130	F8	01	B4	F8	BE	A4	F8	04	BB	F8	00	AB	E0	66	0F	4B
140	32	52	FE	F6	76	33	C7	76	33	5C	76	33	84	EE	69	1B
150	30	DB	7B	7A	13	4B	FF	08	33	30	30	3C	5E	66	20	4B
160	3A	64	F8	01	A9	0E	32	6F	F6	3A	30	66	89	30	71	66
170	48	F8	0A	A8	D4	28	88	C4	3A	74	29	89	3A	71	66	0F
180	EE	6F	30	DB	32	9E	F8	65	AA	2A	C4	C4	8A	3A	89	4B
190	32	3C	FF	01	32	3C	A9	D4	29	89	3A	96	30	3C	F8	0E
1A0	C4	9A	2A	8A	3A	A2	4B	32	3C	FF	01	32	3C	A9	F8	12
1B0	AA	2A	8A	3A	B1	29	C4	89	89	3A	AD	30	3C	D0	F8	CD
1C0	AA	2A	8A	3A	C1	30	BD	4B	EE	5E	FF	08	33	D1	66	2E
1D0	D4	64	2E	C4	C4	C4	6D	E0	66	0F	0E	56	E0	63	FF	34
1E0	E7	F8	00	A8	EE	06	DC	16	96	FF	08	3A	3C	7B	7A	13
1F0	30	ED	F8	01	B3	F8	F9	A3	D3	9B	B0	8B	A0	00	30	FD

Parallel input

The parallel input is implemented by connecting up to eight switches parallel to or instead of keys 0-7 on the keyboard. The switches are tested 75 μ s after pin 14 on IC5 goes high.



When the switches are not being read both sides of the switch will be at 0V. The keyboard need not be disconnected, however care must then be taken that the data are not corrupted by accidental closure of the keyboard switches.



Note: the switch settings are recorded as a binary number, hence if the switch connected parallel with key 0 is closed then the number in memory will be 128, key 1 gives 64, key 2 gives 32, etc. If more than one switch is closed then the number in memory will be the sum of the values of the switches closed.

Provided that the display is not enabled (EF1 switch open) then 26 instructions will be executed by the processor for every parallel input instruction entered by the user, the 100 kHz version of the unit will therefore take 4.2mS to execute one parallel input command.

Counters

Two enables are provided, one per counter:

Counter 1 - pin 9 IC16 Counter 2 - pin 5 IC16

Both enables go high at the same instant that the counter is enabled and go low again when the counter is disabled.

Note: the supply for these enables is taken directly from the batteries and will therefore not be a constant voltage. On the circuit diagram (SDL-TN 1) these are shown OR-tied to provide a single enable output which is used to power a LM324 quad Op-amp.

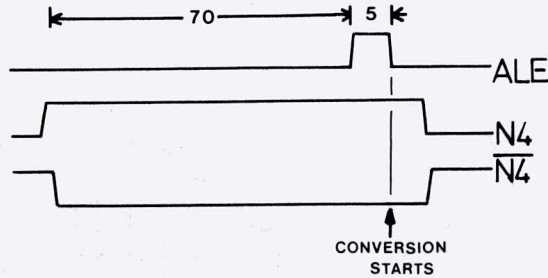
If the op-amps are configured as voltage followers then using the A/D reference (see SDL-TN 2) a constant 6.1V enable can be provided. If required the enable can be level shifted to +5V using one of the spare buffers in IC33, or inverted using IC37 (note:

the supply for IC37 Vcc = +5V).

Analogue inputs

Channels 8-15.

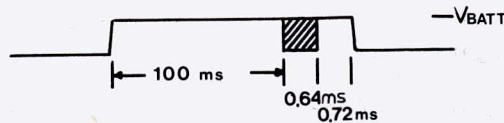
No enable signal is provided for these channels, if a pulse is required to indicate that a conversion is about to start then use the address-latch-enable signal from pin 4 on IC24.



Note: to provide individual enables for channels 8-15 would require extra circuitry or a small change in the program (see SDL-TN 15).

Channels 0-7.

Two sets of enables are provided. There are eight individual enables from the buffers IC22 and IC 23 and the second set are two enables one for channels 0-3 and the other for channels 4-7, the second set were included for use with quad op-amps. Both sets of enables follow the timing shown below:



If inverted enables are required, then ICs 22/23 can be replaced with the pin compatible inverting buffers 4049, note: the counter enables will then no longer be usable.

Channels 0-15

The routine to scan these channels and to store the data takes 5.6mS, this restricts the maximum sampling rate for the channels as follows:

Ch. 0-7 ($5.6 + 101.4$) = 107ms/sample = 9.3 samples/second
 Ch. 8-15 (5.6×10^{-3}) s/sample = 178 samples/second

For both cases the timing is calculated assuming that the display is off (EF1 open). With the display ON the timing between samples will be variable.

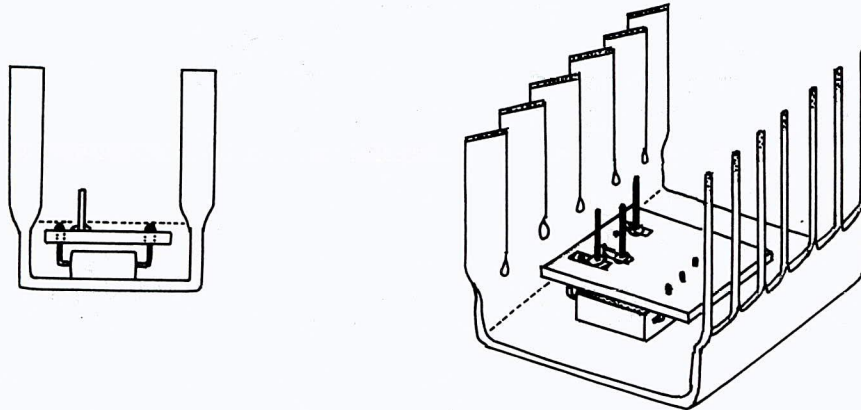
SDL-TN 7 Interfacing: Temperature sensors/solar radiation

The temperature sensor used for most of the experiments on the 1982 Greenland expedition was based on the National Semiconductor IC LM3911. This IC gives a linear output voltage which changes by 10mV for every degree K that the temperature changes.

The connections required to use the IC with the data-logger are given on the

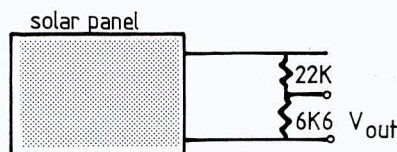
circuit diagram (SDL-TN 1), pins 5-8 are not used and are not connected inside the IC hence they can be used to attach the IC to a heat sink etc. The ICs were powered by the data-logger using the enable outputs associated with channels 0-7 (see SDL-TN 6) which were only switched on by the data-logger for 0.1 sec before a conversion was due to begin. By fixing the enable voltage at 6.1V the current drawn by the temperature sensor is kept to less than 300 μ A and thus self heating effects are kept to a minimum. The outputs from the temperature sensors were then compared with a reference voltage (variable) and the difference was amplified 10 fold. This gave a nominal sensitivity of 0.2 K/digit for the inputs (8-bit A/D converter, V_{max} 4.88 volts).

To protect the ICs from damage by rocks or boots they were mounted inside aluminium heatsinks and then encased in a plastic resin for protection against moisture. The sketch below shows a section view through the completed temperature sensor.



Encasing the sensor IC in resin increases the time constant of the complete sensor, however close contact with the heatsink will keep this effect to a minimum. Measurements on a completed sensor gave a time constant of 6 minutes when the sensor was placed on a horizontal surface with a light wind.

The solar panels (see SDL-TN 14) can also be used to give an indication of the amount of solar radiation present. When used in a light meter the voltage generated by the silicon cells across a very small resistance (typically 10 ohms) is measured, this voltage is then proportional to the incoming radiation. To provide an output suitable for use with the A/D converter without requiring amplification the panel was connected as follows:



When placed horizontally on the ground this circuit gave an output voltage of approximately 3V under full sun conditions (12V panel, 72N lat.).

The spectral response of the solar panels is very similar to that of the eye, yet for many geographical/geomorph. purposes a more useful response might be one which is biased towards the IR part of the spectrum. During experiments 8 and 9 it was found that when a high layer of cirrus type cloud reduced the intensity of the sun, the panels still gave a high output although the readings from ground temperature sensors dropped rapidly indicating a rapid drop in the amount of heat received by the surface. The connection

LM3911: extract from the data sheets in 'National Semiconductor Linear Databook' 1980 ed.

Operating range	-25°C to +85°C
Linearity $\Delta T = 100^\circ\text{C}$	0.5% typ.
Long term stability	0.3% typ.
Repeatability	0.3% typ.
Supply current at 6V	350 μA typ.
Turn "ON" response time	<300 μs

SDL-TN 8 Rotation Sensors

The high input impedance of the amplifiers connected to channels 0-7 on the data-logger means that potentiometers up to 50k ohm resistance can be used to make simple but effective rotation sensors. The two ends of the potentiometer are connected to ground and V enable respectively and the rotation of the wiper is sensed by connecting this to the analogue input. Standard potentiometers have a spindle which will rotate through 300° approximately, giving a sensitivity of about 1.2°/digit with this system or 0.12°/digit if the inputs with x10 amplifiers are used.

Four rotation sensors were used successfully on the expedition to monitor the movement of perched blocks. The body of the potentiometer was attached to the boulder with adhesive and a small pendulum was bolted on to the spindle of the potentiometer. Provided that the potentiometers were shaded from the sun there was no drift in the output reading if the boulder didn't move. If the sun was allowed to fall on the potentiometer then uneven heating of the resistive track would cause a diurnal variation in the readings.

SDL-TN 9 Wind Direction Sensor

This used the parallel data input facility on the data-logger. The wind vane was mounted on a stout mast. A small (15mm dia.) magnet was attached to the underside of the vane, it was positioned so that it was moved around the mast by the vane. There was approximately 10mm clearance between the magnet and the mast. Eight miniature dry-reed switches were mounted in this clearance around the mast with their axes vertical, they were spaced at 45° intervals. The position of the magnet was adjusted so that at any time at least one of the switches was closed by the magnetic field. One end of each switch was connected to a single common wire and this was taken to pin on IC. The other end of each switch was taken to one of the parallel inputs. A 'parallel input' command would then sense which of the switches was closed, from this the direction of the wind vane could be determined.

SDL-TN 11 Soldering Iron for use in the Field

It was expected that there would be some 'in the field' repairs to the circuitry so a simple soldering iron was turned from some 20mm dia. mild steel bar. One end was turned to accept a fine tipped 'Antex' soldering iron bit, and to the other a wooden handle was attached. Between the handle and tip was approximately 100mm of bar which acted as the heat reservoir. The iron was heated over the primus stoves and remained sufficiently warm to melt the solder for between five and ten seconds after being removed from the heat, this was adequate time in which to form one connection.

SDL-TN 12 Data Storage and Processing

The 1024 bytes of RAM available to the user are used by the various programs as follows: bytes 0 to 239 - used to store the user program (see main section of the report) bytes 240 to 255 - workspace area, this will contain random values: bytes 256 to 1023 - recorded data values. Data values are recorded sequentially by the processor and are therefore not segregated into individual channels.

In addition to the values in the user program itself, a typical data processing program will also require the time at which the unit was switched into 'Execute' mode and the power-down time interval set on the unit's selector switch. Given this information it is then straightforward to de-multiplex the data, if individual channel calibrations are included the main computer can then proceed directly to data conversion.

User Program

```

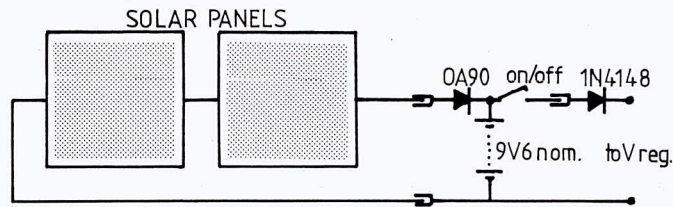
Scan Ch. 1
Scan Ch. 2
Scan Ch. 3
Power-down
Repeat
    
```

locn.	data	iteration
k+6	Ch. 1	N+2
k+5	Ch. 3	
k+4	Ch. 2	N+1
k+3	Ch. 1	
k+2	Ch. 3	
k+1	Ch. 2	N
k	Ch. 1	

SDL-TN 13 Source Code Listing

Requests for a copy of the source code listing of the monitor EPROM should be addressed to the expedition. There will be a small charge for the listing to cover the cost of photocopying.

SDL-TN 14 Power Supply/Solar Panels/Voltage Regulator



Power for the data loggers was provided by two 12V 50mA solar panels (98mm x 128mm, supplied by Maplin Electronic Supplies, P.O. Box 3, Rayleigh, Essex, Stock No. RK24B). With their mirror reflectors attached these panels regularly produced in excess of 30mA current into the partly charged batteries for periods of eight hours or longer. Even on totally overcast days there was often sufficient UV present in the daylight to provide enough power to trickle charge the batteries.

The OA91 diode was included in the circuit to prevent accidental shorting of the batteries through the two external connections, as any data present in the data-logger memory would be lost if this occurred. A germanium diode was used to minimise the voltage loss.

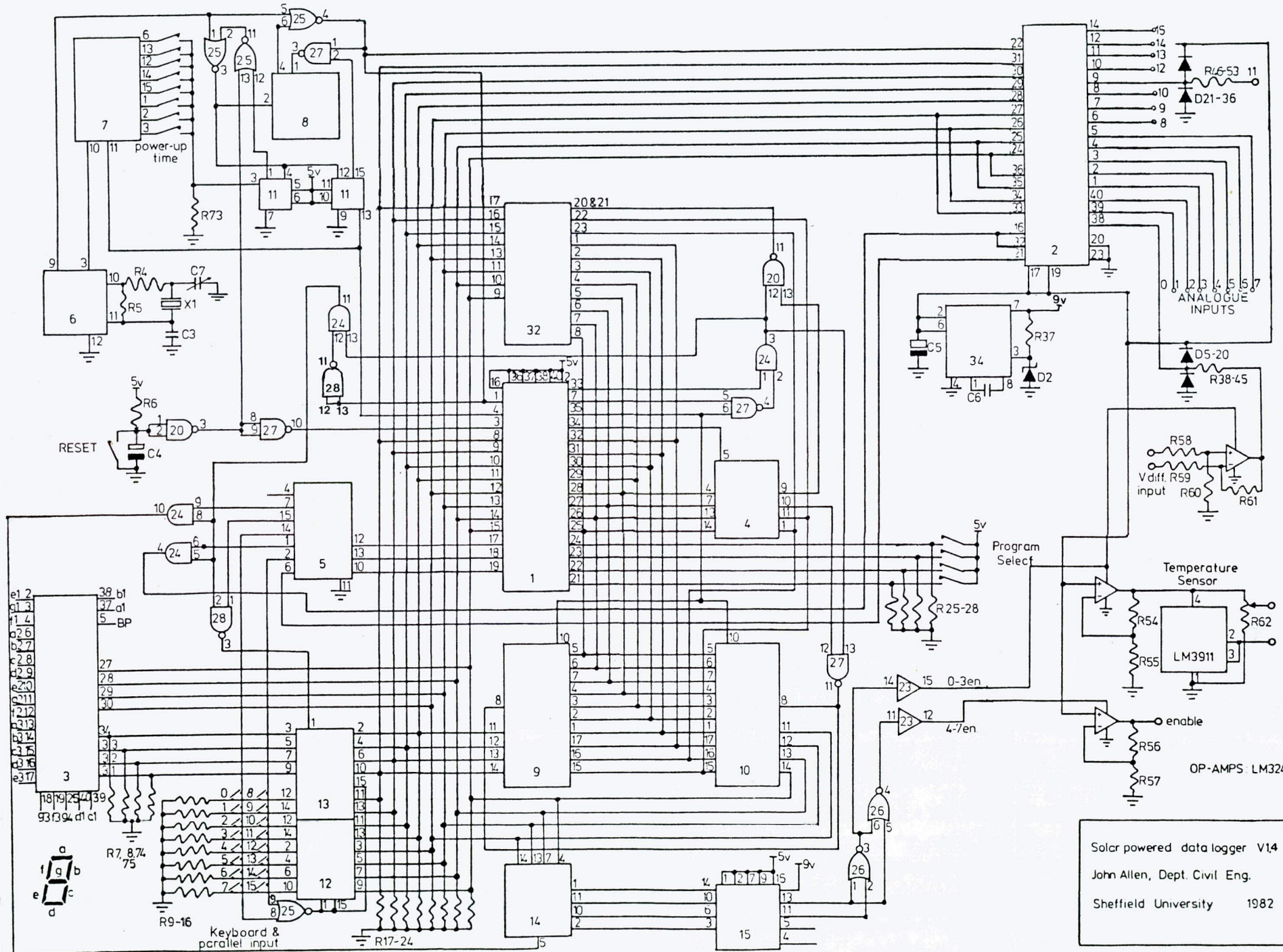
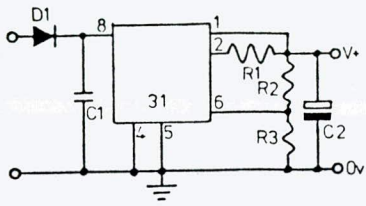
The battery was eight AA sized Nickel Cadmium re-chargeable cells, each of 1.2V nominal voltage. When fully charged the cells reached 1.4V, giving a battery voltage of 9.6V. The charge capacity (C) of the cells was 500 mAh, the maximum current which could be delivered by the panels was 0.1C, it was therefore permissible to leave the panels permanently connected as they were unlikely to damage the cells. Had smaller charge capacity cells been used then there was the possibility that the solar panels would over-charge the cells and destroy them.

The 1N4148 was mounted on the circuit board and was included to prevent damage if the battery pack was connected the wrong way round.

A CMOS voltage regulator was used to provide the 5V required by most of the circuitry, this device had a quiescent current of just 4 μ A. Due to a small mishap this IC was destroyed on one unit; the Vcc supply was then derived by tapping directly off the battery pack, with no apparent ill effect.

SDL-TN 15 Non power-down simplified version

During field trials of the data-logger it was found that the power obtained from the solar panels exceeded the expected value by a factor of five. For applications which only require the analogue inputs the unit can therefore be greatly simplified by removing all circuitry used to power-down the analogue inputs and by removing all the counter circuitry. The simplified version (V1.4) is shown below. Refer to SDL-TN 1 for the circuit diagram of the complete unit.



Solar powered data logger V1.4
 John Allen, Dept. Civil Eng.
 Sheffield University 1982

2.2 MEASUREMENT OF THE FRACTURE TOUGHNESS OF GLACIER ICE

1. Introduction

Some 10% of the world's land area is ice covered (1)*, and large sea areas are either permanently or temporarily ice covered. On land, cracks or crevasses in glaciers and ice sheets are a serious hazard to movement. At sea, the forces required to break through ice cover influence the design of ships. Increasing offshore oil exploration activity in Arctic areas requires knowledge of the forces exerted on large structures by floating ice. In a more exotic field, Poirier (2) has pointed out that knowledge of the creep and fracture properties of ice is essential to an understanding of the moons of the outer solar system. One method of tackling these problems is to use the methods of fracture mechanics to study the brittle fracture of ice.

The aim of this project was to measure the plane strain fracture toughness of the ice of the Bersaerkerbrae Glacier. The concepts of Linear Elastic Fracture Mechanics are presented, and previous work is briefly reviewed. The novel specimen design and the apparatus used on the glacier are described in detail. Although laboratory trials had been successful, the field tests achieved only limited success. The measured fracture toughness was 58 kPa√m, half of the value obtained by other workers in laboratory tests. The reason for this low value was that the specimen contained too few grains to approximate to an isotropic solid.

2. Linear Elastic Fracture Mechanics

This section outlines the basic theory of linear elastic fracture mechanics (LEFM). Good general introductions can be found in Knott (3) and Lawn and Wilshaw (4).

2.1 The stress intensity factor

The results of accurate stress analyses of sharp crack show that the stress, σ_{ij}^{**} on an element close to the tip of the crack, see Fig. 1(a), can be expressed by an equation of the form

$$\sigma_{ij} = \frac{K}{\sqrt{2\pi r}} f_{ij}(\theta) + \text{terms in higher powers of } (r^{1/2}) \quad 1$$

The remaining terms in the series are negligible close to the crack tip. Equation (1) assumes that the material behaves in a linear elastic fashion and that the distance is small compared to the crack size and the specimen dimensions.

The terms $f_{ij}(\theta)$ and $1/\sqrt{2\pi r}$ take account of the position and orientation of the element in the crack tip stress field. The constant K determines the intensity of this stress field and is known as the 'stress intensity factor'. It is a function of the applied loads and geometry of the crack and its surroundings. The form of K varies with the mode of opening of the crack. Figure 1(b) shows the three possible deformation modes, conventionally denoted by subscripts. Generally, mode I loading is the most important mode in brittle fracture studies; it is the only mode considered in this report. The simplest form of K_I is for a crack in an infinite sheet in tension; see Fig. 1(c). In this case:

$$K_I = \sigma \sqrt{\pi A} \quad 2$$

Values of K for many other geometries can be found in the literature, e.g. Rooke and Cartwright (5).

* Numbers in brackets refer to references at the end of this section.

** Symbols are listed in the Nomenclature at the end of this section

Equation (1) implies that the stress will be infinite at the crack tip, where $r = 0$. In real materials, plastic yielding occurs. Provided the extent of the yielded zone is small compared with the elastic stress field, equation (1) remains a valid approximation.

2.2 Fracture Toughness

Although equation (1) describes the stresses at the crack tip, it does not itself provide a fracture criterion. It has been found experimentally that, for brittle materials, the stress intensity factor when fracture occurs is a material property. This critical stress intensity factor is called the fracture toughness, denoted by the symbol K_{Ic} . The subscript 'c' refers to the critical condition. K_{Ic} is more correctly called the 'plane strain fracture toughness'. The specimen dimensions must be great enough to ensure that plane strain conditions exist at the crack tip.

There are standardized methods (6) for the fracture toughness testing of metals. The proportions of the two recommended standard testpieces are shown in Fig. 2. The actual dimensions must be great enough to assume that the plastic zone at the crack tip has a radius less than 1/50 of the crack length, the thickness and the ligament. Hence for a test to be 'valid', the value of K_{Ic} obtained must satisfy the requirements:

$$A \geq 2.5(K_{Ic}/\sigma_y)^2$$

$$B \geq 2.5(K_{Ic}/\sigma_y)^2$$

$$W - A \geq 2.5(K_{Ic}/\sigma_y)^2$$

3

where σ_y is the yield stress. These conditions were originally derived by Brown and Srawley^y (7) from tests on metals, and may not necessarily apply to other materials.

3. Previous Work

Reference (8) presents the results of a series of fracture toughness tests carried out on ice from the surface of the Roslin Glacier (Staunings Alps, Greenland) in 1978. It also discusses the available results of laboratory tests; brief details of these are presented here for completeness.

The tests on the Roslin Glacier used SEN bend specimens similar to the standard proportions shown in Fig. 2(a). The mean fracture toughness was $125 \text{ kPa}\sqrt{\text{m}}$, at a loading rate producing a stress intensity rate of approximately $5 \text{ kPa}\sqrt{\text{m}} \text{ s}^{-1}$.

This result was in agreement with most laboratory tests. Goodman and Tabor (9) obtained a mean value of $116 \text{ kPa}\sqrt{\text{m}}$ in SEN bend tests at comparable loading rates. They also used conical and pyramidal indenters to initiate surface flaws; the results from these tests ranged from 55 to $300 \text{ kPa}\sqrt{\text{m}}$. In a later series of tests (10) Goodman obtained an average value of $115 \text{ kPa}\sqrt{\text{m}}$ at higher loading rates producing a stress intensity rate some two orders of magnitude greater. Liu and Miller (11) used CTS specimens, Fig. 2(b), and obtained fracture toughness values of 200 - $300 \text{ kPa}\sqrt{\text{m}}$ at low loading rates ($\dot{K}_I \approx 2 \text{ kPa}\sqrt{\text{m}} \text{ s}^{-1}$). At high loading rates, K_{Ic} fell to around $100 \text{ kPa}\sqrt{\text{m}}$, comparable to the other results. Gold (12) estimated fracture toughness from the arrest of propagating cracks initiated by thermal shock. These results are difficult to interpret; a discussion of this problem is in reference (8).

All these laboratory tests, and the tests of ref (8), were at temperatures above -15°C ; there appears to be little variation with temperature above this point. The method of specimen manufacture was directional freezing, producing columnar crystals of a size 5 - 10 mm. The ice was free of air bubbles. All the results showed considerable scatter.

In conclusion, laboratory tests give a fracture toughness of around $115 \text{ kPa}\sqrt{\text{m}}$. Tests of ice from the surface of the Roslin Glacier at comparable loading rates were in agreement with these values.

4. Specimen Design

This section describes the novel specimen used for the tests, together with the results of some preliminary laboratory trials to verify the design.

4.1 Choice of Specimen

If tests are to be made on ice from any depth in a glacier, a corer will have to be used to obtain the specimen. The standard testpiece shown in Fig. 2 could be cut from this core, but this involves extra equipment and work. Also the validity requirements of equations (3) dictate the minimum corer diameter. Assuming $K_{IC} = 125 \text{ kPa}\sqrt{\text{m}}$, and $\sigma = 21 \text{ bar}$ (Hawkes and Mellor, (13), for strain rates of 10^{-4} s^{-1} to 10^{-2} s^{-1}), a core of at least 10 cm diameter would be required to produce a SEN bend specimen that would satisfy equations (3).

The specimen chosen should be easy to make, and should use a short length of core. Ideally it should be self-aligning in the test apparatus, to avoid the use of complex grips. The complex gripping methods of ref. (13) are not practical for field tests.

Using published stress intensity factors (ref. (5) and elsewhere), various specimens using discs and round bars were considered. The final choice was a pressurized ring with a radial crack; see Fig. 3. Only 3 - 4 cm of core are needed for this specimen. The crack can either be external Fig. 3(a) or internal, Fig. 3(b). In both cases the pressure p is applied using a pressurized rubber bladder. This obviates the need for seals on the end of the specimen, and contains the fluid when the specimen fails.

4.2 Externally Cracked Ring

See figure 3(a). Stress intensity factors for various wall thicknesses of the ring are presented in (5). For the particular case of $R_i/R_o = 0.5$, the stress intensity factor is given by

$$K_I = p\sqrt{\pi a} \left\{ 0.74 + 0.12 \left[\frac{a}{R_o - R_i} \right] + 1.43 \left[\frac{a}{R_o - R_i} \right]^2 - 0.67 \left[\frac{a}{R_o - R_i} \right]^3 \right\} \quad 4$$

The error is estimated as less than 3%.

This equation was derived from the graph in reference (5), for use with a calculation. The similarity to equation (2) is obvious; the uniaxial stress σ has been replaced by the pressure p , and the polynomial term in brackets incorporates the effect of geometry and the non-uniform stress in the ring wall. Equation (4) can be re-written as

$$K_I = K_o Y \quad 5$$

where $K_o = p\sqrt{\pi a}$

A plot of Y against the dimensionless crack length, α , $\alpha = a/(R_o - R_i)$, is shown in Fig. 4.

4.3 Internally Cracked Ring

The common engineering case, where the pressure acts on the inside of the ring and the crack faces, is also found in reference (5). If the fluid is contained in a flexible bladder, the pressure acts only on the inside of the ring, and NOT on the crack faces. In this case, using results presented by Grandt (14) and the Lamé equations (15), the stress intensity factor is given by

$$K_I = K_o Y \quad 6$$

where $Y = 1.63 + 0.25 \left(\frac{a}{R_o - R_i} \right) - 1.09 \left(\frac{a}{R_o - R_i} \right)^2 + 1.59 \left(\frac{a}{R_o - R_i} \right)^3$

K_o is as given in equations (5). It should be noted that this equation is only valid for the particular wall thickness ratio $R_i/R_o = 0.5$. In the range $0.25 \leq a/(R_o - R_i) \leq 0.65$ the errors are estimated as less than 4%.

Figure 4 also shows the variation of Y with dimensionless crack length $a/(R_o - R_i)$ for the internal crack. The advantage of the internal crack is shown here; for the same crack length the geometry factor Y is greater for the internal crack. This means that the fracture pressure will be lower, which in turn reduces the weight of the apparatus.

4.4 Laboratory Trials

A limited number of laboratory trials were carried out to prove the feasibility of these specimen designs. The apparatus used was a simpler version of the field apparatus described fully in section 5.

Discs of ice were produced by directional freezing of water. A ring of pvc pipe, sealed to a metal plate by silicone grease formed the mould. A fine layer of 'seed' crystals was sprayed into the mould, and the remaining depth filled with chilled water. Expanded polystyrene foam insulation around the mould ensured that the heat flow was mainly through the metal base, causing directional freezing. A small hand corer was used to remove the centre, forming the ring. The rings had an outside diameter of 79 mm, inside diameter 40 mm and an average thickness of 29 mm.

A hacksaw was used to cut the notch, and the tip was sharpened with a fine wire. The ring was then placed over the bladder, and the moveable cup clamped in place to restrain the free section. The pressure was increased until fracture occurred; the maximum pressure was noted. Using equations (4) - (6), the fracture toughness was calculated.

The results are plotted against crack length in Fig. 5. The mean fracture toughness of the 6 internally cracked specimens was $182 \text{ kPa}\sqrt{\text{m}}$ with standard deviation $36.8 \text{ kPa}\sqrt{\text{m}}$. The thirteen externally cracked specimens had a mean fracture toughness of $89 \text{ kPa}\sqrt{\text{m}}$ with standard deviation $23.2 \text{ kPa}\sqrt{\text{m}}$. Applying the F-ratio test (Chatfield (16)) the difference between the standard deviations is not statistically significant. Hence the two samples can be combined to give an estimated standard deviation of $27.9 \text{ kPa}\sqrt{\text{m}}$. Using the t-test on 17 degrees of freedom the difference between the two mean values is significant at the 1% level.

None of the tests would have been 'valid' according to equations (5). However, Fig. 5 shows that the crack length itself does not have an effect on the fracture toughness. Thus it would appear that the cracks are long enough to produce 'valid' results. There are no published results of tests to establish validity criteria for ice in a similar manner to that used for metals in reference (7).

The difference in fracture toughness values between internal and external cracks must be resolved before test results can be fully accepted. One possible reason is a systematic error in the testing. Before testing the majority of the internal cracked specimens, the rig was cooled to reduce melting. The bladder would have been stiffer than during the external crack tests. This stiffness would have increased the apparent fracture pressure. Also, the internally cracked specimens had been stored for longer before testing.

Despite this anomaly, it was decided that these specimens gave the best possible method of testing a large number of specimens. Testing a large number of specimens would allow more accurate statistical analysis of any difference between internal and external cracks.

The ratio $R_i/R_o = 0.5$ was chosen to suit the available stress intensity calibrations in reference (14). A smaller bore diameter would obviously allow longer cracks. The stress analysis for this requires sophisticated mathematical and computational methods. In the time available, it was not possible to carry out this analysis.

The external crack calibration in reference (5) allows $R_i/R_o = 0.35$. To allow the use of the same apparatus for both types, the R_i/R_o ratio was fixed at 0.5. The diameters $R_i = 20 \text{ mm}$, $R_o = 40 \text{ mm}$ were chosen to suit the available equipment, in particular the internal corer and rubber bladder. In addition, 80 mm is a convenient size for hand coring.

5. Apparatus

The final design of apparatus used for the field tests is shown in Fig. 6. The diagram is schematic only; the apparatus is illustrated in Fig. 7. Numbers in brackets in this section refer to item numbers in Fig. 6. Most of the apparatus (with the exception of the Data Logger) was assembled from available materials, and so detailed drawings have not been provided. The construction is straightforward and within the capability of an average workshop.

5.1 Mechanical Components

The specimen (5), notched and measured, is placed over the rubber bladder (6). This is the bladder from a hydraulic accumulator, and has a threaded connection fitted. The bladder is held into the fixed cup (4) by a nut on this connection. To place the specimen over the bladder, the moveable cup (7) is slid to the right along the rods (8).

After the specimen has been placed on the bladder, the cup is slid to the left and clamped to the rods. The two cups restrain the expansion of the sections of the bladder outside the specimen. Both cups and the end pieces were machined from aluminium to reduce weight.

The pump (2) was modified from a hydraulic car jack. Although less elegant than a purpose made unit, this approach was inexpensive (cost £4) and convenient. The large diameter cylinder and ram which lift the car were removed, and the base casting cut in half. A length of 3/16" copper pipe was hard silver soldered into the high pressure passage in the casting. A fitting on the other end of the pipe connected the pipe to a connector carrying the pressure transducer (9), Bourdon pressure gauge (3) and the bladder. Two short lengths of copper pipe were soft soldered into the fluid feed and return passages in the casting. Lengths of pvc hose connected these to the fluid reservoir (1). No lever was taken for the pump, as an ice axe gave more than sufficient leverage.

5.2 Pressure Measurements

Two methods were used for pressure measurements; a transducer interfacing to the data logger and a conventional Bourdon tube pressure gauge. Both were required to measure a range 1.4 MPa (200 psi).

The pressure transducer was a strain gauge type, manufactured by Showa Measuring Instruments Co., model HVK-50. This model had a range of 4.9 MPa (50 kg f cm⁻²) and hence only about 30% of the range would be used. However, the unit had a non linearity of 0.3% full scale, and so would give sufficient accuracy even over only part of the range. The unit was loaned to the expedition by Environmental Equipments (Northern) Ltd. of Nantwich. (This company also loaned us two displacement transducers for taking ice strain measurements using the data logger.)

A separate amplifier unit was built to interface the transducer to the data logger. The input impedance of these transducers is 350Ω, and hence an input voltage of 5V would require a current of 15mA. Thus a separate power supply would be required for the transducer. As the output would only be around 2mV, an amplification of X1000 was required to interface with the data logger. The circuit used is shown in Fig. 8; this is item (11) in Fig. 6. A 9V dry battery provided a regulated 5V input to the transducer, via a semiconductor voltage regulator. The bridge output was input to a differential amplifier designed around the LM324 quad op-amp circuit. The power supply for this amplifier was derived from the batteries of the data logger. A 'non-enabled' data logger input was used. This would allow scans up to the maximum rate of 200/second. It was envisaged that the maximum rate used would be 5/second. The data logger display would be switched 'off' during testing - see section 1 for details.

A conventional pressure gauge was also fitted to the apparatus. This was a 0-200psi 80 mm (3 inch) gauge, donated by the manufacturers, the Budenberg Gauge Company of Broadheath. This gauge was intended to (a) give a visual indication of the progress of the test, and (b) act as a back-up if the electronics should fail.

5.3 Specimen Coring Equipment

A corer was designed and built to cut 80 mm diameter cores from depths of up to

5 metres. The body of the corer was a steel tube, with holes to reduce the weight. Different types of teeth could be fitted to the cutting end, the intention being to adjust the arrangement while in the field to obtain the best results. Five extension rods, each 1 m long, were made and donated to the expedition by Gubb and Hauff Precision Engineering of London. These rods were made of aluminium. A small mild steel corer and plastic jigs for removing the centre of the ring were also used.

5.4 Experience in Use

This section briefly highlights the problems encountered in using the equipment while on the Bersaerkerbræ Glacier.

The performance of the data logging equipment is described in section 2.1. Although it performed satisfactorily before leaving Sheffield, the transducer amplifier did not give a stable output. The problem appeared to involve earthing, as merely touching different parts of the unit caused a shift of 10 or more data logger units. Considerable time and effort was expended in experimenting with earthing and screening arrangements and with modification to the feedback resistors. Some improvement was obtained, but the results were still too poor to be acceptable. The lack of an oscilloscope was a grave disadvantage here.

On our return to Sheffield, testing with an oscilloscope showed a square wave output of frequency 100 Hz and 1V peak to peak. This was unchanged if the frequency of data logger scanning was altered. When the LM324 integrated circuit was powered from a bench power supply instead of the data logger, a sawtooth wave of 2V peak to peak and 1.5 kHz frequency was obtained. It would seem that the circuit was only just stable, and small variations in earthing etc could cause it to break into oscillation.

The malfunction of this unit deprived the project of any pressure-time records. (It also eliminated any trial of the data logger for surface strain measurements, as the displacement transducers could not be used.) Fortunately, the mechanical pressure gauge functioned well. The remainder of the bursting apparatus worked apart from a leak in a joint in the feed pipe to the pump. A thorough cleaning and degreasing, followed by the application of large amounts of quick setting epoxy resin, solved this problem. The adhesive was allowed to cure for 24 hours, rather than the suggested hour, to compensate for the lower temperatures.

The corer required modifications to the teeth before a reasonable cutting speed was obtained. The teeth as designed clogged with chippings, preventing further progress. This was aggravated by surface melt water entering the hole, causing the chips to form slush. Several progressively more drastic alterations to the mild steel body using a hacksaw eventually allowed cutting at the same rate as specimen testing. The greatest depth attained was 2 metres, largely driven by one man, taking about 4 hours. To make a specimen, a length of undamaged core of about 3 cm or more was required. The core would snap off and remain inside the corer when about 7 - 10 cm had been cut. The ends of the section were usually slanted, and had to be trimmed square before the centre hole was cut.

The use of threaded (ISO metric M24) connections for the extension rods was not completely successful. This was due to difficulty in unscrewing the sections after coring. One section did in fact become jammed into the corer body, and resisted all attempts to unscrew it. This was probably due to grit jamming the thread. The decision to use threaded connections was made on the grounds of simplicity of manufacture, and the risk of jamming was accepted. In retrospect, this was a mistake. The manufacture of the poles was not at fault in any way, and two spare sections were used to support the anemometer and wind direction meter at base camp. Another section, with the threads protected, was used as a stage pole for the melt stream hydrology project. The poles were, at some discomfort, recovered at the end of the expedition for possible re-use.

5.5 Ice Crystal Size Measurement

The use of a plane polariscope and universal stage to measure ice crystal size and orientation is an established technique; see, for example, references (17) and (18). The method depends on the optical activity of ice. When a thin (1 - 3 mm) section is

placed between two plane polarizing filters (with polarizing axes oriented at 90°), the grains appear at varying brightnesses. The brightness depends on the orientation of the "C" crystallographic axis (the optic axis of the ice crystal). Using a universal stage, it is possible to measure the exact orientation of the crystal.

In this case, a simple polariscope was improvised, and used to take black and white photographs of the crystals. No attempt was made to assess the orientation.

6 Results

6.1 Test Site and Material

The tests were carried out about 100 metres from the true left lateral moraine of the Bersaerkerbrae Glacier in the vicinity of Base Camp (see Fig. 9). The ice was heavily foliated, the foliations parallel to the glacier flow and being oriented vertically. The foliations were about 2 - 4 cm wide. In the bubbly layers many of the bubbles were elongated, parallel to the glacier flow. Typically, spherical bubbles were 0.5 mm to 1.0 mm in diameter, while the elongated bubbles were 2 mm long and 0.5 mm in diameter.

The material tested had come from the Dunottar Glacier, and had undergone substantial deformation while flowing into the main Bersaerkerbrae Glacier. Allen et al (17) suggested that foliation was caused by deformation of transverse features in areas of compressive stress. Subsequent flow of the glacier causes the transverse orientation to be changed into arcs. Sufficiently far down the glacier, the foliation will be oriented parallel to the flow. It is likely that the foliation observed at the test site had originated in the upper part of the Dunottar Glacier. The foliation throughout the width of the Bersaerkerbrae Glacier below base camp but above the ice fall was oriented parallel to the glacier. There were no signs of the arcs described in ref.(17).

6.2 Fracture Toughness Results

It proved very difficult to produce useable specimens on the glacier, as the majority of samples shattered during the cutting of the centre hole. This had not been a problem during the laboratory tests. Internal flaws also caused the rejection of otherwise usable specimens.

The outside diameter of the rings as tested was 78 mm, the inside 40 mm. This gives a ratio $R_i/R_o = 0.51$, which is sufficiently close to the value of 0.5 for which equations (4) and (6) are valid. All specimens were externally cracked, the cracks being cut with a hacksaw. It was intended to test specimens with internal cracks, but the difficulty in manufacturing specimens precluded this.

Table 1 presents the results of the tests where failure initiated at the sawn crack. The values of Y are calculated using equation (4). The mean fracture toughness is $58.1 \text{ kPa}\sqrt{\text{m}}$, with a standard error of the mean of $3.8 \text{ kPa}\sqrt{\text{m}}$. Table 1 also indicates, where known, the orientation of the crack to the long axis of the elongated bubbles in the ice; see Fig. 3(b). There are, unfortunately, too few tests at angles other than $\phi = 0^\circ$ to draw any conclusions.

Table 2 summarizes the details for specimens which did NOT fracture from the sawn crack. Again, the coefficient Y has been calculated using equation (4), but fracture toughness values have not been included. Any such value would merely be an upper bound which might have been attained if there were no other flaws present. These results will be discussed further in section 7.

The results of Table 1 are presented in Figures 10 to 12. The measured fracture toughness is plotted against the depth from which the sample was taken, the crack length and the specimen thickness. There is no trend apparent in any of these graphs.

6.3 Ice Crystal Sizes

Samples were taken at 10 points on the glacier, shown on Fig. 9. Tracings were taken from the photographic prints, and the number of grains was counted. A planimeter was used to measure the area; it was necessary to correct for the magnification of the

print. A typical tracing is shown in Fig.13(a); the results of all specimens are presented in Table 3. An average grain size, d_{av} , was calculated as:

$$d_{av} = \sqrt{\left[\frac{\text{area of specimen}}{\text{number of grains}} \right]}$$

7

A plot of d_{av} against the depth of the specimen showed no trend. Inspection of Table 3 shows a tendency for lower values of d_{av} higher up the glacier. The mean value for all glacier ice samples is $d_{av} = 9.6$ mm.

Table 3 and Fig. 13(b) also present the result of a similar analysis of one specimen of the laboratory produced ice used in the trials of the specimen. Note that Fig. 13(b) is at a larger scale than Fig. 13(a). For this sample, $d_{av} = 0.9$ mm.

7 Discussion

7.1 Results Obtained

The mean value of $58.1 \text{ kPa}\sqrt{m}$ obtained from these experiments is significantly lower than laboratory tests (9-11) and the earlier tests on the Roslin Glacier (8). A value of around $115 \text{ kPa}\sqrt{m}$ would have been expected from these results. There are two possible causes of this discrepancy: the presence of air bubbles in the ice, and the effect of grain size. These will be discussed separately in the following sections.

7.2 The Effect of Air Bubbles

The effect is shown schematically in Fig. 3(b). The stress causing fracture is the hoop stress (see ref. (15)), σ_{θ} . Figure 3(a) shows the hoop stress distribution through the ring wall for $R_i/R_o = 0.5$. This variation in hoop stress is, of course, taken into account in the stress analyses leading to equations (4) and (6) in section 4. However, in this section, the models used require a uniform uniaxial stress. This has been chosen as numerically equal to the applied pressure, p (although of opposite sign). It can be shown that for equilibrium of half of the ring, the average hoop stress must be equal to the pressure. (This is only true for $R_i/R_o = 0.5$; more generally $\sigma_{\theta av} = p R_i / (R_i - R_o)$).

Also, from Fig. 3(a), if the crack length is about half the wall thickness, the unflawed hoop stress at the location of the tip of the crack is about $1.0p$. This assumption is a substantial simplification, but it is necessary to be able to apply the results of other models. The results will still be qualitatively useful, even if the precise numerical values are doubtful. It is also necessary to assume that the bubbles are crack like, i.e. with sharp tips rather than rounded ends.

Figure 3(b) shows, schematically, a cracked specimen containing elongated air bubbles. The bubbles are drawn regularly spaced for convenience only. Only elongated bubbles will be considered, as these are more 'crack like' than spherical bubbles, and so cause greater stresses. There are three possible effects:

- a) The crack is extended by intersecting bubbles, so that the true length is longer than the measured apparent length.
- b) A bubble near the crack tip, contained in the crack tip stress field, causes an increase in the local stress intensity factor.
- c) A series of co-linear bubbles generate a high stress intensity at the tip of one bubble.

In cases a) and b) the fracture will still initiate from the sawn crack; in case c) the fracture will initiate from the row of bubbles.

7.2a A Crack Intersecting an Air Bubble

In this case, shown in Fig. 14, the crack is lengthened by the bubble, which is assumed co-linear with the crack. The effect can be assessed directly from equation (4), without assuming an average stress, by proceeding as follows:

For a small increase in dimensionless crack length, $\Delta\alpha$, where $\alpha = a / (R_o - R_i)$,

$$\frac{dK_I}{d\alpha} \approx \frac{\Delta K}{\Delta\alpha}$$

Hence, differentiating equation(4),

$$\frac{dK_I}{d\alpha} = p \sqrt{\pi a} \{ 0.12 + 2.86\alpha - 2.01\alpha^2 \} = \frac{\Delta K_I}{\Delta\alpha}$$

Divide by equation(4) to obtain the proportional change,

$$\frac{\Delta K_I}{K_I} = \frac{p\sqrt{\pi a}}{p\sqrt{\pi a} \cdot Y} \{ 0.12 + 2.86\alpha - 2.01\alpha^2 \} \Delta\alpha$$

where Y is as defined in equation (5). Thus the change in K_I , ΔK_I , corresponding to a change in crack length $\Delta\alpha$, is given by

$$\Delta K_I = \frac{1}{Y} \{ 0.12 + 2.86\alpha - 2.01\alpha^2 \} K \Delta\alpha = B(\alpha) \cdot K \cdot \Delta\alpha \quad 8$$

The function $B(\alpha)$ shows the relative increase instress intensity due to the extension by the bubble; it is plotted in Fig. 14(b). In the range $0.3 \leq \alpha \leq 0.6$, the range of the experiments, an approximate value $B(\alpha) = 0.95$ can be used. If the air bubble lengthens the crack by 2 mm, and the ring wall thickness is 20 mm, $\Delta\alpha = 0.1$ and hence, from equation (8), $\Delta K = 0.095K$. Thus the true stress intensity factor would be 10% higher than that calculated from the nominal dimensions. Clearly this is not sufficient to explain the discrepancy between the results in Table 1 and the results of earlier tests.

It should be emphasized that the precise form of equation (8) is only applicable to an externally cracked ring of $R_1/R_0 = 0.5$. Applying the same analysis to the internally cracked ring, equation (6), leads to

$$B^*(\alpha) = \frac{\{ 0.25 - 2.18\alpha + 4.77\alpha^2 \}}{\{ 1.63 + 0.25\alpha - 1.09\alpha^2 + 1.59\alpha^3 \}} \quad 9$$

Figure 14(b) also shows $B^*(\alpha)$ plotted against α . It is interesting to note that in the range $0.3 \leq \alpha \leq 0.6$, with $\alpha = 0.1$, as before, the effect of the bubble is less than 5%. This effect is less than the scatter expected in the results.

7.2b An Air Bubble Near the Crack Tip

In this case, the bubble is near enough to the crack tip to be contained in the crack tip stress field, and hence can modify this stress field. Wilkinson and Vitek (19) have analysed the elastic stress field surrounding a microvoid ahead of a macroscopic crack. This analysis shows that the microvoid has its own local stress field, modifying that of the macroscopic crack. However, it gives little information on the effect of the bubble on the main crack singularity. It also assumes that the crack length is very much greater than the bubble length. This is not true for these specimens, and hence this model cannot be used directly.

An alternative model of two unequal length collinear cracks can be used; see reference (5). This again is a simple case; the bubble is more likely to be at an angle to the crack, as sketched in Fig. 3(b). This arrangement is shown in Fig. 15(a). The shorter crack, A-B, represents the air bubble, while the longer crack C-D is the main crack. The stress intensities at the crack tips are dependent on the relative lengths of the two cracks and the spacing between them. The applied stress is a uniaxial tensile stress, σ , and the cracks are assumed to lie in an infinite sheet. Thus these results are only qualitatively applicable to the pressurized ring specimen.

Figure 15(b) shows the results of considering typical crack lengths. The air bubble is modelled as crack A-B, of total length 2 mm. The main crack C-D has a total length of 20 mm. Thus the half-length a_2 is comparable to the crack length of the specimens. The stress intensity factor of the main crack, unmodified by the shorter crack, would be $K = \sigma\sqrt{\pi a_2}$. The stress intensities at tips A-D are shown relative to this. These intensities are shown for spacings b ranging from 5 mm to 1 mm. When b reduces to 1 mm, the air bubble will have intersected the main crack and this analysis is no longer valid.

At tip D, furthest from the air bubble, the stress intensity is essentially unaffected. Tip A shows an increase in stress intensity as the bubble moves towards the crack, but the value is always less than that of the main crack alone. It is at tips B and C that the greatest effect is found. At a large spacing, the stress fields of the two tips are similar to those of the individual cracks; tips C and D are comparable, as are A and B. As the bubble moves closer to the main crack, the stress intensity factors rise, until both tips B and C have higher stress intensities than the main crack alone.

At tip C, in particular, a stress intensity some 50% above that of the main crack may be reached. Thus the fracture toughness may be exceeded at tip C even though the apparent stress intensity is below the fracture toughness. Although this means that brittle fracture will be initiated, a total failure may not follow. The initiation of fracture at B or C will lead to the rupture of the ligament B-C. This has the effect of lengthening the crack, by an amount A-C. The situation is now that discussed in the previous section, where the air bubble has extended the main crack. If $a_1 = 2$ mm, $b = 1.5$ mm, the increase in crack length is 2.5 mm. If the main crack were 10 mm long, $\alpha = 0.5$ and $\Delta\alpha = 0.125$ if the ring wall thickness were 20 mm. From equation (8) and Fig. 14(b) $\Delta K = 0.12K$ i.e. the stress intensity at the end of the extended crack is about 10% above that of the original crack. This increase is not sufficient to account for the low test results. The air bubble has caused a lengthening of the crack, not a total failure.

This analysis assumes a quasi-static rupture of the ligament B-C between the bubble and the crack, i.e. the crack arrests immediately K_I at its tip falls below K_{IC} . Liu and Miller (11) found K_I at crack arrest to be some 30% below K_{IC} . Thus it is possible that rupture of the ligament might initiate failure of the whole specimen. It is not possible to analyse this without data on dynamic crack propagation in ice.

7.2c A Series of Bubbles Alone Initiate Failure

A very simple model in this case is an infinite array of collinear cracks in an infinite sheet in tension, ref. (5), as shown in Fig. 16(a). A model with differing crack lengths, orientations and spacings would be more accurate, but would be difficult to derive and use. The cracks are each of length $2a$, spaced distance $2b$ apart. The stress intensity factor for one crack alone would be as given in equation (2); $K_I = \sigma\sqrt{\pi a}$. The additional cracks cause an increase in the stress intensity, dependent on the ratio of length to spacing, a/b . This increase is shown in Fig. 16(b) where the ratio $K_I/(\sigma\sqrt{\pi a})$ is plotted against a/b .

For bubbles 2 mm long, spaced at 4 mm between centres, $a/b = 0.5$, whence, from Fig. 16(b), $K_I = 1.13\sigma\sqrt{\pi a}$. Now if the stress σ is 4.14 bar (60 psi, typical of the failure pressures shown in Table 2), the stress intensity would be:

$$K_I = 4.14 \times 10^5 \times 1.13 \times \sqrt{(\pi \times 0.001)} = 26 \text{ kPa}\sqrt{\text{m}}.$$

This is significantly less than the results in Table 1, and is only one quarter of the values obtained in laboratory tests. Thus it is unlikely that the air bubbles alone can initiate failure. Even if the bubbles are much closer together, so that $K_I = 2.1\sigma\sqrt{\pi a}$, the maximum in Fig. 16(b), the stress intensity will be around 50 $\text{kPa}\sqrt{\text{m}}$. This is still only half the values of laboratory tests, although comparable to the lower values in Table 1. It is unlikely that there would be sufficient bubbles all occurring this close together to produce this increase, however.

7.2d General Discussion of Air Bubbles

It is necessary to be cautious in using these very simplified models. In addition to the assumption of a constant stress instead of the true hoop stress distribution, there are further errors.

The air bubble has been modelled as a crack, with sharp tips. Although elongated, the air bubbles are not sharp, having a finite radius at the tips. This will reduce the stresses at the crack tip or bubble end. The case of an isolated elliptic hole (bubble) has been studied, but more complicated arrangements are less known. In addition accurate data on bubble geometry and spacing would be required to use such a model.

A more serious error is in the two-dimensional nature of the models. The analyses assume that the geometry is constant through the specimen thickness, and plane strain conditions exist. Whilst this is the case for the main crack in the specimen, it should also be the case for the 'bubble' ahead of the crack. This is not found in reality. A distribution of bubbles, some intersecting, some ahead of the main crack, occurs through the thickness. Thus the bubbles will be either local extensions of the main crack, or cause perturbations of the crack stress field. The true stress intensity of these variations will be less than that obtained from the assumption of a 'continuous' bubble along the entire crack front. Even if a bubble did initiate local fracture, this may not cause total failure to occur.

The results of the models developed in this section show that it is unlikely that the presence of the air bubbles alone caused the low fracture toughness values. In the laboratory tests described in section 4.4, there was no effect of air bubbles on the results. In each of the three models considered, the increase in stress intensity due to the air bubbles would not be sufficient to cause fracture at the recorded pressure, if the fracture toughness were $125 \text{ kPa}\sqrt{\text{m}}$.

7.3 The Effect of Grain Size

This section discusses the grain sizes measured on the Bersaerkerbrae Glacier and the laboratory ice samples used to test the specimen design. The effect of the grain size on the measured fracture toughness values is then considered. Finally, the implications of these effects for further fracture toughness testing of naturally formed ice and snow are discussed.

7.3a Grain Size Measurements

The method used to assess the grain size, equation (7), provides the size of a square of the same area as an average grain. The small number of grains in each sample made it of little value to measure individual grain sizes and then attempt a statistical analysis. It was also not practical to use the ASTM method, as described in ref. (20). This method counts the number of grains per square inch at a magnification of X100. With these samples, a single grain would have occupied over one square inch. This method is, of course, intended for metallurgical samples, where grain sizes are much smaller. The linear intercept method was used for the laboratory ice sample, as there was a larger number of grains (see Fig. 13).

For the linear intercept method, several randomly oriented lines are drawn on the tracing or photograph. The total line length is measured, and divided by the number of grain boundaries crossed. A correction is made to allow for the magnification. The grain size of the laboratory samples measured by this method was 0.76 mm, which is in reasonable agreement with $d_{av} = 0.91 \text{ mm}$ obtained from equation (7).

These results show that the grain size of the ice produced by directional freezing of water for the laboratory tests was an order of magnitude smaller than the naturally formed ice of the glacier. In addition, the natural ice probably had a relatively random crystal texture. Without a universal stage, fabric diagrams could not be obtained. Allen et al (17) showed that the foliated ice of the Blue Glacier had a 4 maximum C-axis fabric, and related this to the state of stress. It is likely that a similar pattern would have been present in the ice tested. In contrast, the ice made for the laboratory tests had the C-axes all lying in the same plane, parallel to the water surface when freezing. The grains were long and columnar, in contrast to the glacier ice, where the grains would be expected to be approximately equi-axed.

Examination of Table 3 and Fig. 9 shows a tendency to increased grain size nearer the snout of the glacier. There is no obvious variation with depth at a single site. This may be due to the small number and size of the samples taken. Rigsby (18) found that, on a polar glacier, crystal size decreased considerably over the first 6-900 mm depth, where the ice was still below freezing. He suggested that re-crystallisation had caused an increase in crystal size in the surface layer. Thus the samples discussed here would not have been deep enough to show this variation, as they were taken towards the end of the melt season.

7.3b The Effect of Grain Size on the Measured Fracture Toughness

The simple theory of LEFM assumes an isotropic elastic medium. In real metals, the individual grains are anisotropic but are oriented randomly. In addition, the grains are small compared with components and defects. Typically, grains are much less than 0.1 mm in diameter, while components and cracks may be tens of millimetres in size. Hence the component can be analysed as a continuum. If, however, the defect is of a size comparable with the grain size, LEFM methods no longer apply, and more sophisticated theories are required. An example of this is the so-called 'short crack problem' in metal fatigue. Here a crack is contained within one or two grains; see references (21, 22).

This is the situation with the tests on the Bersaerkerbrae. The results of these tests, and other reported work, are summarized in Table 4, showing typical grain sizes where known. Typically, the sawn cracks in the ring specimens were 10 mm long. This is virtually identical with the mean value $d_{av} = 9.6$ mm. Hence it is quite likely that the entire crack would have been within one or two grains. Under these conditions, LEFM theory will not apply, and a meaningful fracture toughness can not be obtained.

In the earlier laboratory trials of the ring specimen, the cracks were also about 10 mm long. However, the grain size of these specimens was 0.91 mm, so the crack would have extended through about 10 grains. The wall of the ring would have contained around 20 grains. Thus the LEFM analysis would be appropriate, and a true fracture toughness value can be obtained.

Table 4 summarizes the test conditions and grain sizes of these tests and earlier work. Goodman and Tabor (9) stated that their grain sizes varied from 1 mm to single crystals. Their SEN bend specimens (Fig. 2(a)) were 130 mm x 20 mm x 20 mm, with a fracture toughness of $116 \text{ kPa}\sqrt{\text{m}}$. It can be assumed that the crack traversed several grains. The tests with conical and pyramidal indenter gave values ranging from 55 - 85 $\text{kPa}\sqrt{\text{m}}$ (pyramidal indenter) to over 300 $\text{kPa}\sqrt{\text{m}}$ (conical indenter). The cracks ranged in length from 1 to 10 mm and were generally formed within a single grain. Thus these indenter tests were testing the fracture resistance of a single grain. The lower end of this range is comparable with the results in Table 1. Liu and Miller (11) used crack lengths of 50 mm in specimens with a grain size of 5 mm. Hence the crack would have traversed about 10 grains. Goodman (10) used specimens with a grain size of 5 - 10 mm, and crack lengths of about 10 mm. The fracture toughness was $118 \text{ kPa}\sqrt{\text{m}}$ at -4°C , although the crack would have occupied only 3 or 4 grains. Tests on the Roslin Glacier (8) used SEN bend specimens, with a mean crack length of 18 mm and width of 43 mm. Unfortunately no measurements were made of grain sizes. If the sizes were similar to those measured on the Bersaerkerbrae, the cracks would have been contained in 2 - 3 grains. Without these measurements, it is not possible to assess the effect of crystal size on these tests.

It would appear that provided the crack traverses 10 or more grains, a continuum response will be obtained and a valid fracture toughness can be measured. The indenter tests (9), where the crack was contained in a single grain, showed a wide variation, which may be due to variation in orientation of the grain. The Bersaerkerbrae tests were probably similar, with the crack contained in only one or two grains. Hirayama et al (23) state that the compressive strength of ice is dependent on grain size if

$$\frac{\text{specimen diameter}}{\text{grain diameter}} < 25$$

10

Above this ratio the strength was independent of the grain size. According to this criterion, all the tests in Table 4 would have shown a size effect.

The large grain size would further weaken the specimens, as flaws would have a greater effect. If the specimen contains many grains, a grain boundary flaw will have little effect, as it will be small and the surrounding grains will provide reinforcement. When there are only a few grains in the specimen, this strengthening effect is lost. A flaw becomes potentially more damaging. This would also account for the great difficulty in producing specimens, as the pre-existing flaws were causing failure.

Air bubbles on the grain boundaries will have a weakening effect on the specimen, independently of the crack. It might be possible to quantify this using analyses of

the creep failure of metals (24). (The nucleation and growth of grain boundary cavities is the main cause of creep failure.) These analyses usually assume a regular array of grains. As the specimens in these tests contained only a few irregular grains, these analyses may not be accurate. In addition, data on the distribution of air bubbles on the grain boundaries is not available.

7.3c Fracture Toughness Testing of Natural Ice

These results have implications for further fracture toughness testing of natural ice. It seems reasonable to assume that the crack should be at least 10 grains in length. Similarly, the distance between the crack tip and the far side of the specimen (the remaining ligament) should also contain at least 10 grains. Thus the minimum dimension of the specimen would be 20 grains. The actual dimensions would be much greater. Consider a standard proportioned SEN bend specimen (Fig. 2(a)), made in ice of grain size 10 mm. Width W would be 200 mm, and the overall size would be 800 mm x 200 mm x 100 mm. Similarly, the ring specimen (Fig. 3) used in these tests would need an outside diameter of 800 mm to produce a wall thickness of 200 mm. These sizes of specimen would be difficult to obtain, even from the surface. For the ring specimen, a reduction in size could be obtained by reducing R_i/R_o , but the minimum size would still be around 400 mm.

7.4 Validity Criteria

Following from the previous discussion, it is necessary to re-consider the validity requirements expressed in equations (3). For a large grain size, these equations may be satisfied, and yet the crack could be contained within a single grain. The criteria

$$A \geq 10 d_{av}, B \geq 10 d_{av}, (W-A) \geq 10 d_{av} \quad 11$$

are suggested as ADDITIONAL to equations (3). The two sets of equations can be combined to give a condition

$$d_{av} \leq \frac{1}{4} \left(\frac{K_{Ic}}{\sigma_y} \right)^2 \quad 12$$

For fine grained material, the limit is expressed by equations (3); for coarse grained material, equations (11). Both sets must be satisfied, and taken into account when designing specimens.

8 Conclusions

1. The mean apparent fracture toughness of ice from the Bersaerkerbrae Glacier, tested using a new design of cracked ring specimen, was 58 kPa \sqrt{m} . This is half the value obtained in other laboratory tests on standard specimens.
2. The low fracture toughness was not caused by the air bubbles in the ice.
3. The large grain size of the ice relative to the specimen size invalidated the assumption of an isotropic continuum. The assumptions of Linear Elastic Fracture Mechanics were not satisfied, and so a valid fracture toughness measurement was not obtained.
4. An additional validity criterion is suggested for fracture toughness testing ice. The crack length, ligament and thickness should all be greater than ten times the grain size.

9 Acknowledgements

In addition to a general acknowledgement to all our supporters, the following specific thanks are due:

To John Allen for the design of the data logger and electronics, and Eann Patterson and John Thompson for their coring of the samples. In the Department of Mechanical Engineering, Messrs Alan Wright and Tom Brown made components for the test rig. The construction of the apparatus and data logger was financed by a Scientific Investigation Grant from the Royal Society. The pressure gauge was donated to the project by the Budenberg Gauge Company of Broadheath, Manchester. Environmental Equipments (Northern)

of Nantwich loaned the pressure transducer, and generously offered other items which we would have used if payload had been available on the Twin Otter. The extension rods for the corer were donated by Gubb and Hauff Precision Engineering of London.

10 Nomenclature

SYMBOL	USE	UNITS
A	crack length	mm
a	crack length	mm
B	specimen thickness	mm
B(α)	function of α showing effect of an air bubble; section 7.2a	
d	average grain size	mm
f_{ij}^{av}	function determining crack tip stress	
K_{ij}	stress intensity factor	kPa \sqrt{m}
K_{Ic}	plane strain fracture toughness	kPa \sqrt{m}
K_{Ic}^o	reference stress intensity factor	kPa \sqrt{m}
p^o	pressure	psi; bar
R_i	specimen inside radius	mm
R_o	specimen outside radius	mm
r^o	distance from crack tip	
W	specimen width	mm
Y	function of geometry in stress intensity factor	
α	dimensionless crack length	
θ	angle	degrees
σ	stress	Pa
σ^y	yield stress of ice	bar
ϕ^y	orientation of bubble axis to crack	degrees

References

- Embleton, C., and King, C.A.M. *Glacial Geomorphology*, 2nd edition, London, Arnold, 1975.
- Poirier, J.P. *Rheology of Ices*. *Nature*, 299 (1982), 683-688.
- Knott, J.F. *Fundamentals of Fracture Mechanics*, London, Butterworths, 1973.
- Lawn, B.R. and Wilshaw, T.R. *Fracture of Brittle Solids*, Cambridge, CUP, 1975.
- Rooke, D.P. and Cartwright, D.J. *Compendium of Stress Intensity Factors*, London, HMSO, 1976.
- British Standards Institution. *Methods of Test for the Plane Strain Fracture Toughness of Metallic Materials*; BS5447, London, BSI, 1977
- Brown, W.F. and Srawley, J.E. *Plane Strain Crack Toughness Testing of High Strength Metallic Materials*, STP 410, Pittsburgh, Pennsylvania, ASTM, 1966.
- Andrews, R.M., McGregor, A.R., Miller, K.J. *Fracture Toughness of Glacier Ice*, IN *Proceedings of the International Karakoram Project*, edited by K.J. Miller, Cambridge, CUP, to be published.
- Goodman, D.J. and Tabor, D. *Fracture Toughness of Ice: A Preliminary Account of some new experiments*. *J. Glaciology* 21 (1978) 651-660.
- Goodman, D.J. *Critical Stress Intensity Factor Measurements at High Loading Rates for Polycrystalline Ice*. *Proc. IUTAM Symposium on the Physics and Mechanics of Ice*, 1979, edited by P. Tryde, pp 129-146, Berlin, Springer-Verlag, 1980.
- Liu, H. W. and Miller, K.J. *Fracture Toughness of Fresh Water Ice*. *J. Glaciology* 22 (1979) 135-143.
- Gold, L.W. *Crack Formation in Ice Plates by Thermal Shock*. *Canadian J. Physics*, 41 (1963), 1712-1728.
- Hawkes, I. and Mellor, M. *Deformation and Fracture of Ice under Uniaxial Stress*. *J. Glaciology* 11, (1972), 103-131.
- Grandt, A.F. *Stress Intensity Factors for Cracked Holes and Rings Loaded with Polynomial Pressure Distributions*. *Int. J. Fracture* 14, (1978), R221-229.
- Dugdale, D.S. *Elements of Elasticity*, Oxford, Pergamon, 1968, pp 94.
- Chatfield, C. *Statistics for Technology*, London, Chapman and Hall, 1975.
- Allen, C.R. et al. *Structure of the Lower Blue Glacier Washington*. *J. Geology* 68 (1960), 601-662.
- Rigsby, G.P. *Crystal Orientation in Glacier and in Experimentally Deformed Ice*. *J. Glaciology* 3 (1960) 589-606.
- Wilkinson, D.S. and Vitek, V. *Stress Analysis and Diffusional Growth of Microvoids*.

IN: Cavities and Cracks in Creep and Fatigue, edited by J. Gittus. London, Applied Science Publishers, 1981, pp 243-258.

20. Reed-Hill, R.E. Physical Metallurgy Principles, 2nd edition, New York, Van Nostrand 1973, pp 712.
21. Hobson, P.D. A Crack Growth Law For Short Cracks. Fatigue of Engineering Materials and Structures, to be published.
22. Miller, K.J. The Short Crack Problem. Mechanical and Thermal Behaviour of Metallic Materials, Soc. Italiana di Fisica, Bologna, 1982, 165-175.
23. Hirayama, K., Schwarz, J., Wu, H. Model Technique for the Investigation of Ice Forces on Structures. Proceedings of 2nd Conference on Port and Ocean Engineering under Arctic Conditions, Reykjavik, University of Iceland, 1974, pp 332-344.
24. Beere, W. Mechanism Maps. IN Cavities and Cracks in Creep and Fatigue, edited by J. Gittus, London, Applied Science Publishers, 1981, pp 29-57.

TABLE 1 Test Results, Specimen Fracturing from Crack

TEST NUMBER	FRACTURE PRESSURE p.s.i.	THICKNESS mm	DEPTH, mm	CRACK LENGTH mm	α	γ	K_{Ic} kPa \sqrt{m}	ORIENTATION OF BUBBLE, ϕ DEGREES
1	78	27		6	0.316	0.899	66.4	
2	67	30	400	8	0.421	0.994	72.8	
3	81	27	500	6	0.316	0.899	68.9	
4	69	27	700	10	0.526	1.102	92.9	
5	81	23	850	6	0.316	0.899	68.9	
6	35	30	220	8	0.421	0.994	38.0	
7	45	27	55	6	0.316	0.899	38.3	0
8	48	15	25	4	0.211	0.822	30.5	90
9	54	32	50	8	0.421	0.994	58.7	0
10	38	20	150	9	0.474	1.046	46.1	0
11	65	24	300	8	0.421	0.994	70.6	0
12	39	10	350	7	0.368	0.945	37.7	0
13	47	18		9.5	0.500	1.074	60.1	90
14	34	12		11	0.579	1.159	50.5	45
15	44	24	1200	8	0.421	0.994	47.8	0
16	54	22	1400	9	0.474	1.046	65.5	0
17	55	22	1750	7	0.368	0.945	53.1	0
18	48	24	1900	10	0.526	1.102	64.6	0
19	34	15	2000	9	0.474	1.046	41.2	0
20	55	24	300	12	0.632	1.217	89.6	0

Mean K_{Ic} = 58.1 kPa \sqrt{m} Standard Deviation = 17.1 kPa \sqrt{m}

TABLE 2 Summary of Specimens Which did not Fail From Sawn Crack

TEST NUMBER	FRACTURE PRESSURE p.s.i.	THICKNESS mm	DEPTH mm	CRACK LENGTH mm	$\frac{a}{R_o - R_i}$	Y	
A1	67	22	150	7.5	0.395	0.969	fracture // to bubbles, at 30° to sawn crack crack // to bubbles, fracture // to bubbles, crack ⊥ to long bubbles, fracture // to bubbles crack ⊥ to long bubbles crack // to bubbles fracture // to crack crack ⊥ to bubbles fracture // to crack crack // to bubbles fracture // to crack fracture // to bubbles fracture // to bubbles and // to crack
A2	55	17					
A3	53	24	8	0.421	0.994		
A4	64	27					
A5	57	25	900	8	0.421	0.994	
A6	56	18					
A7	64	22	1500	8.5	0.447	1.020	
A8	32	23					
A9	53	24	9	0.474	1.046		
A10	69	16				10.5	

// - parallel ⊥ - perpendicular

TABLE 3 Results of Grain Size Samples

See Fig. (9) for location of sample sites. Mean glacier ice size 9.63 mm, S.D. 3.24 mm. All traces except 19, magnification X 1.1

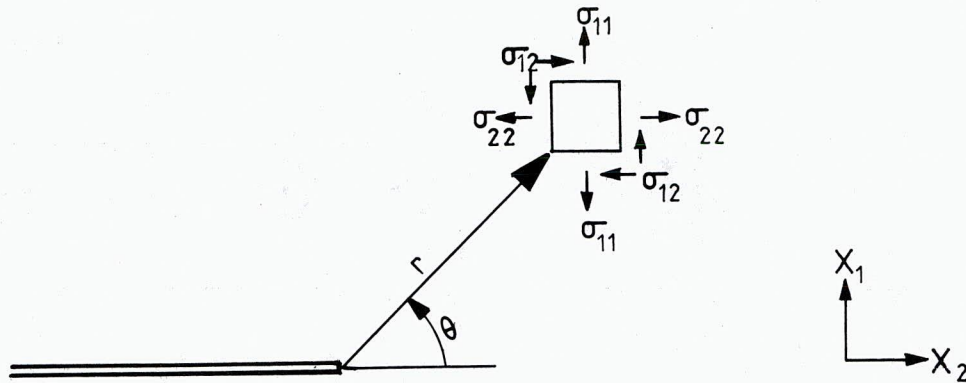
TRACE	SITE	DEPTH mm	NO. GRAINS	AREA MEASURED cm ²	TRUE AREA mm ²	d _{av} , mm	REMARKS
1	1	0	22	31.6	2612	10.9	
2	1	150	5	12.8	1058	14.5	
3	2	100	21	39.5	3265	12.5	
4	2	200	25	36.5	3017	11.0	
5	3	20	39	49.0	4050	10.2	
6	3	180	22	48.9	4041	13.6	
7	4	0	41	20.6	1703	6.4	
8	4	100	15	50.3	4157	16.6	
9	4	150	61	48.9	4041	8.1	
10	5	0	26	45.2	3736	12.0	
11	5	175	69	46.1	3810	7.4	
12	5	220	66	46.2	3818	7.6	
13	6	100	44	23.9	1975	6.7	
14	7	75	50	54.7	4521	9.5	
15	8	50	80	54.7	4521	7.5	
16	8	100	64	45.3	3744	7.6	
17	9	50	116	60.9	5033	6.6	
18	10	80	170	46.4	3835	4.7	
19	LAB	-	666	102.0	552	0.91	

x 4.3 MAGNIFICATION

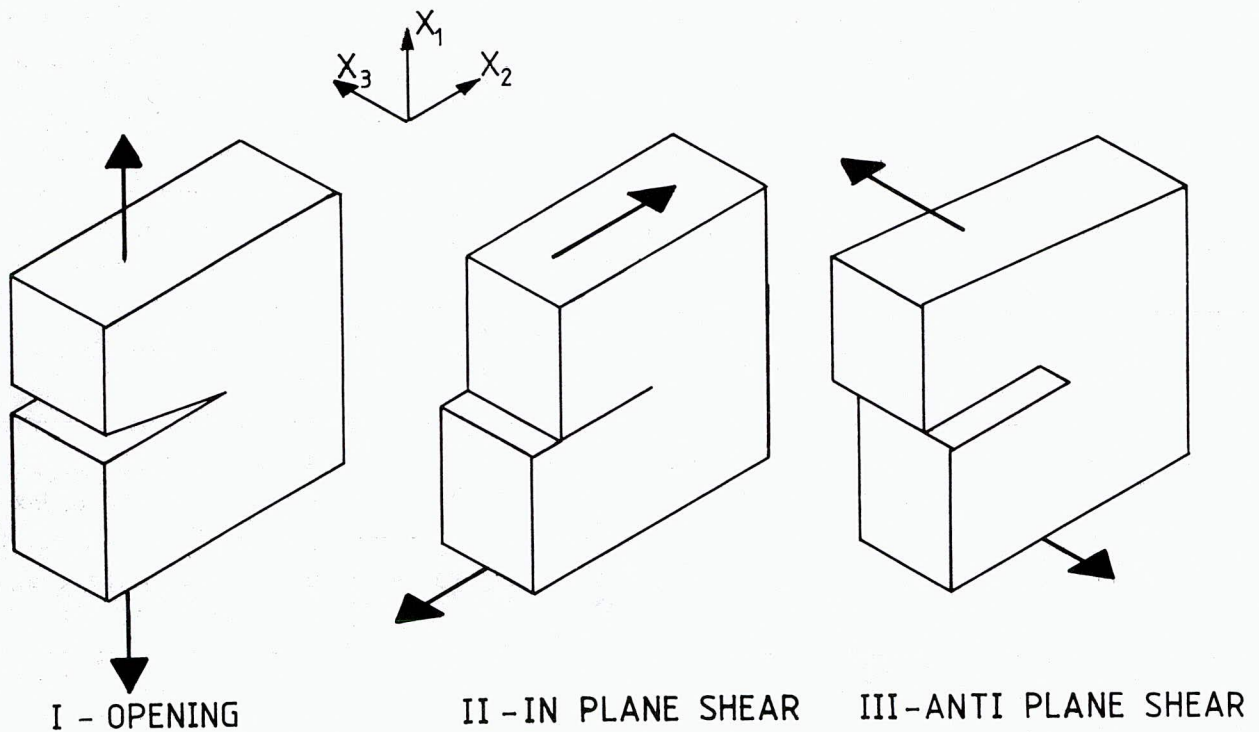
TABLE 4 Summary of Available Fracture Toughness Results

AUTHOR	REF	TEST METHOD	GRAIN SIZE mm	CRACK LENGTH a, mm	K_{Ic} kPa \sqrt{m}	REMARKS
Gold	12	Thermal shock of slabs	1.5-6	2.4-9	50-160	K_{Ic} at arrest of propagating crack
Liu and Miller	11	CTS	5	50	110-340	
Goodman and Tabor	9	SEN bend (3 point)		10	116	Grain size "1mm to single crystals"
		Pyramid indenter Conical indenter		1 - 10 1 - 10	55 170-290	Crack within a single grain Crack within a single grain
Goodman	10	SEN bend (4 point)	5 - 10	10	118	High loading rate tests
Andrews et al.	8	SEN bend (3 point)		18	125	Roslin Glacier ice
This report		Radially cracked ring	0.9	9	182	internal crack external crack
			0.9	9	89	
			9.6	10	58	Bersaerkerbrae Glacier ice

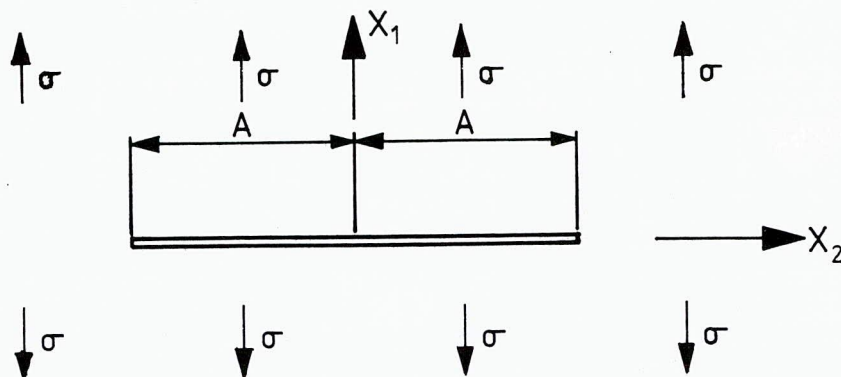
FRACTURE MECHANICS CONCEPTS



a) CRACK TIP COORDINATES (r, θ) AND STRESSES

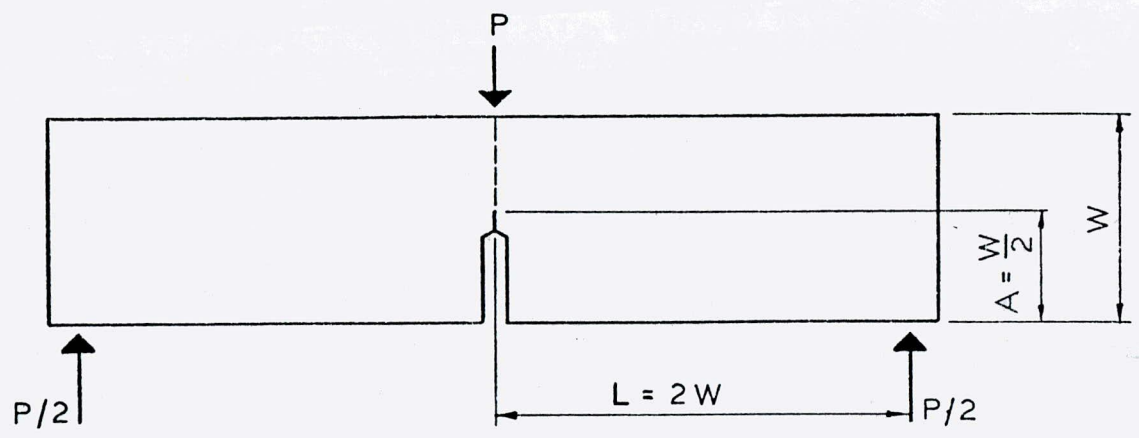


b) DEFORMATION MODES

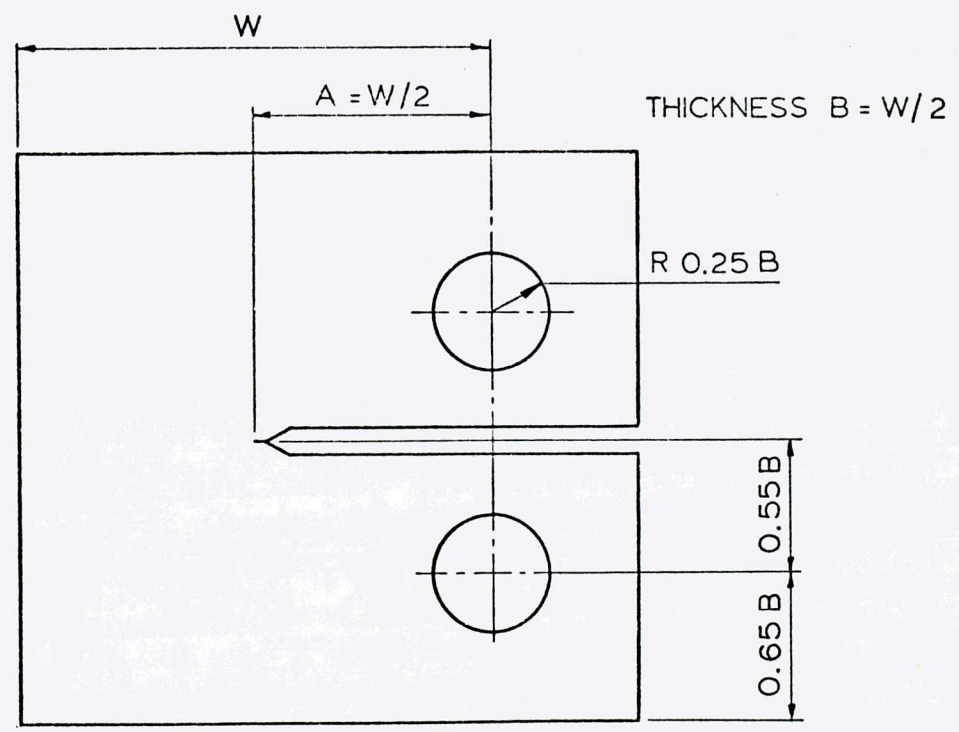


c) CRACK IN AN INFINITE PLANE IN UNIAXIAL TENSION

THICKNESS $B = W/2$

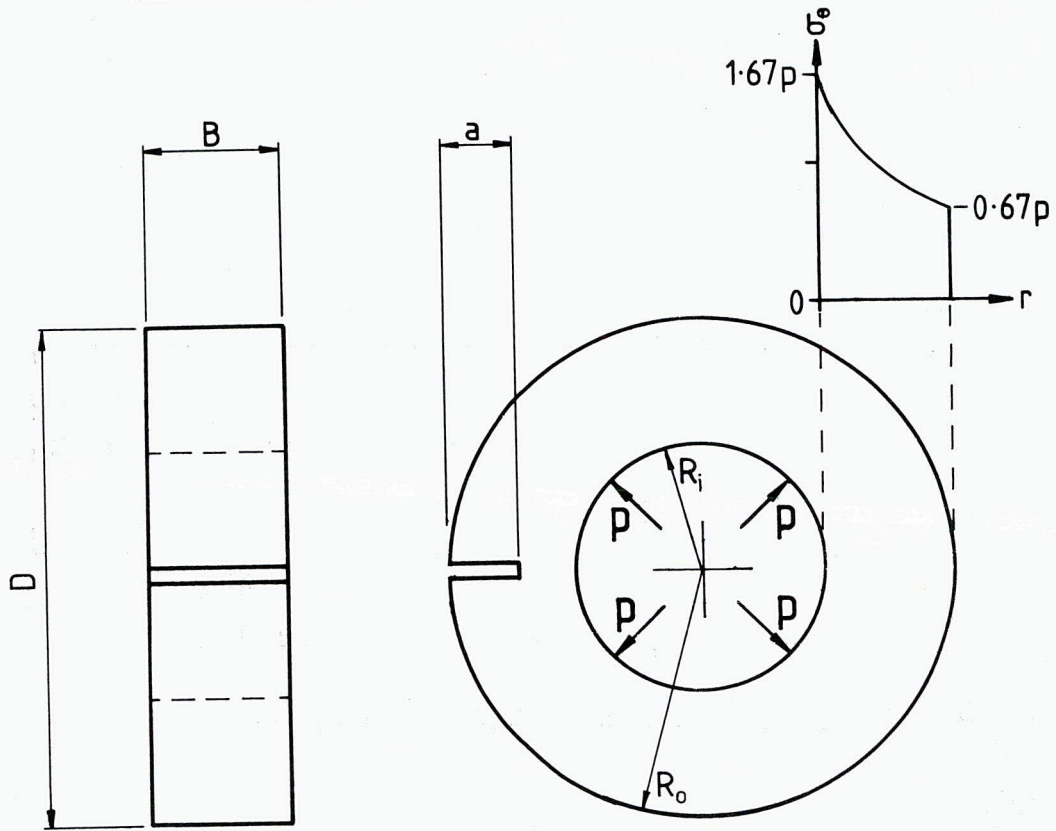


a) SINGLE EDGE NOTCH (SEN) BEND TESTPIECE

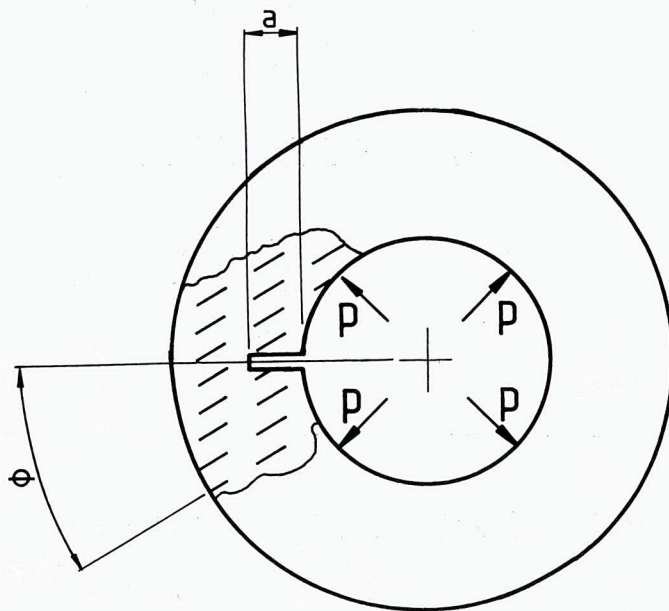


b) COMPACT TENSION (CTS) TESTPIECE

RADIALLY CRACKED RING SPECIMENS



a) EXTERNAL CRACK, SHOWING HOOP STRESS DISTRIBUTION



b) INTERNAL CRACK, SHOWING ELONGATED AIR BUBBLES

STRESS INTENSITY FACTORS FOR RADIALY
CRACKED RINGS

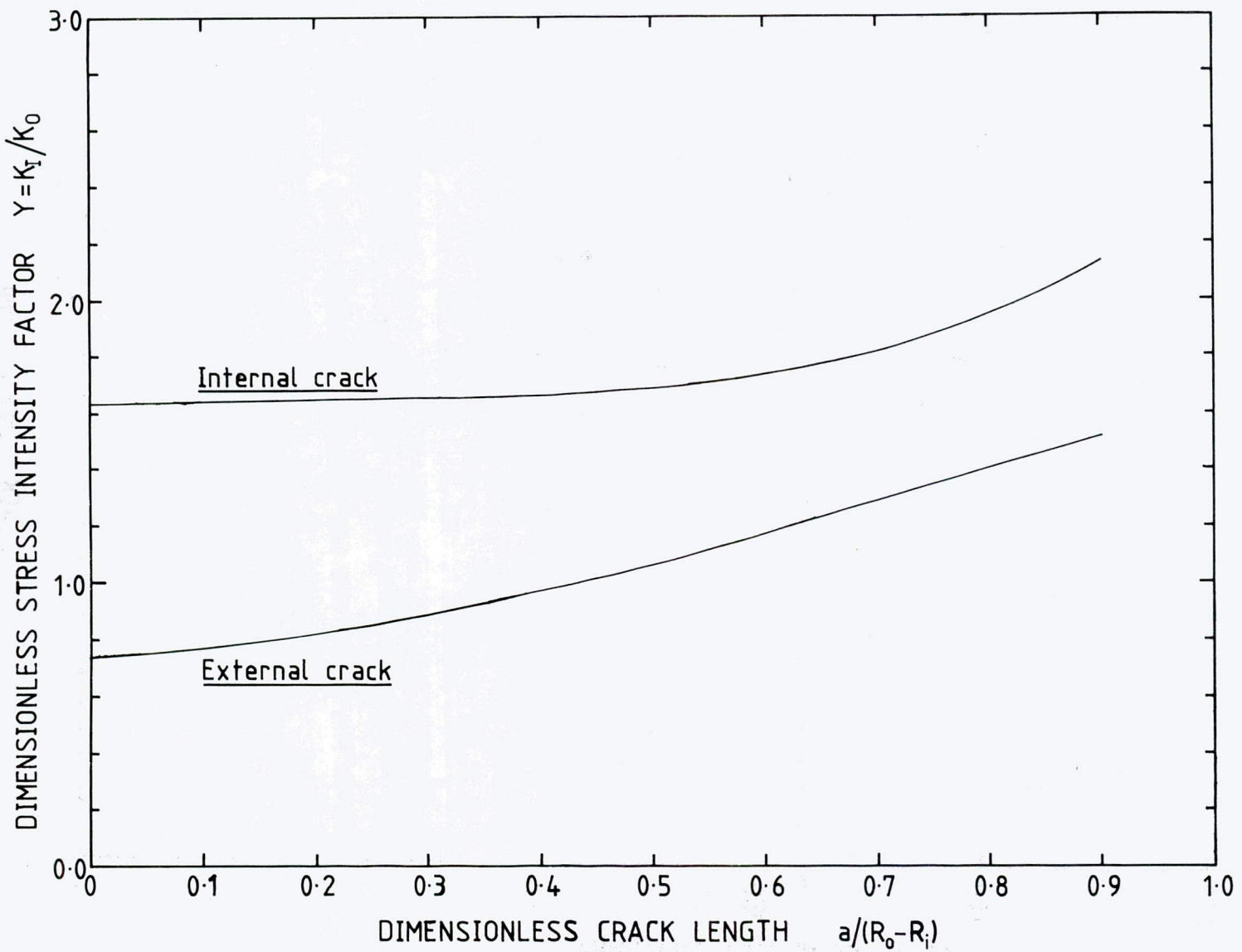
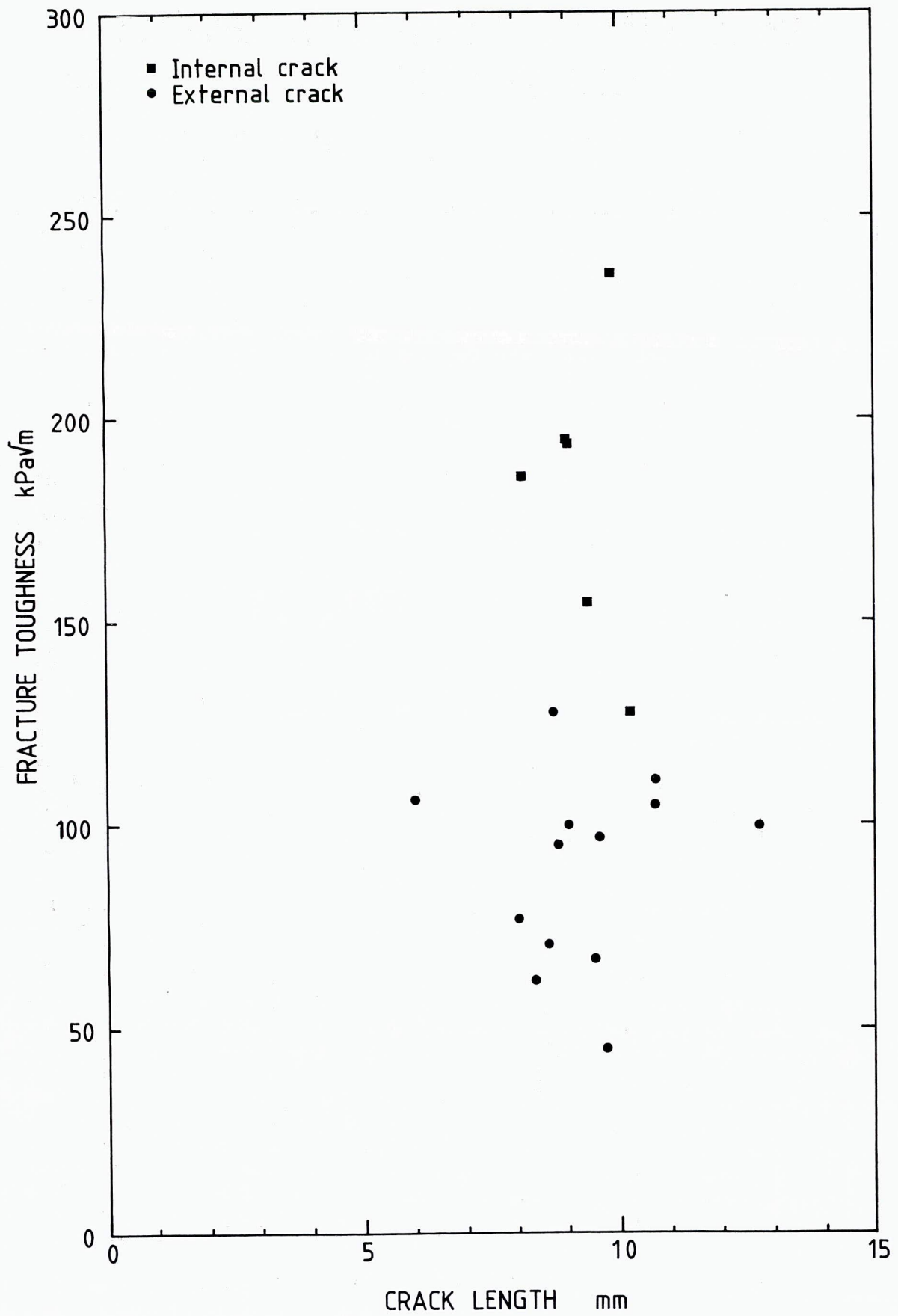
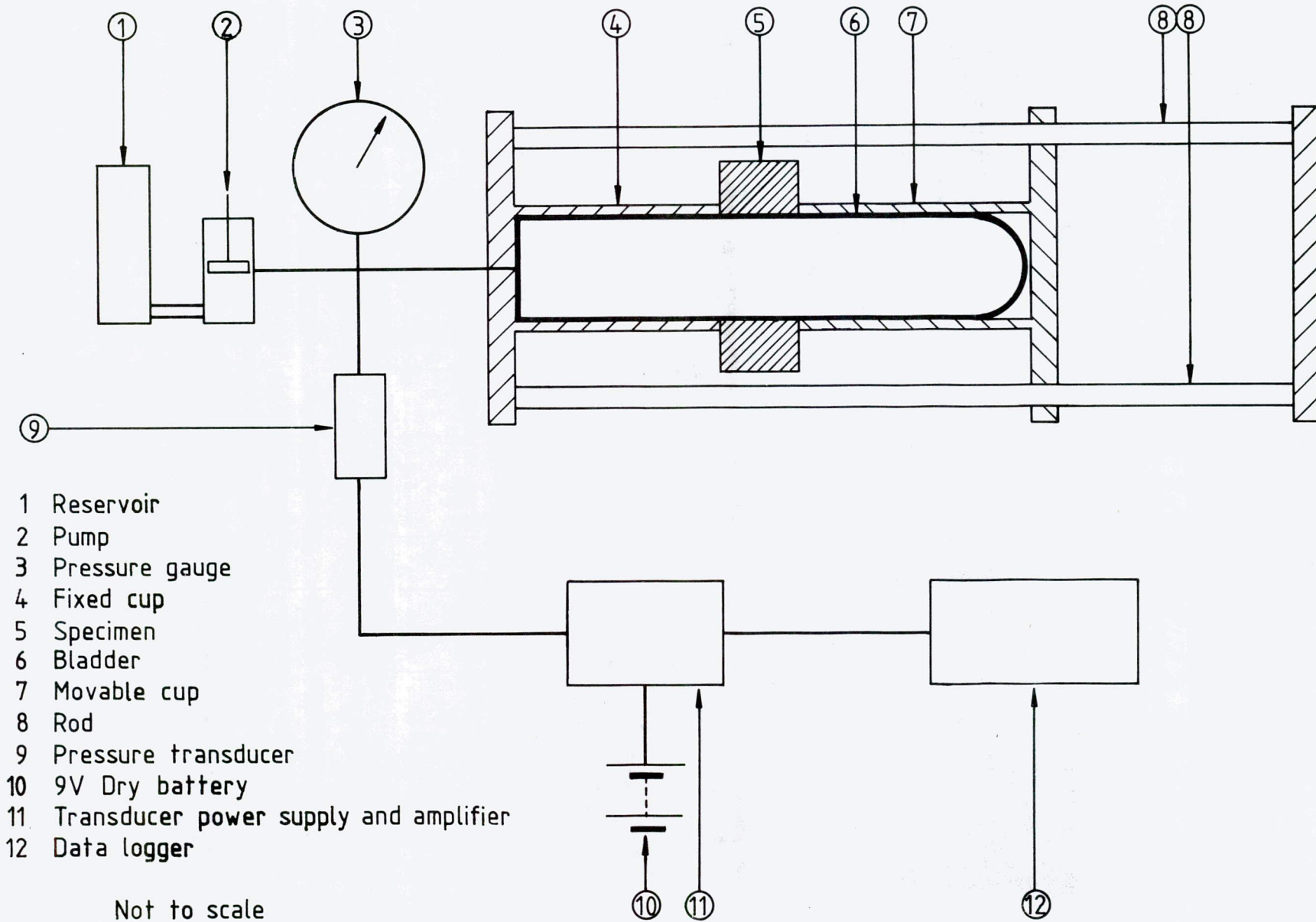


FIG. 4

FIG. 5

LABORATORY TRIALS OF RING SPECIMENS



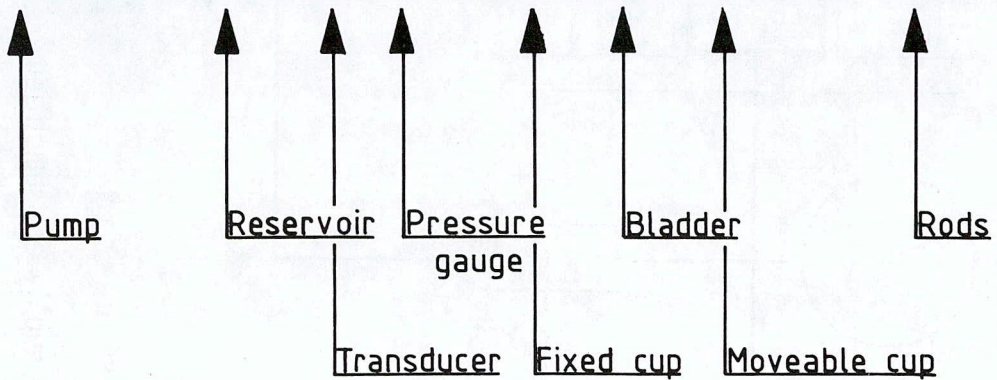
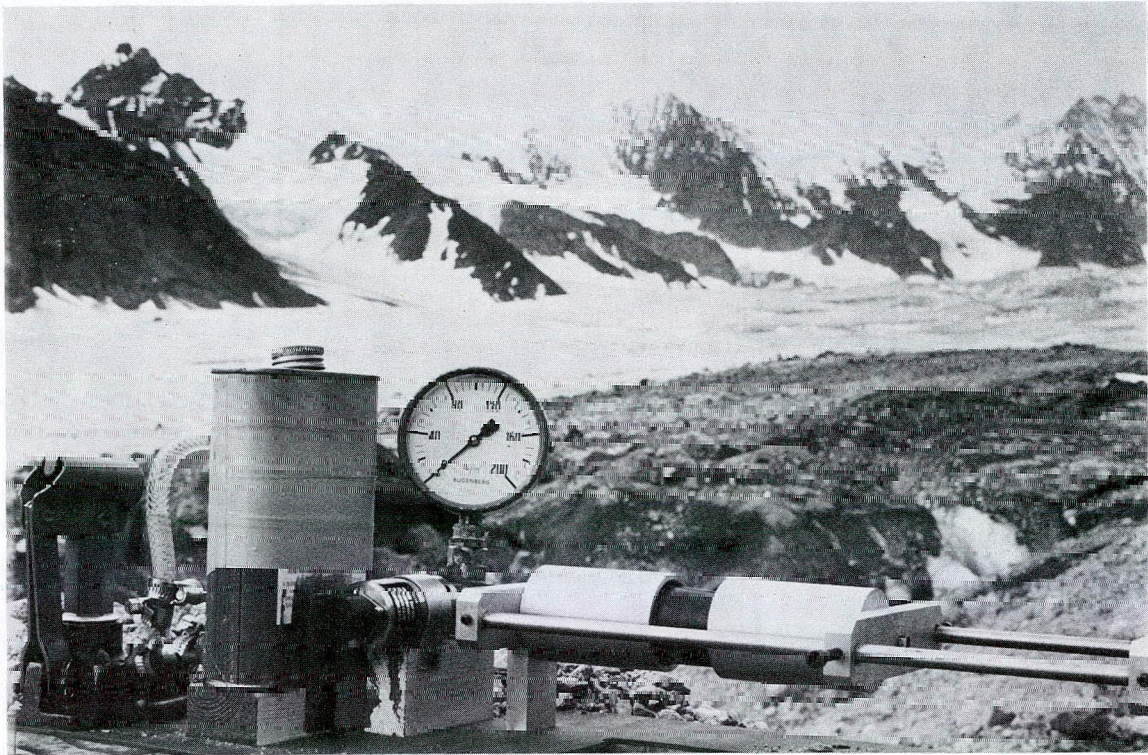


FIELD TEST RIG FOR RING SPECIMENS (Schematic)

FIG. 6

FIG. 7

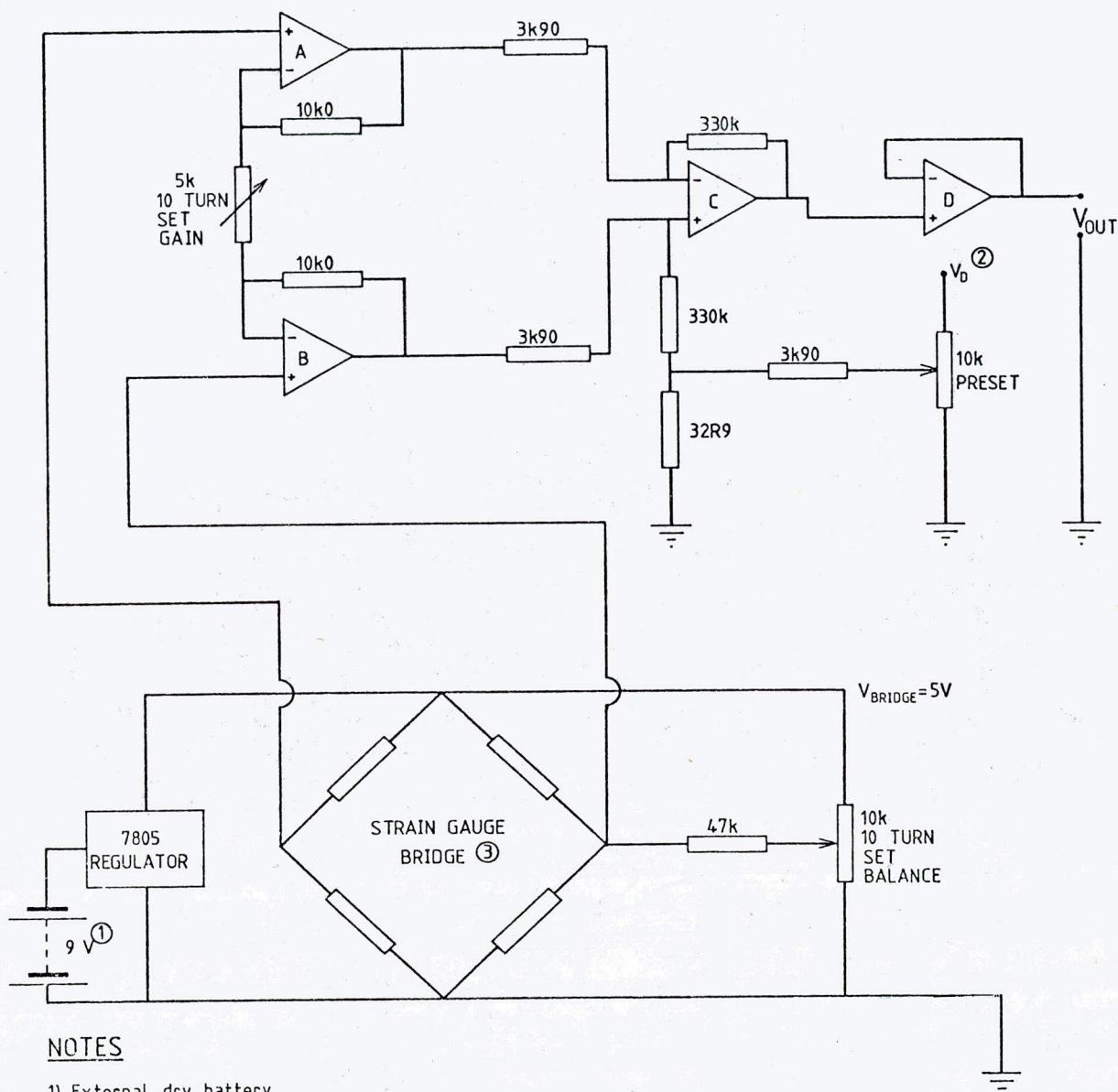
FIELD TEST RIG FOR RING SPECIMENS



The test rig photographed in base camp before being taken out onto the glacier.

FIG. 8

TRANSDUCER AMPLIFIER CIRCUIT



NOTES

- 1) External dry battery.
- 2) $V_D = 9V$ approx., data logger battery voltage.
- 3) Strain gauge bridge is located in the transducer.
- 4) Operational amplifiers A - D each 1/4 LM324.
Integrated circuit is supplied at V_D .

FIG. 9

LOCATION OF TESTS AND GRAIN SIZE SAMPLES

- ⊕ FRACTURE TOUGHNESS TESTS AND GRAIN SIZE SAMPLE
- GRAIN SIZE SAMPLE ONLY

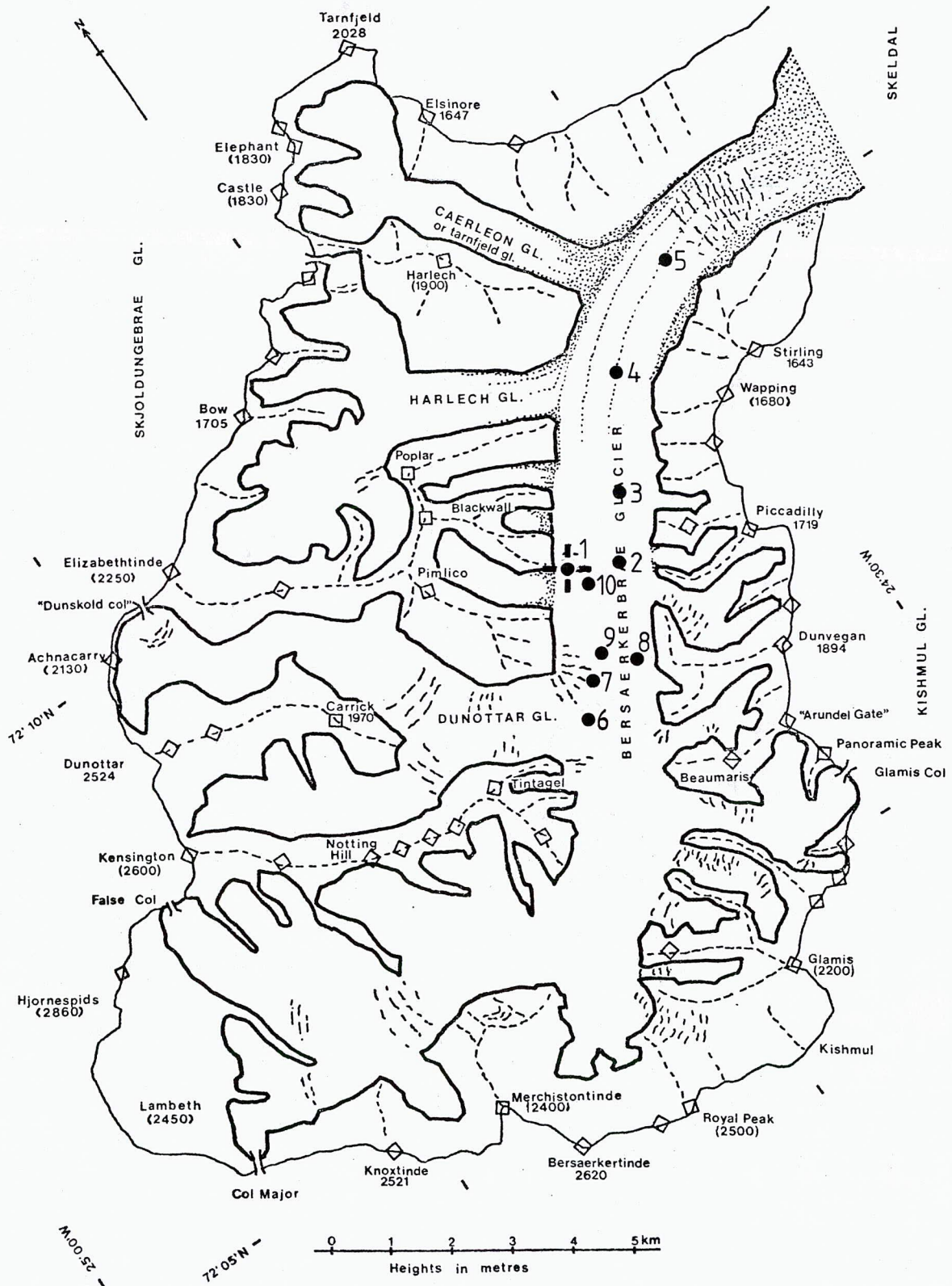


FIG. 10

EFFECT OF SPECIMEN DEPTH

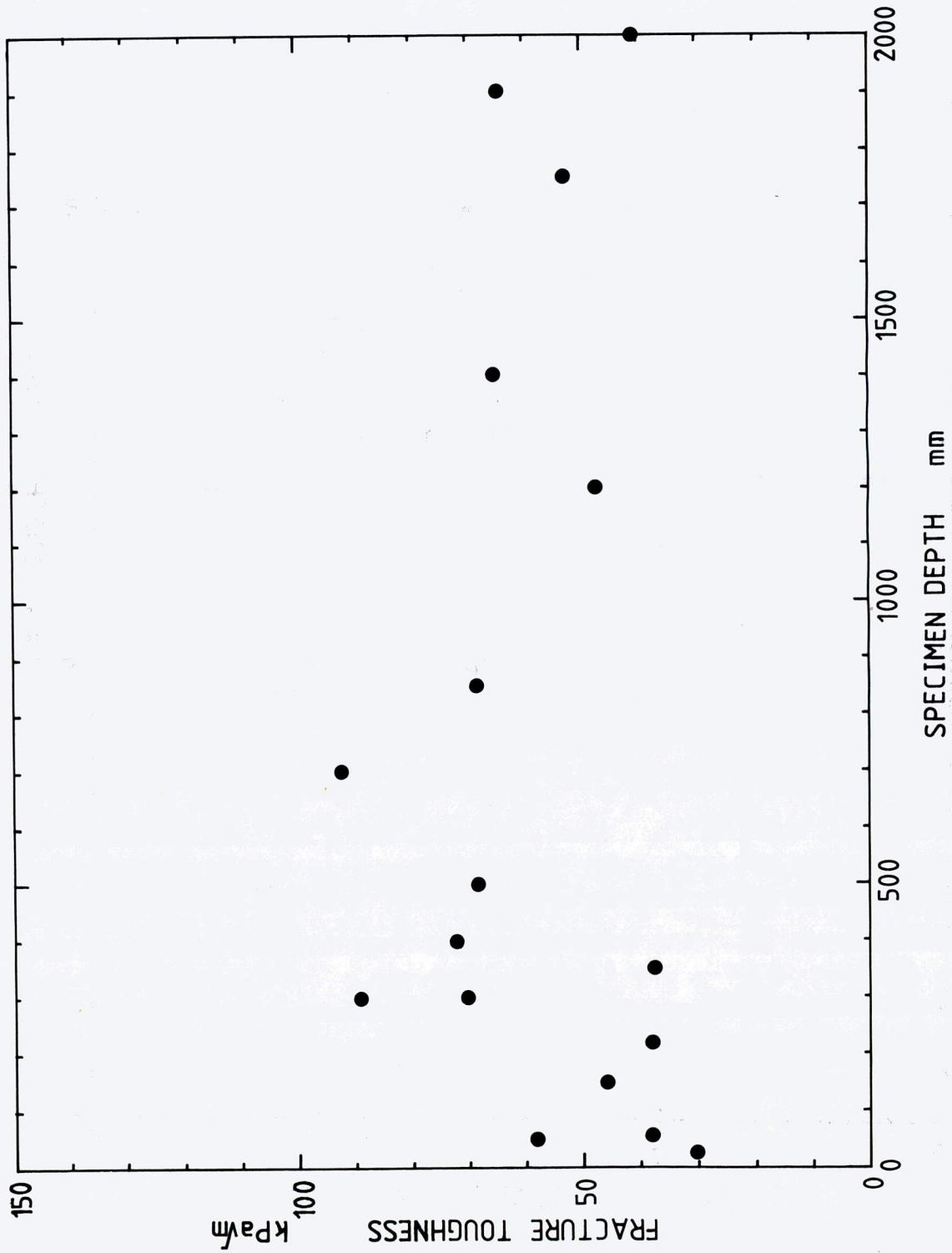
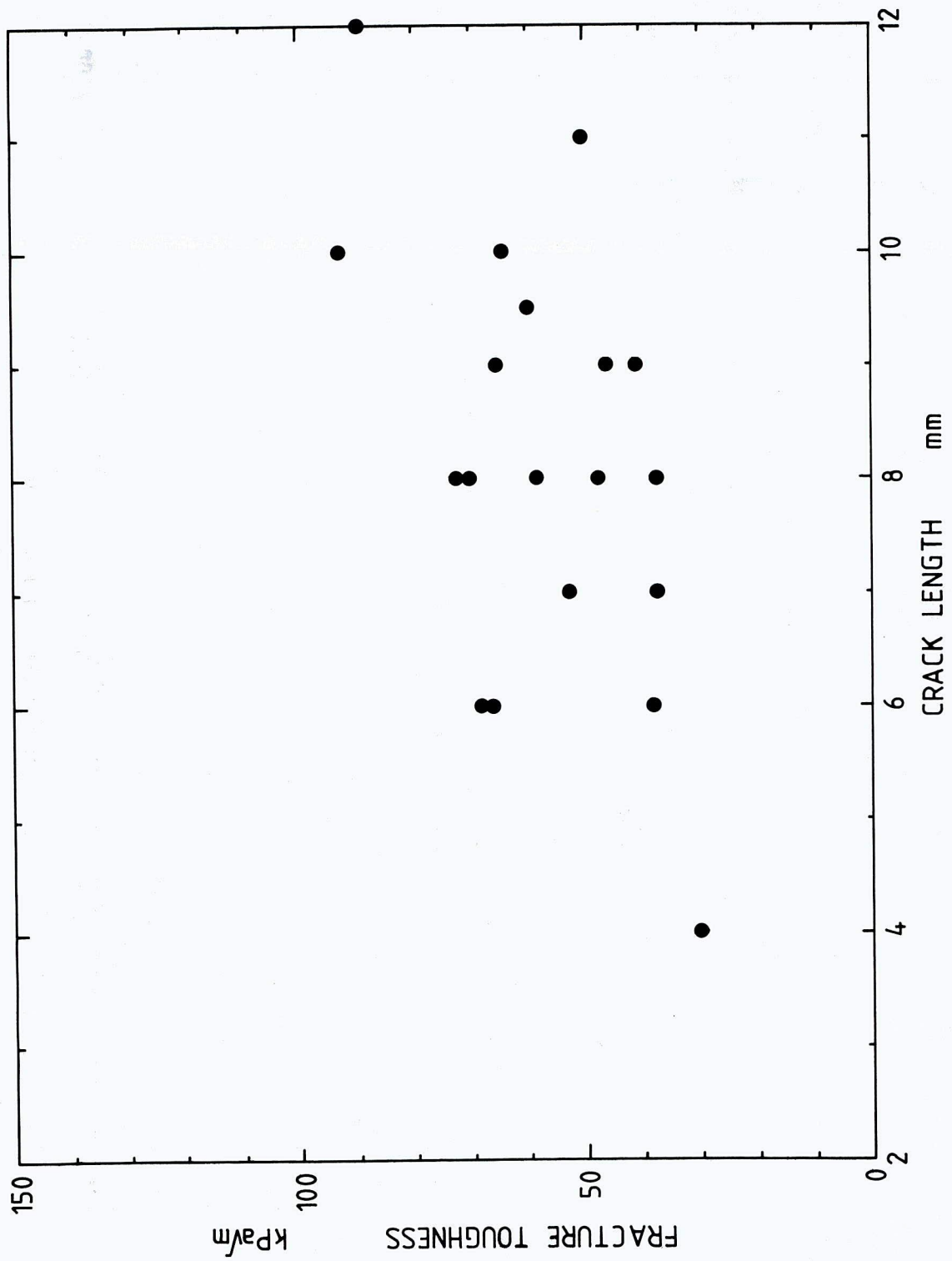


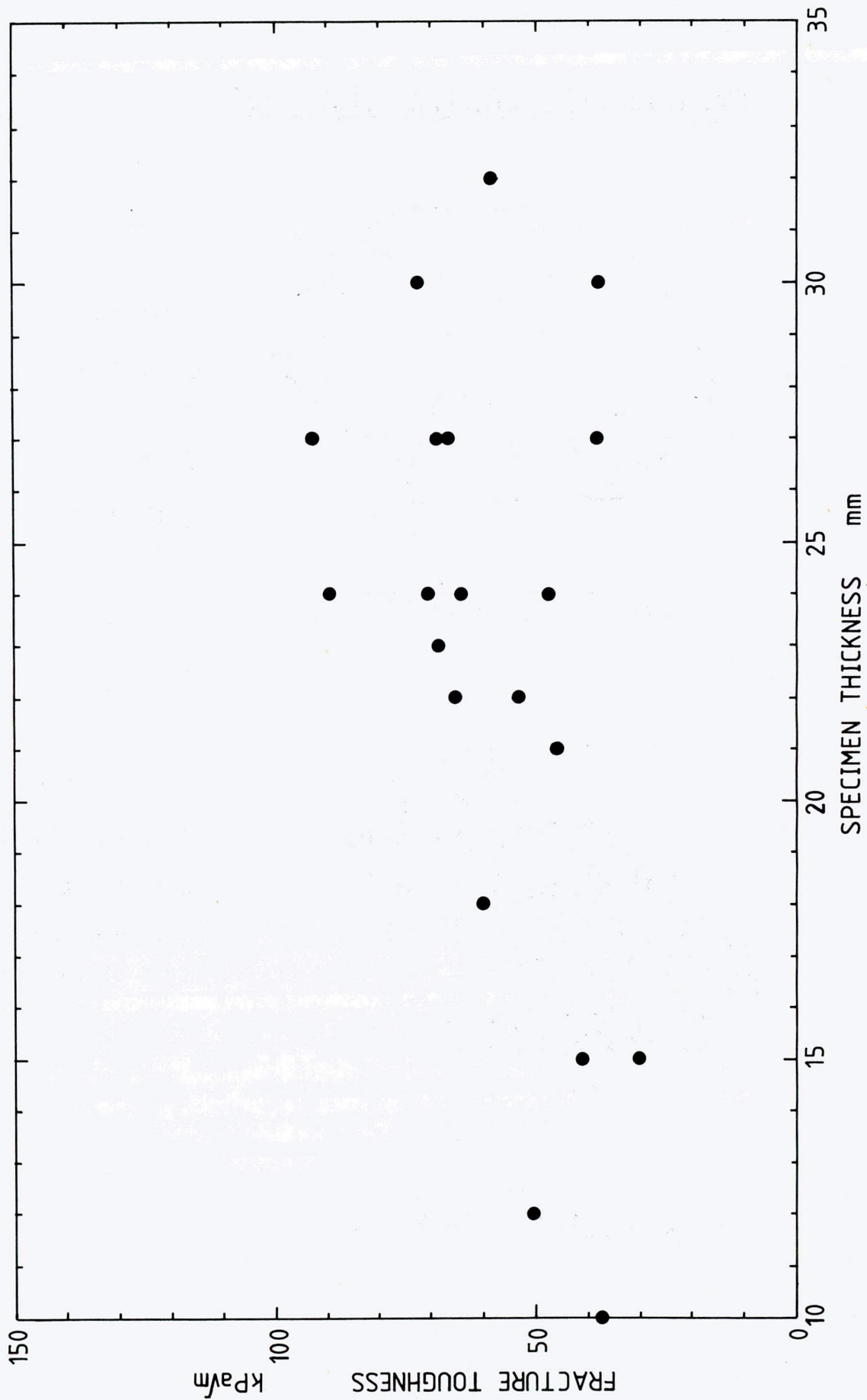
FIG. 11

EFFECT OF CRACK LENGTH

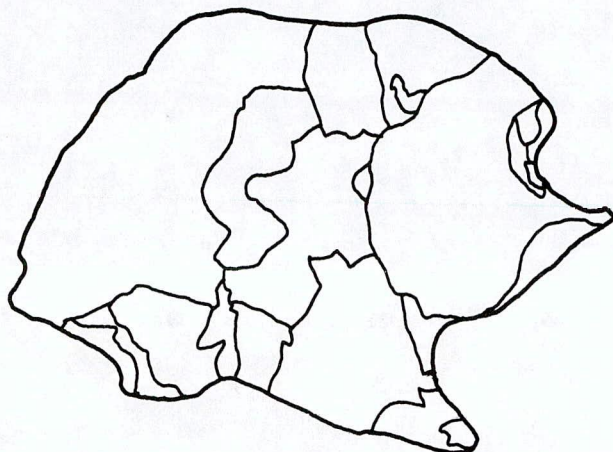


EFFECT OF SPECIMEN THICKNESS

FIG. 12



TYPICAL ICE CRISTAL TRACINGS



┌───┐ 10 mm

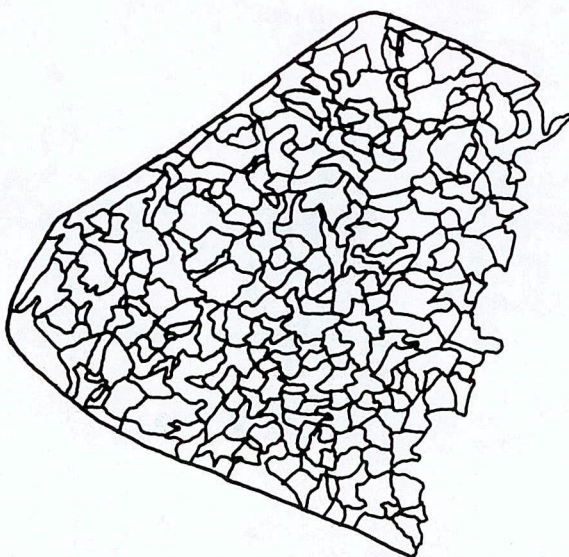
25 Grains

$d_{av} = 11.0$ mm

Site 2

Depth 200 mm

a) GLACIER ICE, BERSÆRKERBRÆ



┌───┐ 5 mm

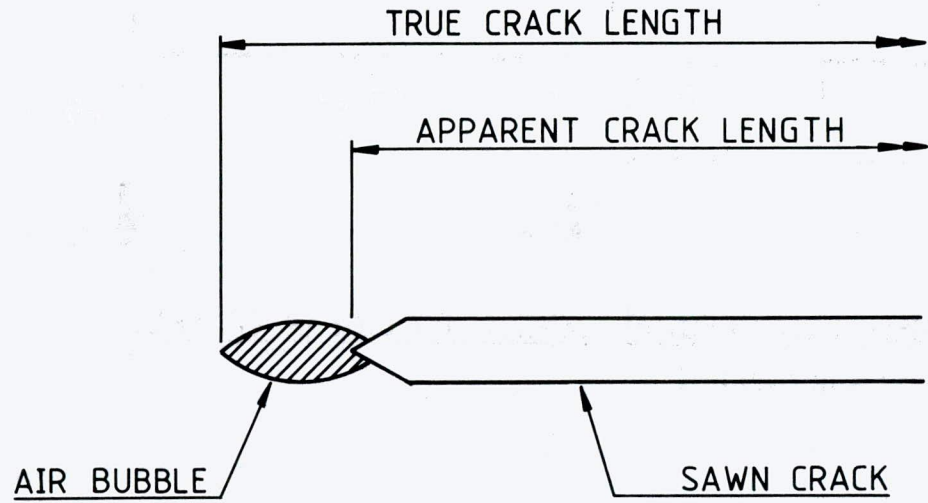
666 Grains (total)

$d_{av} = 0.91$ mm

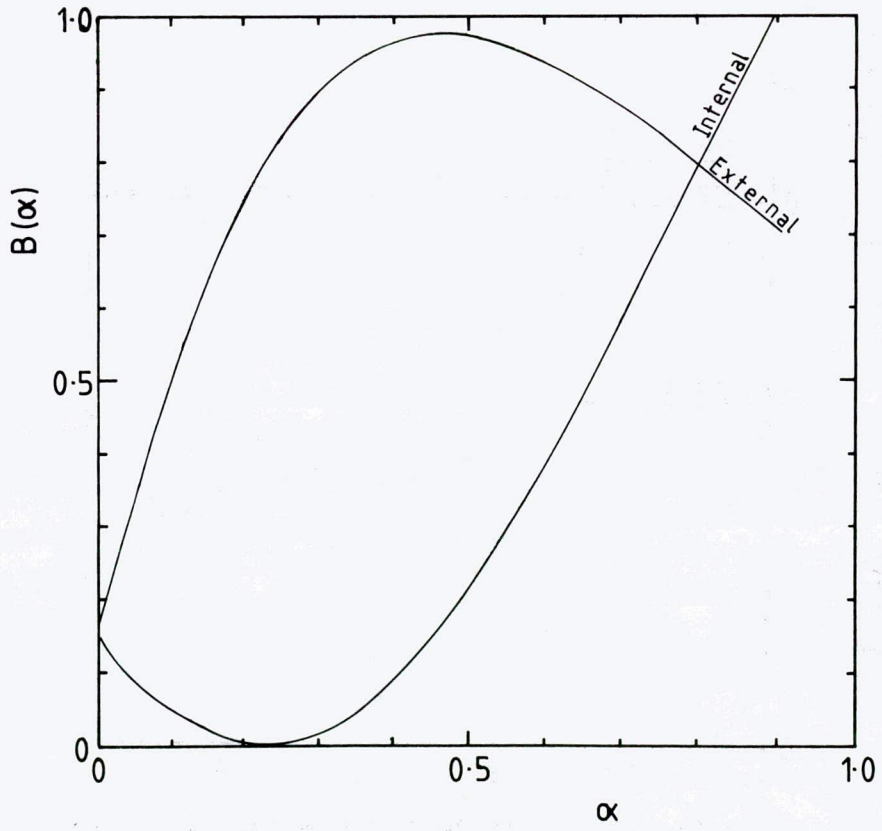
Note the larger
scale of this trace.

b) LABORATORY TRIALS (part only)

CRACK INTERSECTING AN AIR BUBBLE

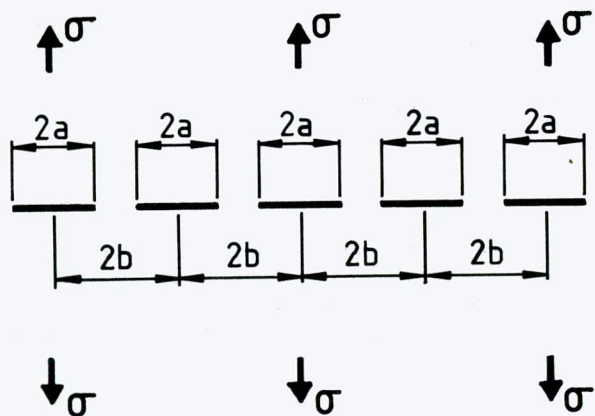


a) CRACK INTERSECTING AN AIR BUBBLE

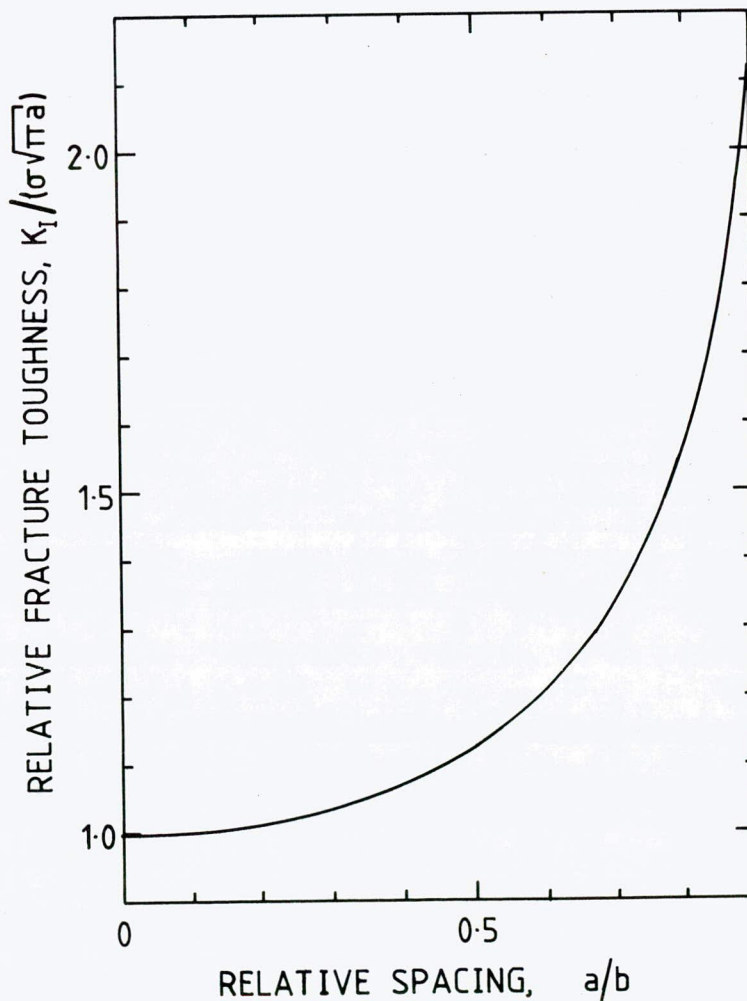


b) VARIATION OF INCREASE IN K_I WITH CRACK LENGTH (see text)

A ROW OF BUBBLES INITIATE FRACTURE



a) THE MODEL: INFINITE ARRAY OF CRACKS IN TENSION
(Rooke and Cartwright)



b) VARIATION OF STRESS INTENSITY WITH SPACING

2.3 PERCHED BLOCK REPORT

Summary

A large number of rocks were observed both qualitatively and quantitatively during the course of fieldwork. The major factors influencing perch block formation have been identified and discussed. A simple mechanism and a mathematical model have been presented. Further field work is necessary to assess the validity of the model.

Nomenclature

a	width of surface perpendicular to flow (m)
A	azimuth of normal to plane ($^{\circ}$)
b	displacement thickness (m)
C _p	specific heat capacity of water ($\text{J kg}^{-1} \text{K}^{-1}$)
d	diameter of cylindrical rock (m)
E	nett energy flux in a 24 hour period (J/m^2)
e _a	atmospheric water vapour pressure at a height at which diurnal fluctuations are negligible (mm Hg)
h	height of cylindrical rock (m)
K	Von Karman's constant
K _h	defined in text by expression (8)
k _h	thermal conductivity of air
l	characteristic length on which Reynolds No. is based (m)
n	fraction of sky observed
Pr	Prandtl number
Q	convective heat transfer flux (W/m^2)
R	radiative heat transfer flux (W/m^2)
R _D	defined in text by expressions (2) and (15)
Re _l	Reynolds Number
T _l	temperature (K)
T _a	temperature at a height at which diurnal fluctuations are negligible ($^{\circ}\text{K}$)
t	local hour angle (radians)
u	wind speed (m s^{-1})
x	symbol used to define scripts
z	height above glacier surface (m)
z _s	surface roughness of the ice surface (m)
α	albedo
β	angle of inclination of plane
δ	angle of declination
ε	emissivity
ρ	air density
σ	Stefan-Boltzmanns constant
φ	latitude
μ _z	dry adiabatic lapse rate
ν ^z	air viscosity

Subscripts

H	horizontal surface
i	exposed glacier surface
r	rock-shielded ice surface
R	rock surface
V	vertical surface

z at height z above surface
0 at the surface, i.e. z = 0
2 at 2m above the surface, i.e. z = 2 m
b at height b, the displacement thickness above the glacier surface

Superscripts

\bar{x} mean value of x, exact definition explained in text

Prefix

Σx total of variable x in 24 hour period

Introduction

Perched blocks are isolated rocks or boulders which are supported above the glacier surface on pedestals of ice. It is easily observable that rocks on a glacier surface either sink into the ice or grow pedestals underneath them. Whether a rock sinks or perches is dependent on a number of factors which are the subject of this project. However it is obvious the shape and size are major factors, the larger the rock the more likely it is to form a perch. Once a rock has perched then it seems reasonable to surmise that it will eventually fall off its perch. When it falls off it may roll for some distance along the glacier surface so that on an annual basis the velocity of the rock and the glacier surface will not be the same. When surveying a glacier it is a common technique to use large rocks as markers to measure the glacier's velocity. If the hypothesis that the rocks move independent of the glacier surface is correct then any survey adopting this method would be prone to error.

A second point of interest related to perch formation is that a structure erected on a glacier would behave in a similar manner to the rocks investigated.

The aim of this project is to identify the factors involved in the perching mechanism, to assess the critical size which determines whether a rock will sink or perch and to observe movement or evidence of movement of rocks along the glacier surface.

Fieldwork

The project's fieldwork was divided into two major parts. Firstly the observation of a number of naturally positioned large rocks, and secondly an attempt to 'grow' perched blocks on an area of flat ice using rocks that had been manhandled there.

The first part, the observation of large rocks, involved searching the glacier for rocks that were considered likely to perch. Fifteen were chosen and numbered for reference. They varied in size from about 0.5m across to 5m. Each boulder was photographed weekly so that its rate of perching or sinking could be assessed. Figure 1 shows three of these rocks on their perches, the development of a perch is shown in figure 8. Except for the three largest boulders which were the size of a small cottage, the dimensions of the rocks were recorded along with the angle of maximum inclination to the horizontal of the upper surface and the bearing of the plane containing that angle.

In addition as part of the datalogger trials rotation meters were attached to three rocks, Nos. 9, 10 and 15, the results are given in fig. 2 (and rock No. 9 with the rotation meter is shown in fig. 3 (b) and (c)). This data has proved of little use in this project because the test period was not long enough. However it was a useful demonstration of the datalogger's capabilities, for further details see the report on the datalogger, section SDL-TN8.

The second part of the fieldwork was delayed until a fresh snowfall cleared from the glacier and then it ran concurrently with the work already described i.e. from 15 July to 21 August 1982. An area of approximately flat ice with no crevasses was found and cleared of all debris. Then twenty rocks of various shapes and sizes were selected and manhandled into the test area. They were arranged in rows and columns far enough apart to assure that they would not influence one another. Figure 3 (a) shows the test site (which became known as the Perch Block Farm) with the rocks in place. Before each rock was finally positioned it was photographically surveyed. The rocks were then left

until the end of the test period when the ice surface around them was surveyed using apparatus constructed in the field.

The rocks were also photographed during this survey. Due to computation difficulties the numerical data has not yet been processed to give contours of surface height around the rocks.

Throughout the test period meteorological data was recorded. During datalogger trials diurnal wet and dry sand, and gravel temperatures were obtained on typical days (experiment 9, in the section 2.1, the Datalogger report).

Mathematical Model for the Perch Mechanism

Ablation and Factors Influencing It

A rock perches because the ice underneath does not receive as much energy for melting as the exposed glacier surface. As a result the glacier surface melts faster leaving the rock perched on a pedestal of ice. To attempt to quantify this process it is necessary to compare the melt rates for the two ice surfaces. To do this the process of ablation, which is the process by which the glacier ice melts, needs to be considered.

The ablation rate of the ice surface of a glacier is dependent on the supply and removal of heat and mass. Mass is supplied by snowfall. Mass removal is controlled by the removal or supply of heat causing freezing or melting. So in considering the local melt rates around the rock the heat exchange is of primary importance. The following factors need to be accounted for in the heat balance, heat being supplied by

- (1) Short-wave radiation.
- (2) Long-wave radiation.
- (3) Molecular conduction from the air, if the temperature gradient above the ice surface is positive.
- (4) Eddy conduction if the temperature gradient above the ice surface is positive and the air is turbulent.
- (5) Conduction from the underlying ice, if the ice temperature increases with distance below the surface.
- (6) Condensation on the surface of water vapour from the air if the water vapour pressure increases with height.
- (7) Freezing of rain.

Heat will be lost due to outgoing long-wave radiation and due to (3) to (6) inclusive if the temperature gradients are reversed. The presence of the rock affects all these processes, however it is possible to simplify the problem. It is generally accepted that radiation, convection (or eddy conduction) and water vapour flux are the only factors that need to be considered, the remainder can be neglected. Taylor and Lister (1) have shown that for the Britannia Glacier ($77^{\circ} 14'N$, $23^{\circ} 49'W$) in North East Greenland the relative importance to ablation of these three energy fluxes is

Radiation	67%
Convection	32%
Water vapour flux	1%

It is therefore possible to consider only radiation and convection, and to neglect condensation and evaporation of water vapour.

Theoretical Energy Balance for Exposed Glacier Ice and Rock-Shielded Ice

If the rock reduces the amount of energy reaching the ice surface beneath it compared to the nett energy flux to the exposed glacier per unit area of surface then the rock will perch. This is because the ice underneath the rock will not melt as quickly as the exposed ice. This assumes the effect of pressure melting due to the weight of the rock can be neglected.

To decide whether a rock is likely to perch it is necessary to consider the energy balances for the rock shielded ice and the exposed ice. Diurnal fluctuations are eliminated by summing the energy balances over a 24 hour period. The variations in temperatures and wind speeds from day to day during the summer months are small compared to the variations from hour to hour during the day.

As has been discussed it is only necessary to consider radiation and convection fluxes for the exposed ice surface. The expression given by Halstead (2) for the solar radiation flux at a horizontal surface is

$$R_H = R_D(1 - n)(1 - \alpha) - (1 - 0.77n)\epsilon\sigma[(T_o^4 - T_a^4) + T_a^4(0.18 + 0.25 \times 10^{0.126e_a})] \quad (1)$$

$$\text{where } R_D = 1395(\sin\phi \sin\delta + \cos\phi \cos\delta \cos t) \quad (2)$$

ϕ is the latitude, δ the declination and t the local hour angle measured from noon and equal to $\pi/12$ radians per hour.

n is the fraction of the sky obscured by cloud and α is the surface albedo.

T_o is the surface temperature and T_a is the temperature at a height at which diurnal fluctuations are negligible. OUTCALT^a(3) has assumed that

$$T_a = (\bar{T}_2 - 22)$$

where \bar{T}_2 is the mean temperature 2 m above the ground. e_a is the atmospheric vapour pressure at the same height as T_a and can be calculated for T_a in the range 258 K to 273 K using

$$0.14179 \log_{10} e_a = \left\{ 0.718966 + 9.18726 \frac{(T_a - 273)}{T_a} \right\} \quad [\text{mm Hg}] \quad (3)$$

σ is Stefan-Boltzmann's constant ($= 5.67 \times 10^{-8}$) and ϵ is the emissivity of the surface, approximately 0.9 for most surfaces.

Hence for the ice surface the radiation flux is given by

$$R_{H_i} = 1395(\sin\phi \sin\delta + \cos\phi \cos\delta \cos t)(1 - \bar{n})(1 - \alpha_i) - (1 - 0.77\bar{n})\epsilon\sigma[(273^4 - T_a^4) + T_a^4(0.18 + 0.25 \times 10^{0.126e_a})] \quad (4)$$

where \bar{n} is the mean cloud cover for the month.

To calculate the total nett radiation flux to the surface in 24 hours integrate expression (4) for a 24 hour period

$$\Sigma R_i = \frac{3600}{\pi/12} \int_0^{2\pi} \left\{ 1395(\sin\phi \sin\delta + \cos\phi \cos\delta \cos t)(1 - \bar{n})(1 - \alpha_i) - (1 - 0.77\bar{n})\epsilon\sigma[(273^4 - T_a^4) + T_a^4(0.18 + 0.25 \times 10^{0.126e_a})] \right\} dt \quad (5)$$

simplifying

$$\Sigma R_i = 1.2 \times 10^8 (\sin\phi \sin\delta)(1 - \bar{n})(1 - \alpha_i) - 4.9 \times 10^3 (1 - 0.77\bar{n})\epsilon[(273^4 - T_a^4) + T_a^4(0.18 + 0.25 \times 10^{0.126e_a})] \quad (6)$$

The energy flux to the glacier surface due to convection cannot be calculated using the standard convective heat transfer formulae because the glacier surface has to be considered as an infinite surface with special boundary conditions. Drake (4) gives the following empirical expression

$$Q = K_h \rho C_p \frac{(T_z - T_o + \mu_z)}{z} \quad (7)$$

where

$$K_h = \frac{K U_z z}{[\ln(z/z_s)]^2}$$

K is Von Karman's constant ($= 0.42$), U_z and T_z are the wind speed and air temper-

ature at height z . As most meteorological data is recorded at about 2 m it is convenient to take $z = 2\text{m}$. z_s is the surface roughness of the ice surface, typically 0.005m. μ is the dry adiabatic lapse rate ($= 0.0098$) and ρ and C_p are the density and specific heat capacity of air respectively.

The temperature at 2 m above the glacier surface is a function of time. It can be approximated by

$$T_2 = \frac{(T_{2_{\max}} - T_{2_{\min}})}{2} \cos t + \bar{T}_2 \quad (9)$$

where $T_{2_{\max}}$ and $T_{2_{\min}}$ are daily maximum and minimum. Means of the daily maxima and minima during the month under study can be used. Similarly \bar{T}_2 is the daily mean and can be averaged for the month or months considered. For a comparison of this distribution with experimental data see figure 4. To find the total convective flux over 24 hour integrate with respect to time, hence from (7), (8) and (9)

$$\Sigma Q_I = \frac{3600}{\pi/12} \int_0^{2\pi} \frac{K U_{2.2}}{(\ln 2/0.005)^2} \frac{\rho C_p}{2} \left[\frac{(T_{2_{\max}} - T_{2_{\min}})}{2} \cos t + \bar{T}_2 - 273 + \mu_z \right] dt \quad (10)$$

simplifying

$$\Sigma Q_I = 1.29 \times 10^6 [\bar{T}_2 - 273 + \mu_z] \quad (11)$$

The total energy absorbed by the exposed ice surface in 24 hours is

$$E_i = \Sigma R_i + \Sigma Q_i \quad \text{J/m}^2 \quad (12)$$

Now consider the rock shielded ice. Apply the 1st Law of Thermodynamics to the rock as a system. The 1st law is the principle of conservation of energy in terms of heat and work transfer applied to a system of constant mass. In the case of the rock there is no work transfer but there is heat transfer. Assume that at the end of a 24 hour period the internal energy state of the rock is the same as the state of the start of that period. Then in the same period to satisfy the 1st law the sum of the heat transfer across the boundaries must be zero. There are three types of heat transfer, conduction, convection and radiation. There will be conductive heat transfer between the rock and ice beneath it and this will be equal to the convective and radiated heat transfer across the other boundaries, i.e.

$$E_r = \Sigma R_R - \Sigma Q_R \quad (13)$$

ΣQ_R has a negative sign because it is a heat loss from the system, as is the conductive heat transfer, E_i .

The most convenient shape of rock to consider is a cylinder standing on end of height h and diameter d . The wind direction and sun's bearing then have no effect on the geometry of the situation.

The radiation flux for the horizontal surface from expressions (1) and (2) is

$$R_{H_R} = \left\{ 1395(\sin\phi \sin\delta + \cos\phi \cos\delta \cos t)(1-\bar{n})(1-\alpha_R) - (1-0.77n) \right. \\ \left. \epsilon\sigma[(T_{O_R}^4 - T_a^4) + T_a^4(0.18 + 0.25 \times 10^{0.126e_a})] \right\} \frac{\pi d^2}{4} \quad (14)$$

To avoid complicated integration assume in this case that T_{O_R} is constant. If the median value is used then for the data collected on the expedition the error is less than 3 percent.

For the vertical faces the geometric factors in expression (2) are changed to give

$$R_D = \left\{ 1395 \cos \beta (\sin \phi \sin \delta + \cos \phi \cos \delta \cos t) + \sin \epsilon (\cos A [\tan \phi \{ \sin \phi \sin \delta + \cos \phi \cos \delta \cos t \} - \sin \delta \sec \phi] + \sin A \sin \delta \sin t) \right\} \quad (15)$$

where β is the angle of tilt of the plane, and A is the azimuth of the normal to the plane. The radiation flux for the vertical face projected towards the sun is

$$R_{V_R} = dh \left\{ (1395 \cos A [\tan \phi (\sin \phi \sin \delta + \cos \phi \cos \delta \cos t) - \sin \delta \sec \phi] + \sin A \sin \delta \sin t) \right. \\ \left. (1 - \bar{n})(1 - \alpha_R) - (1 - 0.77\bar{n}) \epsilon \sigma (T_o^4 - T_a^4) + T_a^4 (0.18 + 0.25 \times 10^{0.126e_a}) \right\} \quad (16)$$

The total radiated heat transfer in 24 hours is found by integrating expressions (14) and (16) with respect to time

$$\Sigma R_R = \frac{3600}{\pi/12} \int_0^{2\pi} R_{H_R} + R_{V_R} dt \quad (17)$$

i.e.

$$\Sigma R_R = 1.2 \times 10^8 (1 - \bar{n}) (1 - \alpha_R) (\pi d^2/4 \sin \phi \sin \delta + dh \cos A [\tan \phi \sin \phi \sin \delta - \sin \delta \sec \phi]) \\ - (\pi d^2/4 + dh) (4.9 \times 10^{-3}) (1 - 0.77\bar{n}) \epsilon [(T_{o_R}^4 - T_a^4) + T_a^4 (0.18 + 0.25 \times 10^{0.126e_a})] \quad (18)$$

From classical heat transfer theory (see Ede (5)) the forced convective heat transfer from a finite surface is given by

$$Q = 0.037 Pr^{1/3} Re_1^{4/5} a k (T_{o_R} - T_2) \quad (19)$$

where Pr is the Prandtl number (0.71) and Re_1 the Reynolds number based on l the length of the surface parallel to the flow, for a circle l is taken as $0.785 d$

$$Re = \frac{\rho u l}{\eta} \quad (20)$$

which is the mean length

ρ and η are the air density and viscosity respectively ($\rho = 1.27$ and $\eta = 1.75 \times 10^{-5}$).

The wind speed u is a function of the height above the glacier surface while within the boundary layer. Assuming that the boundary layer is larger than any rocks considered, the boundary layer profile can be approximated using the 1/7th power law (see Streeter and Wylie (6))

$$u_z = U_b (z/b)^{1/7} \quad (21)$$

where z is the height of the glacier and U_b is the wind speed at the displacement thickness. Assume the displacement thickness is 2 m then $U_b = u_2$.

' a ' is the width of the surface normal to the flow, and k is the thermal conductivity of the air ($= 2.47 \times 10^{-2}$).

$$T_{o_R}, \text{ the rock surface temperature is a function of time of the same form as } T_2 \text{ i.e.} \\ T_{o_R} = \frac{(T_{o_{Rmax}} - T_{o_{Rmin}})}{2} \cos t + \bar{T}_{o_R} \quad (22)$$

hence substituting (20), (21) and (22) into expression (19) and integrating over 24 hours the total convective heat transfer in that period is

$$\Sigma Q_R = \frac{3600}{\pi/12} \int_0^{2\pi} \left\{ 0.037(0.71)^{1/3} \frac{([T_{oRmax} - T_{oRmin} - T_{smax} - T_{2min}] \cos t + \bar{T}_{oR} - \bar{T}_2)}{2} + \bar{T}_{oR} - \bar{T}_2 \right\}^{4/5} (\rho u_2/\eta)^{4/5} k \left[\left\{ (u_2/2)^{1/7} 0.785d \right\}^{4/5} 0.785d + \left\{ 2 \int_0^h (z/2)^{1/7} \frac{\pi d}{2} dz \right\}^{4/5} \right] dt$$

simplifying

$$\begin{aligned} \Sigma Q_R &= 5.45 \times 10^5 (\bar{T}_{oR} - \bar{T}_2) u_2^{4/5} (0.598 h^{33/35} d^{9/5} + 2.075 h^{68/35} d^{4/5}) \\ &= 5.45 \times 10^5 (\bar{T}_{oR} - \bar{T}_2) u_2^{4/5} h^{0.94} d^{4/5} (0.598d + 2.075h) \end{aligned} \quad (23)$$

hence substituting expressions (18) and (23) in (13)

$$\begin{aligned} E_r &= \{ 1.2 \times 10^8 (1 - \bar{n})(1 - \alpha_R) (\sin \phi \sin \delta + 1.27hd^{-1} \cos A [\tan \phi \sin \phi \sin \delta - \sin \delta \sec \phi]) \\ &\quad - (1 + 1.27hd^{-1})(4.9 \times 10^{-3})(1 - 0.77n) \epsilon [(T_{oR}^4 - T_a^4) + T_a^4 (0.18 + 0.25 \times 10^{0.126e_a})] \\ &\quad - 6.88 \times 10^5 (\bar{T}_{oR} - \bar{T}_2) u_2^{4/5} h^{0.94} d^{-6/5} (0.598d + 2.075h) \} \quad J/m^2 \end{aligned} \quad (24)$$

for the rock to perch the exposed ice must receive more energy so that it melts faster, i.e. the criterion for a rock to perch is that

$$E_i - E_r > 0 \quad (25)$$

this can be evaluated for a particular location i.e. an entire glacier (in terms of the rock dimensions h and d), by substituting expressions (6), (11) and (24) and the necessary data. However rocks are not cylinders as has been assumed. To apply the criterion to particular rocks h is given by the mean height of the rock and d can be taken as the mean of the diameter of the largest inscribed and smallest circumscribed circles it is possible to fit on the upper surface. This approach avoids misleading values which large protruberances or incisions might otherwise produce.

Discussion

The mathematical model presented in the previous section had its genesis while the expedition was in the field, but it was not developed in detail until after the expedition had returned to the United Kingdom. Unfortunately insufficient data was gathered to allow the model to be applied to rocks observed. The expedition lacked enough spare apparatus to allow meaningful rock surface temperatures to be measured when it was realised that this data was needed for the model. It is therefore not possible to comment on the validity of the mathematical model using experimental data.

However, the following comments can be made on the observations gathered in the field. Solar radiation is a key factor in the perch mechanism. Figure 5 shows a frequency plot for the bearing towards which the rocks tilted. The peak occurs at the interval $210-220^\circ$ which corresponds to the bearing of the sun at midday local time until half-hour after (Figure 6) when the incident solar radiation will be at peak intensity. The side of the rock facing the midday sun will receive the most radiation which will melt the ice in that region faster causing the rock to tilt downwards at that side. This tilting was observed both on rocks that were already perched and those attempting to perch on the Perch Block Farm.

The prevailing wind direction was 245° , it was a katabatic wind blowing down the glacier. The wind will cause further accelerated melting of ice pedestals on the south westerly side. However from the reports of the direction of tilt on the Roslin glacier and the fact that the rocks with no pedestals attempting to perch tilt towards the midday sun, the solar radiation is more important than the forced convection caused by the katabatic wind. This agrees with conclusions of Lister and Taylor (1) on the relative importance of radiation and convection to ablation.

The rate of perching for rocks occurring naturally and the ones of similar size and shape on the Perch Block Farm is very different. The perched blocks that were

manhandled may have been 'planted' too late in the season. The test which started on 15 July was delayed by a fresh snowfall in early July. For the fifteen large rocks that were observed in their natural position, three had made large movements by 22 July, eight by 30 July and ten by 4 August. The remaining five made no large movements between 17 July and 21 August. This would seem to indicate that the majority of perching occurs early in the season, i.e. by early August.

Early in the season the quantity of meltwater runoff will be at a peak due to snow melting. At peak meltwater flow as well as the streams and rivers water also flows off the glacier surface in something approaching sheet flow. When this sheet of water meets a rock it will be diverted around the rock as shown in figure 7a. The effect of this will be to erode a channel around the rock, the development of which is shown in figure 7b. The result of this will be to erode a pedestal until the rock is undermined so that it falls over. On the Bersaerkerbrae because of the glacier's orientation the meltwater and solar mechanisms work hand in hand resulting in the series of developments shown in figure 7 and illustrated in figure 8.

Further support for the importance of meltwater flow comes from the Perch Block Farm. This was sited on a flat piece of ice on top of a slight rise, as a result there was little if any waterflow across the site. There was no evidence of the water channels seen around the naturally positioned rocks. In addition the ice surface was dirtier because of the lack of waterflow and this would retard the exposed ice ablation making the difference between exposed ice and rock-shielded ice melt rates smaller and hence the likelihood of perching smaller.

The cycle of events described in figure 7 appears to happen only once a season usually, however considerable evidence of rocks migrating across the glacier was seen (figure 3(c)).

Conclusions

Large rocks do move relative to the glacier surface by a mechanism summarised in figure 7. Rock size, shape, solar radiation, forced convection and meltwater water flow are the major factors in the perching mechanisms. A mathematical model involving all these factors except meltwater flow has been developed and can be used to predict whether a rock will perch. Further field work is needed to assess the model's accuracy.

References

1. Taylor, P.F. and Lister, H. Meddelelser om Grønland 158, 7, 1 (1961)
2. Halstead, M. H., Richman, R.L., Covey, W. and Merryman, J.D. 'A preliminary report on the design of a computer for micro-metrology. J. Meteorology, 14 (1957) 306-325.
3. Outcalt, S. I. 'The development and application of a simple digital surface simulation' J. Appl. Meteorology 11 (1972) 629-636.
4. Drake, J.J. 'The effects of surface dust on snow melt rates' Arctic and Alpine Research 13(2) 1981 219-223.
5. Ede, A. J. 'An introduction to heat transfer principles and calculations' International Series of Monographs in heating, ventilation and refrigeration, vol 2, Pergamon Press (1967) Chapter 5, p 76.
6. Streeter, V. L. and Wylie, E.B. 'Fluid mechanics' 6th edition McGraw-Hill Book Company (1975) Chapter 5 p 272.

Bibliography

1. Robinson, N. 'Solar Radiation' Elsevier Publishing Company (1966).
2. Paterson, W.S.B. 'The Physics of Glaciers' Pergamon Press (1972)

FIGURE 1(a)

Naturally positioned rock no. 12 photographed on 22 July 1982, on the Bersaerkerbrae, looking on a bearing of 250° .

This is the most spectacular perched block observed. It slowly fell towards the man in the photograph.

Photo: E.A. Patterson

FIGURE 1(b)

Naturally positioned rock no. 11 photographed on 11 August 1982, on the Bersaerkerbrae looking on a bearing of 150° .

This rock has already fallen off its perch and is starting to grow a new perch c.f. figure 7(a)

Photo: R. M. Andrews

FIGURE 1(c)

Naturally positioned rock no. 13 photographed on 4 August 1982, on the Bersaerkerbrae looking on a bearing of 245° .

Photo: R. M. Andrews

FIGURE 1

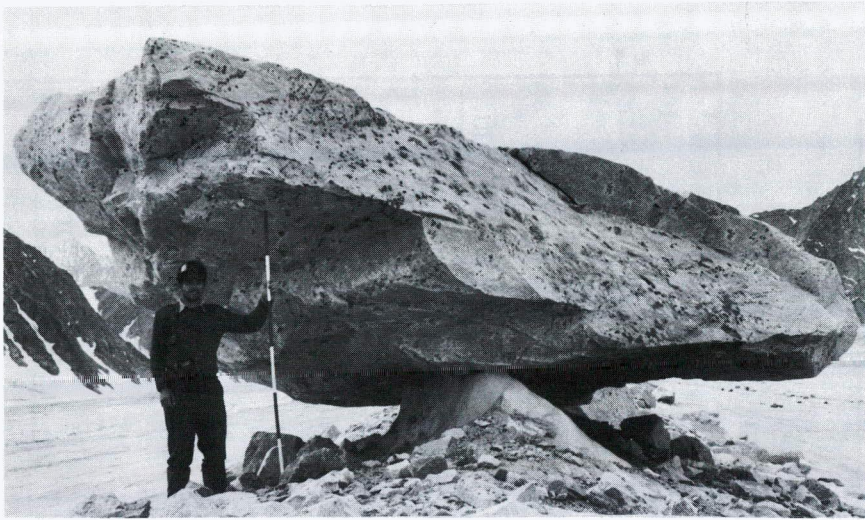


FIGURE 2(a) PLOT OF ROTATION-METER RESULTS FOR 31 JULY
TO 5 AUGUST 1982.

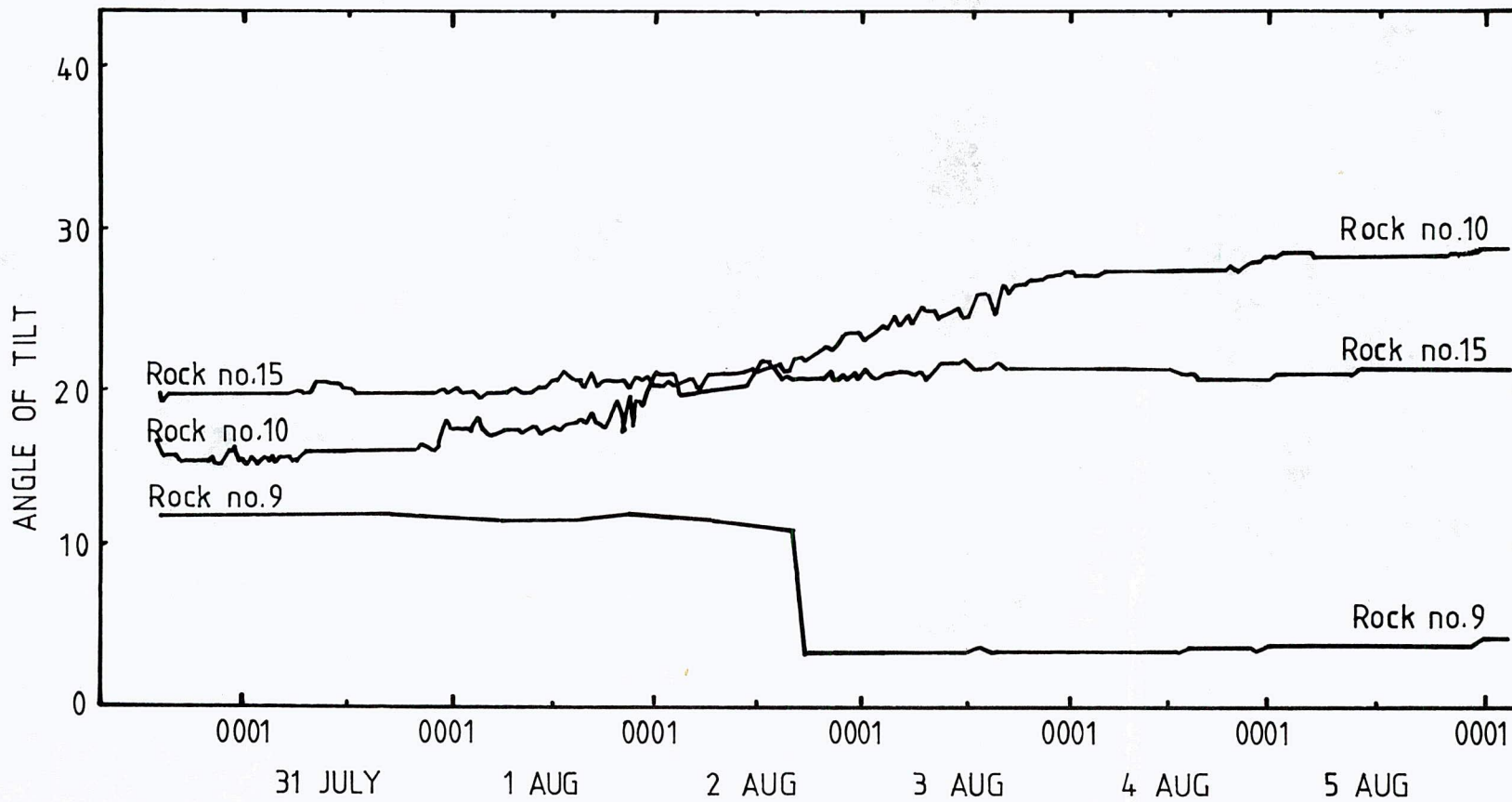


FIGURE 2(b) PLOT OF ROTATION-METER RESULTS FOR 6th TO 12th
AUGUST 1982.

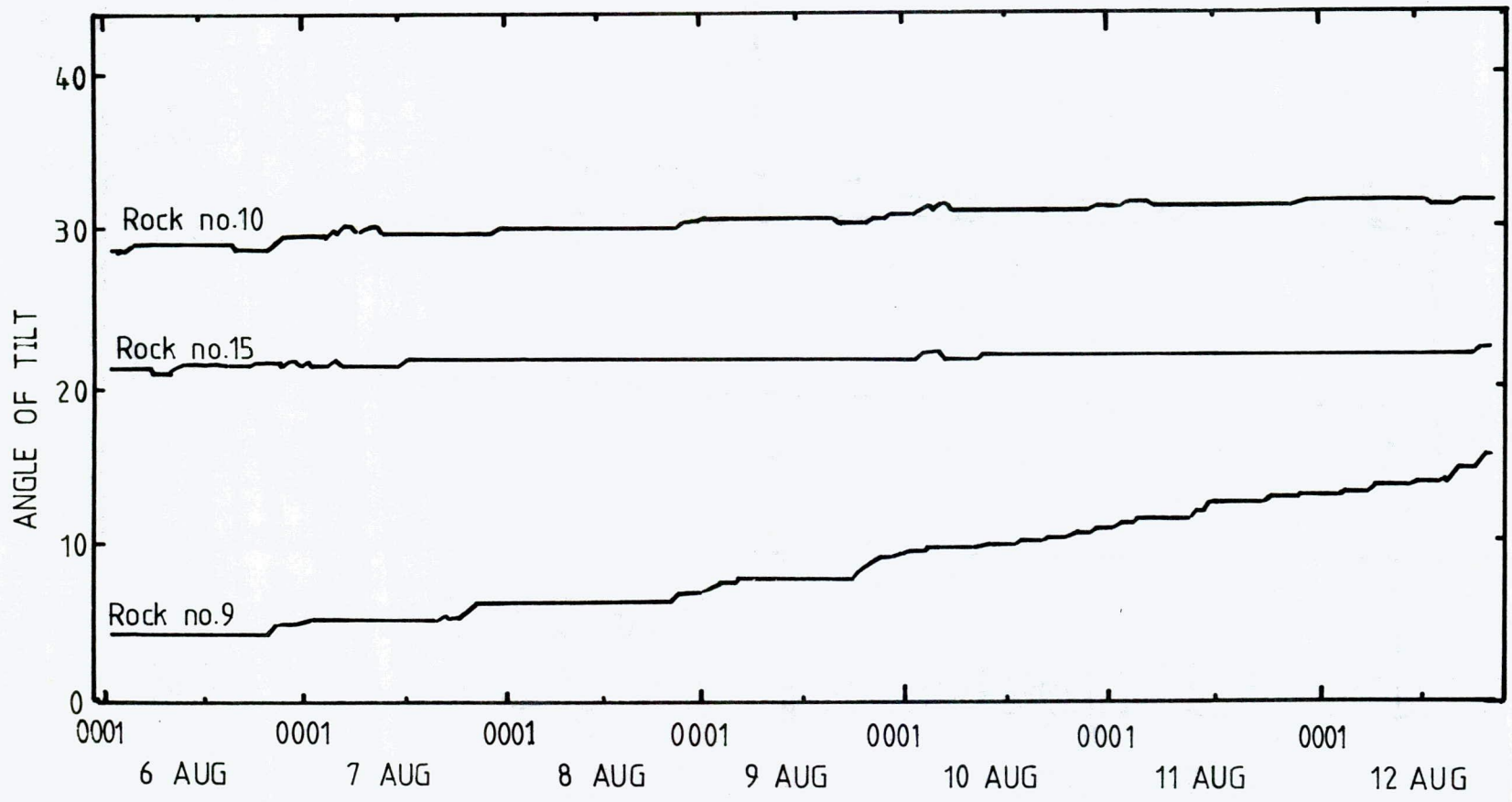


FIGURE 2(c) PLOT OF ROTATION-METER RESULTS FOR 13th TO 19th
AUGUST 1982.

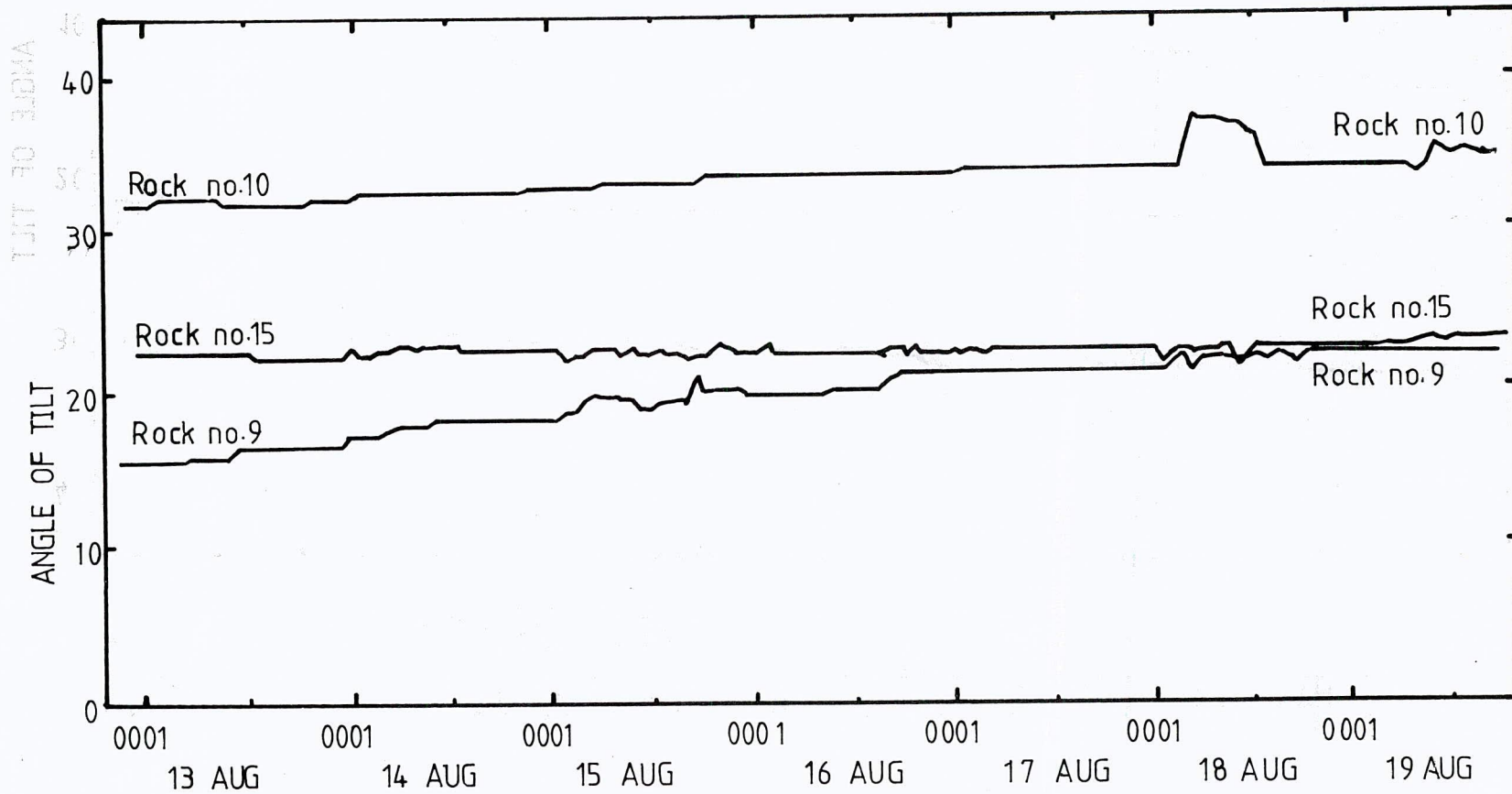


FIGURE 3(a)

The perch block test site (Perch Block Farm), shortly after the rocks had been manhandled into position

Photo: R. M. Andrews

FIGURE 3(b)

Naturally positioned rock no. 9, photographed on 30 July 1982 on the Bersaerkerbrae, looking on a bearing of 244°

This rock is fitted with a rotation-meter which is not connected in this photograph. The rock fell of its perch the following day before the rotation meter was connected.

Photo: R. M. Andrews

FIGURE 3(c)

Naturally positioned rock 9, photographed on 4 August 1982 on the Bersaerkerbrae looking on a bearing of 250° .

The photograph illustrates the rock movement across the glacier surface since it moved to its present position from where the man is standing by forming and falling off a number of perches.

Photo: R. M. Andrews

FIGURE 3



FIGURE 4 TEMPERATURE DISTRIBUTION IN EXPRESSION (9)
AGAINST AIR TEMPERATURES AT A HEIGHT OF 2m.

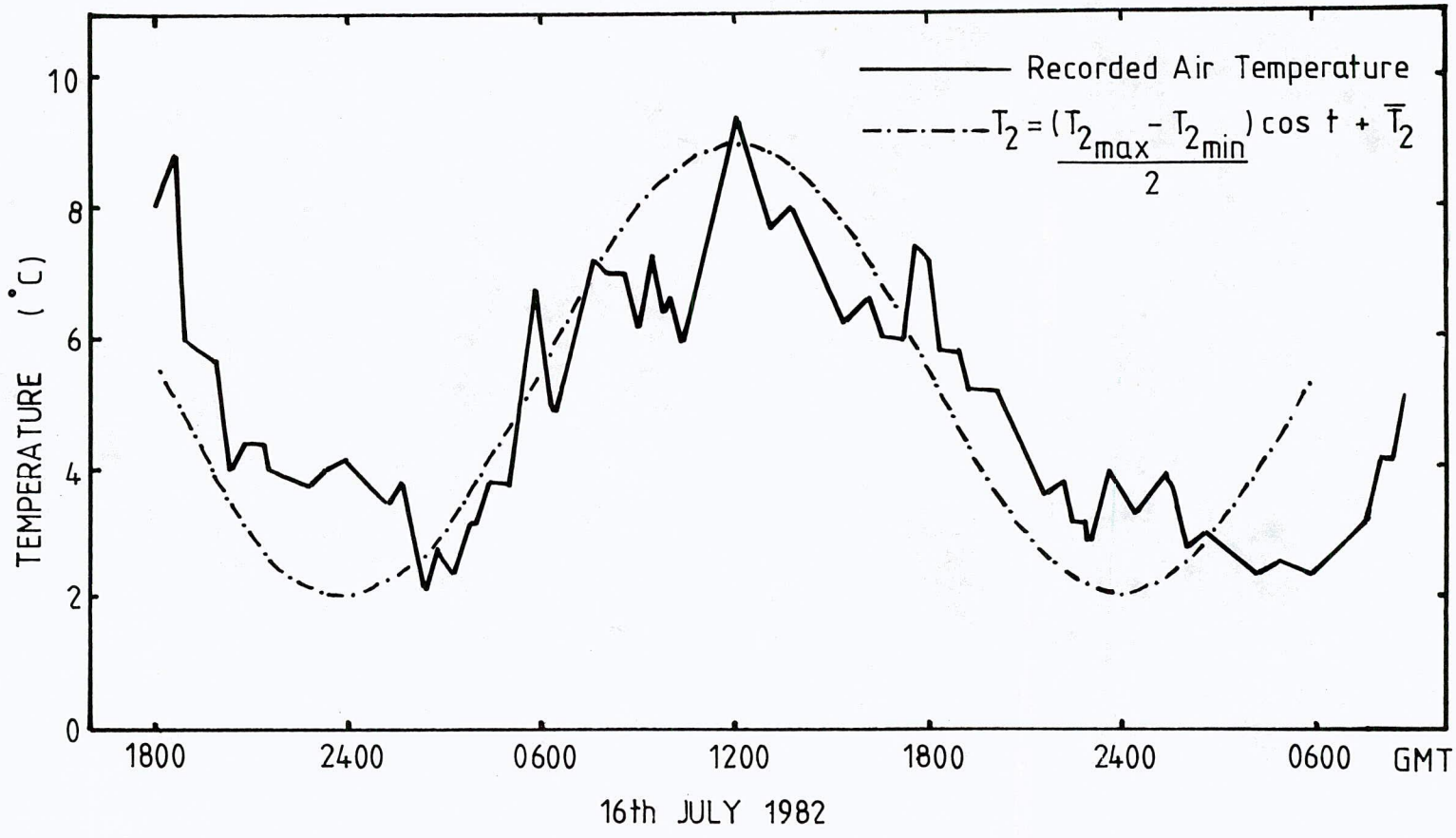


FIGURE 5 FREQUENCY DISTRIBUTION OF BEARING OF
MAXIMUM INCLINATION OF TOP OF ROCK.

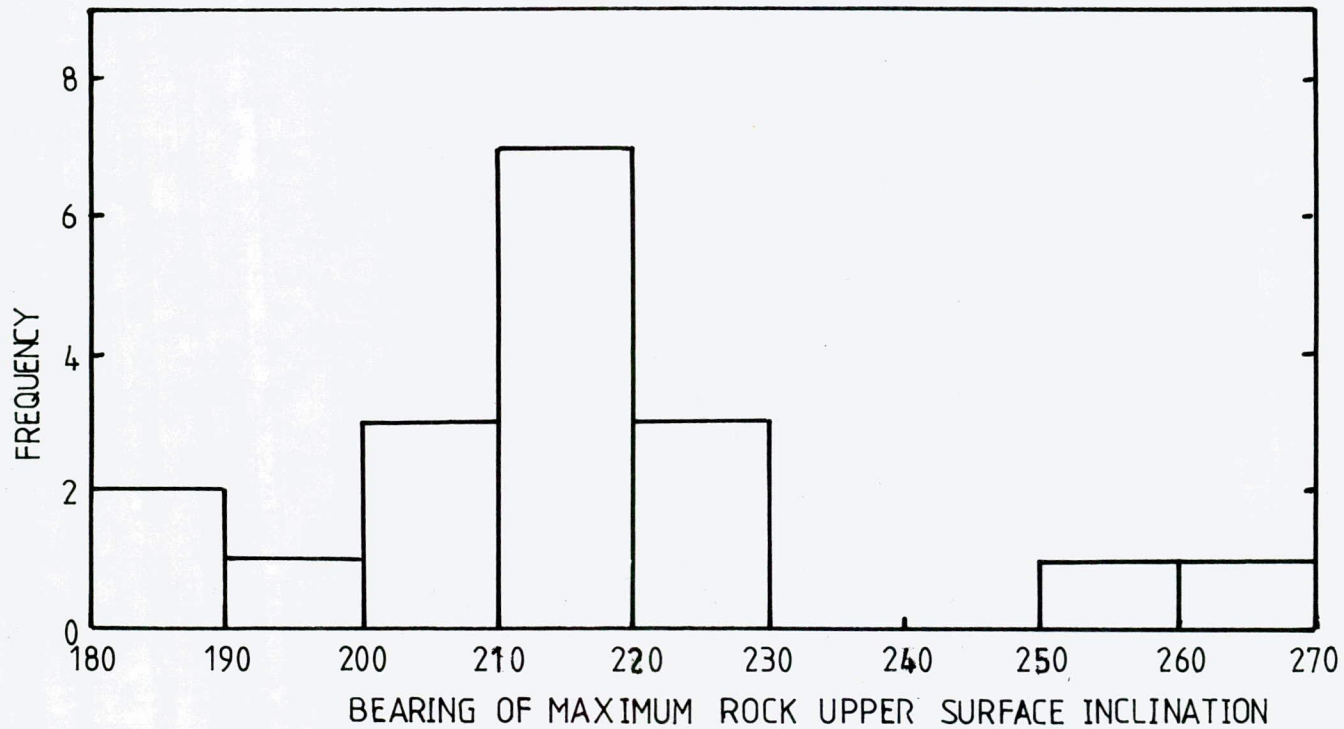


FIGURE 6 GRAPH OF SUN'S BEARING AGAINST TIME.

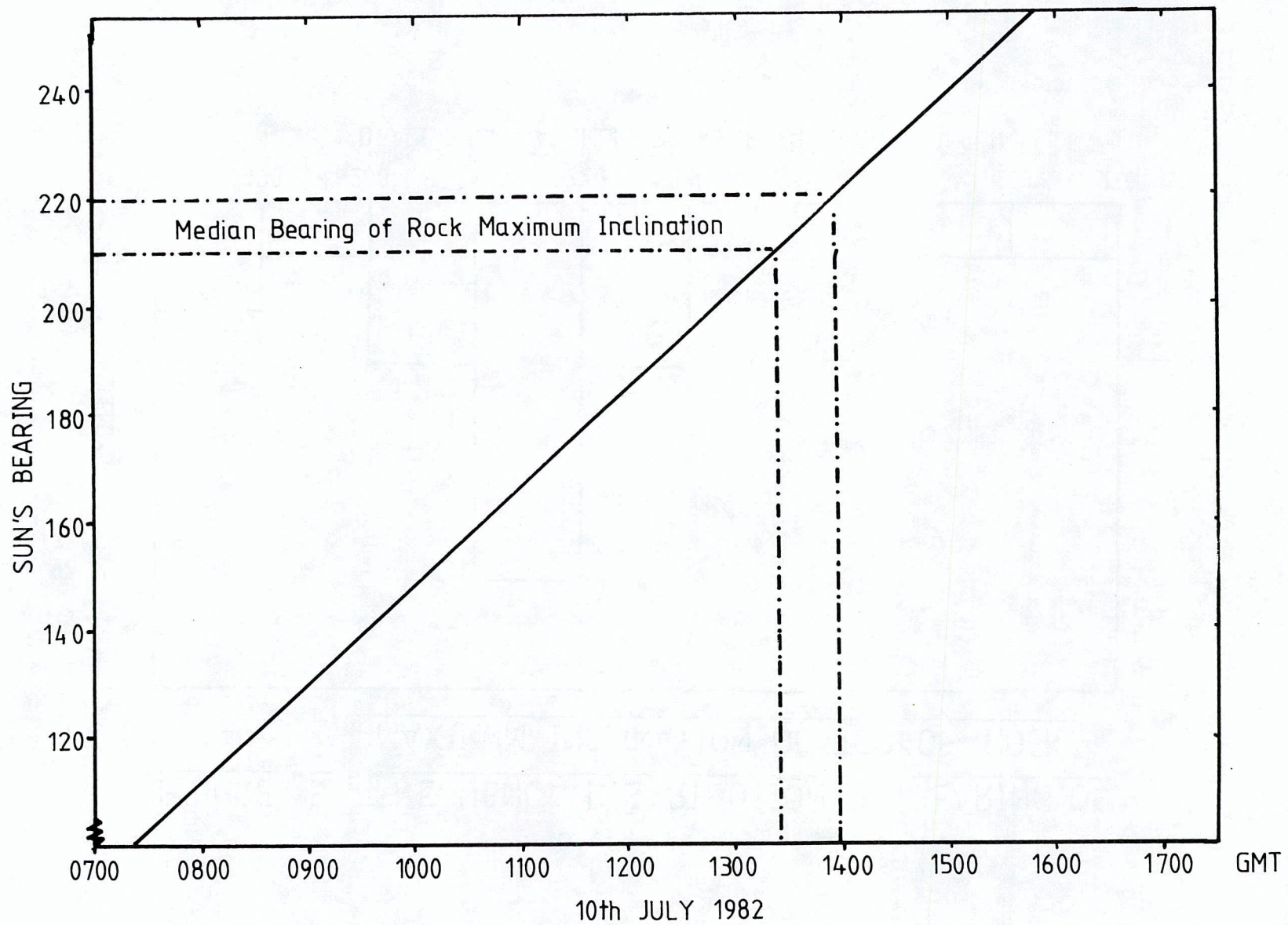
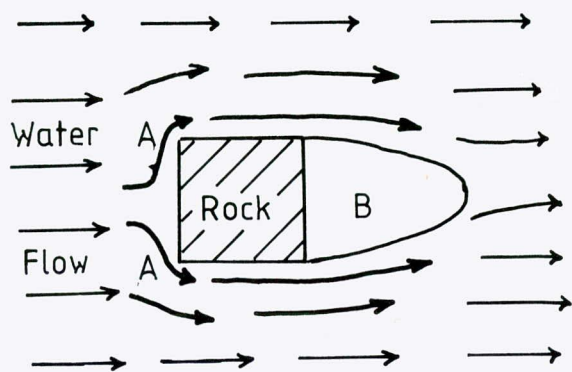


FIGURE 7 SIMPLE MECHANISM FOR PERCH FORMATION BY MELTWATER ACTION.



Diagrammatic representation of meltwater flow around the rock in plan view. Water is channeled around the rock increasing ablation in the vicinity of 'A'. There is no water flow over 'B', which is a separation bubble. The ablation at B is therefore less than elsewhere on the glacier.

FIGURE 7(a)

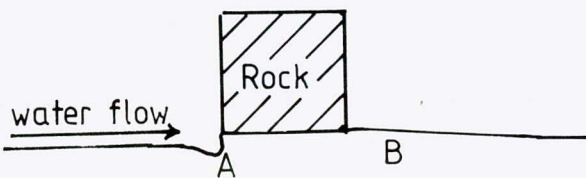


FIGURE 7(b)

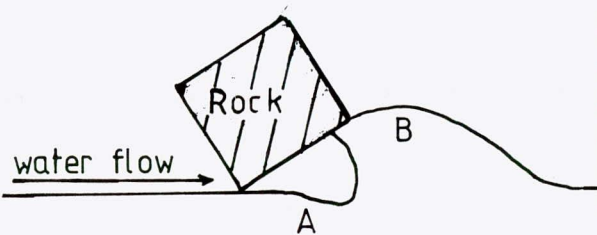


FIGURE 7(e)

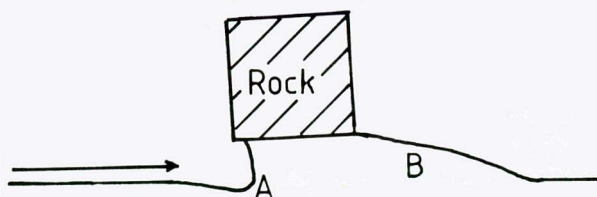


FIGURE 7(c)

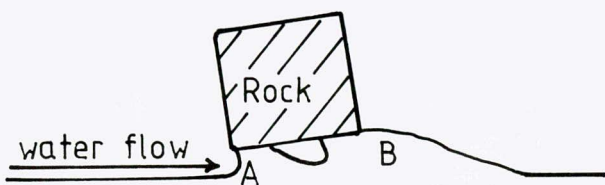


FIGURE 7(f)

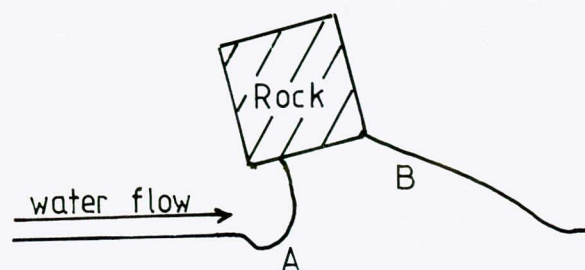


FIGURE 7(d)

Figure 7(b) to (e) show the gradual formation of a perch by water action. Followed by the undercutting of the perch causing the rock to fall off [Figure 7(d) & (e)]. A new perch then starts to form [Figure 7(f)]. This mechanism [illustrated in Figure 8] is assisted by solar radiation.

FIGURE 8(a)

Naturally positioned rock no. 4, photographed on 15 July 1982. Compare with figure 7b, the water channels on the right hand side have started to develop as has the mound down stream of the rock (The arrow marks the direction of melt-water flow).

Photo: R.M. Andrews

FIGURE 8(b)

Rock no. 4, photographed on 22 July 1982. Compare with figure 7c, the rock is perching and there is evidence of water action at (X) (The arrow marks the direction of melt-water flow)

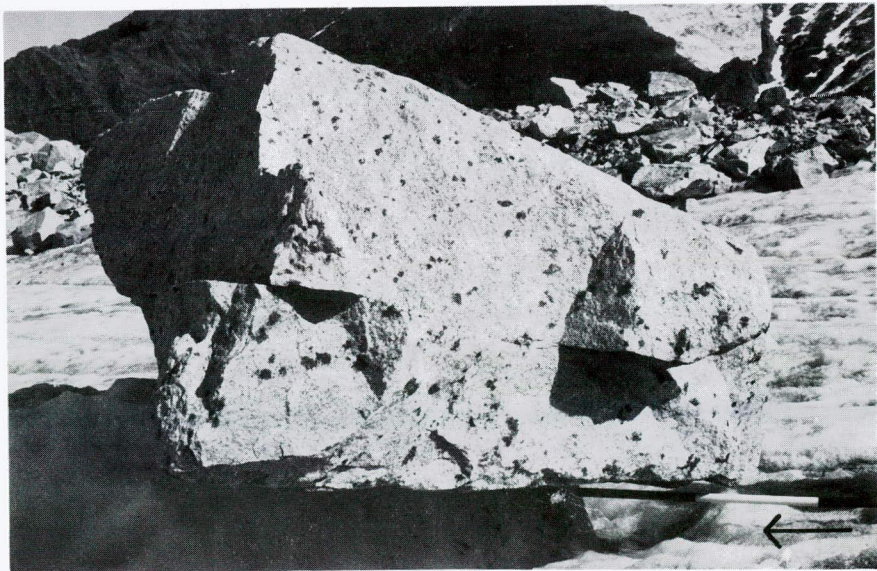
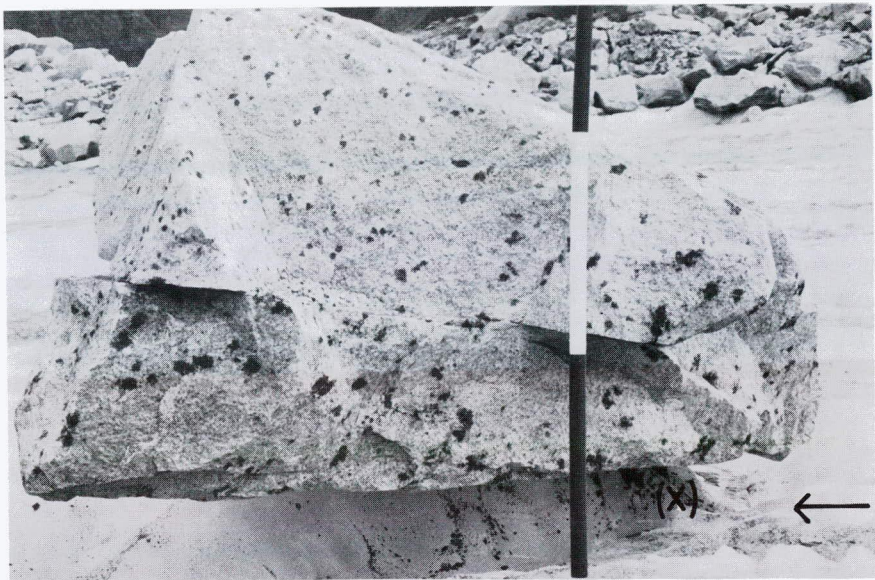
Photo: R. M. Andrews

FIGURE 8(c)

Rock no. 4, photographed on 30 July 1982. Compare with figure 7d, the rock is clearly perched with a large overhang on the up-stream side. The dry mound is evident down-stream. (The arrow marks the direction of melt-water flow)

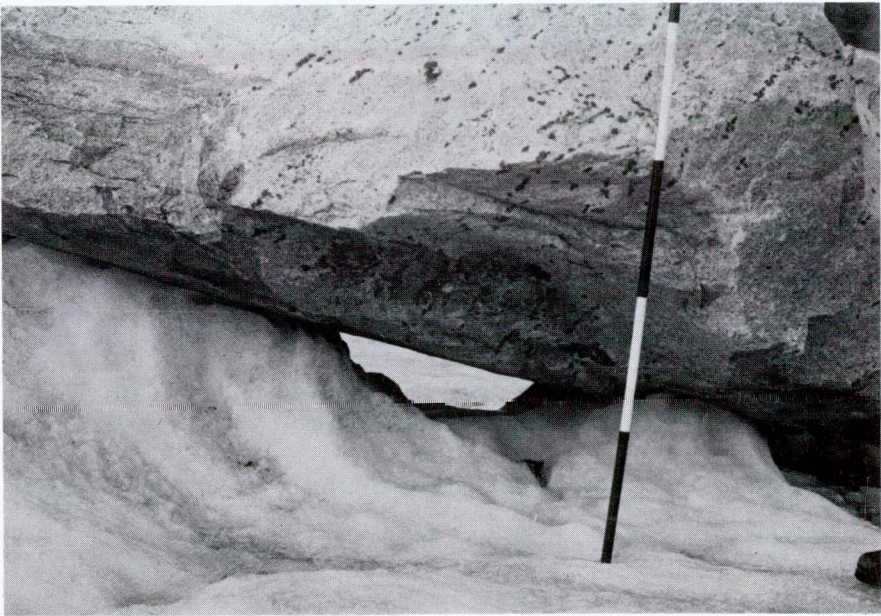
Photo: E. A. Patterson

FIGURE 8



continued over

FIGURE 8 (continued)



2.4 MELT STREAM GEOMORPHOLOGY

Introduction

This project measured the discharge of a supraglacial stream and related this to such factors as incoming solar radiation and air temperature. The project was not planned before the expedition but developed in the field. The 'instruments' used were adapted and borrowed from equipment left over from the planned projects. In addition to measuring discharge, sketches were made of the channel to show the changes with time over the melt season.

The study stream was the left lateral supraglacial stream of the Bersaerkerbrae glacier. The discharge was measured in the reach immediately below our camp. The stream received much sediment from the moraines and scree near its channel. It became apparent that much of the change in channel morphology was occurring because the stream had to cope with so much sediment.

The datalogger was used to record some solar radiation data and an attempt was made to set up an automatic stage recorder. This was abandoned because of a lack of resources.

A glacial stream must surely be one of the most interesting features a geographer can observe. Features evolve visibly each day on a glacial stream which take years on a typical English stream. In the sections which follow there are descriptions of melt and flow processes which were observed. The methods used for recording data are described and the data presented and discussed.

The Melt Season on the Bersaerkerbrae

Much melting had undoubtedly taken place prior to our arrival on the Bersaerkerbrae Glacier. The residents of Mesters Vig claimed two weeks of fine weather before the bad weather which accompanied our arrival set in. Despite missing the early stages of the melt new snow had fallen during our journey so that when the sun eventually appeared the effect was that of the sudden first thaw following the winter. The daily floods of this early period increased in volume each day until they were undoubtedly the largest experienced that year. This can be deduced from the obvious inadequacy of the channel to handle the flow.

The concept of 'bankful discharge' is difficult to apply in a glacial channel but the upper surface of undercut notches provides a reference which is useful in visually assessing the relative size of a flood. This surface marks the level of a previous maximum stage. Providing it is not too old, i.e. a relic from the previous year, it is reasonable to assume that a stage which passes this level must be representative of a discharge greater than that experienced that year. When melting began in earnest on 6-7 the notch was reached and raised. It is likely that the discharge of 6-7 was the greatest of the summer up to that date.

Our departure for Antarctic Havn from the Bersaerkerbrae on 12-8 meant that we could not see the end of the melt season. However, we had some cold weather and snow on 11-8 and 12-8 with dramatic effects on the stream flow. Therefore we were fortunate to record the effects of the onset of winter if not the entire event.

The Extent of the Study Stream's Catchment

Defining the bounds of a particular glacial stream is nearly impossible. The surface of the glacier constantly changes as it moves and there are frequent stream captures by crevasses. In addition the study stream flowed within an ice cave for much

of its course where the existence of tributaries cannot be seen. It is only possible to describe the most obvious sources, not to define their limits. They are:-

1. The glacier surface.
2. The moraines.
3. Water released from storage in pools on glacier and on the moraines.
4. Tributaries from the mountains.

These sources are shown on a diagrammatic representation of the catchment in fig. 1.

1. The glacier surface. Water from the glacier surface probably contributes the bulk of the water in the total stream discharge. Visual assessment puts the limits of this area some 10-20 metres from the study stream channel, about half way to the next supraglacial stream as you go towards the middle of the glacier. The upstream limit of the catchment appears to be just up-glacier from the icefall. The drainage in this area is rather complicated and the study stream mostly flows within ice cave passages.

Early in the season it is difficult to see how water from the glacier surface reaches the main stream channels. The surface of the glacier appears to be a continuous blanket of snow with only the largest of perennial channels visible. Water freed from the surface must percolate through the snow pack and flow down-slope over the ice surface. This is broadly analogous to the 'interflow' concept of hillslopes. Water is first visible around the bases of large boulders which have surfaces above the snow to absorb the heat from the sun. They melt the surrounding snow; more on the sun-facing side. The melt water ponds-up around the base of the boulder and is drained by an often sinuous channel. These narrow channels often disappear beneath the snow pack once away from the warming influence of the boulder.

The larger boulders sometimes have quite well developed channels draining their bases and they are clearly reactivated each summer.

By the time water can be seen in these channels water can be heard in countless small channels at the ice/snow interface. Initially flow is very inefficient because snow, slush and ice inhibit flow. Slush in the channel slows flow so that on a clear night the channel is likely to freeze over. Observations would seem to suggest that it takes only a couple of days of sunshine to remove the majority of such obstructions. However this is probably much faster than at the start of the melt season proper. As melting proceeds the channel network increases in efficiency and probably is close to maximum efficiency before the snow has entirely melted from the surface of the glacier. In theory this increase in efficiency should be detectable as a reduction in delay before peak flow.

In addition to an increase in efficiency, the size of the network feeding the study stream can increase or decrease quite suddenly because of stream captures. These occur in the normal way, by headward erosion, and also by the opening of crevasses.

2. The moraines. Much of what has been said above about the glacier surface also applies to the area I have called the moraines. In fact most of the moraines are ice-cored on active ice but they merge into the scree slopes from the mountain sides. The study stream is incised some 15 metres below the mean surface level of the glacier. The environment is shown in fig. 2. During the day the slopes of the valley provide sheet flow into the stream channel. Not surprisingly this is greatest on the debris-strewn, south-east facing slope. This meltwater locally concentrates into small channels supplied from an area of a few square metres. These small catchments act as 'funnels' for debris loosened from the moraine and the debris collects as small cones in the stream channel.

The moraine debris affects the melting of the ice beneath in quite a complex way. Such melting has been the subject of much research because of the possibility of dating glacial events once the melting rate is known. Some 0.5 metres of moraine is thought to be necessary to prevent melting of the ice beneath. A thinner layer will probably promote melting so that from observations it seems reasonable to divide the moraines into three regions.

- (i) Thick debris. More than 0.5 m.
- (ii) Debris between 0 and 0.5 m in thickness.

(iii) Negligible debris - fine dust layer.

A study was made of the temperature fluctuations within different parts of the moraine*. The results are shown in fig. 3. A thick debris layer has a greater capacity to store heat than a thinner one but ultimately a debris layer 0.5 m thick effectively insulates the ice beneath. A thinner debris layer will cool more quickly at night. In fig. 3 the temperature sensors were placed about 5 cm beneath the surface of the moraine. This meant that the one in wet sand was close to the ice and the dry one was some way from the ice where the debris was thicker. The temperature for wet sand dropped below zero between 0300 and 0630 on 16-7 where the thin moraine cooled so that melting ceased. The thicker moraine represented by the curve for dry sand maintained a temperature above 3 degrees centigrade. It is possible that on particularly clear nights the cooling is enough to freeze water in the margins of the moraines but where the moraine is thicker melting could continue. In this way water is stored in the moraine until the margins are thawed the following morning.

The composition of the moraine is another variable which affects the way the ice melts. Where the moraine is mainly sand the sand becomes wet as the melted water rises by capillary action. Flow over the ice surface and beneath the sand is slow. Where the moraine is mainly of pebbles and rock the meltwater can run off rapidly over the ice surface. Losses through evaporation are probably much greater from the surface of more sandy moraine.

Where there is only a fine dust-covering over the ice the ice surface seems to contribute very little meltwater to the main stream. Such surfaces can feel almost dry to the touch, while individual dust specks appear to be quite dry. The large surface area of the dust particles promotes effective evaporation of most of the melt. Estimates made from the observations of ice-screws in a dust-covered ice surface suggest that the surface could retreat as much as 5 mm per day largely by evaporation.

In detail therefore, the melting which occurs in the moraine-covered parts of the catchment is extremely complex and would reward a detailed study of spatial variations.

3. Storage on the glacier and among the moraines. Ultimately the source of this water would be the areas described above but some pools may have been filled during the previous season only to be thawed and drained later. Pools which drain suddenly can be thought of as a randomising factor which confuses the stream hydrograph. Part of the catchment was in the icefall area where the disrupted surface caused many pools to form. Continual movement opened many crevasses which caused sudden draining of several pools. The hydrograph for 8-7 shows evidence of such 'surges' though the source was not observed at the time.

Storage within the moraine-covered part of the catchment takes the form of large pools which fill from snow melt. These fill quite rapidly because of the rapid melting among the rocky debris. The pools drain steadily in most cases over several days. The drainage probably occurs by interflow between the ice and the base of the moraine and sometimes by the opening of crevasses. This source of water is probably an important part of the hydrograph at the start of the melt season but disappears towards the end. It is certainly a major component of the night-time 'base-flow'.

4. Tributaries from the mountains. This source of water was also of greatest importance at the start of the melt season. Several large snow patches in the mountains fed waterfalls which dropped onto the scree and moraine at the glacier margin. These waterfalls were active during the first couple of weeks only. They were also extremely sensitive to the position of the sun and may be the main cause of the second peak which was a feature of the hydrographs in the early weeks. In all cases the water sank into the moraine and scree and could not be seen to join with the main stream. Although a cave passage is possible it could not be proved. The majority of the tributary water probably follows a more diffuse route through the moraine debris.

* This is experiment 9 in the datalogger project report, section 2.1 - Editor

Methods

An extremely simple method was used to obtain an hourly measurement of the discharge. The 'velocity-area' technique was used. Stage was measured from a stage pole installed in the stream channel. The cross section of the stream at the stage pole was surveyed each day to give a figure for the cross sectional area at each stage. The velocity was measured by timing floats over a measured reach.

This method has many draw-backs which will be familiar to anyone who has attempted such a study on any stream. On a glacial stream there are many other problems.

The first problem is fixing the pole. This rarely presents much trouble in an English catchment. The pole was an extension rod for the ice-corer and it was secured at the top by guys which were tied to ice-screws in the sides of the ice-valley. The site had to be chosen with care because the only way the bottom of the pole could be fixed was to bury it in sediment. Unfortunately the changes in channel morphology were so rapid that it was easy to lose all the sediment in a channel in one day. It was important to choose a position which seemed to be aggrading fairly slowly.

Reading the water level on a stage pole is fairly easy at low stage but at high stage the water surface fluctuates over 2 cm or so. Some estimating is necessary but as long as a consistent approach is adopted the errors are acceptable.

Movements of the pole occurred despite determined attempts to prevent it. The ice-screws which attached the guys to the walls of the ice valley would unscrew as they warmed in the sun. They had to be jammed to prevent rotation. Melting around the ice-screw caused the guys to become slack so that the ice-screws had to be repositioned occasionally. This caused no problems but demanded the attention of someone to prevent the loss of the pole should the guys pull out.

It also appeared that the pole tended to sink into the bed of the stream. Usually it was embedded in sediment to the ice floor so that scour does not seem a likely cause. Possibly the pole was warmed sufficiently by the sun to conduct heat to the ice floor and cause the pole to sink. A survey tape was stretched across the channel. This provided the reference level for the cross section surveys and also a reference against which the movement of the pole could be measured. The maximum sinking was 2 cm in one day. This is far too much to be a result of melting alone. The measurement of pole movement was used to correct the stage readings recorded on the pole. By ensuring that you measure such movements it should be possible to measure stage to the nearest 0.5 cm at low flow and nearest 1.0 cm at peak flow.

The cross section of the channel was surveyed using a staff and measuring from the survey tape to the stream bed. This was carried out each morning before the rising of the main flood. The cross sectional area for each stage is therefore easily calculated. However, the cross section of the stream channel changes so rapidly that you really need to measure the cross section every hour. Using the staff and tape you would hardly finish one survey before needing to start the next. It might be worthwhile to try and distribute changes in cross section in proportion to the discharge each hour. This assumes a particular relationship between discharge and channel change and so was not adopted. The discharges were calculated assuming a constant cross section. Thus discharges after the peak are a little lower than reality. It would only be justifiable to spend a lot of effort in improving the cross section accuracy if velocity measurements were reasonably accurate.

Timing floats over a measured reach is more acceptable in a small stream than a large one but even so it is completely inadequate. The flow was so turbulent at peak flow that it was an achievement for a float to reach the end of the measured reach without sinking. Alternatively the floats became caught in waves near rocks for several seconds. Inevitably you must choose a route which will allow your float to remain on the surface so that you lose a randomness in the measurement. The only practical way was to take the average of as many runs as possible along courses which seemed to represent the majority of the flow down the reach.

This method probably gives quite good results for low flows where the water is restricted to a narrow channel. At peak flows the velocities measured are probably

rather higher than reality because of a tendency for the floats to move into the most rapidly flowing part of the channel regardless of where they start off.

A better method of velocity measurement would have been the single best improvement of this study. Preferably it would be an automatic measurement recording of the datalogger because much time was taken making manual measurements.

Chemical methods of discharge measurement would be much better in this environment and have been used successfully by many field groups. The problems of setting up such a method for this stream are that you have to transport the chemical release instrument to the site. This costs money. If you have to take water samples for analysis in a laboratory you need another piece of heavy expensive equipment. Salt would be a useful chemical in conjunction with a conductivity meter. The conductivity readings could be easily recorded on the datalogger. All you have to do is carry sufficient salt to the site for several weeks of recording. Construction of a weir or flume for more accurate discharge measurement is impossible. The range of flow is very great and the stream simply melts an easy route around the edge of any construction. The rapid upstream migration of small waterfalls would be a risk to such a structure.

The velocity area technique is probably the only option for an expedition with limited ability to transport equipment and limited finances. The secret is to refine the method to reduce the amount of human intervention required and improve the accuracy and frequency of measurements.

Back in England a cross sectional area was calculated for each stage. The discharge was calculated from velocity x area and plotted against time. The results are in fig. 4 a - d.

Solar radiation was recorded on the datalogger by measuring the output of the solar panels which charged the datalogger. The solar panels were not very good for such a purpose because they saturate beyond a certain level.*

Air temperature was measured using a hand-held whirling hygrometer. Air temperatures were also recorded by the sensors* attached to the datalogger. The recording was not carried out on a regular basis so the manual recordings are used here. The datalogger provides a much easier method of temperature measurement and would have been adopted if one could have been dedicated to the task throughout the study period.

The Data

The stream hydrograph data is presented in fig. 4 a - d. In the upper portion of each graph, discharge is plotted against the dry air temperature. The air temperatures were smoothed by plotting three-point moving means to show the trends. Beneath this graph the solar radiation is plotted against the cloud cover. The solar radiation units are arbitrary units based on the output of one solar panel as measured by the datalogger. The cloud cover is shown in octals with some indication of the cloud type and thickness.

Interpreting these graphs is very difficult. The shapes of the hydrographs are very different but there seems to be some consistency over two or three day periods. It was hoped that the results would allow a model to be proposed to approximately relate the discharge to solar radiation and air temperature. This proved impossible because there was no clear relationship even between the total daily discharge and the mean air temperature. This is shown in fig. 5. Only the period 6-8 to 12-8 seems to show some kind of relationship. Even so the total discharge for 10-8 was greater than that for 9-8 despite a lower mean air temperature. The relationship between discharge and mean solar radiation was even worse. Part of the problem was that solar radiation was not specifically recorded for this study during the second period of study from 5-8 to 12-8. The datalogger was needed to record solar radiation in the vicinity of the perched-block study out on the glacier. Although the graphs are not representative of the solar input in the study stream area they are reproduced here for comparison from day-to-day. In addition to this the flat top of the solar radiation curves suggests that the panels may be saturating before maximum solar input so that the radiation on sunny days is too low.

* See SDL-TN7 and SDL-TN14 in the datalogger report, section 2.1. Editor

Air temperature measurements showed much fluctuation which was why the moving mean was employed to show the trends. The reason for this was that the wind was generally very calm and there was very little mixing of air. It was possible to feel cool gusts from the glacier immediately followed by warm gusts from the south-east slopes of the mountains. This infers that the mean air temperature over the moraines could be much higher than over the glacier. So half of the catchment could be responding to warmer air temperatures than the other.

The data is therefore rather disappointing. As explained in the method, there is reason to be unhappy with the quality of the data. Despite this it is possible that the variation in discharges could be real and merely reflect the many unpredictable changes which occur within the catchment. The hydrograph of 8-7 certainly suggests that 'surges' are a component of the stream hydrographs. While this was particularly large, other smaller surges may be responsible for more subtle features of the hydrographs.

The hydrographs of 10-7 and 11-7 show that there is a component which arrives after the main peak. During 12-7, 13-7 and 17-7 it is possibly responsible for the shelf in the recession limb. The second sampling period from 5-8 to 12-8 does not show this features.

The timing of the main peak is earlier (14:30) during 10-7 to 13-7 when the weather was sunny than during 16-7 to 18-7 when the weather was particularly cloudy. Indeed the 16-7 to 18-7 hydrographs show a clear peak around 16:00. This is explained by supposing that there is a component which responds rapidly to sunshine and produces the peak on sunny days at about 14:30. The rising limb of the hydrographs is much steeper on sunny days than on cloudy days. This may be because a clear night normally precedes a sunny day. On a clear night the moraines lose a lot of heat by radiation. The margins freeze and water could be stored in the moraine to be released suddenly the next morning. Much water is stored in the network and released suddenly when the obstructions are melted. On cloudy nights the network does not freeze over because radiation cooling is much less. There is less delay in flow the following morning and flow increases at a more steady rate. On cloudy days there is an almost linear approach segment before the rising limb begins proper at about 09:30.

During the period 10-8 to 12-8 the weather gradually worsened. A clear night and a sunny start to 10-8 produced a slowly rising approach segment then the steep rising limb at 09:30. Cloud thickened during the evening and remained overnight. On 11-8 there is still a steep rising limb and this is due to a thinning in the cloud around 10:00 which was sufficient to produce a response. The extra sunshine was only just noticeable yet there was a response. Observations of the channels draining the moraine showed that melting had begun at about 10:00. On 12-8 the diurnal flood did not occur for the first time since our arrival. The cloud was thick and low with snow falling. The snow drifted into the channels and prevented passage of water into the study stream. Pools on the margins of the stream channel remained frozen throughout 12-8. A fall of snow is clearly most effective at reducing the peak flows in glacial streams.

Channel Morphology

A sketch of the stream channel was made nearly every day. A series of these is shown in fig. 6. The channels shown are some 2 to 3 m wide and 75 m in length. The streams issued from an ice cave which had the familiar 'drainpipe' cross section of a passage formed in the phreas. Two to three metres downstream from the resurgence the water fell over a 1.5 m waterfall. This waterfall migrated upstream as shown by the 'F' in fig. 6. By 15-7 the waterfall was inside the cave. The cave passage then had the 'keyhole' cross section so characteristic of limestone caves.

Between A and B there was a comparatively steep reach which culminated in a small waterfall at B. Between B and E the channel was generally straight but the stream meandered between the ice banks which defined the channel. In long profile the stream bed showed a succession of pools and riffles. The pools were in the outsides of the meanders. The riffles were in the centre of the channel. During the waning of the daily flood much sediment was deposited. An attempt has been made to show the distribution of sediment in the channel with time in fig. 6.

A glacial stream finds it very difficult to achieve a smooth long profile. Continuous movement of the glacier results in many knickpoints throughout the length of the stream. The waterfalls at F and B produced dramatic changes in the channel morphology within a few days. Between A and B the combination of slope and sediment produced a wider channel with a tendency towards braiding. The majority of the flow was along the true right and the waterfall migrated up this side from B. The waterfall left a clean ice trench along the true right hand side of the channel. This trench increased in depth upstream so that by the time the waterfall was at A it was some 1 m high. Sediment was easily carried along this channel but was deposited at B where the channel slope reduced and where there was already a substantial bar. The sediment slowly filled the ice channel from B to A.

The contrast between the roughness of an ice channel and a sediment filled channel is so great that there is continuous instability in channel form. In general it can be stated that erosion is most rapid where sediment is thinnest. A pattern was observed where ice channels gradually became filled with sediment during the waning of the daily floods. Eventually flow in these channels became so inefficient that the emphasis in flow switched to the other side of the channel. This pattern is shown diagrammatically in fig. 7. Pools are marked P. Riffles are marked R. Initially the deepest part of the channel was on the true right despite the meanders. The pools gradually fill with sediment which build up behind the riffle. This sediment layer protects the ice beneath from melting. Erosion in this part of the channel is now mainly sideways. The efficiency of flow is reduced because the roughness increases. Eventually a peak flow removes the now thinner sediment layer on the true left. Once the sediment layer is removed, melting of the ice floor occurs rapidly. The channel has now two distinct parts. The ice channel on the left continues to widen and deepen. The channel on the right becomes more choked with sediment and is eventually abandoned. This is demonstrated in the sequence of sections shown in fig. 8. These are sections which correspond to the position of the line Z-Z in fig. 7.

The whole sequence described above repeats for the next meander upstream. This is shown in diagrams C to F in fig. 7. In E and F the ice channel on the left has deepened sufficiently to start undercutting the bar recently abandoned on the right.

This process results in a transference of the main flow from the true right to the true left of the stream channel. The substantial sediment load, which is moved effortlessly along the smooth ice channel on the left, is brought to rest further downstream. A change in gradient has caused a large bar to form. Sediment carried down the ice channel backs up from that bar to slowly fill the ice channel. Eventually this channel will choke and it is likely that flow will switch to the right again.

When a large boulder falls into the stream, as many did, the channel can change quite suddenly. With reference to fig. 6, two large rocks fell into the stream at point D on 13-7. During peak flow the upstream 'bow-wave' at these rocks was so high that water overflowed into the abandoned oxbow (18-7). By 5-8 the whole of the small islet had been melted and the main course of the stream was along the line of the oxbow.

The large rock at A caused the main flow to be directed toward the true right of the channel. Nearly a metre of undercutting occurred at this point.

Conclusions

It was disappointing that the discharge measurements could not be related to solar radiation and air temperature. This may have been because there were too many 'random' events occurring such as 'surges' from storage release. The methods employed for measuring discharge and solar radiation needed improvement. Testing of the dataloggers in different roles meant that one could not be dedicated for the whole of the study period to recording for this project.

The changes in the channel morphology were of great interest. It would have been more worthwhile to concentrate on more quantitative studies of changes in channel morphology. This will certainly be the objective of my next glacial project. With the assistance of a reliable datalogger and well designed instruments it should be possible to produce the data needed to relate channel change to discharge. The big challenge will be to do this in a way which is both economic and requires the minimum of human attention in the field.

FIG. 1

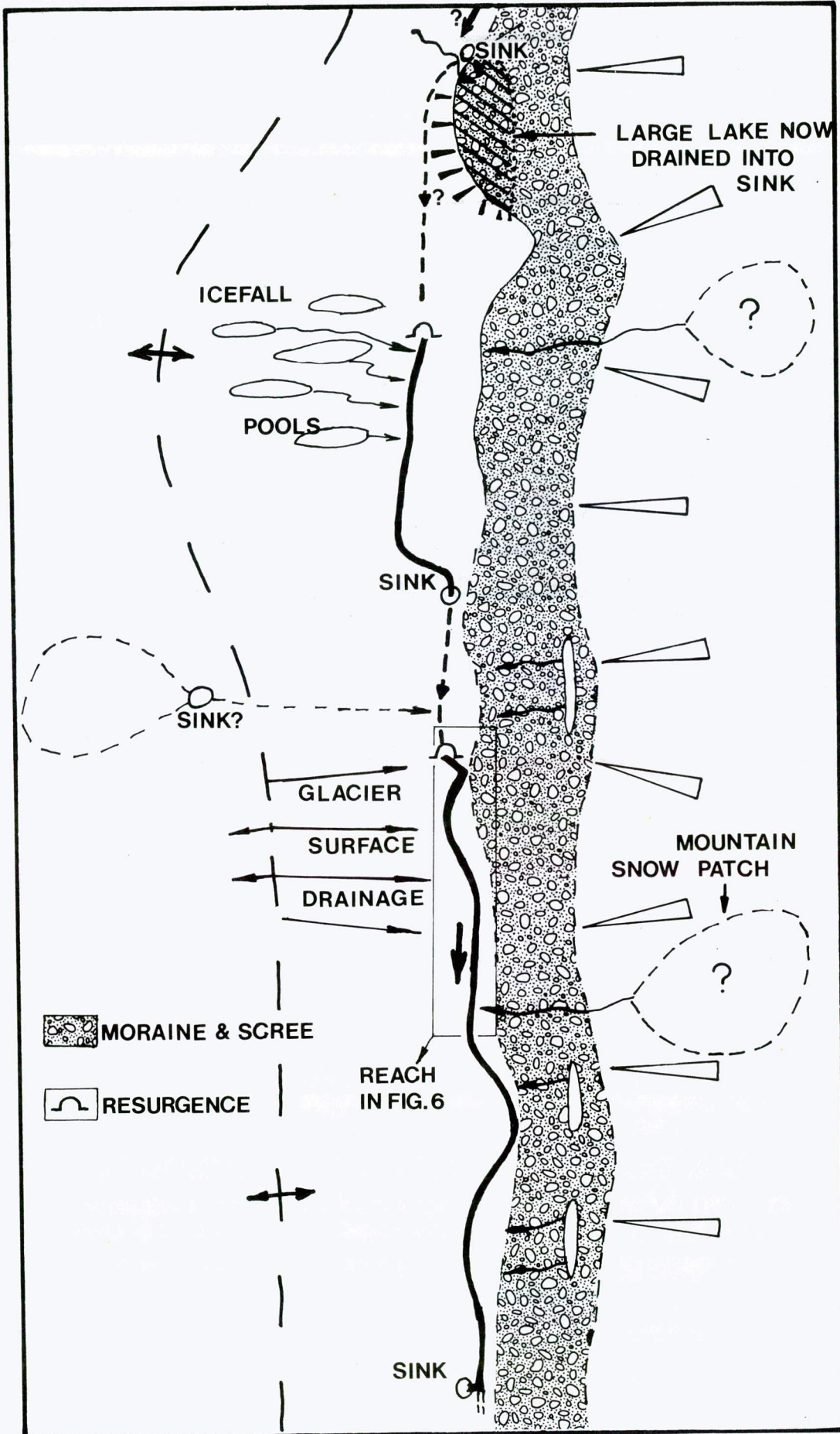


FIG. 2

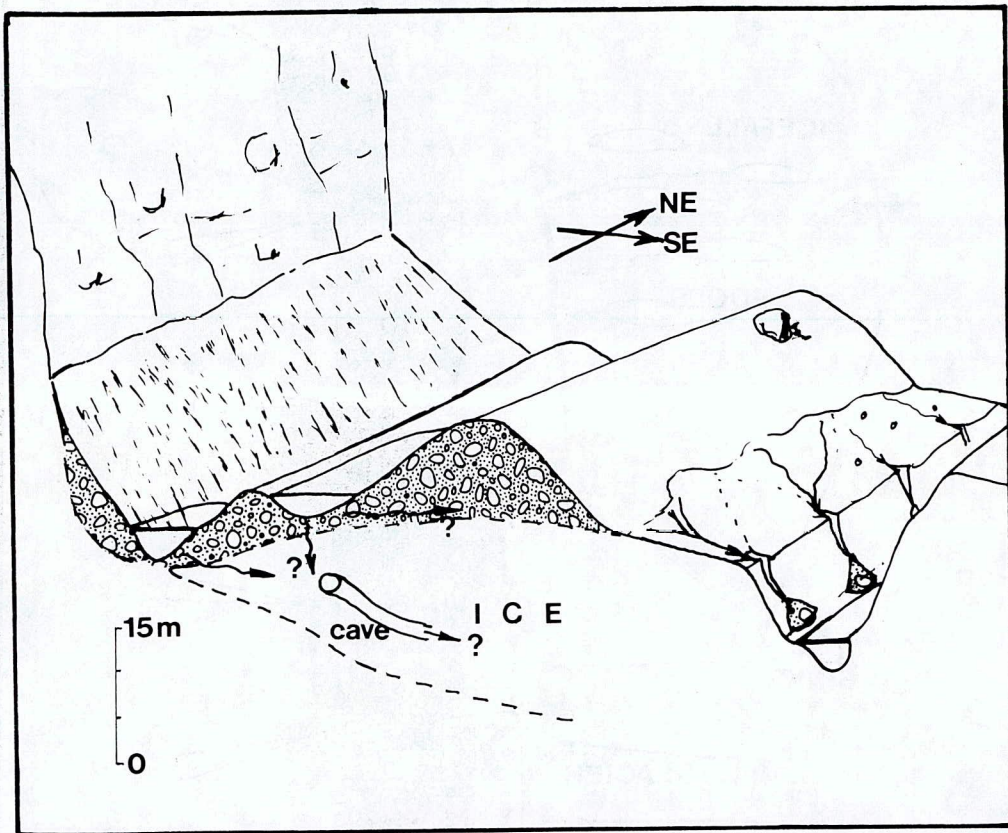
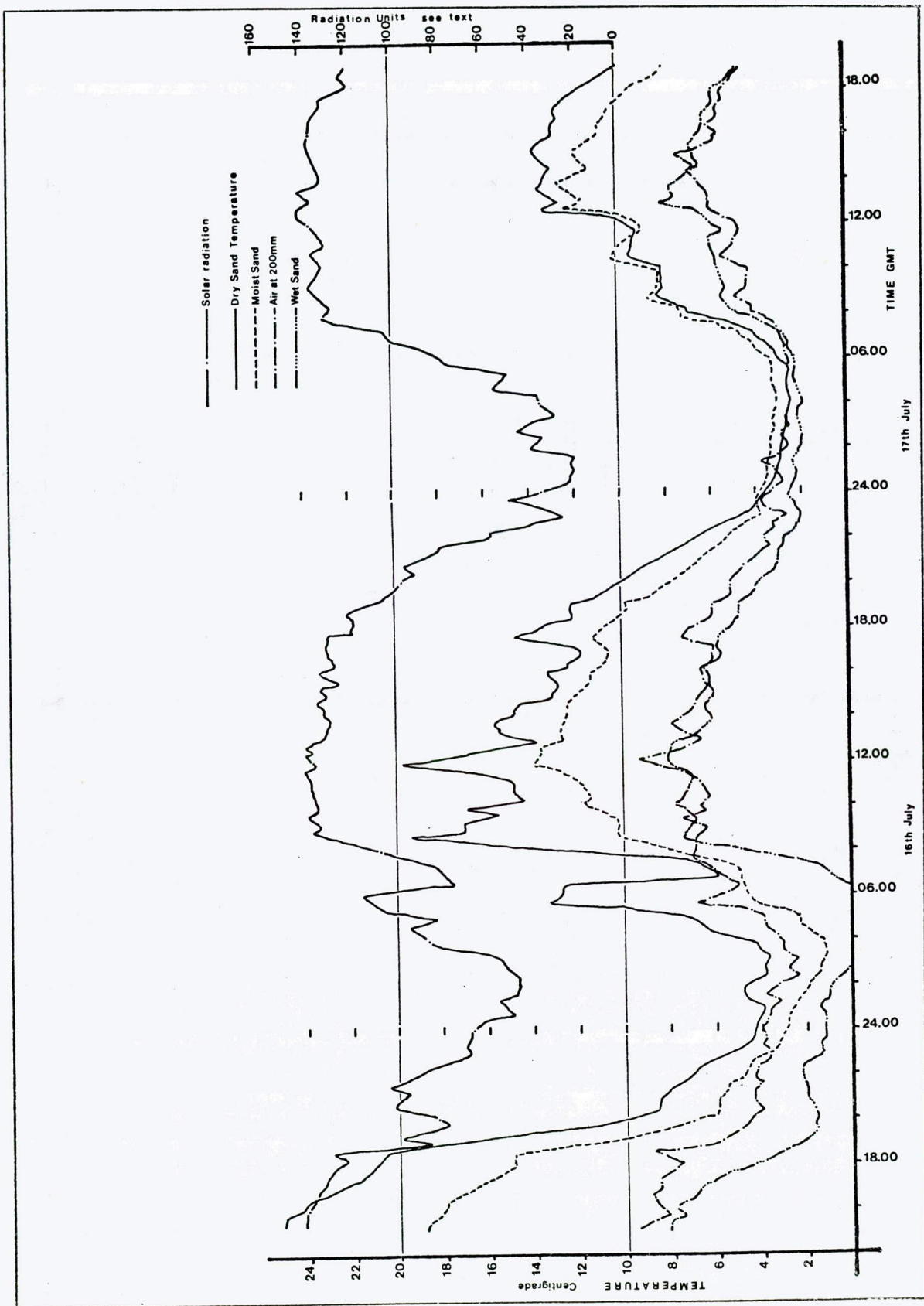


FIG. 3



76

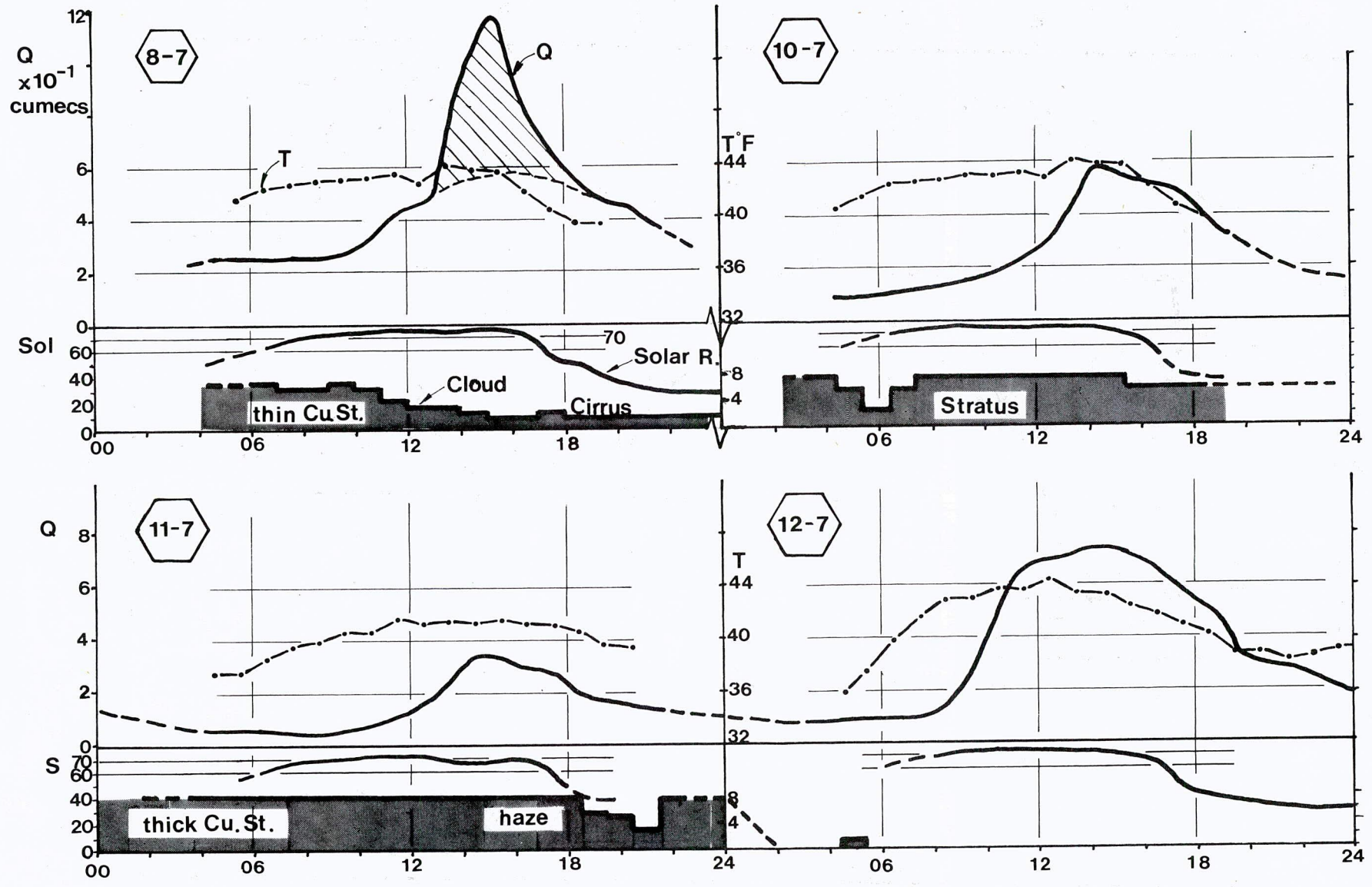


FIG. 4a

95

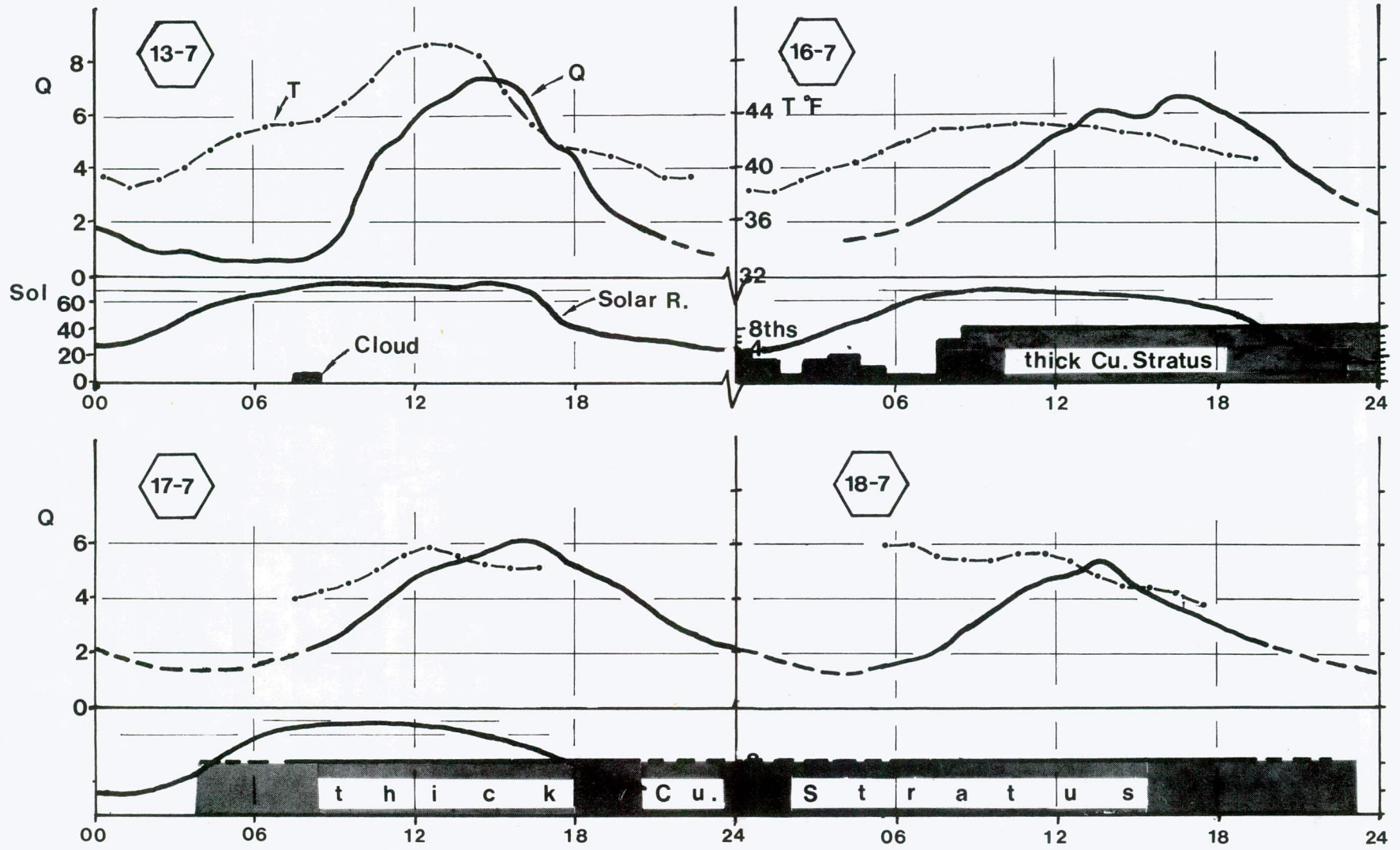


FIG. 4b

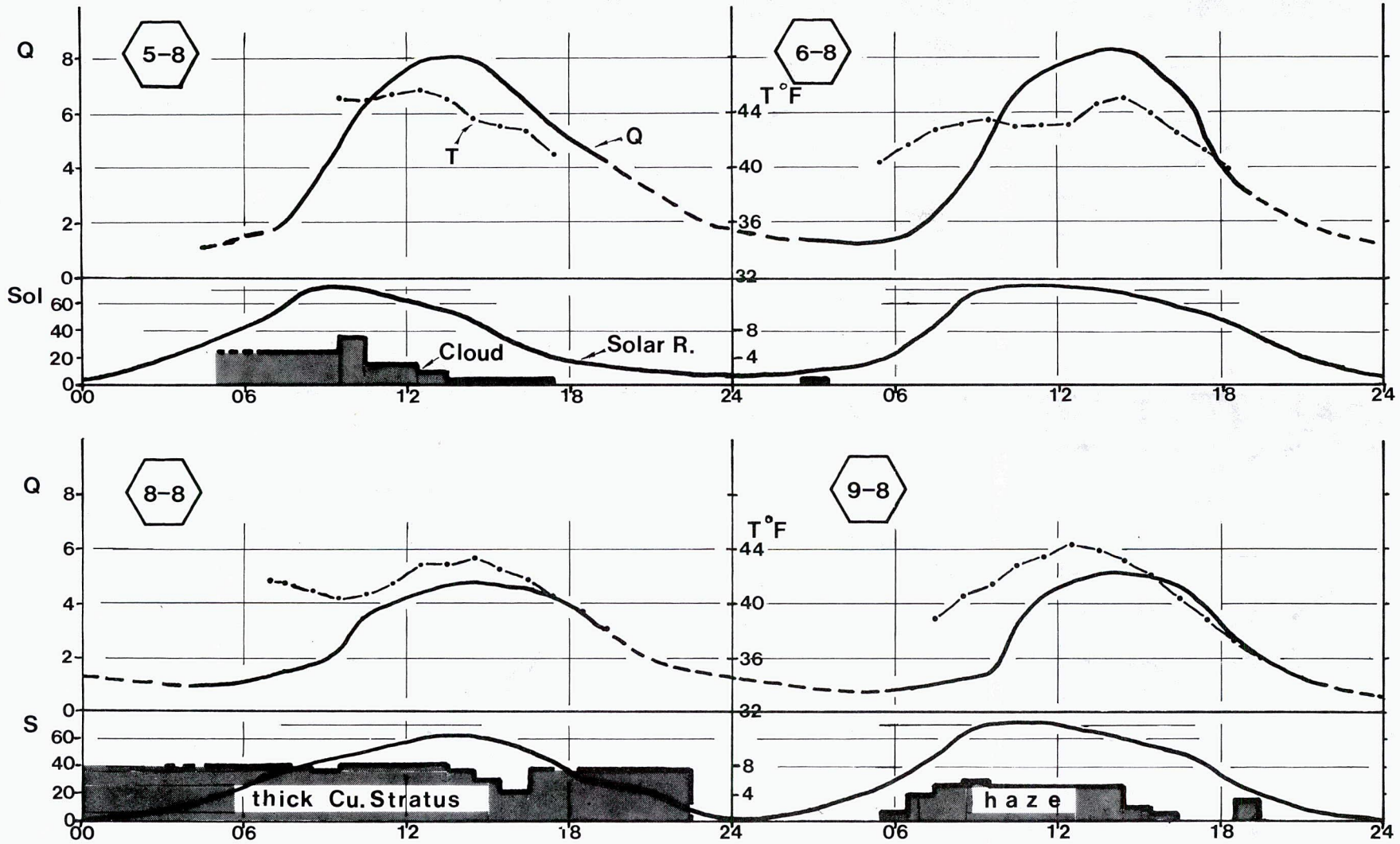


FIG. 4c

97

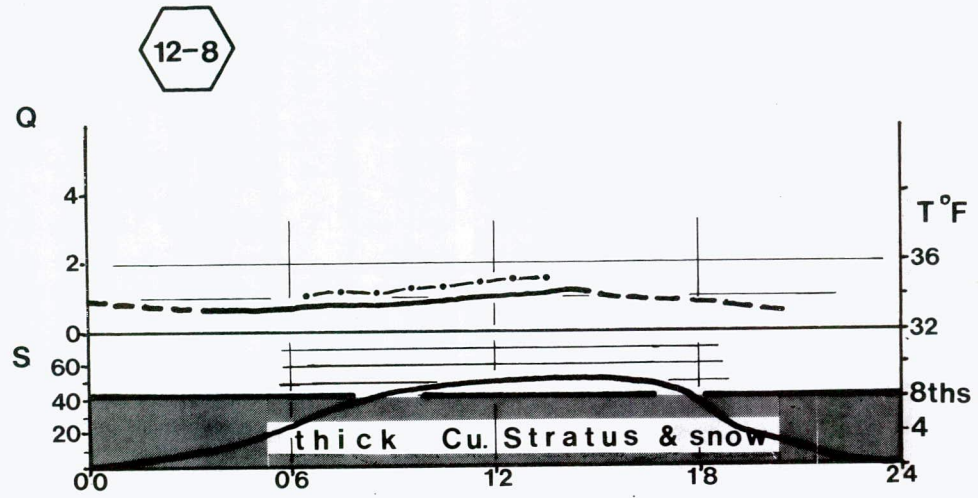
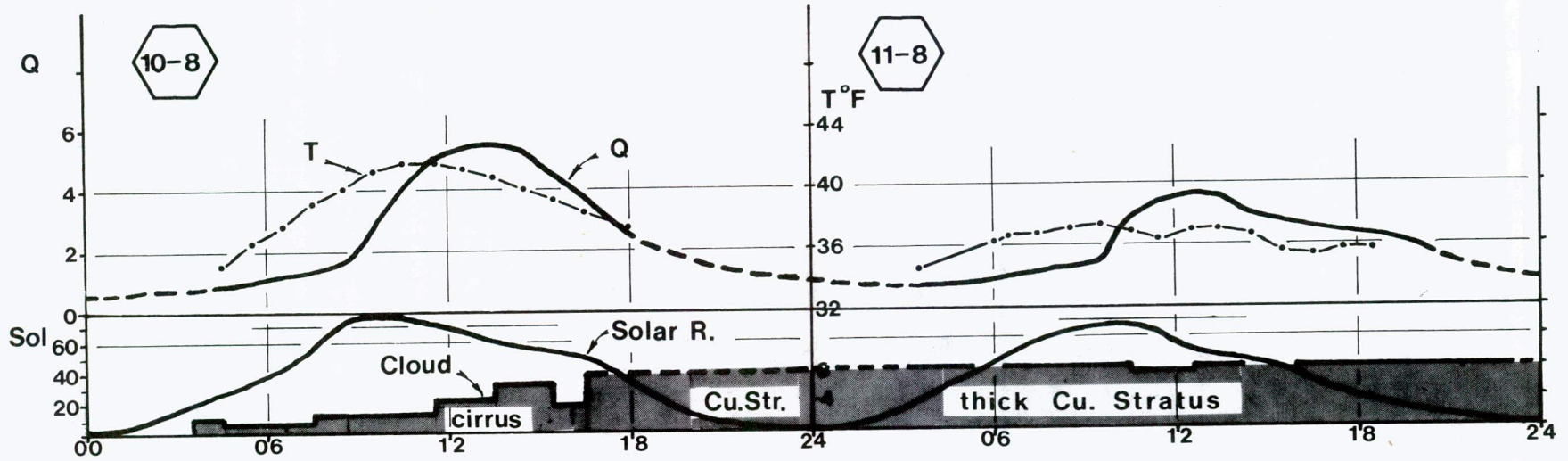


FIG. 4A

FIG. 5

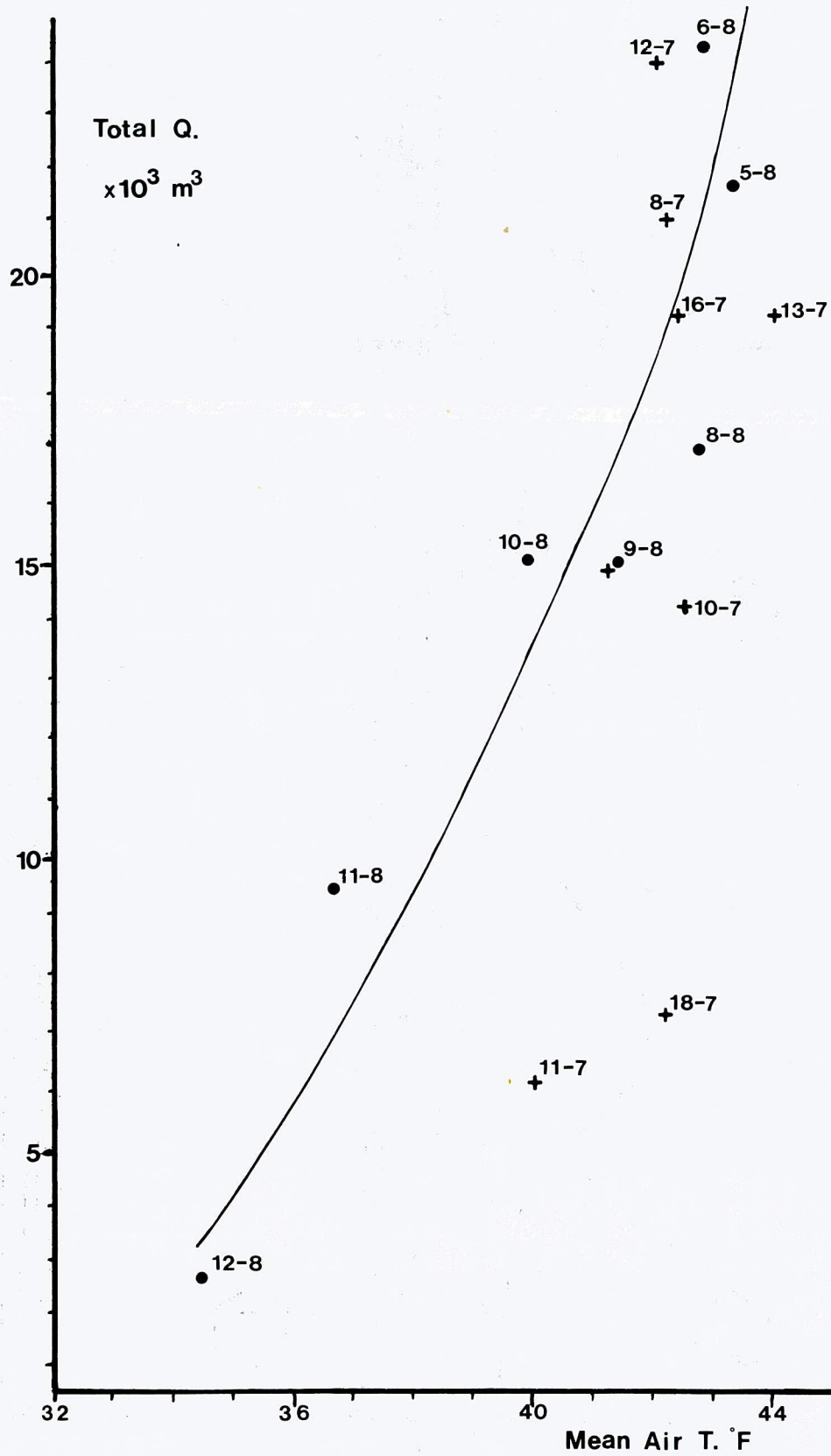


FIG. 6

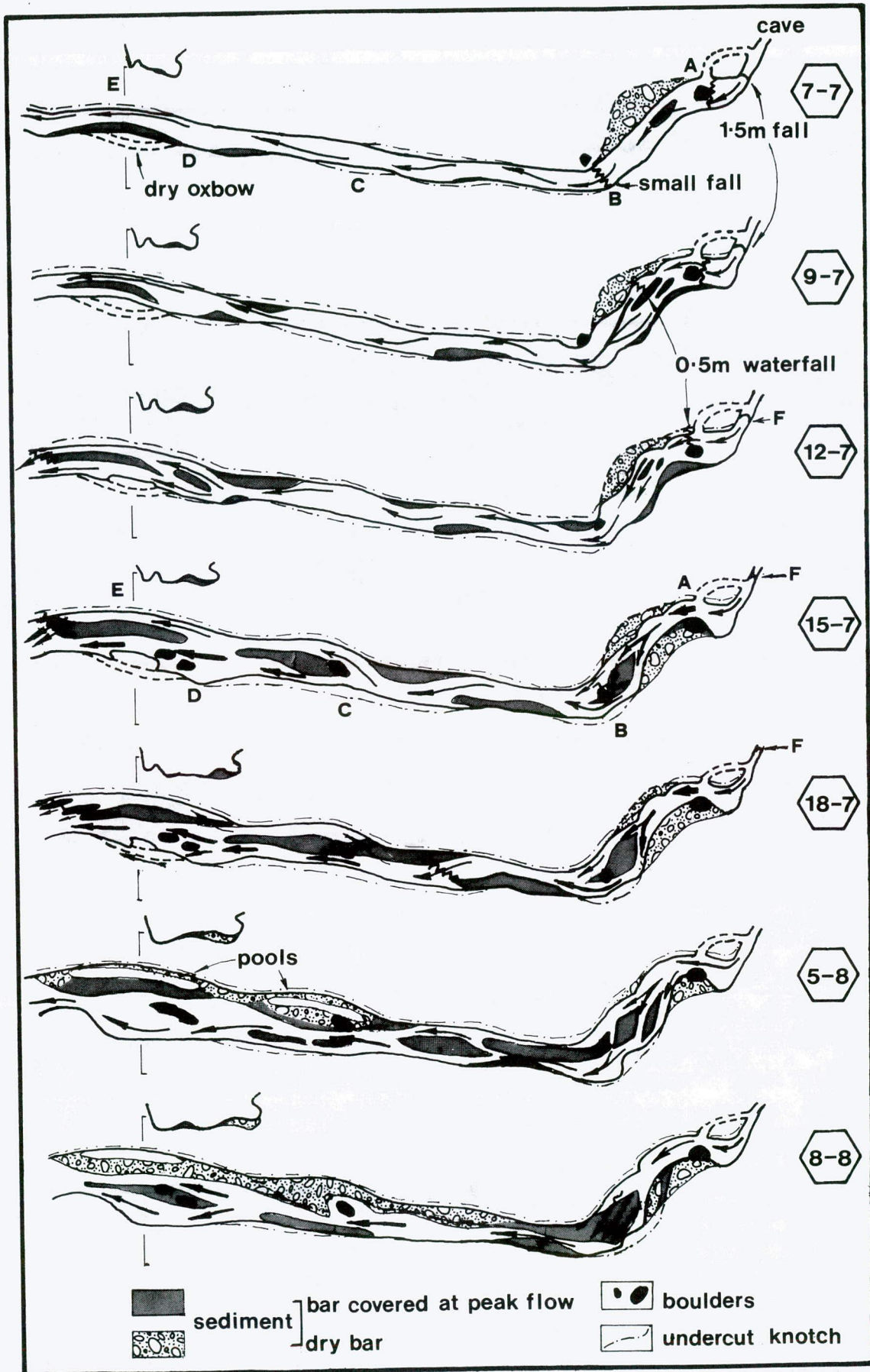


FIG. 7

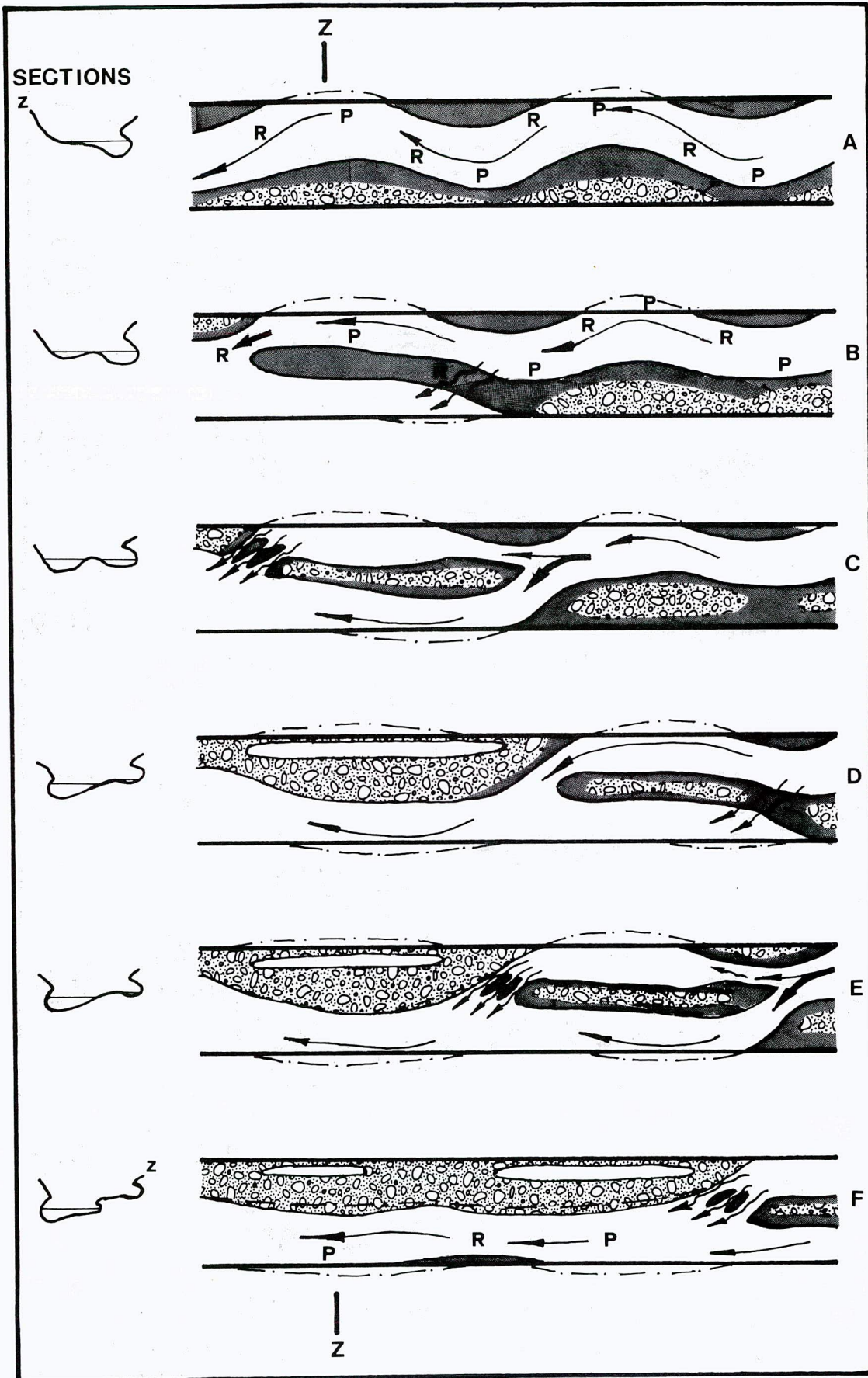
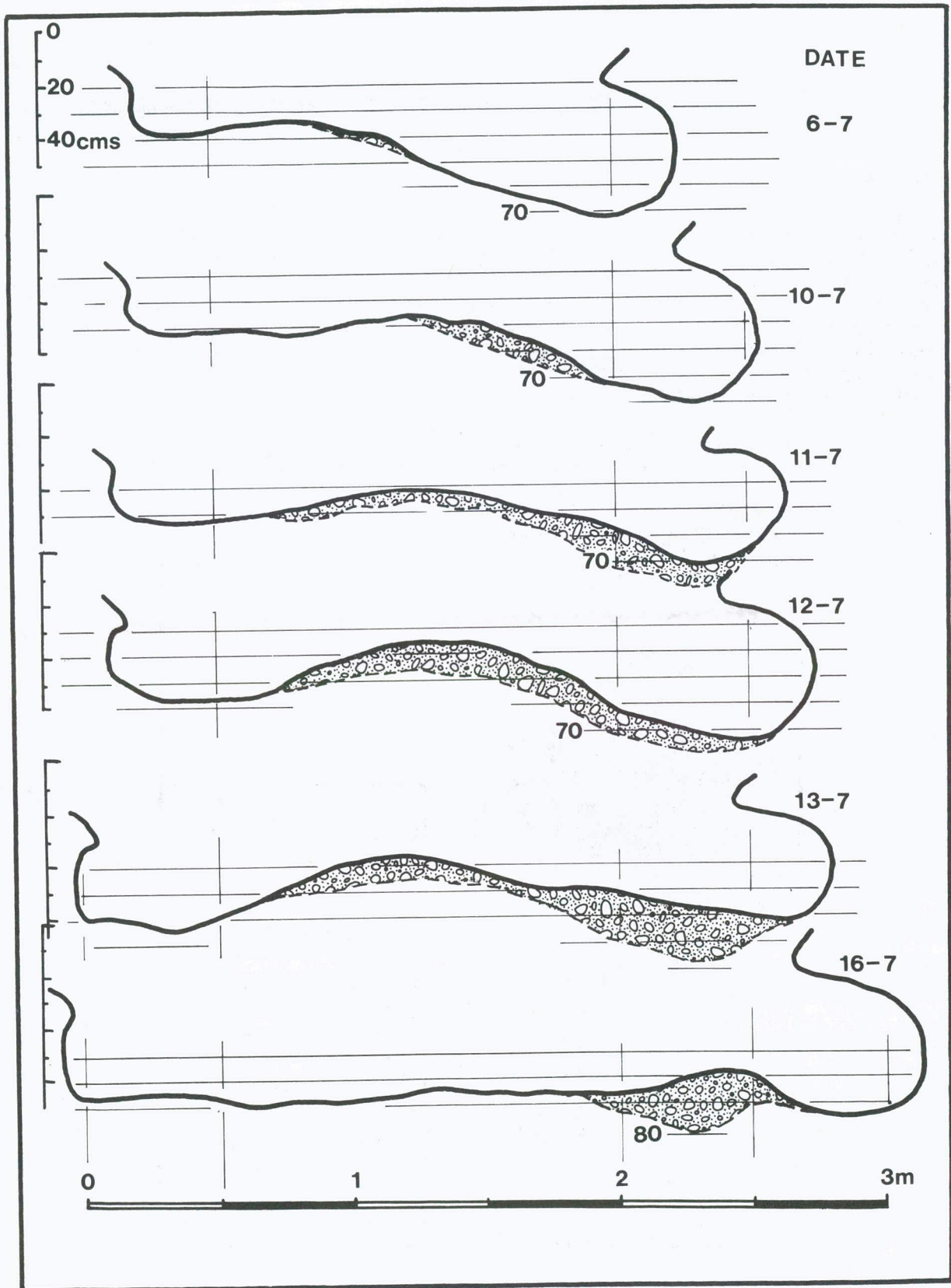


FIG. 8



2.5 LOWER JURASSIC SEDIMENTS AT ANTARCTIC HAVN, CENTRAL-EAST GREENLAND

Introduction

The virtually complete succession of Jurassic sediments found in Jameson Land and Scoresby Land have been extensively studied in the past few decades since the expeditions of Lauge Koch in the late 1920's. As the most complete sequences are found in southern Jameson Land, in particular the western shore of Hurry Inlet, it is not surprising that the bulk of research has taken place in this area. The sediments found in the Antarctic Havn area, which constitute the most northerly outcrop of the Lower Jurassic in Scoresby Land, have not been the centre of such detailed attention. The following report provides a general description of sediments exposed in a low cliff on the southern shore of Antarctic Havn.

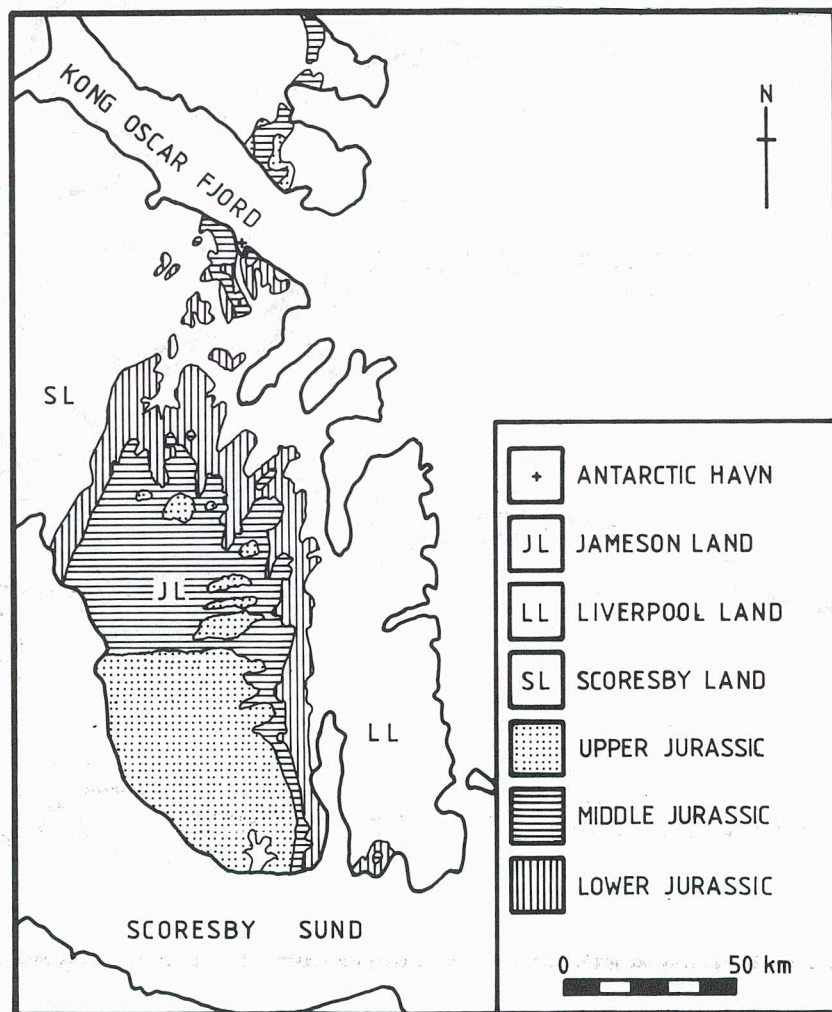


Fig. 1 Distribution of Jurassic sediments in East Greenland.
(after Birkelund and Perch-Nielson (10))

Lithostratigraphy

The sediments exposed to the immediate south of Antarctic Havn are of Lower and Middle Jurassic age, which have been downfaulted into position (1). These have been subdivided into units defined by Rosenkrantz (2) and later by Surlyk et al (3), after investigations in southern Jameson Land. Information on these units can be found in the works of Rosenkrantz (2), Donovan (4) and Surlyk et al (3) where they have been discussed in great detail.

The sediments forming the low cliff at Antarctic Havn are believed to be of the Neill Klinger Formation, which has been subdivided into the Rævekløft, Gule Horn and Ostreaelv Members. The lithostratigraphical scheme for the Jurassic sediments of Jameson Land is shown in fig. 2.

It can also be seen in fig. 3 that the Neill Klinger Formation increases in thickness towards the north. Thus the Neill Klinger Formation is represented by up to 300m of sediments in north Scoresby Land; whereas the formation is 220 m thick along Hurry Inlet, southern Jameson Land.

UPPER JURASSIC	JAMESON	Raukelv Fm	Fynselv Mbr
			Salix Dal Mbr
			Sjællandselv Mbr
MIDDLE JURASSIC	LAND	Hareelv Fm	
		Olympen Fm	
		Vardekløft Fm	Fossilbjerget Mbr
			Pelion Mbr
			Sortehat Mbr
LOWER JURASSIC	GROUP	Neill Klinger Fm	Ostreaelv Mbr
			Gule Horn Mbr
			Rævekløft Mbr
RHAETIC - L. LIASSIC		Kap Stewart Fm	

Fig. 2 Stratigraphical scheme of the Jurassic in Jameson Land, East Greenland (after Surlyk et al (3))

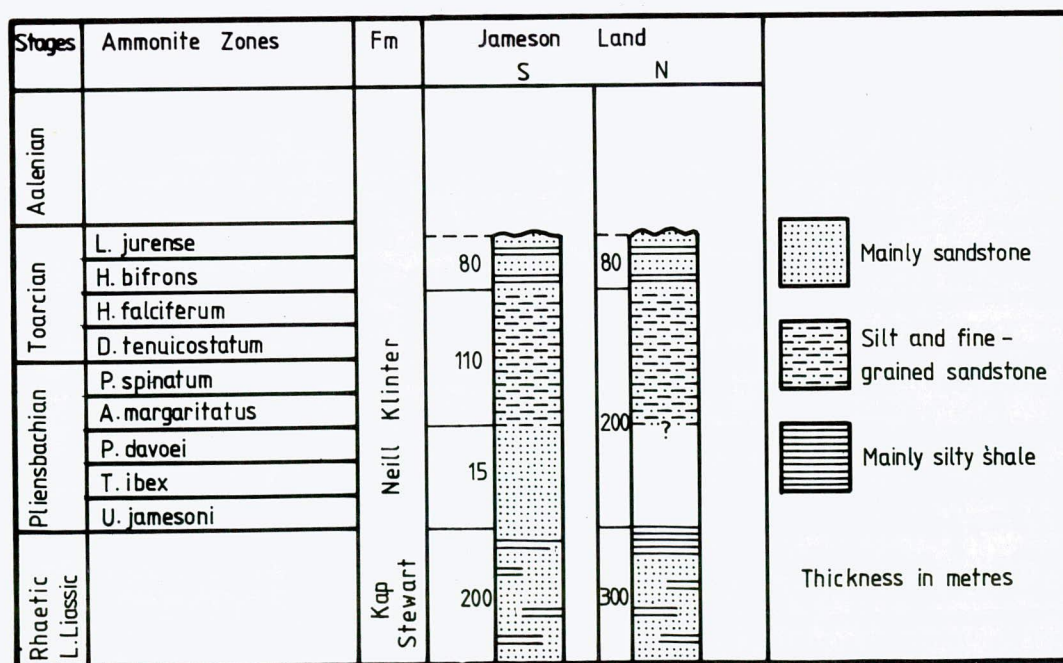


Fig. 3 Ammonite zonation of the Lower Jurassic in Jameson Land, East Greenland (after Birkelund and Perch-Nielsen (10))

Biostratigraphy

The faunas in the Neill Klintner Formation are dominated by bivalves in those horizons that are fossiliferous. The faunas found in this formation have been described by Rosenkrantz (2, 5) and are closely related to their European counterparts. Fortunately sufficient ammonites have been found to enable correlation with the ammonite zones of the Lower Jurassic (fig. 3).

The Raevekløft Member has been dated as the Pliensbachian by fossils found in four prominent sandstone horizons. The two basal sandstones are characterised by faunas dominated by *Entolium*, which have been subscribed to the *Uptonia jamesoni* zone of the Pliensbachian. Whereas the third sandstone has yielded ammonites, including *Lytoceras fimbriatum*, indicative of the *Prodactylioceras davoei* zone (2).

No body fossils have been found in the Gule Horn Member although trace fossils are plentiful in the lower half.

The Ostreaelv Member, like the Raevekløft Member, is dominated by bivalves with belemnites, crinoids and ammonites also present. The ammonites include *Hildoceras bifrons* and *Lytoceras jurense* of Toarcian age.

Sedimentology

Sedimentological studies have been made of the Neill Klintner Formation (7) and the underlying Kap Stewart Formation (6, 8). The main aim of these reports was to define the various lithofacies present in order to interpret the depositional environments. The Gule Horn Member was used to define offshore-estuarine regressive sequences in the Neill Klintner Formation (7), while the Raevekløft and Ostreaelv Members have not been studied.

The cliff section along the southern shore of Antarctic Havn is believed to be part of the Ostreaelv Member. The sediments, which dip 3° - 5° in a southeasterly direction, range from muddy siltstones to fine grained sandstones. In the top half of this section are found three prominent limestone horizons, in which belemnite and bivalve remains were found. The cliff forms a low barrier about 250 m in length and is divided into two parts by an area of slumped material. The western part of the cliff forms the base of the section, with the eastern part containing the upper section. Figure 5 shows the sections studied in simplified form and their location along the cliff. The five sections were then used to identify three major types of lithofacies based on lithology, sedimentary structures and fossil content.

Sections 4 and 5 were then used to produce a detailed log of the complete cliff section (fig. 6).

Facies 1a

This facies is dominated by dark grey muddy siltstones interbedded with several sandstone horizons. The unit varies in thickness from 0.5 m to 1.0 m. Ripple-cross laminations are the main structures in the muddy siltstones, although horizontal laminations are occasionally found. The thickness of these laminations varies from a maximum of 10 mm to less than 2 mm. The thinnest laminations are often associated with a fining in grain size and an increase in fissility, forming paper shales. These paper shales appear to contain a higher percentage of carbonaceous material than the rest of the siltstones. Large muscovite grains are found throughout the siltstones, orientated parallel to the laminations.

The finegrained sandstones, with abundant muscovite grains, are found throughout this facies as lenses. This lenticular bedding has two distinct sizes, the smallest is less than 1.0 cm thick and up to 7.0 cm in length. While the larger size may form prominent sandstone beds that may attain a thickness of 10 cm and several tens of metres in length. Both types exhibit ripple-cross laminations.

This facies is devoid of body or trace fossils.

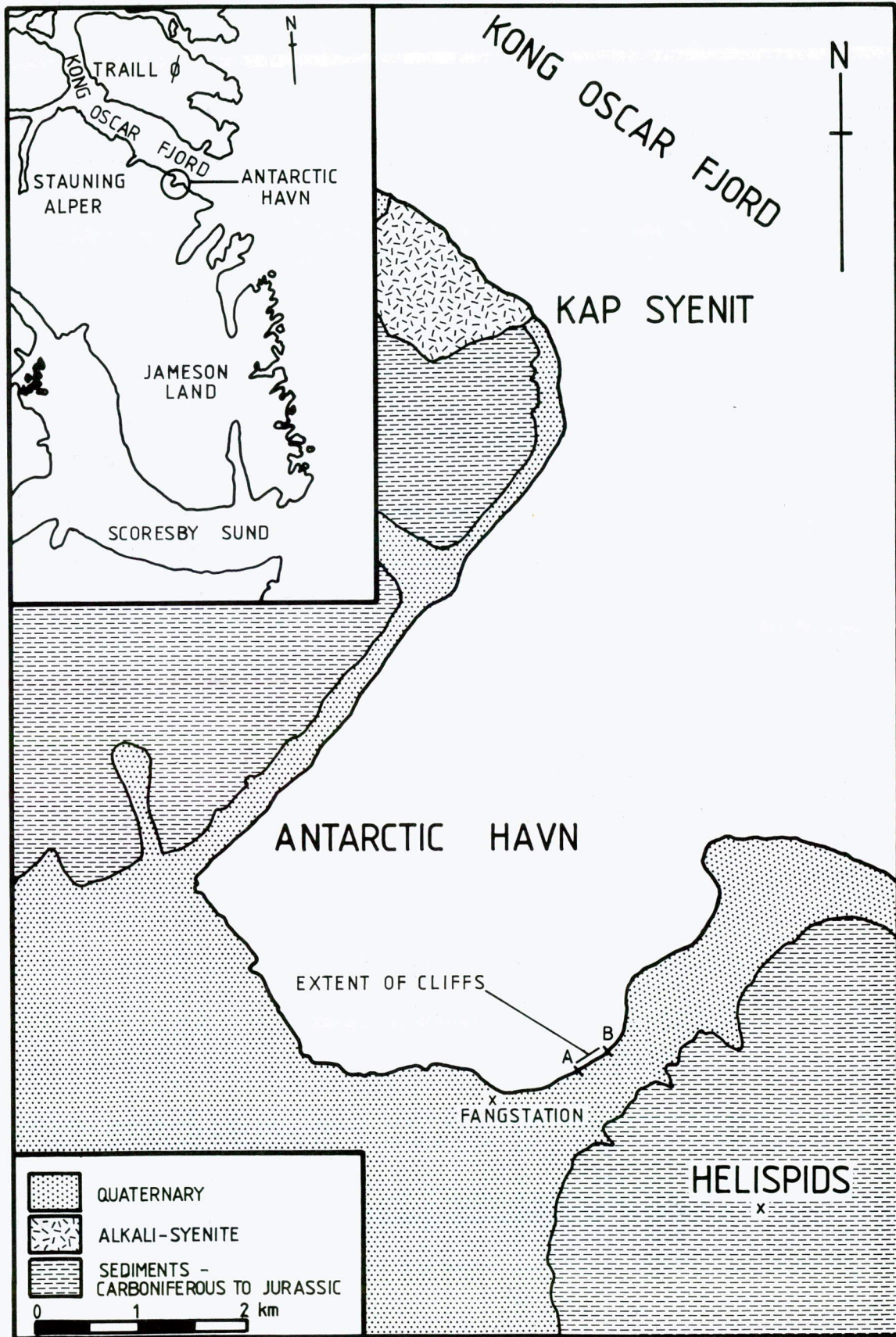
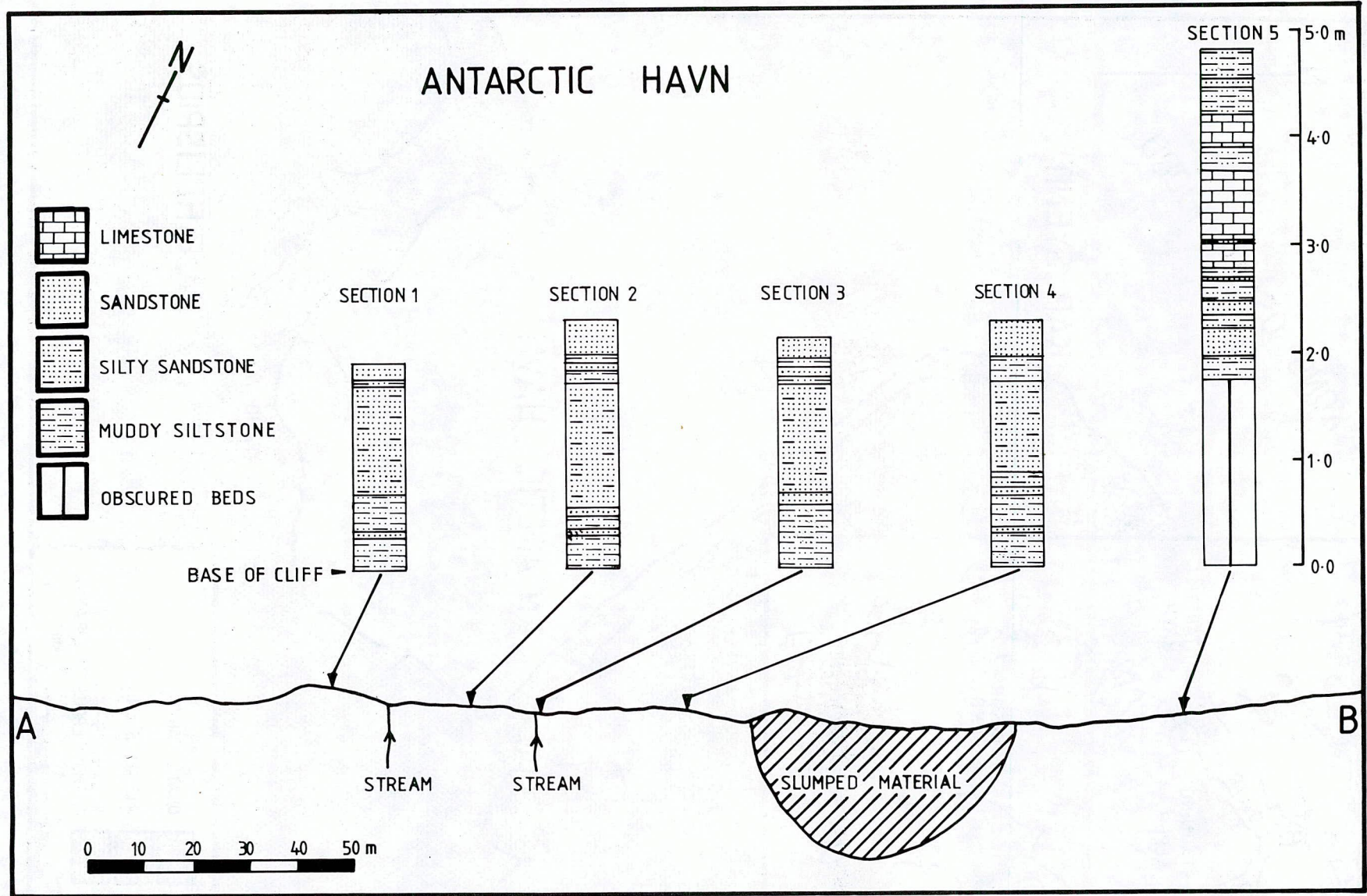


Fig. 4 Simplified geological map of the area around Antarctic Havn, East Greenland (adapted from Koch and Haller (15))

Fig. 5 Plan of the Antarctic Havn southern shore, showing the cliff section locations



Facies 1b

This facies is basically the same as facies 1a except that the sandstones are more thickly developed and dominate some parts. Flaser bedding and ripple-cross laminations are the major sedimentary structure in these thicker sandstones.

Facies 2

Light brown silty sandstones form this facies which ranges from 0.8 m - 1.3 m in thickness. Flaser bedding and ripple-cross laminations are the structures found in this facies. The laminations vary in thickness from 0.75 cm - 5.0 cm, the finer muddy material forming the thinnest laminations. Small muscovite grains are found throughout the facies.

In the top half of this facies poorly preserved burrow-like structures are present. These vertical structures may reach a length of 9.5 cm and 0.5 cm in diameter, always appearing to taper towards the bottom. Despite poor preservation it is possible to make out the alignment of muscovite grains parallel to the burrow walls. No other fossils were found in this facies.

Facies 3

This facies consists of the limestones that form three prominent horizons near the top of the measured section. The limestones have been designated as 1, 2 and 3; with 1 being the bottom limestone bed.

Although limestones 1 and 2 are separated by only 3 cm of muddy siltstone their lithology is quite different. 1 and 3 are fine grained limestones containing very little bioclastic material; whereas limestone 2 is oolitic containing belemnite and oyster remains. All the limestones appear to have very few sedimentary structures apart from the occasional wavy bedding plane and a general fining upwards in grain size. The latter is emphasized in areas where bivalve remains can be seen near the base of beds.

All limestones contain ellipsoid iron concretions, in some areas this is so widespread as to form the appearance of bands. Pyrite was also found throughout the facies, often replacing the carbonate material in ooliths.

Thin sections were made from samples of the limestones and will be discussed later.

Interpretation of Facies

Reliance on current directions and the interpretation of sedimentary structures from past work (6, 7, 8) has been necessitated by the lack of current data collected from Antarctic Havn.

Facies 1a and 1 b

This facies is mud dominated with ripples and ripple-cross laminations. Despite the lack of data indicating bi-polar current directions past research into the Gule Horn Member would seem to indicate a marine rather than a fluvial or deltaic environment (7). The presence of sand lenses would then be interpreted as the reworking of nearby material introduced into the area by storms and heavy tides.

Except that the sand lenses are more thickly developed in facies 1b than 1a, the depositional environment would appear to be basically similar.

Facies 2

The formation of flaser bedding needs periods of high and low current flow. Together with the presence of burrows this would seem to indicate a shallow water environment. A tidal flats environment can be ruled out by the lack of root beds and bioturbation. Therefore it is probable that Facies 2 was deposited in a tidally-influenced shallow water marine environment.

Facies 3

The bioclastic material contained in the limestones, especially limestone 2, would suggest the reworking of sediments. Broken belemnite pyragmacones and bivalve shells, particularly oysters, reinforce the idea that the sediments originate from a fairly open marine environment before being introduced into a shallow water area. The lack of current structures in the limestones, apart from the occasional ripples on top surfaces, suggest deposition during a high energy event such as a storm.

The facies distribution can be seen in fig. 6 and is dominated by facies 1a and 1b. This would tend to agree with past work in which the Ostreaelv Member has been interpreted as a mud dominated coarsening upwards sequence (7).

Detailed Petrology

The making of thin sections from limestones 1, 2 and 3 enabled the identification of structures that could not be resolved in hand specimen. The following provides a brief description of the more important features.

Limestones 1 and 3

Both are micritic limestones in which quartz grains and the occasional feldspar grain are supported in a micritic matrix. The major constituents of the matrix are calcite and an iron mineral.

Limestone 2

Oolites form at least 45% of this limestone and are supported in a micritic matrix. The petrology is basically similar to that of the other limestone beds apart from the addition of oolites. The oolites are ≤ 0.5 mm in diameter and formed of concentric rings of calcite, often with a rim of sparry calcite. Most of the oolites have been flattened in an orientation roughly parallel to the bedding. Replacement of oolites by pyrite has also taken place and is found in all three limestones.

In all the limestones an iron mineral is found in the matrix, often so concentrated that it forms ellipsoid concretions ≤ 10 mm in length and ≤ 2 mm in thickness. In these concretions remnants of the original fabric, such as oolites, can be identified. In some areas these concretions are so numerous that they give the appearance of thin horizons. Although the very fine grained nature of this iron mineral makes identification difficult, together with information of the depositional environment, siderite would appear to be the most likely candidate.

The fact that original sedimentary structures can be seen in the siderite concretions would seem to indicate that it is of secondary and not primary origin.

Regional Setting

The underlying Kap Stewart Formation has been identified as fluvial (6) and tidally influenced deltaic deposits (8) in which the overall transport direction was to the north. During the Pliensbachian a marine transgression occurred and this persisted until the late Toarcian. During this period clastic sediments were being deposited in a shallow sea where the transport direction was to the south. The area can be described as a N - S trough with Antarctic Havn situated near the northern margin (fig. 7). The shallow water deposits identified at Antarctic Havn would be consistent with a shoreline to the north. The source for the clastic sediments being the area to the north of Kong Oscar Fjord.

It has been postulated that a NW - SE trending fault along the approximate centre of Kong Oscar Fjord was an important barrier during the Lower Jurassic (8, 9). This fault would have prevented deposition and has been used to explain the lack of Lower Jurassic sediments north of Scoresby Land. This barrier would have been submerged by the Middle Jurassic (Bajocian) allowing deposition to take place in northern areas.

The faunas of Northern Europe, Arctic Canada and Spitsbergen are similar to those found in Jameson Land and Scoresby Land, so these areas were probably interconnected (10).

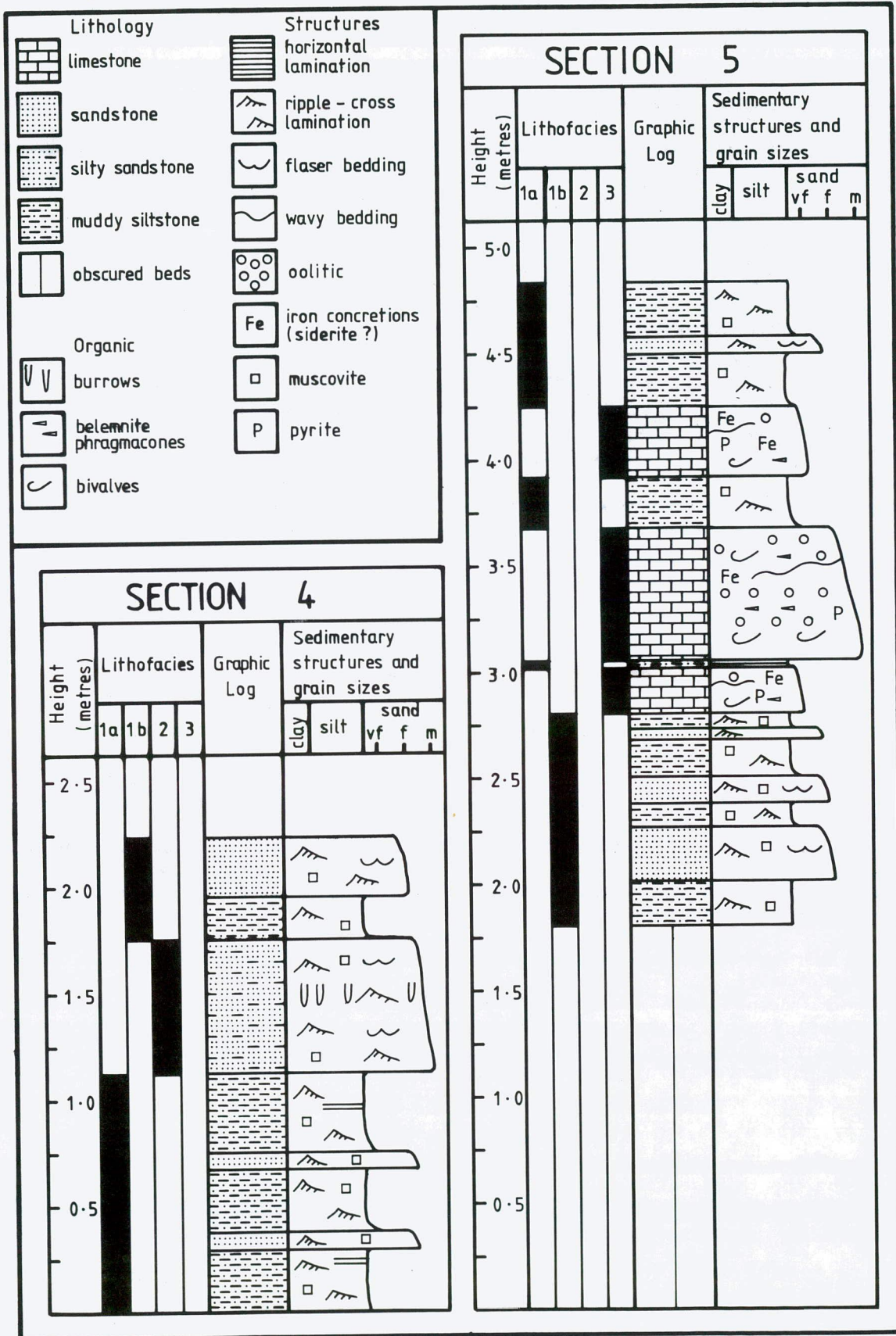


Fig. 6 Detailed log of the sediments exposed in a cliff along the southern shore of Antarctic Havn

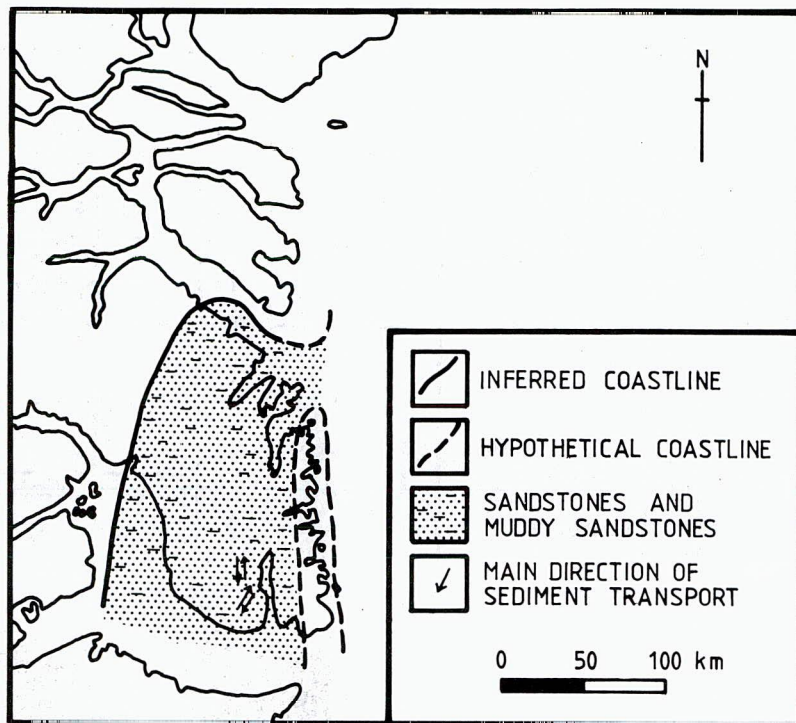


Fig. 7 Early Jurassic (Pliensbachian-Toarcian) palaeogeography of East Greenland (after Surlyk (9))

Conclusions

The lack of current data and the relatively small section measured makes it difficult to define the depositional environments of each facies. Although it is possible to infer a shallow water marine environment that was tidally influenced, but this relies heavily on past work in southern Jameson Land.

The section is dominated by muddy siltstones interbedded with thin sandstones. The limestones form three prominent horizons in the top half of the section and are at least partially oolitic. They appear to be reworked sediments from deeper water washed into the area by a catastrophic event such as a storm.

The author has reservations about the assigning of these sediments to the Ostreaelv Member of the Neill Klintner Formation especially when dating of the sediments relies on past work, despite the scant attention the area has received. Obviously the lack of body fossils, such as ammonites, has hampered dating when ammonites are the major method of correlation in the Jurassic of East Greenland. Therefore a study of the microflora might prove useful in determining the age of these sediments.

Acknowledgement

The author would like to thank Stan Rae of Gearhart Geodata Services Ltd., Aberdeen, for preparing the thin sections.

References

1. SURLYK, F. and BIRKELUND, T. (1972) The Geology of Southern Jameson Land. Rapp. Grønlands. geol. Unders. 48, p 61-74.
2. ROSENKRANTZ, A (1934) The Lower Jurassic rocks of East Greenland. I. Meddr. Grønland; 110, 1, 122 pp.
3. SURLYK, F; CALLOMON, J.H.; BROMLEY, R.G. and BIRKELUND, T. (1973) Stratigraphy of the Jurassic-Lower Cretaceous sediments of Jameson Land and Scoresby Land, East Greenland. Meddr. Grønland; 193, 5, 76 pp.

4. DONOVAN, D.T. (1957) The Jurassic and Cretaceous systems in East Greenland. Meddr. Grønland; 155, 4, 214 pp.
5. ROSENKRANTZ, A. (1942) The Lower Jurassic rocks of East Greenland II. The Mesozoic sediments of the Kap Hope area, southern Liverpool Land. Meddr. Grønland; 110,2, 56 pp.
6. SYKES, R.M. (1974) Sedimentological studies in southern Jameson Land, East Greenland I. Fluvial sequences in the Kap Stewart FM (Rhaetic-Hettangian). Bull. geol. Soc. Denmark 23, p 201-212.
7. SYKES, R.M. (1974) Sedimentological studies in southern Jameson Land, East Greenland II. Offshore-estuarine regressive sequences in the Neill Klint FM. (Pliensbachian-Toarcian). Bull. geol. Soc. Denmark 23, p 213-224.
8. CLEMMENSON, L.B. (1976) Tidally influenced deltaic sequences from the Kap Stewart FM (Rhaetic-Liassic), Scoresby Land, East Greenland. Bull. geol. Soc. Denmark 25, p 1-13.
9. SURLYK, F. (1977) Stratigraphy, tectonics and palaeogeography of the Jurassic sediments of the areas north of Kong Oscar Fjord, East Greenland. Bull. Grønlands. geol. Unders; 123, p 1-56.
10. BIRKELUND, T. and PERCH-NIELSEN, K. (1976) Late Palaeozoic-Mesozoic evolution of central East Greenland. in 'Geology of Greenland'; - 305-339, eds. Escher, A. and Watt, W. S. (GGU, Copenhagen).
11. BATHURST, R.G.C. (1975) Carbonate Sediments and Their Diagenesis. No. 12 in 'Developments in Sedimentology' series (Elsevier, Amsterdam).
12. BIRKELUND, T. and PERCH-NIELSEN, K. (1969) Field observations in Upper Palaeozoic and Mesozoic sediments of Scoresby Land and Jameson Land. Rapp. Grønlands. geol. Unders; 21, p 21-36.
13. BROMLEY, R.G.; BRUUN-PETERSEN, J. and PERCH-NIELSEN, K. (1970) Preliminary results of mapping in the Palaeozoic and Mesozoic sediments of Scoresby Land and Jameson Land. Rapp. Grønlands. geol. Unders; 30, p 17-30.
14. CALLOMON, J. H. (1961) The Jurassic System in East Greenland. In Raasch, G.O. (ed) Geology of the Arctic; 1, p 258-268 Toronto U.P.
15. KOCH, L. and HALLER, J. (1971) Geological Map of East Greenland 72°-76° N. Lat; 1:250,000. Meddr. Grønland; 183.
16. PETTIJOHN, F.J. (1975) Sedimentary Rocks, 3rd edition, (Harper and Row, New York)
17. READING, H.G. (1978) Sedimentary Environments and Facies. (Blackwell Scientific Publications, Oxford).
18. REINECK, H. E. and SINGH, I.B. (1975) Depositional Sedimentary Environments, corrected reprint of 1st edition, p 82-113. (Springer-Verlag, Berlin)
19. ROSENKRANTZ, A. (1929) Preliminary account of the geology of the Scoresby Sund district. In Koch, L. 'The Geology of East Greenland' Meddr. Grønland; 73, 2.
20. SURLYK, F., BROMLEY, R.G., ASGAARD, U. and RAUNSGAARD PEDERSEN, K. (1971) Preliminary account of the mapping of the Mesozoic formations of South-East Jameson Land. Rapp. Grønlands. geol. Unders; 37, p 24-32.

2.6 A REPORT OF MUSKOX OBSERVATIONS FOR 1982

Introduction

Conducting a survey of muskoxen was not a primary aim of the expedition. However we did undertake to keep a record of muskoxen that were sighted during our time in the field and this is presented in this report. The expedition base camp was half way up the Bersaerkerbrae glacier surrounded by ice and rock and too high to be hospitable to muskoxen. Parties from the expedition visited Schuchert Dal and Antarcitics Havn providing opportunities to observe muskoxen. On these trips the parties had to be self-sufficient and so carried heavy loads making it difficult to devote much time to detours to observe herds of muskoxen closely. Where possible an attempt was made to note the composition of herds as well as their size. Calves and yearlings could be distinguished by their size, however assessing the age of adults was too speculative.

The expedition arrived in Mesters Vig on 3rd July 1982 and flew by helicopter direct to the Bersaerkerbrae. The first party departed on 23rd July for Schuchert Dal.

Until 25th August there was a continuous stream of movements in and out of base camp. The observations made by these parties are given in Table 1.

Muskoxen and their North East Greenland range

The muskox (OVIBUS MOSCHATUS) looks rather like a modern mammoth with a head like a battering ram and a long shaggy coat. The bulls stand about five feet high at the shoulder, the cows about four feet. It has an extremely thick long coat to protect it against the rigours of the Arctic winter. The coat has two layers. The inner is a very dense, fine fleecy coat called qivint. This is covered by a dark brown coarse top coat on which the hairs may be as long as two feet on the chest, neck and hindquarters.

Muskoxen live in herds ranging in size from three or four to a hundred. The herd is usually ruled by a single bull; the bulls rut in the autumn. They charge at each other at full gallop, head down crashing their skulls together. The horns and bone at the front of the skull is usually eight or nine inches thick!

The bulls that lose spend a solitary life wandering the tundra alone. When threatened the herd forms into a circle with horns outermost with the young in the centre. The bulls will charge an enemy but they seldom press home their attack as this could mean leaving their herd.

During winter muskoxen stand around on the snow swept tundra huddled together with the adults acting as windbreaks for the young, protecting them from the worst of the Arctic weather. They scrape away snow where they can to feed on the vegetation underneath. They therefore need a dry stable winter climate in which the snowfall is not too great and there are no mild spells to thaw the snow which then ices over depriving the muskoxen of the forage buried beneath. Their main food is Arctic Willow (SALIX ARCTICA) and sedges (CYPERACEAE) which require little rainfall if water is available from melting snow patches, permafrost or glaciers.

Muskox calves are usually born in April or May after a gestation period of eight or nine months. They are born without the characteristic shaggy coat but they have a thick, short curly coat which is slowly replaced. The lactation period is about 18 months and because of this cows are only in season every other year or if they have lost their offspring. Muskox are probably more dependent than any other animal on climate for their survival and reproduction.

Muskoxen are thought to have existed in Greenland at least 4000 years ago (1) † However due to changes in climate it is unlikely that they have been in continuous occupation. Relatively recently, wet periods around 1200 - 1300 AD and 1500 AD made muskox extinct in north east Greenland. However following these periods they invaded from the north and inland refuges. Muskox bones found around Kong Oscars Fjord indicate that they lived there in the late seventeenth century (2). The drift ice pulsation and melting stages from 1740 to 1810 severely affected the population. The first positive sighting of muskoxen in North East Greenland occurred in August 1869 when KOLDEWEY (3) sighted and shot a lone bull. The population declined during a bad winter between 1895 and 1900 but during the 1920's, 30's and 1940's it thrived.

North Jameson Land provides some of the best pasture available to muskox. To the west are the inhospitable glaciated mountains of Scoresby Land. To the south and east is the barren central plain of Jameson Land where the vegetation is too sparse to support a large summer population. However the abundance of carcasses found there (4) and the relatively thin winter snow cover it receives may indicate that it is an important wintering place for muskox (5).

In summer northern Jameson Land is snowfree except on the high mountains. Despite their appearance muskoxen are remarkably agile. However the lack of vegetation of the steep mountain sides limits their grazing to the valleys and foothills. The greatest number are found in the large river valleys.

Distribution and Density in 1982

The record of daily observations is given in Table 1. The total number of muskox for each area are given in Table 2; these give an indication of the regional population. Care has been taken not to count animals twice in the census. This is fairly easy to avoid with herds since they can be recognised by the number of adults, yearlings and calves present. However repeated counting of solitary bulls is far more difficult to avoid, especially when visiting an area after an absence of a fortnight or more. These totals have been compared with totals collected by the Cambridge East Greenland Expedition (4), the 1962 Oxford University Expedition (4) and the 1974 Joint Biological Expedition to North East Greenland (6). The Cambridge expedition was in Greenland between 8th July and 9th September 1961 and journeyed mainly in the region to the south of our studies. However their figures for Antartics Havn are comparable. The figures from the Oxford expedition are difficult to compare since their figure for Schuchert Dal includes observations taken between Malmberg and the Konglomeratelv Valley. The majority of the animals were sighted in the valley between the Holger Danskes Briller Lakes. Whereas we only operated between Malmberg and the snout of the Roslin glacier on the west side of Schuchert Dal.

FERNS (6) has suggested that the most efficient way of comparing years is to use the maximum daily totals for comparable sites. This method eradicates the bias in the mean and total counts brought about by varying numbers of observers involved and number of days spent in an area. These figures are presented in Table 3. If the totals are used as an index of the population then between 1974 and 1982 there has been an increase of 1.1% per annum compared with 2.2% per annum between 1961 and 1974 (6). Ferns suggests that a modest increase in the range 1 - 4% per annum has occurred in the population in the 20 years preceding 1974 and the figures obtained for the last eight years suggest that this increase is just being maintained.

Ferns has estimated the total population for the regions visited in 1974, based on observations made on foot and from the air. He states that the summer forage in these areas is limited to land between 200 m, and on this basis he calculates population densities shown in Table 4. In 1982 muskoxen were sighted at over 700 m on the mountains on the north side of the Bersaerkerbrae and on the Gefion Pass (see figure 1). Hall (1964) also reports animals above 500 m. Population densities for 1982 have been calculated using the total number of animals observed and the area of land below 700 m that was actually visible to parties on their treks. As can be seen in Table 4 this gives considerably lower densities than Ferns obtained, but still higher on average than the 0.2 animals/km² he gave for the inclusion of all mountainous land.

† Numbers in parenthesis refer to the references listed at the end of the section.

The summer range in Northern Jameson Land supports a slightly larger density of animals than other regions in the Arctic. For example Devon Island in the Canadian Arctic and Nunivak Island off the west coast of Alaska support summer muskox densities of 0.3 animals per km² (7) and 0.2 animals per km² (8) respectively. However it is not the summer densities which limit the population but the winter density. In winter they will be restricted to much smaller area limited by the depth of snow through which they can dig to uncover food. No figures are available for muskoxen densities in North East Greenland in winter. However the point is illustrated by the figures for Nunavik Island where in₂ summer muskoxen wander over the entire island. In₂ winter they are restricted to 25 km² area giving a winter density of 29.7 animals per km².

Breeding Trends

Table 5 shows calf production figures for years between 1954 and 1982. The enormous variation is almost certainly caused by the varying severity of the winters. The winter of 1953-4 was catastrophic for the muskox population and combined with a bad winter in 1938-9 it reduced the population by half. A description of the 1953-4 winter is given by MALMQUIST (9) - the coast was free of drift ice during the early part of the winter. In February there were ten days of mild weather which melted a layer of snow. This layer of snow froze again when the cold weather returned covering everything in a sheet of ice. This cut off the muskox from their forage, decimated the population of young and old muskoxen. The 1954 calf production figure bears witness to the results of a disastrous winter. However 1955 showed a considerable increase in the number of calves per head of muskox, since the majority of cows that survived the 1953-4 winter would not have had a surviving calf to suckle and so would be available to breed in the autumn of 1954.

The winters of 1958-9 and 1959-60 were bad (see figure 2) and are responsible for the exceptional high percentage of calves in 1961, many of whom probably perished in the winter of 1961-2 which was also poor and followed by low calf production in 1962. The 1973-4 winter was also severe giving a low percentage of calves in 1974. The snow depths in the winter of 1980-1 and 1981-2 were not exceptional and this is reflected in the average number of calves in 1982. If the small sample sizes of 1955 and 1971 are neglected then the average percentage of calves is 8.3%, extremely close to the 1982 figure. This is not very promising for the future of the muskox, since it is thought that a mean of 10.5% is needed to stabilise the population in the long term (10). However when all the data is used a mean of 11.25% is obtained which is more encouraging and agrees well with the estimate of animal population increase of 1.1%.

Seasonal migration

It is difficult to give an accurate indication of seasonal migration because of the lack of observations of numbers, movement and feeding habits in winter.

We rarely sighted a herd in the same location on recurrent visits even after only a days absence. This would seem to indicate that the muskoxen are always on the move looking for new pasture. It was not obvious when an area had been grazed by muskox by examining the vegetation alone. It was noticeable that no muskox were seen around Mesters Vig or in the Tunnelelv in late August when we were in those areas. This supports the theory that there is a summer migration away from the coastal plain (6). In summer the coastal plain is likely to be wetter than further inland. Muskox prefer a dry climate because heavy rainfall will encourage the growth of dwarf birch (*BETULA NANA*), northern bilberry (*VACCINUM ULGINOSUM*) and other plants to the disadvantage of arctic willow (*SALIX ARCTICA*), one of the main components of the muskox diet.

In Schuchert Dal muskox were never seen near marshy or boggy areas indicating their probable dislike for this sort of ground. The summer of 1982 was particularly wet with several periods of very damp weather bringing low cloud and rain in from the sea for three or four days at a time. The weather never really set fair in its normal manner. This weather would be expected to force muskox further inland away from the wet coastal plain and this is reflected in our lack of observations around Mesters Vig and Tunnelelv.

A similar migration may occur in a winter when the absence of drift ice makes the coast extremely wet. Aerial photographs show that the lower slopes near the icecap are relatively snowfree in winter, as the cold air near the icecap blocks the intrusion of

the warmer wet air. These inland sites may well be of importance to muskox in bad winters.

Herd Size

The herd sizes (Table 6) appear to be correlated to the number of calves present in that year as one would expect.

Conclusions

Muskoxen in North Jameson Land are maintaining an average calf production rate high enough to stabilise the population under normal climatic conditions. The increase in population over the last 30 years is between 1 and 4% per annum which is encouraging after the muskox's chequered history in Greenland. However although they have few predators (there are no wolves in Jameson Land) and they are no longer killed for meat for trappers' dogs the population is still in danger of being decimated by a single catastrophic winter. They now face a new danger - losing their traditional grazing territories to man in his society's thirst for oil. Prospecting was being carried out in parts of Jameson Land whilst this expedition was in Greenland. Insufficient is known of muskoxen winter movements and habits to predict what effect an increase human presence would have on them.

Acknowledgements

The expedition would like to thank the Secretary of The Commission for Scientific Research in Greenland, and the Danish Civil Aviation Directorate for supplying the snow depth figures.

References

1. VIBE, C. 'Arctic animals in relation to climatic functions' Meddelelser om Grønland 170 (5) 1967
2. DEGERBØL, M. 'Animal bones from Kong Oscars Fjord region in East Greenland' Meddelelser om Grønland Vol 102, Part 2, pp 93-97 (1935)
3. KOLDEWEY, K 'Die zweite deutsche Nordpolarfahrt in den Jahren 1869 und 1870 unter Führung des Kapitan Karl Koldewey' p 325, Leipzig.
4. HALL, A.B. 'Musk-oxen in Jameson Land and Scoresby Land, Greenland' Journal of Mammology Vol 45, No. 1, 1964, p 1-11.
5. PEDERSEN, A. 'Polar Animals' London: Harrop 1962.
6. FERNS, P. N. 'Muskox Abundance in the Southern Part of the Range in East Greenland' Arctic, Vol 30, No. 1, March 1977.
7. HARRINGTON, C.R. 'Remarks on Devon Island Muskoxen' Canadian Journal of Zoology 43(1): 79-86 (1964).
8. SPENCER, D.L. and LENSINK, C.J. 'The muskox of Nunivak Island, Alaska' Journal of Wildlife Management, 34(1), p 1-15, 1970.
9. MALMQUIST, Steen 'Dansk patruljetjeneste i Nordøstgrønland' Grønland 1955 p 412-422.
10. FREEMAN, M. M. R. 'Population characteristics of musk-oxen in the Jones Sound region of Northwest Territories' Journal of Wildlife Management 35(1), p 103-8, 1971

TABLE 1 Musk-oxen herds in 1982

Area	Site	Date	Number	Herd size
Mesters Vig	Skeldal	7 August	4	4
	Ovre Gefion	20 August	2	2
	Nedre Fundal	13 August	6	6
		20 August	8	8
		22 August	1	1
Antarctics Havn	Delta dal	21 August	3	3
		22 August	9	8, 1
	Kolledalen	16 August	21	5,2,9,1,4
		20 August	20	8,1,2,(9)
Schuchert Dal	Flexurdal	19 August	14	2,3,6,3
	N. of Lang glacier Between Lang and Roslin glaciers	30 July	7	7
		23 July	8	1,7
		30 July	11	11
		16 August	14	8,4,11

() indicate animals observed before

TABLE 2 Regional enumerated populations

Area	1961	1962*	1974	1982
Mesters Vig			18	33
Antarctics Havn	42	11	47	46
Schuchert Dal		86		40
TOTAL	42	97	65	119

* These observations are not comparable because the areas involved are slightly different

TABLE 3 Maximum Daily Totals for Comparable Areas

Site	1961	1962	1974	1982
Skeldal		7	4	4
Ovre Gefion	2		5	2
Nedre Fundal			5	8
Delta Dal			3	9
Kolledalen	5	8	23	22
Flexurdal	14		14	14
TOTAL			54	59

TABLE 4 Population Densities

Area	Animals/km ² (1974)	Animals/km ² (1982)
Mesters Vig	0.3	0.13
Antarctics Havn	0.8	0.3
Schuchert Dal	-	0.5

TABLE 5 Calf Production for years for which data are available

Year	Sample size	Percentage Calves
1954 ¹	323	1.5
1955 ²	14	12.0
1961 ²	267	23.6
1962 ²	71	<5.6
1971 ³	28	25
1974 ⁴	233	3.0
1982	111	8.1

- 1 Vibe (1963)
 2 Hall (1964)
 3 Halliday (1974)
 4 Ferns (1977)

TABLE 6 Distribution of herd sizes

Herd size	1961	1974	1982
1	4	25	7
2	7	5	4
3	3	6	3
4	2	9	1
5	7	9	1
6	5	2	2
7	7	0	2
8	8	3	3
9	2	2	1
10	0	2	0
11	1	1	1
12	1	0	0
13	1	0	0
14	1	1	0
Mean	5.7	3.6	4.1

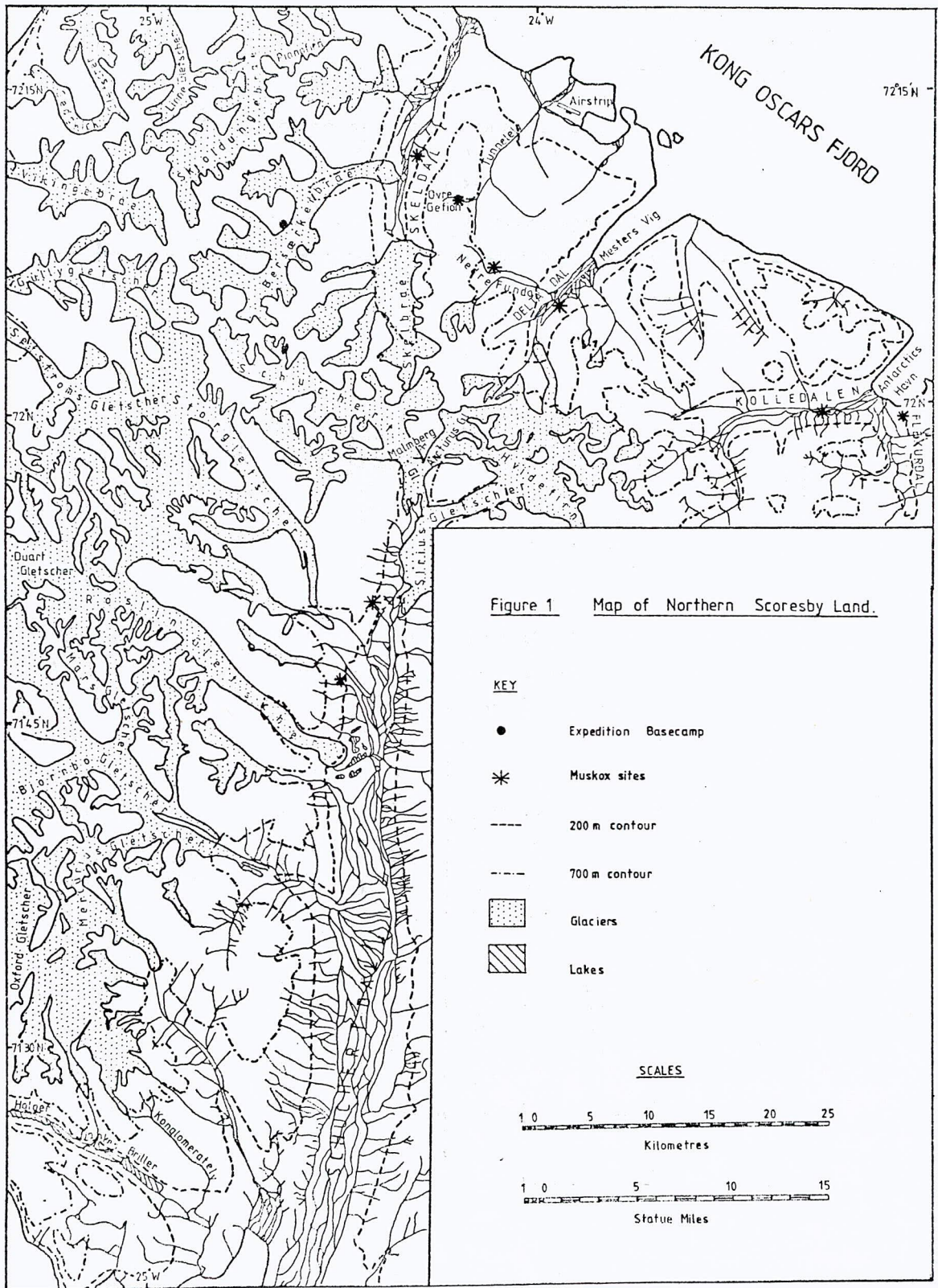
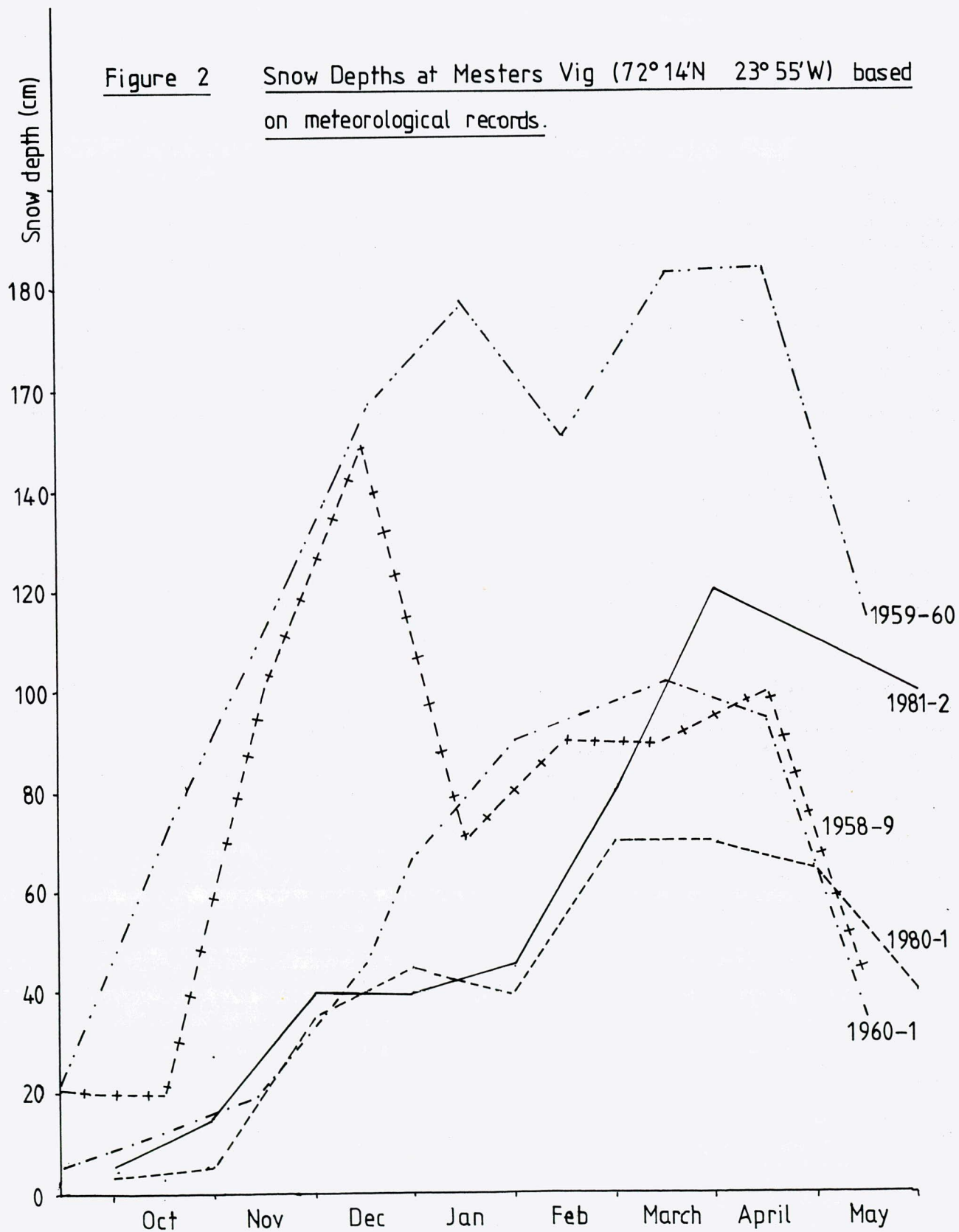


Figure 2 Snow Depths at Mesters Vig (72°14'N 23°55'W) based on meteorological records.



2.7 DETERMINATION OF PLASMA CORTISOL LEVELS

Introduction

Much has been written about the endocrine system's response to cold stress. Evidence for changes in plasma cortisol concentration in response to cold is conflicting. Both normal and increased levels have been reported in humans on exposure to cold for a period of a few hours (1, 2). Nagata et al (3) report approximately the same values of plasma cortisol during summer and winter for a population exposed to temperatures of minus thirty to minus six degrees centigrade during winter and fifteen to thirty degrees centigrade during summer. Experiments on rats (4) show that in the first few hours of cold exposure the blood levels of adrenocorticoids increase, but after several days, and perhaps because food intake has increased in response to the cold, the levels return to normal. A recent report (5) showed an increase in urinary 17 OHCS in 'non-prior adapted', and no change for 'prior adapted' individuals exposed to working temperatures of minus twenty degrees centigrade for two weeks.

It was decided to monitor plasma cortisol levels in members of the expedition to determine whether they would change, and also to see whether the diurnal variation might be abolished because of the twenty four hour daylight.

Normally venous blood samples for cortisol assay are centrifuged immediately and assayed soon afterwards. As the radioimmunoassay could not be performed in the field a method of storing samples for a long period had to be developed.

Development of a Technique for Storing Samples

Venous blood samples were taken into heparinised tubes from patients not receiving medication. The samples were then centrifuged within ten minutes of collection to remove cellular content. The plasma was removed by pipette and divided into six portions. Three portions were placed in plain glass tubes. Three portions were placed in commercially available plastic tubes, pretreated with fluoride, to which fifty microlitres of a nought point eight percent solution of merthiolate had been added.

A plain tube and a treated tube were frozen at minus twenty degrees centigrade and assayed the next day. A plain tube and a treated tube were left in a warm room (twenty to thirty degrees centigrade) for three weeks and then assayed. A plain tube and a treated tube were kept on ice for ten weeks and then assayed.

All assays were performed using the Amerlex radioimmunoassay kit for cortisol.

Graphs were drawn of the assayed value for each set of conditions, against the control value of the sample kept overnight at minus twenty degrees centigrade taken from the same patient.

See table 1

It was concluded that samples could be kept satisfactorily for ten weeks by centrifuging them and then storing the plasma in glass tubes kept on ice.

PATIENT NUMBER	FROZEN 1 DAY		ROOM TEMP 3 WEEKS		ICE 10 WEEKS	
	PLAIN	F+M	PLAIN	F+M	PLAIN	F+M
1	/	249	/	264	/	280
2	/	/	/	/	/	290
3	270	322	308	367	/	325
4	495	498	459	592	/	/
5	271	299	222	338	289	297
6	711	808	500	927	676	555
7	187	207	159	205	232	181
8	244	258	221	300	265	107
9	278	298	259	311	333	312
10	231	231	112	264	205	194
11	122	126	71	94	102	99
12	322	368	281	452	366	376
13	508	477	501	528	542	448
14	472	478	432	428	439	530
15	276	287	256	343	280	288
16	391	382	348	462	374	397

All values in nmol/ml

Method

Venous blood samples were removed from the antecubital fossa using disposable plastic syringes. The samples were placed in heparinised tubes and centrifuged within ten minutes of the blood being taken. The plasma was removed and placed in a plain glass tube which was then stored on ice. All samples were assayed in the same batch using the Amerlex cortisol radioimmunoassay kit on return to the United Kingdom.

It was planned to take samples at regular one weekly intervals from each member of the expedition. Unfortunately due to parties moving away from base camp it proved impossible to do this. Samples were collected from each expedition member at the same time each day (GMT). Five members of the expedition had samples taken at 0800 GMT, one member at 1600 GMT and one at 2100 GMT. During the last week of the expedition samples were also collected from four members of the expedition at different times of the day to determine the presence or absence of any diurnal variation.

Control samples were taken in a warm environment (approximately 22 degrees centigrade) before leaving the United Kingdom.

Results

See Graphs

There is a significant drop in plasma cortisol concentration between the control samples collected at 0800 before leaving the United Kingdom and those collected at the same time during the first eight days of the expedition ($P < 0.05$). There is no significance between samples obtained later in the expedition and those obtained before leaving the United Kingdom.

There appeared to be no loss of diurnal rhythm, despite the twenty four hour day-light present for most of the expedition.

Discussion

As has been mentioned previously there is a great deal of apparently conflicting evidence for changes in adrenocortical activity in response to cold. Some of the controversy seems to arise because there is not an accurate correlation between urinary 17 OHCS and plasma cortisol levels (3). A direct comparison of results is therefore not valid. Some authors have interpreted a steady level of plasma cortisol during cold exposure as an increase in secretion. They argue that if it were not for increased levels of secretion the level would have fallen with the normal diurnal variation. Others would interpret this as showing no change in the rate of secretion.

There is strong evidence to suggest that if people were exposed to cold over a long period of time then plasma cortisol levels will return to their 'normal' levels (2, 5). This idea fits well with the results of the present study which shows levels returning to their control values shortly after arriving in Greenland.

The initial decrease in plasma cortisol levels was rather unexpected as animal studies have shown an initial increase in cortisol levels in rats subjected to cold, followed by a return to normal levels a few days later. Sheep which have died in, 'severely cold, wet and windy conditions' have lipid laden and haemorrhagic adrenals suggesting that they have been excessively stimulated by adrenocorticotrophic hormone.

No comparable studies seem to have been performed over the two month period studied here. The initial decrease requires further study.

It is, of course, possible in any experiment where conditions are difficult to control that factors apart from temperature had a part to play in the results obtained. It seems unlikely that exercise had an effect in the initial period as little physical activity took place because of poor weather conditions. Changes in plasma cortisol levels in response to activity would, in any case, seem unlikely to account for the decrease in plasma cortisol concentration observed (6). Changes in relation to food intake during the expedition can have played no part as the diet for each day was, with the exception of the flavour of vegetable, identical.

Conclusion

This study shows a significant decrease in plasma cortisol concentrations when seven healthy subjects, aged twenty two to twenty six, were removed from the temperate conditions of the United Kingdom to an environment with air temperatures around four degrees centigrade. These concentrations then returned to their original, United Kingdom, levels during the course of the eight week expedition, though the air temperature did not increase appreciably.

References

1. J. GOLSTEIN-GOLAIRE, L. VANHAELST, D.D. BRUNOA, R. LECLERCQ and G. COPINSCHI. *Journal of Applied Physiology* 1970 Vol. 29 No. 5. Acute effects of cold on blood levels of growth hormone, cortisol and thyrotrophin in man.
2. H. NAGATA, T. IZUMIAMA, K. KAMATA, S. KONO, Y. YUKIMURA, M. TAWATA, T. AIZAWA and T. YAMADA. *J. Clin Endo Metab* 1976 Vol. 43 No. 5. An increase of plasma triiodothyronine concentration in man in a cold environment.
3. O. WILSON, P. HEDNER, S. LAURELL, B. NOSSLIN, C. RERUP and E. ROSENGREN. *Journal of Applied Physiology* 1970 Vol. 28 No. 5. Thyroid and adrenal response to acute cold exposure in man.
4. O. WILSON, P. HEDNER. *Acta Univ Lund. sct ii* No. 18 1966. A field study of physiological adjustment to increased muscular activity with and without cold response.
5. M. RAOOMSKI and C. BOUTELIER *J. Applied Physiology*, Vol. 53 1982 Hormone response of normal and intermittent cold-preadapted humans to continuous cold.
6. C. LEACH, P. TAMBAUT, J. VERNIKOS-DANELIS, C. WINGET, B. CAMPBELL. The effect of hypokinesia on plasma ACTH and cortisol. In Ferin, H. (editor), *Biorhythms and Human Reproduction*, pp 409-416, New York, Wiley, 1974.

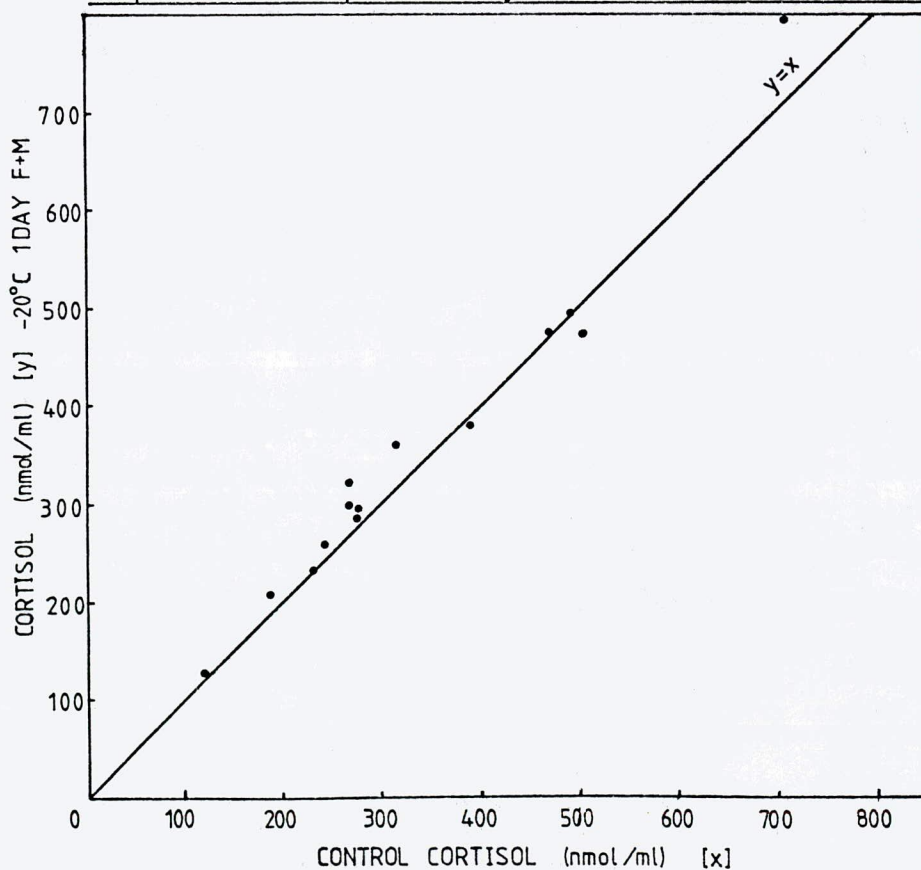
Acknowledgements

I would like to thank Dr. P. Howard of the Royal Hallamshire Hospital, Sheffield for agreeing to supervise this project.

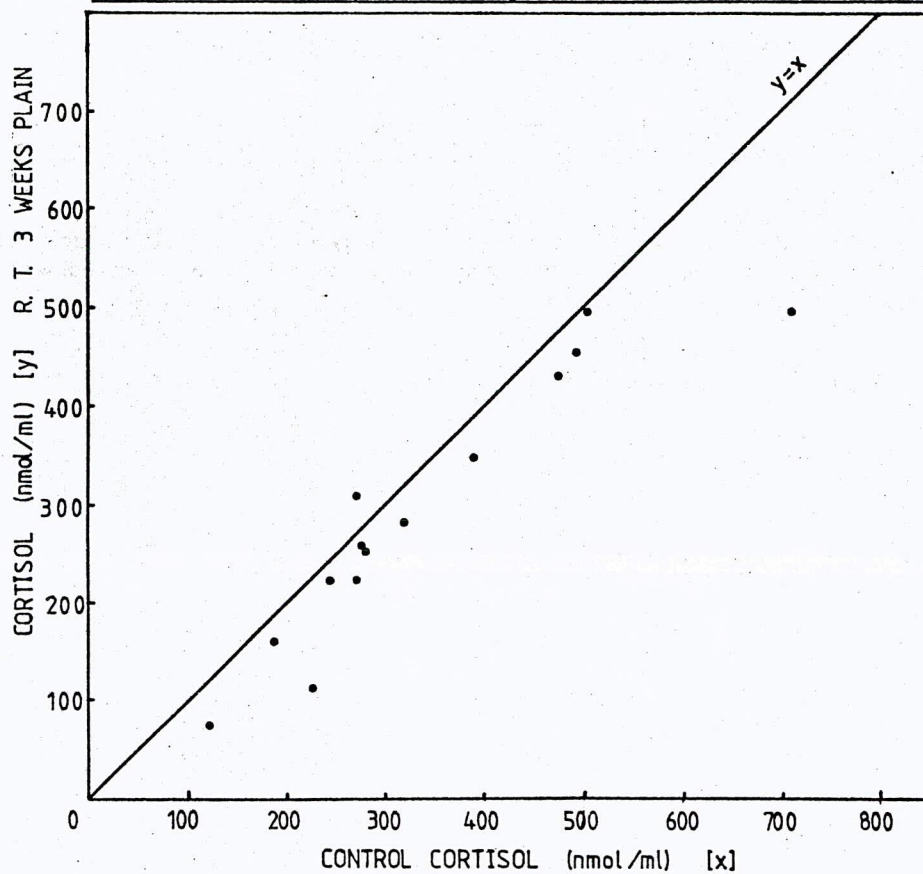
Thanks are due to Dr. Pennington and the members of his Department at the Jessop Hospital for Women in particular Mrs. C. Blair, for carrying out the cortisol assays and offering advice.

Thanks are also due to Mr. McClellan of Science and Technology Education on Merseyside (STEM) for his help in obtaining replacement hand cranked centrifuges at short notice.

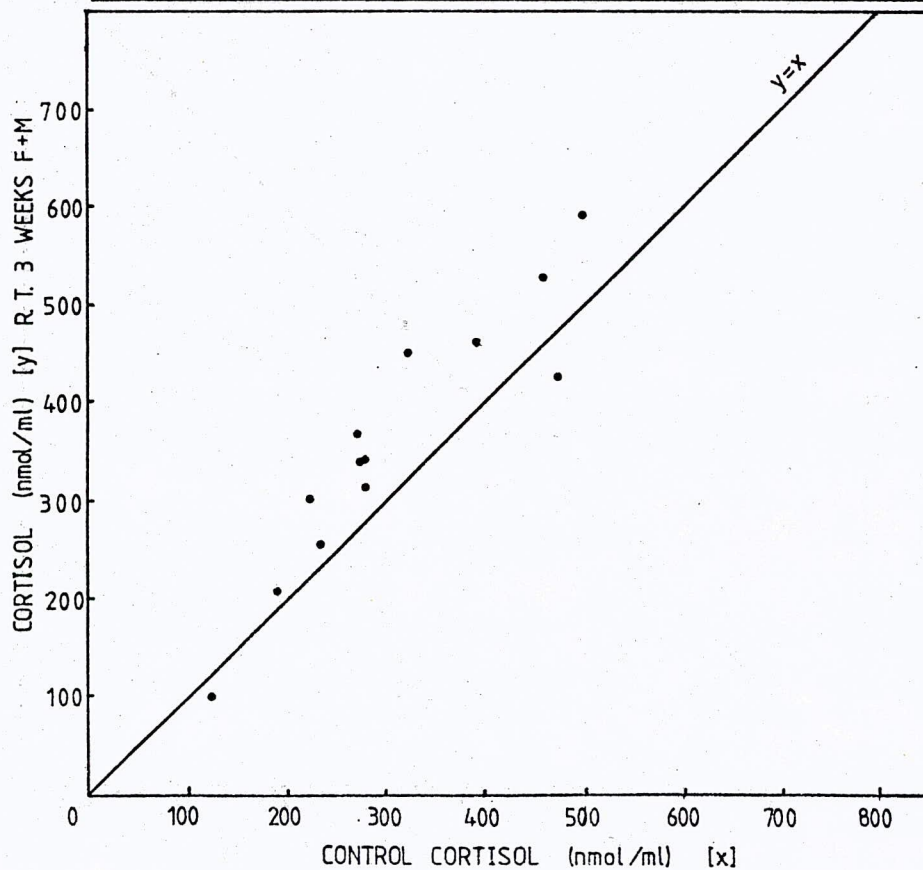
Graph to show reproducibility with time of cortisol assay



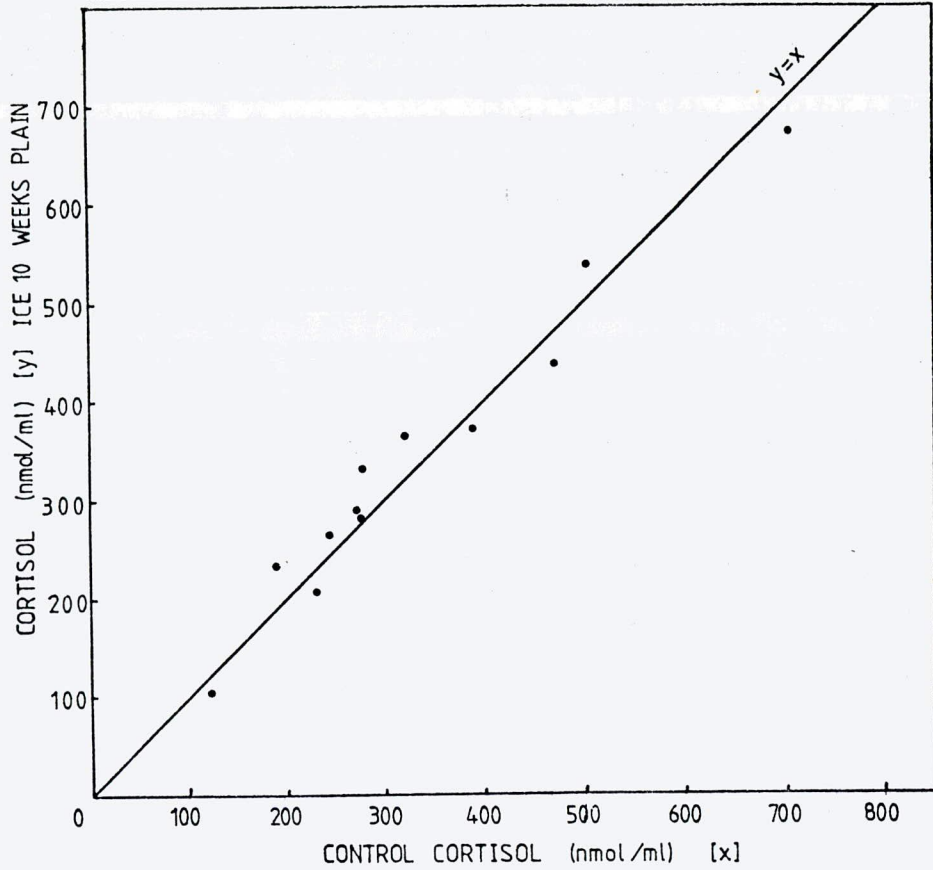
Graph to show reproducibility with time of cortisol assay



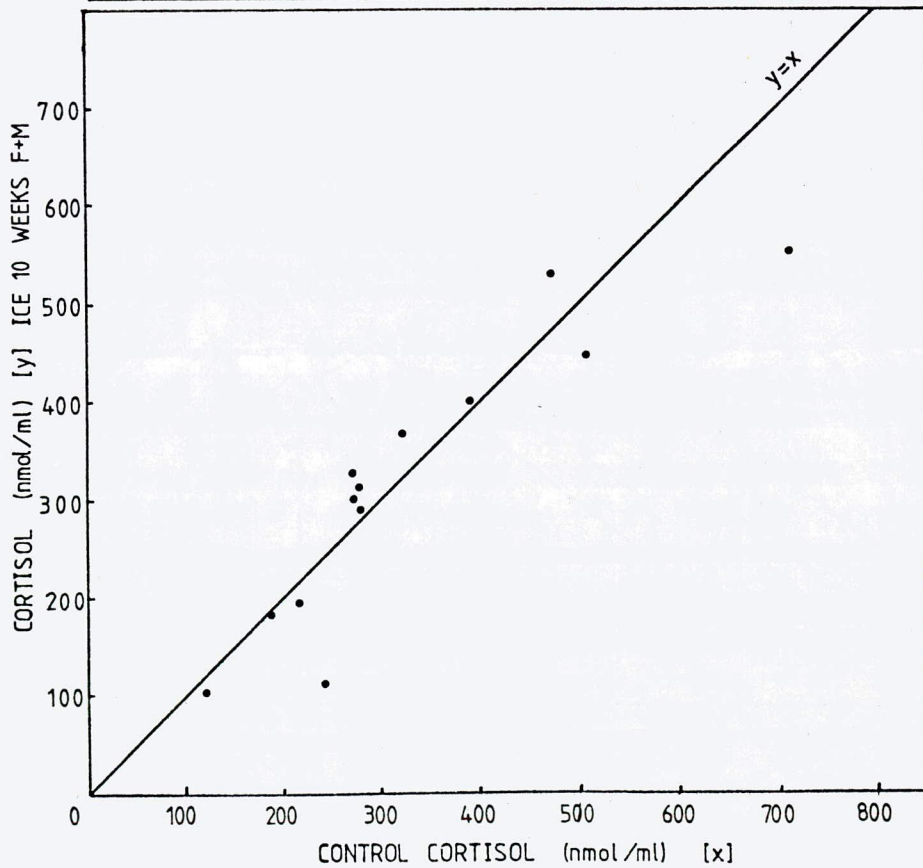
Graph to show reproducibility with time of cortisol assay



Graph to show reproducibility with time of cortisol assay

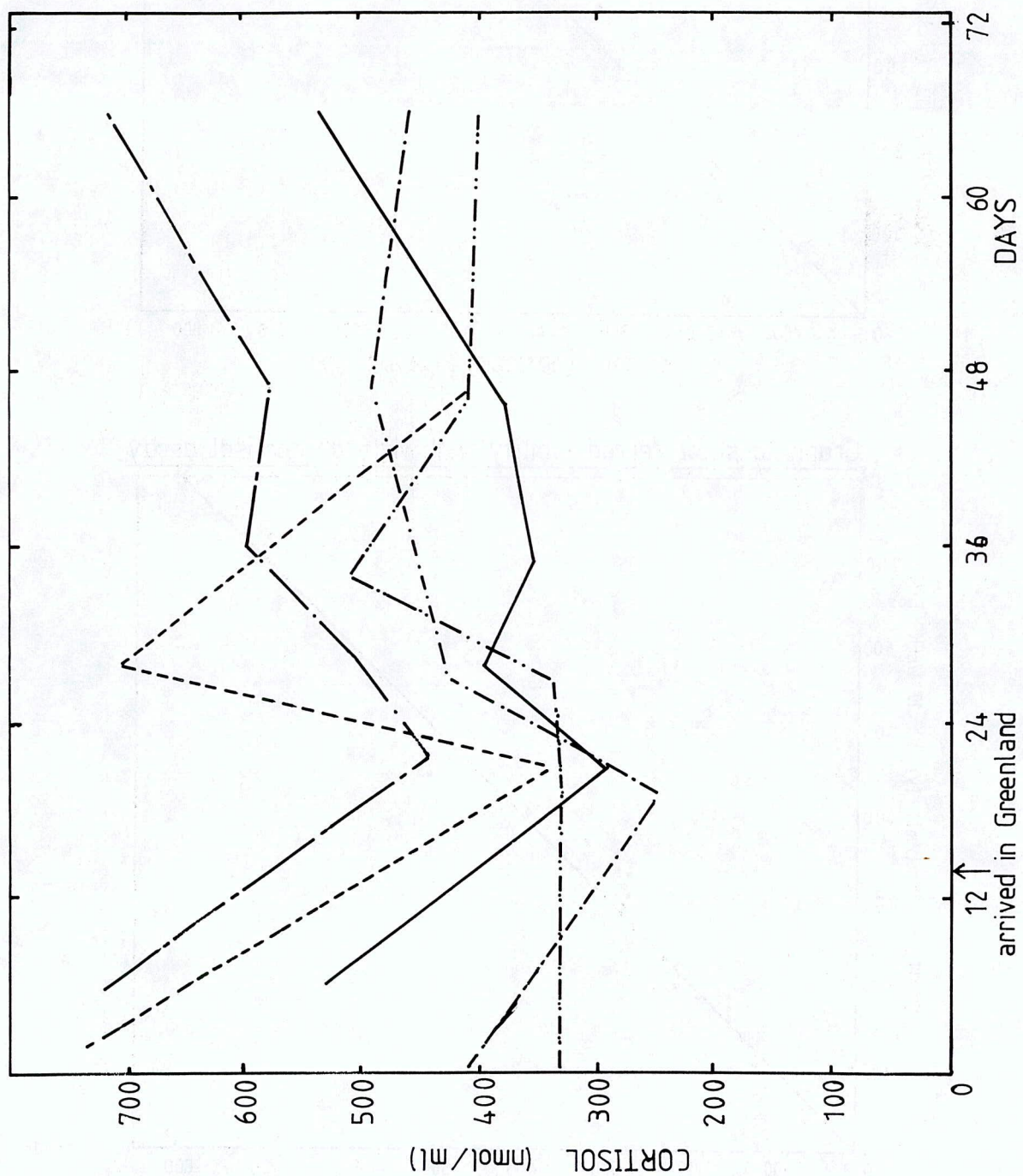


Graph to show reproducibility with time of cortisol assay



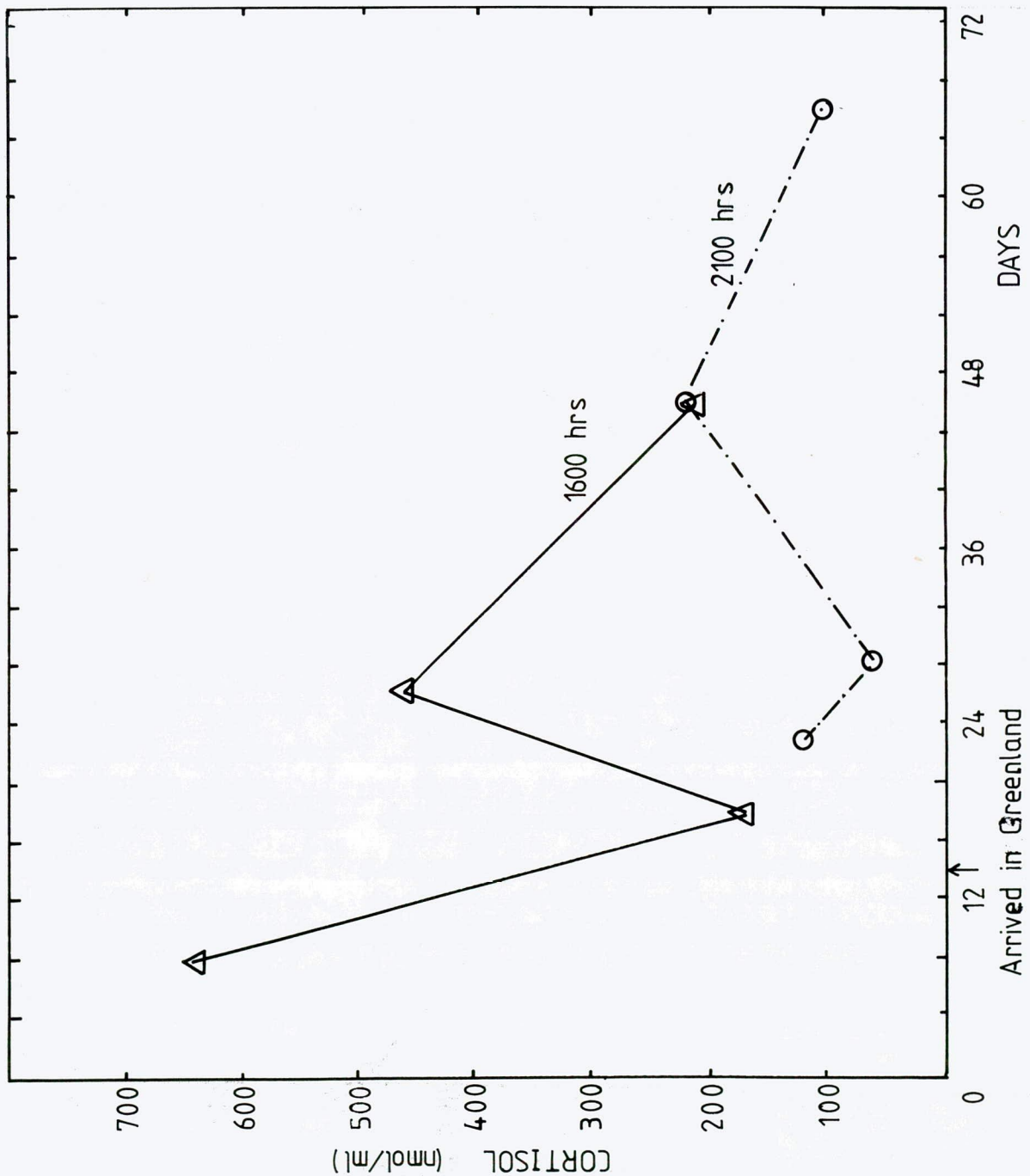
GRAPH TO SHOW VARIATION IN PLASMA CORTISOL CONCENTRATION WITH TIME.

Samples taken at 0800 GMT.

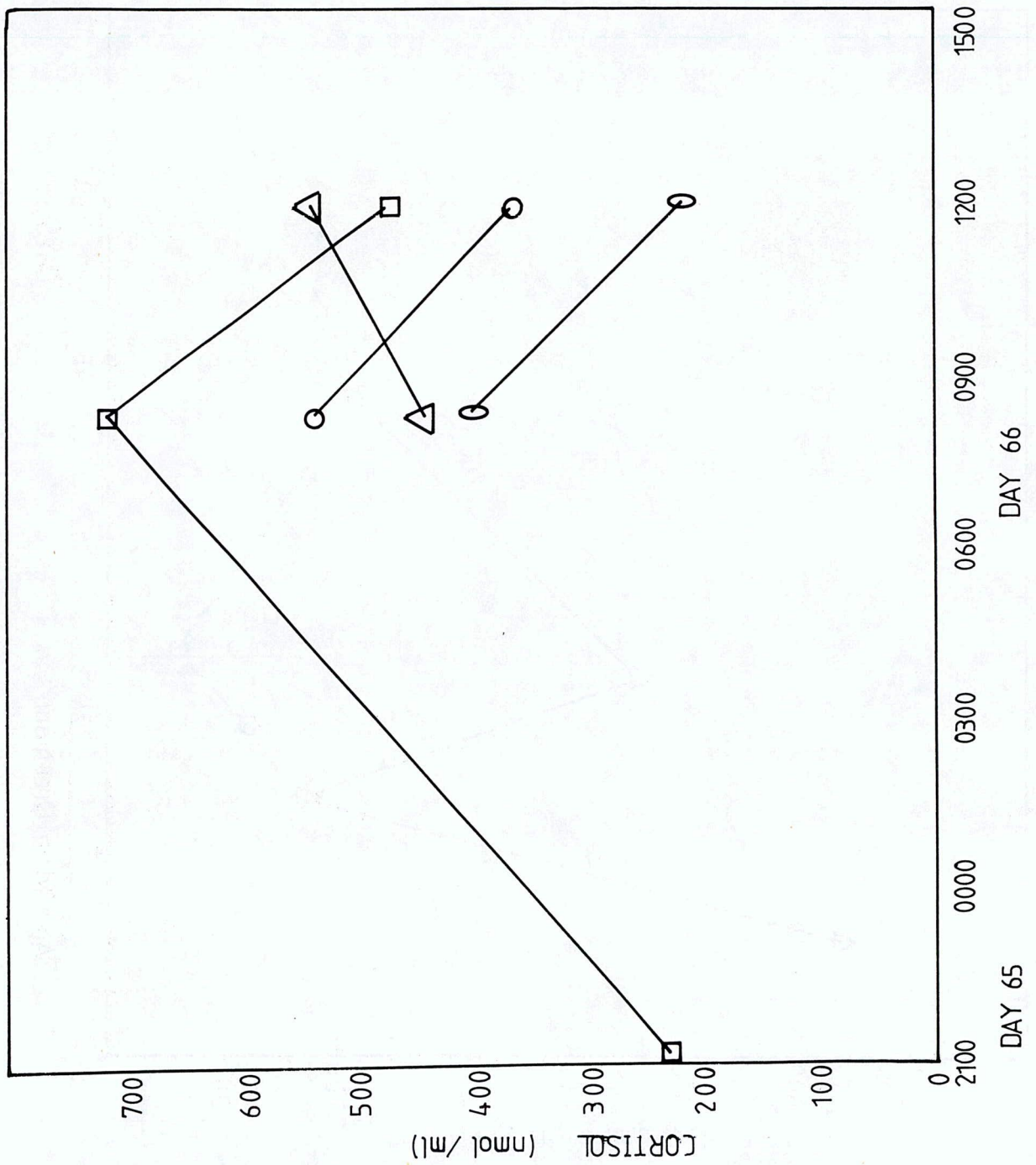


GRAPH TO SHOW VARIATION IN PLASMA CORTISOL CONCENTRATION WITH TIME.

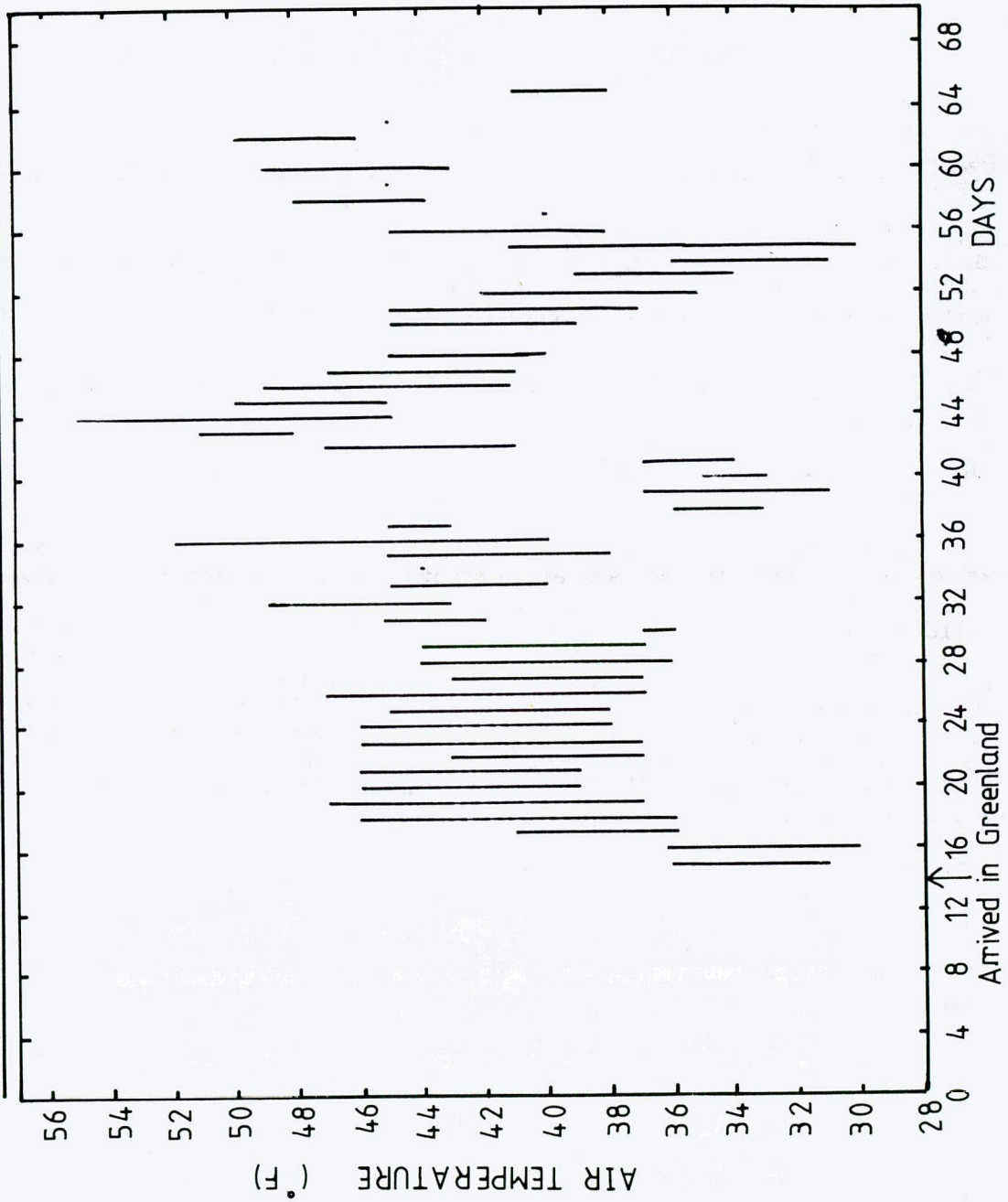
Samples taken at 1600 and 2100 GMT.



GRAPH TO SHOW DIURNAL VARIATION OF PLASMA CORTISOL CONCENTRATION



Graph of air temperature (waking hours) against time.



2.8 METEOROLOGICAL CONDITIONS OBSERVED IN THE NORTHERN STAUNING ALPS

DURING JULY AND AUGUST, 1982

In contrast with the weather conditions experienced by some of the expedition members during the 1978 Sheffield University Expedition to the area, the conditions during July and August were generally changeable with several spells of total overcast and precipitation. The observed weather conditions appeared to follow a regular pattern of 11 to 14 days duration. After eight to ten days of dry generally sunny and warm conditions there would be a day during which the cloud cover would noticeably thicken and the altitude of the cloud base would fall. Over the following two days either light rain or snowfall would be noted and the cycle would then end with a day during which the cloud cover would once again thin and rise in altitude. Precipitation was recorded on nine days during the first six weeks in the field.

The expedition arrived in the area on the 3rd July and was deposited on the glacier during a period of light snowfall. During the first few days the maximum and minimum air temperatures were both close to 32°F. The next spell of precipitation occurred over the 16th, 17th and 18th of July when there were several showers. This was followed by light snowfall on the 28th and 29th of July. Between these periods of precipitation it was generally sunny and warm with air temperature around base-camp reaching 44 to 48°F during the day and falling to 37 to 38°F during the night. The period 30th July to 9th August was notable for several successive cloud free days and was undeniably the best period experienced by the expedition. Snow returned on the 12th of August and this was followed by a week of unsettled weather with frequent snow and rain showers. During this week the wind was particularly strong, in contrast with the almost calm conditions during the rest of the period. The final spell of clear dry conditions started around the 20th of August although by then it was generally colder, with the night-time temperatures on the tundra often reaching below 32°F. During the month of August the day time air temperatures in the base-camp area reached typically between 41°F and 44°F and fell to between 34°F and 37°F during the night, the colder night-time temperatures occurring when the sky was cloud free.

The low wind speeds which are prevalent along this part of the Greenland coast lead to frequent development of local weather systems. On the small scale this included the katabatic winds which frequently developed overnight on the glacier. On a larger scale was the thick layer of mist which developed over the pack-ice in Kong Oscars Fjord and which occasionally was brought up the glacier past base-camp by the reversal in wind direction on the glacier which generally occurred about mid-day.

It was noted that this year there was substantially more pack-ice still present in Kong Oscars Fjord at the end of August than there was in 1978.

3.1 PERMISSION TO ENTER GREENLAND AND TRAVEL TO THE AREA

These sections have been combined, as there is no point in attempting to travel to the area without permission. In fact the flight to Mesters Vig will not be cleared to land unless permission has been given.

A Permission to Enter Greenland

The rules stated here are as they applied in 1981/82; later parties should ascertain the current position from the Ministry for Greenland. For scientific expeditions the rules are summarized in a booklet entitled "Welcome to Greenland", published by the Commission for Scientific Research in Greenland.

Authority to enter the National Park (in which the Stauning Alps lie) vests with the Landstyre in Godthab. However, application should be made to the Ministry for Greenland on the form available from the Ministry or the Commission. The Ministry will inform the expedition of the result. This procedure is simple, but will take several months. The expedition did not receive permission until the beginning of May 1982. The letter granting permission will specify certain conditions. Care should be taken to observe these. In particular, an insurance policy covering rescue expenses will be required; in our case a sum of 200 000 Danish kroner was specified.

Address: Ministry for Greenland
Hausergade 3,
DK-1128 Copenhagen K

The Commission for Scientific Research in Greenland
Øster Voldgade 10, tr. G, st.,
DK-1350 Copenhagen K

B Travel to Greenland

Mesters Vig receives only one ship per year, at the end of July or early August. This is too late in the season to be of use to most expeditions, although it may be worth considering shipping stores for use the following year. The passenger fare is in any case comparable to the cost of flying once the costs involved in joining the ship in Denmark are included.

The only practical air route to Mesters Vig from the U.K. is via Iceland. From Iceland an aircraft must be chartered for the flight to Mesters Vig. The payload of this flight is likely to be the major factor in much of the planning, and must be settled at an early stage. Whilst the weight of food and bodies can be estimated with some certainty, it is less easy to estimate scientific and other equipment. The expedition finally used a DHC6-300 Twin Otter for the outward flight and returned in a Mitsubishi MU2. The smaller MU2 was significantly cheaper and is probably the most economical aircraft presently available for this flight. The payload needed for the return flight will, of course, be reduced by the weight of the food eaten. It is worth noting that if these flights are costed in U.S. dollars exchange rate fluctuations can make a large change in the sterling cost. Both flights were chartered from:

Flugfelag Nordurlands HF,
Box 612,
602 Akureyri,
Iceland.

We can thoroughly recommend this company.

The expedition flew to Iceland using the scheduled Icelandair service from Glasgow. Icelandair no longer have a U.K. office, and so the flights were arranged through:

Iceland-Airtours,
11 Royal Exchange Square,
Glasgow G1 3BD.

We would like to offer our thanks, in particular to Mr. Ronnie Macaulay, for the assistance we received. Some stores were carried as baggage; the remainder were sent air freight. The air freighted stores were bonded at Keflavik and loaded directly onto the Twin Otter, avoiding customs formalities.

The alternative route to Iceland is by ferry from Scrabster to Seydisfjordur via the Faeroe Islands, taking two days. The agents in this country are:

P & O Ferries,
Orkney and Shetland Services,
P.O. Box 5,
Ferry Terminal,
Aberdeen AB9 8DL.

This route was discounted on the grounds of cost. The cheapest passenger fare is not significantly less than the advanced booked air fare. To move the volume of stores a vehicle would have been needed both in the U.K. and Iceland. Hire costs would have approached the air freight charges. Approaches to shipping agents concerning sea freight direct to Reykjavik proved fruitless, presumably due to the small amount.

In conclusion, future parties would be wise to investigate all possibilities, as the relative costs can change from one year to another.

3.2 TRAVEL WITHIN THE STAUNING ALPS

The expedition used two methods of travel, on foot and by helicopter. Space does not allow a detailed description of all the routes taken on foot. In any case, glacier movement and events such as flash floods can alter preferred routes, as we found to our cost in the Schuchert moraines. The descriptions in Donald Bennet's "Stauning Alps" guide give a good basis for route planning, allied with the 1:250 000 maps of the area (see section 3.6). Detailed route planning can only be done on the ground.

Ice axes are necessary for work on the glaciers, as are ropes if cols are to be crossed or work carried out above the snowline. Crampons are recommended; the lower parts of the glaciers can become very slippery after rain has washed away most of the surface roughness which normally provides traction for boot soles. The diurnal variation in glacier melt water flow makes a significant difference to the difficulty of crossing rivers and supra glacial melt streams, and crossings should be timed accordingly.

Travel by helicopter is fast, but very expensive. Thanks to a very generous grant from the University Expeditions Committee, we were able to charter one flight from Mesters Vig to the Bersaerkerbrae. The helicopter, a Bell 212, was just able to carry seven passengers and all the stores. The constraint was volume rather than weight. It may be possible to arrange at extra cost, the use of a cargo net to carry bulky items, but this requires a ground party in place before the flight. The major part of the cost was a flying time charge at the rate of about £1000/hour. It was not possible to spend time selecting a base camp site from the air. Instead, a landing was made in the general area chosen, and the final site was located on foot. Details of current costs, helicopters available etc can be obtained from the Copenhagen office of Greenlandair:

Greenlandair A/S,
Nyropsgade 26,
DK-1602 Copenhagen V.

3.3 FINANCIAL REPORT

The expedition has a credit balance as can be seen from the balance sheet presented overleaf. There are only a few outstanding expenses, including the distribution of the report and submitting papers to scientific journals. It is probable that the final balance will be extremely small and will be carried forward to the next Sheffield University Greenland Expedition.

The initial estimate of the cost of the expedition was about £6000; in fact it cost £7500. We underestimated the following expenditures: air freighting stores to Iceland, report printing and to a small extent insurance. In addition, mainly due to the University's generosity the expedition was able to charter a helicopter to fly into base-camp. This cost was not included in the initial estimates.

The expedition's fund raising was unexpectedly successful. £2655 was donated to the expedition. The Royal Society also gave a Scientific Investigation Grant of £169 to the Fracture Toughness of Ice Project. This grant and the project's expenses were not included in the balance sheet since the grant was specifically allocated to the project.

The expedition bought \$6300 in May 1982 when the pound was at \$1.7965. By the time the expedition left for Greenland the pound had dropped to around \$1.65. It was certainly worth being prepared for a severe weakening of the pound since this would have bankrupted the expedition.

The expedition's bankers were the Yorkshire Bank Limited and more recently Lloyds Bank plc. The Yorkshire Bank was chosen because it was felt that the expedition should support local business since local business and industry was supporting the expedition. However in retrospect it should be pointed out that a large city centre branch of one of the large clearing banks is better equipped and more experienced to perform the foreign currency dealings required by an expedition.

Finally I would like to thank the Manager of Lloyds Bank's Eastern Branch (Whitechapel High Street, London) for the personal assistance and guidance he has given me throughout the 1982 and the 1981 expedition.

INCOME

Carried forward from 1981 expedition	107.00
Expedition members (£600 each)	4200.00
Gilchrist Education Trust	150.00
Laverick-Webster-Hewitt Travelling Scholarship (University Prize)	125.00
Mount Everest Foundation	600.00
Royal Geographical Society (Geographical Magazine Trust Fund)	500.00
Royal Navy (Flag Officer Plymouth)	100.00
Scott Polar Research Institute (Gino Watkins Memorial Fund)	200.00
Sheffield University	600.00
Makro Self-Service Wholesalers Limited	50.00
Miscellaneous donations	330.38
Prof. K. J. Miller (payment for 2 places on flight from Greenland)	300.00
Sale of U.S. dollars	543.00
Sale of Danish and Icelandic currency	34.10
Sale of primus stove	43.00
Interest from savings account	17.53
Interest from deposit account	61.40
	<hr/>
	7961.41

Expenditure

Insurance - Personnel	388.03
Danish Indemnity	112.50
Scientific Equipment	80.00
Scheduled airfares	1123.00
Airfreight charges	388.28
Purchase of U.S. dollars for charter flights	3506.82
Helicopter charges	544.80
Sherpa van hire (Sheffield to Glasgow)	72.89
Car hire (Sheffield to Glasgow)	66.00
(Iceland in June)(2220.30kr)	110.57
(Iceland in August)(703.85kr)	30.60
Food (bought at Makro wholesale)	459.08
Food (bought at International Stores)	9.02
Miscellaneous hardware *	100.53
Data logger components	50.00
Medical supplies	15.00
Stationery, photocopying and prospectus	38.16
Postage and telephone	48.76
Report printing	378.67
Report typing	100.00
Cash expenses - Iceland	181.40
Greenland	24.69
United Kingdom	11.72
Bank charges	23.58
Public Relations Fund	35.75
Photographic services	14.03
	<hr/>
	£ 7923.88
Outstanding credit balance	<hr/>
	37.53

* Detailed expenditure on miscellaneous hardware

Primus stove	48.90
Billies	18.09
Nylon Groundsheet	15.60
Kitchenware	4.34
Carboard boxes	2.56
Cow Gum adhesive	1.47
Primus stove spare parts	9.57
	<hr/>
	£ 100.53
	<hr/>

3.4 FOOD REPORT

The main aim of this brief report is to help other people who might be planning an expedition for the first time, in the hope that our experiences will prove useful. It is therefore intended to highlight some of the more important factors which had to be considered.

One must realise that in organising the rations for a small expedition, with limited financial resources, that compromises are inevitable. The main problems being weight, bulk, price and calorie content. Thus the ideal ration is always brought down to the 'relatively' mundane level by the fact that any other variation would not prove feasible. It would be useful if anyone organising the rations for the first time, or going on an expedition for that matter, understood this.

The menu shown below was designed to produce a calorific intake in the range 3000-3500 calories, with a weight per manday of 1.0 kg maximum. The payload of the charter flight from Iceland to Greenland made the weight per manday factor of paramount importance. Fortunately the proposed menu was able to meet these specifications despite many modifications. Major modifications are usually caused by the incorporation of donated foodstuffs into the menu.

Table 1 SAMPLE MENU

BREAKFAST:- porridge oats with sultanas (hot or cold); digestives with marmalade; tea
LUNCH:- digestives with jam or peanut butter; chocolate bar; tea or fruit juice
drink
DINNER:- soup; meat product; dried vegetables; spaghetti; coffee, cocoa or tea.

It should be recognised that with such a menu there will be times when the amount of food is too much or too little; but overall, expedition members felt that the rations were more than adequate. Although with hindsight the amounts per manday of some items could have been altered. Certainly the margarine and dried milk allowances would have been decreased allowing an increase in the sugar ration.

Table 2 shows the actual amounts per manday of the foodstuffs consumed and their calorific values.

No mention has been made of the methods of packaging as they tend to vary considerably according to circumstances and are largely a matter of common sense. See the equipment report, section 3.4, for brief details of packaging.

In the final analysis with the severe limitations placed on the weight per manday by aircraft payloads the changes possible were very few indeed; unless the menu was radically changed and financial constraints removed.

Perhaps the following statement found accompanying 'notes on food packing' sums up the expedition rations ...

'if in doubt - STARVE!'

We would like to thank Mr. P. Morris of Makro Sheffield for arranging day pass facilities to purchase the food, and a £50 donation towards the cost.

TABLE 2

ITEM	WEIGHT PER MANDAY (g)	CALORIFIC VALUE (KCAL)	CALORIFIC VALUE PER 100g (KCAL)
OATS	72.0	288	400
DRIED MILK	40.0	141	353
SUGAR	95.0	372	392
DIGESTIVES	125.0	604	483
MARGARINE	143.0	1091	763
CHOCOLATE	65.0	250	385
PEANUT BUTTER		124	620
OR JAM/HONEY	20.0	54	268
MARMALADE	20.0	53	265
PASTA	107.0	364	340
MEAT PRODUCT	75.0	75	100
SOUP	29.0	9	30
DRIED VEG	20.0	15	75
SULTANAS	54.0	134	248
COFFEE	2.85		
TEA	2 BAGS		
COCOA	2.85		
FRUIT JUICE DRINK	2.85		
	874	3550*	

* Approximate total; there are minor variations between meat products, vegetables etc.

Source of calorific value data - Expedition Food and Rations Planning Manual
Young Explorers' Trust.

Assistance Received

Listed below are the companies who donated food, together with comments on the items. Our thanks are offered to all these concerns for their generous support.

COMPANY	FOOD	COMMENTS
Rowntree-Mackintosh	'Yorkie' chocolate bars Peanut butter	Re-packed to save the weight and hazard of the glass jars
Colman Foods	Assorted sauce mixes Honey; peanut butter;) lemon juice)	Added to boxes at random; adds welcome variety to the meat course Re-packed - see comment above
Quaker Oats	Porridge Oats; Spaghetti	
Trebor Ltd	Trebor mints Extra strong mints	A great help in passing a day out on the glacier
Hunni Foods	Porridge Oats; Spaghetti Muesli; Sultanas Soups - various flavours Dried Vegetables	The plastic re-sealable pots were very good, and used for other purposes once empty.
Dairy Crest	Dried milk powder	

3.5 EQUIPMENT

Introduction

The expedition was primarily a scientific enterprise and once base camp was established our only method of transport was on foot. As a result we only carried sufficient mountaineering and camp equipment to fulfil our basic requirements. We did however carry a range of support equipment for the scientific apparatus commensurate with remaining a 'lightweight' expedition.

The equipment list given below has been made as comprehensive as possible so that it can be used as a guide for future expeditions. The comments are inevitably based on personal experience although the entire expedition was canvassed for opinion. The comments on general equipment are mine and the scientific equipment comments belong to John Allen and Bob Andrews. Items specific to one project only are not included here; only 'general' scientific items have been listed.

Much of the equipment was already owned or bought by individuals, rather than the expedition. This made us more critical of the equipment. In certain cases I have been rather scathing, my intention is solely to forewarn other people who plan expeditions. However if any manufacturers read this report they may find it useful as well.

Items donated to the expedition are indicated by an asterisk against the supplier's name. Our thanks are offered to these concerns. We would also like to thank Don Morrison Mountaineering Equipment for supplying general and personal equipment at discount prices.

A. GENERAL EQUIPMENT

ITEM	QUANTITY	MAKER/SUPPLIER	COMMENTS
Mk III Force 10 Tents	2	Vango	Both were cotton throughout, one had a lightweight groundsheet which was too thin for the moraines. Snow and Rock vallances would be a very useful addition to these tents. (This modification is available by special order from the manufacturers.)
Ultimate Tent	1	Ultimate Equipment	A spacious three man tent, susceptible to condensation and fitted with too thin a ground sheet. However like the Force 10, it proved very stable in high winds and snow despite the ground subsiding underneath it.
Large lft tent pegs	24	Specially made by expedition member	These pegs were made from 1/16" x 1" x 1" aluminium angle iron. They were originally destined for use as tent pegs, they worked well in snow, sand and loose moraine but bent too easily if they had to be hammered home. However they provided an invaluable source of raw material for modifying scientific equipment.
Spare tent rubbers	10		
½" x 2m drain-pipes (Plastic) + connectors	6	Arnold Laver DIY	They were intended as survey markers, they were lightweight making portorage easier but they lacked rigidity even when packed with sand. They were however successful as part of the rotation meter pendulum.
1" x 2m drain-pipe (Plastic)	1	Arnold Laver DIY	Used as a water-pipe in the melt water stream to fill our water containers.
10 Litre Water Bladders	2	Blacks	20 litres of water lasted us 24 hours, these plastic containers were starting to split when we left Greenland. Their major fault is that the tap tends to fall out whilst pouring. They would be virtually impossible to fill in a stream without a water pipe. Advantages, light and small when empty.
5 Litre plastic bottles	10	Sorby Hall*	These were used detergent bottles which we took to Mesters Vig empty. Some were badly crushed en route however none were punctured. They were used as fuel bottles - a very cheap and successful innovation!
Optimus III Parafin Primus Stove	4	Don Morrison Ltd Bryan Stokes Ltd	These stoves were bought by the expedition in the expectation that they would live up to Optimus' fine reputation. They failed dismally! We were assailed by a series of minor faults which one should not have to experience from stoves in their price bracket. We would recommend that future expeditions thoroughly test these stoves to iron out these teething problems, before taking them into the field.
3" Plastic funnels	4	Prestons Ltd	Used to refuel the stoves. Funnels with filters would be better, but were unavailable at the time of purchase.
Trangia Billy Set	1	Optimus S.A.	Excellent, well-designed, robust billies. To save weight we took only one lid for three billies, two lids would be more useful.

ITEM	QUANTITY	MAKER/SUPPLIER	COMMENTS
Bull Dog Billy Set	2	Blacks (Greenock Ltd)	Cheap, lightweight billies, but they dint and buckle very easily. Both sets were new at the start of the expedition and had to be thrown away at the end.
Meta Fuel	8 x 40 tablets	Don Morrison Ltd	An excellent clean method of starting a primus stove, needed minimum of $\frac{1}{4}$ tablet to start each stove. One word of warning; they appear to be hygroscopic.
Wooden spoons	3	-	An essential piece of kitchen equipment, a ladle would have been useful.
Mugs and plates	-	-	Everyone took their own, a bad move! It makes sharing out food too difficult. Mugs and plates should be all the same, although they should be kept by individuals to avoid infection.
Brillo pads	16	-	Planned to use two per week, however after being used once they were practically useless.
Zoflora disinfectant	1 bottle	-	A concentrated disinfectant, used to clean cooking utensils after a nocturnal visit by an Arctic hare.
Jeyes Cloths	10	-	Good strong, hardwearing, usually thrown away because they were greasy, not worn through.
Travel wash, cold water detergent	4 tubes	Boots Ltd	We needed at least double the quantity, works well once out of the tube (it freezes in the tube), although specified as useable in cold water, the manufacturers obviously didn't mean meltwater at $\frac{1}{2}^{\circ}\text{C}$.
Pan scourers	16	-	Clog with grease after first use, really needed one per day, or more detergent which ever is lighter.
Plastic bags 5 $\frac{1}{2}$ " x 5 $\frac{1}{2}$ ", 3 $\frac{1}{2}$ " x 4"		Transatlantic Plastics	These were resealable, excellent for sample collection and storage of small electronics components
Thin plastic bags 12" x 8" 3" x 5"		Grangewood* Plastic Packaging Ltd Leesack Ltd*	Excellent for packing rations by the day and as a general purpose waterproof bag. They did tend to puncture easily.
Cardboard boxes	40	J.A. Henderson & Son Ltd.*	Two types were used (a) 1ft cubes of thick 3 layer water resistant card, these were excellent, rigid waterproof and doubled as good building blocks. They were used to carry rations in and were perhaps too small. (b) 9"x9"x18" thin card boxes, useless, no rigidity, fortunately we only had a few.
2oz nylon sheet 3m x 3m with eyelets	1	Specially made for the expedition	Designed as a cover for a base camp kitchen area. A heavier weight of nylon is really needed and stronger eyelets in say a 1" rather than $\frac{1}{2}$ " hem. Loops for roofing poles would also stop it ballooning in strong winds.
String	4 balls		We took two types, a thin twine that was virtually useless as it snapped too easily and a thick good quality cord that was really multi-purpose.

ITEM	QUANTITY	MAKER/SUPPLIER	COMMENTS
Cloth adhesive tape	12 rolls	Advance Tapes (UK) Ltd *	Used to seal cardboard boxes in the U.K., waterproof and strong, we only carried one spare roll, needed 2 or 3.
PVC insulating tape	various colours and widths	Advance Tapes (UK) Ltd *	Used for data logger trials, making a polariscope from cardboard boxes, identifying kit, general repairs. Invaluable!
Refuse sacks		Grangewood* Plastic Packaging Ltd Leesack Ltd*	One to line each box of rations, others to line rucksacks, etc. Essential when stores may be left exposed as airports or unloaded straight onto a glacier in falling snow.
Ropes	2		Climbing ropes, 1 off 11mmx45m, 1 off 9mmx45m.

B. SCIENTIFIC EQUIPMENT

ITEM	QUANTITY	MAKER/SUPPLIER	REMARKS
Coding sheets		University	To record data logger readings for immediate card punching in Sheffield
Graph paper	1 pad		
Marker pens	2		1 per member as personal kit would have been better.
"Araldite Rapid" Epoxy Adhesive	2 packs	CIBA-Geigy	Not very rapid at 0°C; joints were weak even after allowing an extended cure time.
Paint stick	3		Used for numbering boulders.
Jewellers' screwdrivers	4		
Tweezers	1		
Whirling hygrometer	1	Casella	
Multicore solder	1m length		Used with a soldering iron heated over the primus stoves for in the field repairs.
Rubber bands			
Small bulldog clips			
Protractor	1		360°, plastic
Rulers	3		300mm, one plastic, two steel
Thermometers	2		1 max/min
Calculator	1	Texas Instruments	Scientific; LCD display became sluggish when cold.
Digital Multimeter	1		Essential for trouble shooting the data loggers.
Resistors	various values		For rotation meters etc; see data logger report.
Terminal strip	25 connections		Quick method of connecting rotation meters etc. Could have used more.
Polythene beakers	2		150 ml, calibrated as rough measuring cylinders.
Junior hacksaw	1		Plus spare blades
Needle files	3		Flat, round, threesquare. Would have taken 8" round and flat in addition if weight constraints had allowed.
Aluminium cooking cooking foil	2 rolls 300mmx3m	BACO	Used to shield thermometers and blood sample cool box from solar radiation.
30m Fibron tape	1	Rabone-Chesterman	
20m steel tape	1	Rabone-Chesterman	Tape only, sections used for stream survey and perched block survey.
Allen screws and nuts	Assorted		M3 and M5, various lengths. Appropriate keys required!
Re-sealable polythene sample bags	several	Transatlantic Plastics	Several uses, especially useful for preventing 'bits' becoming lost in the sandy moraine.

3.6 MAPS, AERIAL PHOTOGRAPHS AND LANDSAT IMAGE

1. Maps

Three sheets of the 1:250 000 series are needed to cover the entire area:

7101 Carlsberg Fjord
7102 Stauning Alper
7202 Kong Oscars Fjord

Sheet 7202 is based on 1930's survey, and the area of the central Stauning Alps, around the head of the Stor Glacier, does not show the glaciers accurately. Sheets 7101 and 7102 are more recent (1960's survey in general) and are more accurate. It should be borne in mind that the scale prevents a very detailed representation of the mountain regions.

The area is also covered by two sheets in the 1:1 000 000 series. Only the Northern sheet, 2040 Kong Christian X's Land is currently available. This covers the East coast from 72°N to 75°N inclusive, from the inland ice to the Greenland Sea.

The maps are very difficult to obtain in this country; it is easiest to order them directly from:

Geodaetisk Institut,
Rigsdagsgarden 7,
DK-1218 Copenhagen K.

Delivery is usually 3-4 weeks; the price in 1981 was about 30 Danish kroner each sheet.

The two sketch maps compiled by Donald Bennet for his Stauning Alps guide book were also used. Although at a scale of 1:100 000, they show only the outline of the glaciers and the location of peaks. They may still be available from:

West Col Publications,
1 Meadow Close,
Goring,
Reading,
Berks. RG8 OAP

2. Aerial Photographs

Individual stereo pairs and a composite mosaic were used before departure in an attempt to choose a suitable site for base camp. This was frustrated by the amount of snow cover obscuring the glacier and moraines. Copies of the mosaic were used in the field as a substitute for large scale maps of the glacier. I would like to thank Mr. R. Brown of the Geography Department of the University for the loan of his prints and mosaics.

The scale of the prints was about 1:35 000 at sea level. A total of 25 prints in 4 runs covered the Bersaerkerbrae, Skeldal and Deltadal. The photographs were taken in July 1973. The Geodaetisk Institut will provide information on the most up to date coverage, price, etc.

3. Satellite Imagery

To provide an overview of the whole of the Staunings Alps a copy of the Landsat

scene for Path 248 Row 9 was purchased from Earthnet through NPOC (National Point of Contact - for address see below). This approximately 185 km square scene is centred on the head of the Roslin Glacier and provides coverage from Kong Oscars Fjord in the North down to Scoresby Sund in the South and from Carlsberg Fjord on the East to well beyond Alpefjord in the West. The whole of the Staunings Alps are present on the scene. Four dates with cloud free imagery were available:

3 July 1979
20 March 1980
7 April 1980
6 March 1981.

The 1979 image was thus the most likely to be free of snow cover, so a 1:1 million black and white film positive copy of band 6 (near infra-red) was purchased. The choice of band was related to the enhanced appearance of rivers, lakes and saturated snow on imagery taken on the IR part of the spectrum. Film positive was chosen as the medium so that contact negatives could be made off selected portions of the scene. It also was the most suitable format for digitizing using a stereocomparator.

A users guide, order form and current price list can be obtained from:

NPOC,
Royal Aircraft Establishment (Space Dept.),
Farnborough,
Hants,
GU14 6TD.

(The May 1982 price of one image was approximately £19, prices increased end October 1982.)

3.7 MEDICAL REPORT

A fairly comprehensive medical kit was carried by the expedition; (see contents list). The bulk of the supplies were transported in two boxes with the main stores. The drugs were carried by the medical officer as hand luggage to simplify customs formalities.

Fortunately we had no serious accidents during the course of the expedition. We were, however, able to offer medical assistance to two members of another expedition in the area, who were later evacuated on medical grounds.

No vaccinations were required for entry to Greenland. All members were advised to ensure they had up to date Tetanus protection. It is also worth noting that Rabies is endemic in the wildlife of the region. Care should be taken to maintain high standards in camp, as scavenging raids by foxes are likely.

Our thanks are extended to Mr. D. Fergusson of the Royal Hallamshire Hospital, Sheffield and to the staff of the University of Sheffield Student Health Service for their advice and assistance in preparing the medical stores.

Medical Supplies

Each box contained:

2 x Sterile Dressing (10cm x 40cm)(Parafin Gauze Dressing B.P.C.)
3 x Latex Medical Procedure Gloves
1 x 7.5cm porous elastic adhesive bandage
1 x 5 cm porous elastic adhesive bandage
1 x Suture set
7 x 'Melolin' Non Adherent Dry Absorbent Dressing (10cm x 10cm)
4 x 'Propax' Gauze Swabs B.P. (10cm x 10cm)(5 swabs 12 ply)
2 x Sterile Dressing Pack (1 Absorbent Dressing Sheet 50 cm x 45 cm)
3 x Sterile Dressing Pack (5 Large Absorbent Cotton Balls B.P.)
2 x Triangular Bandage
7 x Sterile Dressing Pack (1 Gauze Tissue Pad 20cm x 27.5cm)
1 x 4 Plain Dissectors
1 x Dressing Scissors
1 x 20cm Plaster of Paris Bandage B.P.C.
1 x 15cm Plaster of Paris Bandage B.P.C.
1 x 10cm Plaster of Paris B.P.C.
1 x 5cm Plaster of Paris Bandage B.P.C.
3 x 15cm Crepe Bandage
3 x 10cm Crepe Bandage
4 x 7.5cm Cotton Conforming Bandage
10 x Savlodil
1 x Disposal Airway
4 x 'Steri-Strip' Skin Closures (6mm x 75cm)
1 x Roll of 1cm Zinc Oxide Plaster
In addition Box 1 contained: Assorted Silk Sutures
4 x Surgical Blades
10 x 2ml ampoules Lignocaine Hydrochloride 2%w/v
1 x 500g Cotton Wool
In addition Box 2 contained: 1 x Roll 20cm Zinc Oxide Plaster
Assorted Silk Sutures
4 x Surgical Blades

1 x 100 Cotton Buds
1 x 7.5cm Roll of Zinc Oxide Plaster B.P.C.
2 x Thermometers
10 x 2ml ampoules Lignocaine Hydrochloride 1%w/v

Also taken: 1 x 3ft x 4ft sheet thermoplastic splinting

Drugs

Amoxyl	100T x 250mg
Erythromycin	250T x 250mg
Flagyl	60 x 200mg
Piriton	50 x 4mg
Maxolon	20 x 10mg
Avomine	20 x 25mg
Polyfax	2 x 4g
Amethocaine	1% 2 x 10ml
Streptotriad	20 Tablets

3.8 RADIO REPORT

A high frequency radio set was taken to Greenland by the expedition in order to maintain an emergency rear link to the airstrip at Mesters Vig.

Whilst at base camp on the Bersaerkerbrae Glacier Mesters Vig was contacted every two days in order to test the equipment. The set was used to arrange flights out of Greenland for two members of another expedition who had to leave early on medical grounds.

The set, with its small hand generator, proved both robust and simple to operate.

Our thanks are extended to the Commanding Officer of the University of Sheffield Officers Training Corps for his permission to use the set.

Radio type UK/PRC 320
Frequency range 2.0 to 29.9999 MHz
Mode SSB 30w PEP(HP)
 3w PEP(LP)

3.9 MOUNTAINEERING REPORT

The nature of the terrain in and around the Stauning Alps is so varied that generalized comments are of limited value, and in fact could be misleading. The report below relates to just a small part of the Staunings. As with any unfamiliar region, the degree of severity depends partially on the individual's experience. This should be borne in mind while reading. - Editor's note.

GENERAL INTRODUCTION

It has been said that people require mountaineering skills to do scientific work in the Staunings. This has been disproved many times, although common sense and walking experience is essential. Indeed, one of the most important Staunings' skills, river crossing, might not even be considered as mountaineering in Europe.

Melt streams on glaciers are another exaggerated problem, as most glacier ice is exceptionally rough (except after rain or snow). Mid-day July temperatures can be high on the tundra, but not on the glacier with their permanent Katabatic winds. Even so, 'night' crossings of cols are advisable, to obtain firm ground. In crossing such cols (even the Skel Pass) long axes and possibly snow shoes, are useful.

As the rock seems to be poor, ice/snow routes are more attractive. The range is still immediately post Golden Age as regards small peaks and alternative routes on major peaks awaiting first ascents.

DIAMOND PEAK 2150 metres

This peak's almost unbroken NE snowface dominates the right hand side of the Roslin Glacier, just below the junction of the Dalmore Glacier.

NE Face and NW Ridge (AD) 950 metres

Eases its way up the main snow-slope (30° - 50°) to emerge on the right hand ridge below the conspicuous gendarme.

From the camp, cross the glacier to the foot, trending up glacier to cross melt streams - $\frac{3}{4}$ hour. Easily up to a flattening ($\frac{1}{2}$ hour), where some crevasses are crossed. Trend right up one of several gullies/rock to reach the N.W. ridge - 2 hours from foot. Follow this to the 5 metre gendarme (a move of IV gains its top) and further to the summit. Total 3 hours from the foot.

N Face and NW Ridge (PD+)

Gains the right hand ridge from one of two 500 metre 45° couloirs to its left.

Follow the ridge past its junction with the N. spur and past the gendarme to the summit (1 hour in descent).

DUNOTTAR-SKJOLDUNGEBRAE COL circa 1900 metres

Between the Northernmost reach of the Dunottar Glacier and the Skjoldungebrae, at the foot of the SW arete of the Elizabethtinde.

Ascent the Left (North) bank of the Dunottar, near the scree. Gain the upper right hand basin and the col more easily. The far side, not descended, is 45° PD for about 600 metres. ($3\frac{1}{2}$ hours up, $2\frac{1}{2}$ down from Sun Valley camp.)

"ARUNDEL GATE"

The next mountain N.W. of Panoramic Peak on the main Bersaerkerbrae watershed. It is at the head of the South branch of the double-headed glacier North of the glacier leading to Glamis col.

NW Face (PD)

Up this glacier to the upper basin North of the summit then directly 300 metres up to the top.

W Ridge (F)

In descent, diverge left down scree to the Peveril col.

"PEVERIL"

The "Bunny's Ears" between Arundel Gate and Beaumaris.

Traverse East-West (PD+)

Ascent left on to the highest summit and descend steeply (IV -, probably avoidable) to the col between the two ears. Avoid the West ear on the left (South) to reach the col below Beaumaris.

BEAUMARIS

1½ kilometres NW of Glamis col, 3 kilometres SW of Dunvegan; wrongly named on Bennet's map. A varied loose mountain with snow low down and a final rock ridge/tower. Generally there are dip slabs on the North and ledges on the South, where difficulties are turned.

East Ridge (PD)

Ascend the ridge (100 metres, III) until ledges on the left can be followed to the summit tower.

West Spur and Ridge (PD)

From the mountain's foot up scree/ice and a snow ridge to the foot of a rock ridge. Follow ledges on the right to avoid difficulties on the crest (including the West Tower) except for a fine level solid section before the final steepening.

SORRY, WRONG MOUNTAIN

Ian and Ken wanted a view, so why not Panoramic Peak, although Keith correctly called it Beaumaris. The West spur was obviously an easy descent, and doubts about altitude suggested the traverse of a trio of summits accessible from the glacier on the North. Leaving camp at 0730, they headed out across and up the glacier.

On reaching the first, uncairned, summit at 1030 it was obvious that Panoramic Peak was 1 kilometre away, invisible from base. The other nearby summit seemed to fit the description of Beaumaris. They pressed on, spending most of the day on Staunings rock-Danger, Handle With Care. However, once the feasibility of the ledges on the South side was established, they moved together. Despite Ken's unspoken preference for a steep "whimp out" gully they passed over the cairned high point revelling in a 50 metre Chamonix-sharp section.

On the snow by 1530, they were down within the hour, even allowing for an attempted short cut down an ice slope to the North. They were re-united with John Allen and Kev by 1715 - 10 hours being about the longest endurance without cooking for oneself!

COASTAL TREK *

A circular route from base camp on the Bersaerkerbrae down to the coast via the

* written by John Thompson

Skjoldungebrae and back up the Skel Valley was planned by John Thompson and Charles Hird.

We left camp at 1100 and walked up the Harlech Glacier, keeping to the middle most of the way up, and then towards the true left, where the most easterly col into the Skjoldungebrae lies. On entering the basin the snow became quite soft and we found several large crevasses, fortunately only ever losing one leg through at a time. The final ascent to the col is ice for which we needed crampons. An alternative approach is to climb loose scree to the east of the ice slope.

A stop for tea took place at the top whilst we enjoyed the magnificent view. Fears of changing weather made us press on down to the Skjoldungebrae. The snow was very soft and it proved a long slog. The area is very crevassed and crawling on hands and knees over snow bridges was necessary on occasion. At midnight we bivvied two thirds of the way down to the Skjoldungebrae and set off again at 0915. Keeping to the right hand side avoids the worst of the crevasses. On reaching the Skjoldungebrae we again kept to the right and only later crossed to the centre.

The lower reaches of the Skjoldungebrae provide easy walking until the snow is reached. Keeping to the left we were hoping to get to the coast over the moraine but this was so loose that we went over a col some half mile or so from the end of the glacier, walking northwards. This is higher than it looks from the bottom, but provides a good view of the coast and gives a route to the Cap Petersen hut which can be seen from the top of this "pass".

We spent a pleasant night in the hut and rested the next day, taking a short stroll to the west along the coast admiring the scenery. That afternoon the Danish Army Sledge Patrol, Sirius, arrived by boat to stock the hut with provisions for the winter. A brew was put on and friendly relations established. They kindly offered us a lift along the coast by boat to the bottom of the Skel Dal. This provided us with an unequalled view of the mountains, perfectly reflected in the still water between areas of pack ice.

The next day we walked up the Skel Valley, an easy walk with abundant wildlife, camping just below the snout of the Bersaerkerbrae Glacier.

The next morning was started with a walk up the moraine on the true left side of the glacier. This is quite hard going in parts but was still only a comfortable day's walk from base camp.

ACKNOWLEDGEMENTS

The acknowledgements have been divided into three sections - financial support, support in kind and general assistance. Within each section supporters have been listed alphabetically. Supporters of the cancelled 1981 expedition are also included.

FINANCIAL SUPPORT

Mrs. M. Andrews
Barclays Bank plc
Geographical Magazine Trust Fund
Gilchrist Educational Trust
Gino Watkins Memorial Fund
Lloyds Bank plc
Makro Self-Service Wholesalers Ltd
Mount Everest Foundation
National Westminster Bank plc
Mr. J. Peach
Royal Navy (Flag Officer Plymouth)
The Royal Society
Sheffield Twist Drill and Steel Co. Ltd.
Stanley Tools Ltd
University of Sheffield
Williams and Glyns Bank plc
Yorkshire Bank plc

SUPPORT IN KIND

Advance Tapes (UK) Ltd.
Budenberg Gauge Company
Carrich Ltd.
Colman Foods
Don Morrison Mountaineering Eqpt.
Environmental Equipments (Northern) Ltd.
Gubb and Hauff Precision Engineering
Grangewood Plastic Packaging Ltd.
Hatton Colour Company
J. A. Henderson & Co. Ltd.
Hunni Foods Ltd.
Leesack Ltd.
Makro Self-Service Wholesalers Ltd.
Mechanical Engineering Department, University of Sheffield
Quaker Oats Ltd.
Rowntree-Mackintosh Ltd
Sheffield Newspapers
Trebor Ltd.

GENERAL ASSISTANCE

Mr. Sigurdur Adalsteinsson
Airport Manager and Staff, Mesters Vig
Lt. Col. G. Barton
Mr. P. Belcher
Mr. Olafur Benedictsson
Mrs. C. Bown
British Embassy, Reykjavik
Mr. R. D. Brown,
Mr. T. Brown
Civil Engineering Department, University of Sheffield
Commission for Scientific Research in Greenland
Directorate of Civil Aviation, Copenhagen
Mrs. J. Edwards
Expedition Advisory Centre
Flugfelag Nordurlands HF

Flugfrakt HF
Mr. T. B. Ferguson
Mr. D. Fergusson
Mr. R. J. Forster
Greenlandair A/S
Greenland Technical Organization
Prof. T. Hanna
Mr. B. Hauff
Mr. T. Herbert-Jackson
Dr. C. Hird
Dr. P. Howard
Icelandair
Dr. B. Kenny
Dr. H. Lister
Mr. I. Mackley
Mr. R. Macaulay
Mr. McClellan
Mechanical Engineering Department, University of Sheffield
Prof. K. J. Miller
Ministry for Greenland
Mr. B. Mole
Mr. P. Morris
Mr. P. Morrison
Mrs. N. Parkes
Mr. J. Peach
Dr. Pennington
Royal Geographical Society
Scott Polar Research Institute
Sorby Hall, University of Sheffield
Mr. C. Stacey
Student Health Service, University of Sheffield
Mr. K. H. Sutherland
University of Sheffield
Mr. A. F. Wright



